Analysis of Protein Kinase D1's Role During Reactive Oxygen Species-mediated Signaling

By Sanaz Sobhani

A thesis submitted to the School of Graduate Studies

In partial fulfillment of the requirements for the degree of

Master of Science in Medicine

(Cancer and Development)

Division of Biomedical Sciences, Faculty of Medicine

May 2025

Memorial University of Newfoundland

St. John's, Newfoundland

ABSTRACT

Protein Kinase D1 (PKD1) is a critical component of cellular responses to reactive oxygen species (ROS)-mediated apoptosis. Previous studies demonstrated that upon oxidative stress, PKD1 is activated through a signaling pathway mediated by the Src/Abl non-receptor tyrosine kinases. Subsequently, PKD1's translocation to different cellular compartments can regulate gene expression and promote cell survival through the NF-kB signaling pathway. Additionally, PKD1 deficiency increases ROS sensitivity in mouse embryonic fibroblasts (MEFs), leading to mitochondrial membrane depolarization and apoptosis when exposed to oxidative stress. Our study examined PKD1's protective role against oxidative stress-induced apoptosis and its impact on gene expression. Using wild-type (WT) and PKD1-deficient (*PKD1-/-)* MEFs, we found that the absence of PKD1 significantly increases oxidative stress-induced apoptosis, as evidenced by H_2O_2 stimulation and serum starvation experiments. To better understand the molecular mechanisms underlying PKD1's protective function, RNA-Seq analysis was performed, comparing gene expression levels between WT and *PKD1-/-* MEFs. RNA-Seq analysis revealed differentially expressed genes (DEGs) between WT and *PKD1-/-* genotypes, with 383 DEGs in primary and 1705 DEGs in immortalized MEFs. Notably, BCL2L11 (BIM), a pro-apoptotic protein, was more than two-fold down-regulated in both primary and immortalized *PKD1-/-* MEFs, suggesting its interaction with PKD1 on the mitochondrial outer membrane through the mitochondrial apoptosis pathway. In addition, KEGG pathway analysis highlighted enriched differentially expressed pathways, including those associated with apoptosis, cell survival, and response to oxidative stress. This study sheds light on how PKD1 defends against oxidative stress and influences gene expression, potentially contributing to the development of treatments for oxidative stress-linked diseases.

General Summary

This study investigates the role of protein kinase D1 (PKD1) in protecting cells from oxidative damage caused by free radicals in the body, which can lead to programmed cell death. When cells experience this damage, PKD1 is activated and plays a key role in regulating genes that promote cell survival. Previous research from our group showed that cells lacking PKD1 show higher sensitivity to these molecules, resulting in enhanced cell death in a mouse cell line called mouse embryonic fibroblasts (MEFs). In our experiment, we compared two cell types: normal (wild type) and PKD1-deficient cells. We found that PKD1-deficient cells died at a much higher rate when exposed to oxidative damage. Our analysis also revealed a significant number of genes that were expressed differentially in the PKD1-deficient cells, including a decrease in protein called BCL2l11 (BIM), which is involved in cell death. Additionally, we discovered that important pathways related to cell survival and death were also affected.

In conclusion, our findings highlighted PKD1's role in protecting cells from oxidative damage, which could lead to new treatments for diseases related to this type of damage, such as cancer.

CO-AUTHORSHIP

The experimental design was supported by Dr. Michael Leitges, who also provided both wild-type and PKD1-deficient mouse embryonic fibroblasts (MEFs), facilitated the immortalization process, and contributed to manuscript preparation. Ursula Braun conducted the Western blotting experiment and image acquisition for Figures 7B, 7C, 8A, and 8C. The RNA-Seq analysis, including DESeq2 and pathway analysis, was conducted by Jocshan Loaiza Moss utilizing R software, resulting in Figures 14 and 15 and Tables 4 and 5. Additionally, he contributed to cell culture and RNA extraction procedures for RNA-Seq analysis. For the TUNEL assay, Hematoxylin staining and mounting were assisted by Iliana Dimitrova and Danielle Gardiner from the Histology Department.

ACKNOWLEDGMENTS

I would like to express my deepest gratitude to Dr. Michael Leitges for his expertise and invaluable support, which have been instrumental to the success of this project. I am sincerely thankful to my advisor, Dr. Jessica Esseltine, for her insightful guidance throughout the writing of my thesis, and I extend my heartfelt appreciation to Dr. Thomas Belbin for his generous assistance with the RNA-Seq analysis.

I am deeply grateful to the School of Graduate Studies for their financial support, which has been essential to the successful completion of my research project. I would also like to acknowledge the Canadian Institutes of Health Research for their support of this project.

I am also profoundly grateful to my colleagues and friends for their unwavering encouragement and emotional support throughout this journey.

To Elyas and Hannah, your boundless love, patience, and support have sustained me in every step of this process, and for that, I am forever thankful. I am incredibly grateful for your understanding when I was not by your side when I should have been.

Lastly, I wish to thank my family for their unconditional love and support, which have been a constant source of inspiration and strength.

LIST OF TABLES

LIST OF FIGURES

List of Appendices

LIST OF SYMBOLS AND ABBREVIATIONS

1X: One time

4X: Four times

10X: Ten times

6-OHDA: 6-hydroxydopamine

Abl: Abelson tyrosine kinase

Adam8: A disintegrin and metalloproteinase 8

ADM: Acinar to ductal metaplasia

A-loop: Activation loop

Apaf-1: Apoptotic protease activating factor 1

APS: Ammonium persulphate

ARF: Alternative reading frame

aPKCs: Atypical protein kinase Cs

ATP: Adenosine triphosphate

Bak: B cell lymphoma-2 antagonist/killer

BAM: Binary alignment/map

Bax: B cell lymphoma-2 associated protein

Bcl-2: B-cell lymphoma-2

BCL2L11: B-cell lymphoma 2-like 11

Bcl-xl: B-cell lymphoma extra large

BH3: B-cell 2 homology 3

BIM: B-cell lymphoma-2 interacting mediator of cell death

BM-MSCs: Bone marrow mesenchymal stem cells

Bmp2: Bone morphogenetic protein 2

BSA: Bovine serum albumin

Btk: Bruton's tyrosine kinase

cAMP: Cyclic adenosine monophosphate

Ca^{+2}: Calcium ion

C1a: Conserved domain 1a

C1b: Conserved domain 1b

C2-C4: Conserved domain 2-4

C2-like: Conserved domain 2-like

Cd68: cluster of differentiation 68

Cdkn2d: Cyclin-dependent kinase inhibitor 2D

cGMP: Cyclic guanosine monophosphate

CIN: Chromosomal instability

Csf2rb: Colony-stimulating factor 2 receptor beta

Csf2rb2: Colony-stimulating factor 2 receptor beta 2

Csf3r: Colony-stimulating factor 3 receptor

Ctsc: Cathepsin C

Cx3cr1: C-x3- motif chemokine receptor 1

Cys: Cysteine

cMYC: Cellular myelocytomatosis

cPKCs: Classical protein kinase Cs

DAB: 3, 3'-diaminobenzidine

DAG: Diacylglycerol

DAPK: Death-associated protein kinase

DBD: Dynein light chain-binding domain

DCLK1: Doublecortin-like kinase 1

DE: Differentially expressed

DEGs: Differentially expressed genes

DESeq2: Differential expression analysis based on the negative binomial distribution, version2

DMEM: Dublecco’s modifies eagle’s medium

Doc2: Docking protein 2

DPI: Diphenyleneiodonium

dUTP: Deoxyuridine triphosphate

Ece2: Endothelin-converting enzyme 2

EDTA: Ethylenediaminetetraacetic acid

EGFR: epithelial growth factor receptor

EMT: Epithelial to mesenchymal transition

Erbb4: Erb-b2-receptor tyrosine kinase 4

ERK: Extracellular signal-regulated kinase

FASTQC: Fast quality control

FC: Fold change

FCS: Fetal bovine serum

Fgf2: Fibroblast growth factor 2

FOV: Field of view

GAPDH: Glyceraldehyde-3-phosphate dehydrogenase

Gata3: GATA binding protein 3

Gly: Glycine

GO: Gene ontology

H_2O_2: Hydrogen peroxide

HEK 293 T: Human embryonic kidney 293 T

Hcls1: Hematopoietic cell-specific Lyn substrate 1

HISAT2: Hierarchical indexing for spliced transcript alignment 2

Hoxa13: Homeobox A13

HPRO: Human Prohibitin

HRP: Horseradish peroxidase

Hspa8: Heat shock protein family A member 8

IHC: Immunohistochemistry

IkBα: Inhibitor of kappa B alpha

IKK: Inhibitor of kappa B kinase

Il7r: Interleukin 7 receptor

Il12rb1: Interleukin 12 receptor subunit beta 1

Itgam: Integrin alpha M

JC-1: JC-1 fluorescent dye

JNK: c-Jun N-terminal kinase

KEGG: Kyoto encyclopedia of genes and genomes

Kras: Kirsten rat sarcoma viral oncogene

Lama3: Laminin subunit alpha 3

log2FC: logarithm base 2-fold change

ml: Milli litter

μM: Micro molar

μg: Micro gram

mM: Milli molar

Mef2c: Myocyte enhancer factor 2C

MEFs: Mouse embryonic fibroblasts

MKK 3/6: Mitogen-activated protein kinase kinase 3 and 6

MnSOD: Manganese superoxide dismutase

MOMP: Mitochondrial outer membrane permeabilization

mRNA: Messenger RNA

mROS: Mitochondrial reactive oxygen species

MSI: Microsatellite instability

NES: Nuclear export signals domain

NF-kB: Nuclear factor kappa-light-chain-enhancer of activated B cells

NIH 3T3: National institutes of health 3T3 cells

nPKCs: Novel protein kinase Cs

NLS: Nuclear localization signals domain

O_3: Ozone

OD: Optical density

P38 MAPK: p38 mitogen-activated protein kinase

PanIN: Pancreatic intraepithelial neoplasia

PB1: Phox and bem1 domain

Pbp2: Penicillin-binding protein 2

PBS: Phosphate-buffered saline

PCA: Principal component analysis

PC1/2: Principal component 1/2

PDAC: Pancreatic ductal adenocarcinoma

PDK1: Phosphoinositide-dependent kinase 1

Pdpn: Podoplanin

PH domain: Pleckstrin homology domain

PHB1: Prohibitin 1

PI3-P: Phosphatidylinositol 3-phosphate

PIF: PDK1 interacting fragment

Pim1:Pim-1 proto-oncogene, serine/threonine kinase

PIP3: Phosphatidylinositol 3,4,5-triphosphate

PKA: cAMP-dependent Protein Kinase A

PKC: Protein kinase C

PKCδ: Protein kinase C delta

PKCδ-/-: PKC delta-deficient

PKD: Protein kinase D

PKD1-/-: PKD1-deficient

PKG: cGMP-dependent protein kinase G

PMA: Phorbol-1-2-mystrate-13-acetate

Prkd1: protein kinase D1

PS: Pseudosubstrate site

Psd4: Post-synaptic density protein 4

PT: Permeability transition

PTPs: Protein-tyrosine phosphatases

p-value: Probability value

RACKs: Receptors for activated PKCs

Rpl34: Ribosomal protein L34

RIE-1: Rat intestinal epithelial cells-1

RIPA: Radioimmunoprecipitation assay

RNA-Seq: RNA sequencing

ROS: Reactive oxygen species

SAM: Sequence alignment/map

SAPK: Stress-activated protein kinase

SDS-PAGE: Sodium dodecyl sulfate-polyacrylamide gel electrophoresis

SEM: Standard errors of the mean

Ser: Serine

SFKs: Src family tyrosine kinases

siRNA: Small interfering RNA

Sirt1: Sirtuin 1

SOD: Superoxide dismutase

Src: Sarc tyrosine kinase

STAR: Spliced transcripts alignment to a reference

Stmn1: Stathmin1

STRING: Search tool for the retrieval of interacting genes/proteins

T2DM: Type 2 diabetes mellitus

TAZ: Transcriptional coactivator with PDZ-binding motif

TDT: Terminal Deoxynucleotidyl Transferase

TEMED: N, N, N', N'-Tetramethyl ethylenediamine

Tgm2: Transglutaminase 2

Tifa: TRAF-interacting protein

Tlr13: Toll-like receptor 13

TM: Turn motif

Tnf: Tumor necrosis factor

Tnfa: Tumor necrosis factor alpha

Tnfaip8l3: Tumor necrosis factor alpha-induced 8-like 3

Trem2: Triggering receptor expressed on myeloid cells 2

Trim34b: Tripartite motif-containing 34B

TUNNEL: Terminal deoxynucleotidyl Transferase dUTP Nick End Labeling

Tyr: Tyrosine

Ucp2: Uncoupling protein 2

Usp13: Ubiquitin-specific peptidase 13

Ugg2: UDP-glucose glycoprotein glycosyltransferase 2

V1-V5: Variable region 1-5

VDAC: Voltage-dependent anion channel

Vegfb: Vascular endothelial growth factor B

Vegfc: Vascular endothelial growth factor C

WT: Wild type

TABLE OF CONTENTS

1. Introduction

1.1. Background of Study

1.1.1. Kinase Signal Transduction

Intracellular signal transduction is a process by which an external signal is transmitted into the cell to convert external signals into various events. Signal transduction can initiate events within the cell nucleus, such as activating transcription factors, thereby potentially altering the cell metabolism or shape by regulating the expression of specific genes. Protein Kinases are the principal components of cell signaling cascades that mediate protein phosphorylation in many signal transduction pathways, including those controlling cell growth, proliferation, initiation, and regulation of immune responses (1,2).

1.1.1.1. Protein Kinase C Family

The Protein Kinase C (PKC) family belongs to the AGC family, which consists of cAMP-dependent Protein Kinase A (PKA), cGMP-dependent protein kinase G (PKG), and protein kinase C (PKC). The AGC family is the most evolutionarily conserved group of kinases and is widely expressed in eukaryotes, with more than 60 protein kinases in humans. These kinases play critical roles in diverse cellular functions related to health and disease, making them important potential drug targets for conditions such as cancer, diabetes, and neurological disorders (3). The catalytic (kinase) domain varies among different AGC kinase families. However, they all share a common conserved catalytic core consisting of two lobes, an ATP-binding site, and a Gly-rich loop. The activation loop and peptide substrate-binding site are located between the small and large lobes. Activation of AGC kinases is mediated by the phosphorylation of the regulatory domain and the interaction of the regulatory site called PIF-pocket (PDK1 Interacting Fragment) with the C-terminus (3). The PKC family includes

the classical isoforms (cPKCs), which consist of α, ßI, ßII, and γ, and are regulated by calcium ions, diacylglycerol (DAG), and phospholipids. The novel PKC isoforms (nPKCs) (δ, ε, η, and θ) are calcium-independent, and the atypical isoforms (aPKCs) (ι, and λ) are insensitive to calcium and DAG (4). PKCs are multifunctional kinases that are known to be involved in cell growth (5) and proliferation (6), differentiation (7–9), neural development (10), oxidative stress (11–14), apoptosis (15,16), aging (17,18), and tumor promotion and progression(19). Distinct protein-protein interactions of individual PKC isoforms with their protein substrates can trigger specific cell functions or initiate specific responses by activating other protein kinases or downstream targets (20).

The structures of PKCs comprise N-terminal regulatory and C-terminal catalytic domains, as outlined in Figure 1. The classical and novel isoforms of the PKC family consist of four conserved functional domains (C1-C4) separated by five variable regions (V1-V5). All members of the PKC family possess an autoinhibitory pseudo-substrate (PS) domain located in the N-terminal region. In addition, cPKCs and nPKCs contain a Diacylglycerol (DAG) binding domain (C1a-C1b) that confer the ability to interact with DAG at various sites within the cell. cPKCs include a Calcium-binding domain (C2) capable of binding to Ca^{2+} ions as part of their activation process, while in contrast, nPKCs do not possess a C2 homologous domain but instead contain a C2-like domain, a variant of the C2 domain that lacks the essential sequences for Ca^{2+} binding but is involved in mediating protein-phospholipid interactions (21). Two aPKC isoforms lack C2/C2-like and functional C1 domains. Instead, they contain a special Phox and Beam 1 (PB1) domain, a PS domain, a non-functional C1 domain in the N-terminus, and a kinase domain in the C-terminal. In addition, aPKCs contain

Nuclear Localization Signals (NLS) and Nuclear Export Signals (NES) in their N-terminal regulatory domain (4,22–24).

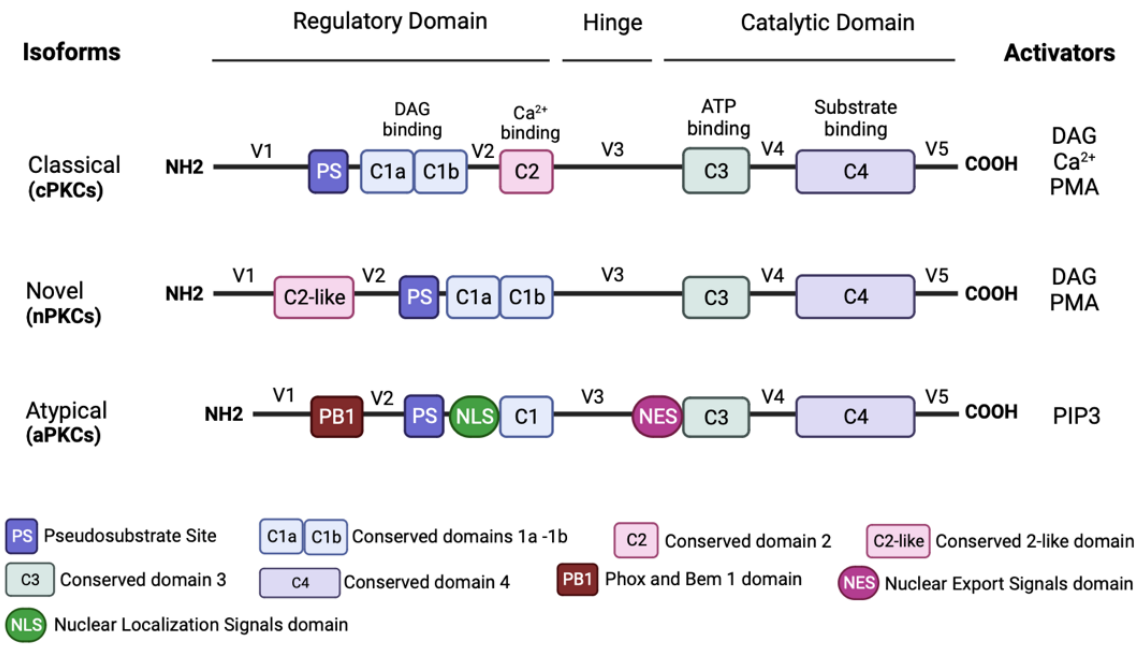
Isoforms
Regulatory Domain
Hinge
Catalytic Domain
Activators
Classical (cPKCs)
NH2
V1
PS
DAG binding
C1a
C1b
V2
Ca2+ binding
C2
V3
ATP binding
C3
V4
Substrate binding
C4
V5
COOH
DAG
Ca2+
PMA
Novel (nPKCs)
C2-like
DAG
PMA
Atypical (aPKCs)
PB1
NLS
C1
NES
PIP3
Pseudosubstrate Site
Conserved domains 1a -1b
Conserved domain 2
Conserved 2-like domain
Conserved domain 3
Conserved domain 4
Phox and Bem 1 domain
Nuclear Export Signals domain
Nuclear Localization Signals domain

Figure 1 Structural characteristics of PKC family members, including domains involved in enzyme activation. The structure of PKC family members comprises regulatory N-terminal and C-terminal domains. While cPKCs and nPKCs exhibit substantial similarities, nPKCs differ in possessing a C2-like domain instead of a C2 domain. The aPKCs lack a C2 domain; alternatively, they contain a single C1 domain but include PB1 and NLS domains in the N-terminus and an NES domain in the C-terminus. **V1-V5:** Variable regions 1-5, **DAG:** Diacylglycerol, **Ca^{2+}:** Calcium, **ATP:** Adenosine triphosphate; **PMA:** Phorbol-1-2-Mystrate-13-Acetate, **PIP3:** phosphatidylinositol 3, 4, 5-triphosphate (4,23). The image was created in Biorender.com.

PKC isoforms (α, ßI, ßII, γ, δ, ε, η, θ, ι, and λ) are differentially expressed in tissues and cells, and their subcellular localization, along with distinct expression profiles in specific cells demonstrate their unique functions of each isoform (23,25,26). Individual PKCs have specific substrates and activators (e.g., DAG, Ca^{2+}, and phosphatidyl inositol). Additionally, different protein kinases can phosphorylate and activate each other. For instance, protein kinase D1 (PKD1) is a substrate of PKCδ (27), and PKCε activates protein kinase D3 (PKD3) via activation loop phosphorylation (27,28).

The function of PKCs can be specified mainly by intracellular localization from the cytosol to different locations within the cell. These processes are tissue-and cell type-specific. For instance, PKCδ has been shown to translocate to the nucleus (29,30), Golgi (31), or mitochondria (32) upon stimulation in response to various stimuli and functions either as a promoter of apoptosis or as a facilitator of cell survival (33). The activation process of PKCs is also isoform-specific. Three specific phosphorylation sites in the C-terminal catalytic domain of PKC isoforms are crucial for their proper functioning and catalytic activation. The activation loop (A-loop), turn motif (TM), and hydrophobic motif (HM) are three conserved motifs found in the catalytic domain of both cPKCs and nPKCs. The aPKCs lack the HM motif and instead contain a negatively charged glutamic acid residue, which is thought to mimic irreversible phosphorylation (34). In addition, a conformational change within the protein is necessary to eliminate the PS domain inhibition, which prevents PKC activation by blocking the catalytic domain. Mutations at the PS site can result in a constitutively active form of PKCs (35). The binding of DAG to cPKCs increases the likelihood of their binding to phosphatidylserine and Ca^{2+}, leading to a conformational change and the release of the PS motif, which is crucial for catalytic activity. Although nPKCs lack a calcium-binding motif,

they are also regulated by DAG. Moreover, nPKCs can bind to phospholipids using their C2-like structure, a domain that enables interaction with specific proteins called receptors for activated PKCs (RACKs). These RACKs serve as scaffolding proteins, helping to localize activated PKCs to specific subcellular sites where they perform their functions. In contrast, aPKC isoforms are insensitive to DAG and calcium because of the absence of functional C1 and C2 domains. They may be regulated through intracellular translocation, controlled by NLS and NES in their N-terminal regulatory domain through binding to regulatory proteins. Compounds such as phosphatidyl inositol and phosphatidic acids can activate aPKCs (4,22–24).

1.1.1.2. Protein Kinase D Family

Protein kinase D (PKD) was initially identified as a new member of the PKC family in 1994 (36) but was assigned later to the calcium/calmodulin-dependent kinases (37) based on structural specifications. PKD family members are serine-threonine kinases that are described to act downstream of the PKC family (38). PKDs comprise three members: PKD1/PKCμ, PKD2, and PKD3/PKCν, with PKD1 being the first to be identified and, thus, the most comprehensively studied (38). PKDs play diverse roles in cellular processes, including epithelial-to-mesenchymal transition (EMT) (39,40), vesicular transport (41,42), cell migration (43–45), cell proliferation (45–48), angiogenesis (45,49,50), invasion (51,52), differentiation (53), gene transcription and survival responses (54), oxidative stress (12,55–61), and apoptosis (62–64).

Like the PKC family, PKDs comprise both N-terminal regulatory and C-terminal kinase domains, as illustrated in Figure 2. In addition to the DAG-binding domains (C1a and C1b), the N-terminal domain contains a lipoprotein-binding pleckstrin homology (PH) domain,

which includes a Tyr phosphorylation site that regulates PKDs activity via autoinhibition. It was shown that deletions or point mutations in the pleckstrin homology domain could increase the kinase activity of PKD1 (65). The C1 domains are tandem cysteine-rich zinc-finger motifs (C1a and C1b) separated by a zinc-finger linker segment that binds to DAG and phorbol esters. C1 domains have a critical function in the localization of PKD to different cell compartments. For instance, the transportation of PKD1 to the trans-Golgi network is mediated by its C1a domain, whereas its C1b domain facilitates its translocation to the nucleus (66–68).

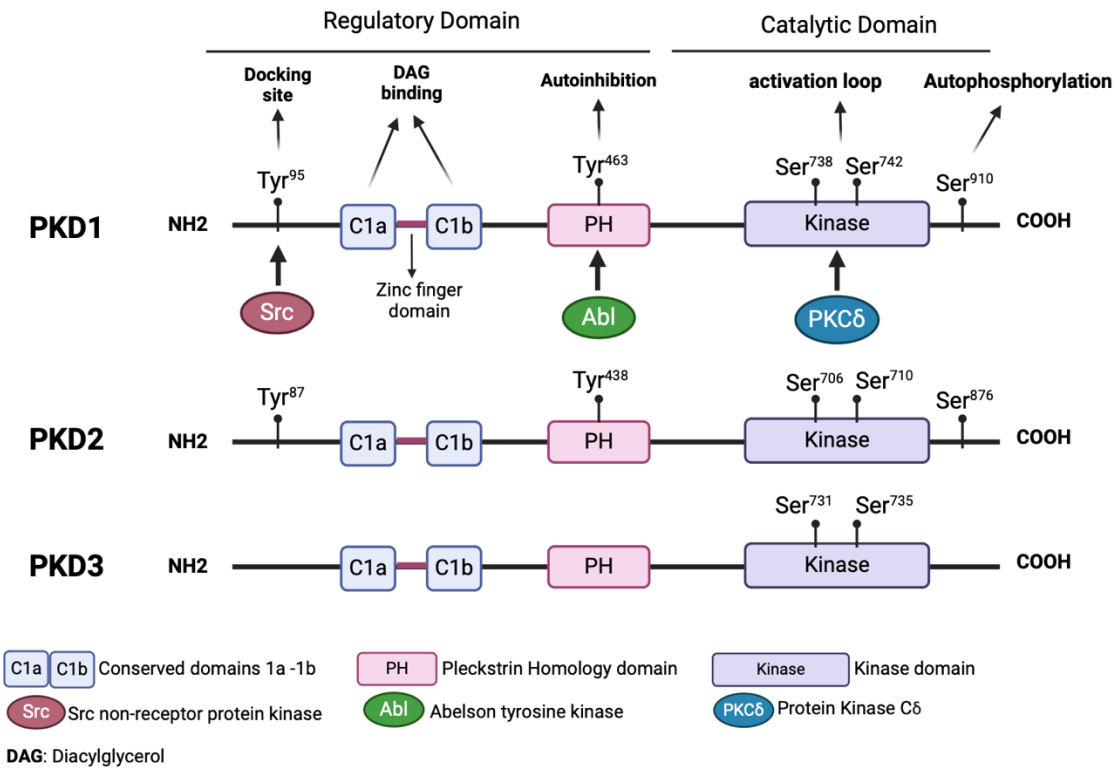
Regulatory Domain
Catalytic Domain
Docking site
DAG binding
Autoinhibition
activation loop
Autophosphorylation
PKD1
NH2
Tyr95
C1a
C1b
Zinc finger domain
Tyr463
PH
Ser738
Ser742
Kinase
Ser910
COOH
Src
Abl
PKCδ
PKD2
Tyr87
Tyr438
Ser706
Ser710
Ser876
PKD3
Ser731
Ser735
C1a C1b Conserved domains 1a -1b
PH Pleckstrin Homology domain
Kinase Kinase domain
Src Src non-receptor protein kinase
Abl Abelson tyrosine kinase
PKCδ Protein Kinase Cδ
DAG: Diacylglycerol

Figure 2 Structural characteristics of PKD family members, including domains involved in enzyme activation. PKDs contain a regulatory domain in the N-terminus and a kinase domain in the C-terminus. PKD1 and PKD2 share approximately 80% amino acid sequence similarity and exhibit significant homology in their catalytic and C1 domains. In contrast to PKD1 and PKD2, PKD3 lacks docking sites, autoinhibition, and autophosphorylation sites (66). The image was created in Biorender.com.

The PKD family exhibits a significant degree of homology among its members. Nevertheless, structural variations have been identified that may reflect differences in their activation mechanisms and downstream signaling (67–69). Unlike PKD3, PKD1 and PKD2 contain C-terminal autophosphorylation motifs (Ser^{910} in PKD1 and Ser^{876} in PKD2) (70) and N-terminal docking sites (Tyr^{95} in PKD1 and Tyr^{87} in PKD2) (56), which are phosphorylated by Src following oxidative stress, creating a docking site for PKCδ. This interaction enables PKCδ to phosphorylate the activation loop, resulting in the activation of PKD1(56). Interestingly, this Tyr residue is absent in PKD3, suggesting that this isoform is not involved in ROS-mediated signaling.

The principal mechanisms regulating PKD activity include intramolecular autoinhibition, phosphorylation of the activation loop, and subcellular localization (71). Biological factors such as DAG, growth factors, G-protein activators, initiation of immune cell receptors, and oxidative stress can induce PKD activation via pathways modulated by PKC isoforms (56,68). In most cases, established signaling pathways that activate PKC subsequently can lead to its interaction with PKDs, resulting in PKDs' activation. In this context, nPKCs have been shown to phosphorylate PKDs at two specific serine residues within their activation loop, including Ser^{738} and Ser^{742} in PKD1, $Ser^{706,}$ and Ser^{710} in PKD2, and Ser^{731} and Ser^{735} in PKD3, thereby inducing PKD activation (66). Alternative mechanisms of PKD activation through PKC-independent pathways have been identified *in vivo*. For example, G beta gamma (Gßγ) protein complexes can directly activate PKD isoforms by binding to their PH domain, independently of PKC. Activated PKD then regulates Golgi structure and protein secretion (69).

In general, PKD family members translocate in response to various cellular stimuli, including the translocation of PKD1 and PKD2 from the cytosol to areas of the plasma membrane containing DAG and the following translocation of PKDs from the plasma membrane to the cytosol, which requires PKCs. The PKDs then relocate to the nucleus. PKD3 commutes between the cytosol and nucleus after stimulation. Moreover, PKD family members could be in the Mitochondria and the Golgi complex in response to specific stimuli (38,68). The regulatory subdomains of PKD family members are crucial for subcellular translocation, assisting in the transportation of PKD isoforms to various cell sections (68).

1.1.2. Reactive Oxygen Species And Oxidative Stress

Reactive Oxygen Species (ROS) are inevitably generated in cells that reside in environments with a high concentration of oxygen. They can originate from physiological by-products of the mitochondrial electron transport respiratory chain or from the extracellular environment. ROS are generally categorized as either radical or non-radical and have the potential to cause damage to various biomolecules, including lipids, DNA, and proteins. The radical group contains compounds such as superoxide ion, hydroxyl, peroxyl, and alkoxyl radicals with at least one unpaired electron in their atomic shells. Non-radical ROS represents a large group of compounds with the potential to generate free radicals within living organisms, including hydrogen peroxide (H_2O_2), ozone (O_3), organic peroxides, and aldehydes (72–74).

Cells need mechanisms to neutralize ROS because they can cause significant harm to biomolecules, leading to the development of various diseases and accelerating aging processes. Antioxidant defenses in cells are crucial for managing and counteracting fluctuations in ROS levels. Therefore, effective neutralization mechanisms are essential for

maintaining cellular integrity and function under oxidative stress conditions. Various cellular mechanisms can neutralize ROS through the degradation of hydrogen peroxide, including non-enzymatic molecules like vitamins A, E, and C, as well as enzymes such as superoxide dismutase (SOD) and catalase. Since these mechanisms are not constantly efficient, oxidative stress may occur (74,75). The fact that antioxidant expression increases in response to high production of ROS indicates the presence of cellular surveillance and detection mechanisms that activate signaling from mitochondria to the nucleus to promote the activation of protective genes. A known signaling pathway that regulates cellular detoxification and survival is initiated by mitochondria and is referred to as the PKD-regulated detection system (76).

Oxidative stress, resulting from ROS, contributes to various disorders, including the development of type 2 diabetes mellitus (T2DM) (77). A significant contributor to the progression of T2DM is the presence of oxidative stress induced by the activation of multiple molecular pathways. Initially, oxidative stress is triggered when the production of free radicals exceeds the body's antioxidant defenses, causing cellular damage and dysfunction that are essential to T2DM pathogenesis. Furthermore, pancreatic beta cells, responsible for insulin production, are especially vulnerable to oxidative stress due to their inherently low antioxidant capacity. Consequently, a progressive decrease in beta-cell mass and function, a hallmark of T2DM, occurs. Additionally, free radicals activate signaling pathways sensitive to stress, such as NF-κB, c-Jun N-terminal kinase /stress-activated protein kinase (JNK/SAPK), and p38 MAPK, which further impair insulin action and promote insulin resistance. Inflammation is another pathway in T2DM, which is activated by oxidative stress and exacerbates insulin resistance and beta-cell dysfunction. Inflammatory mediators such

as cytokines can further increase oxidative stress, creating a vicious cycle that worsens T2DM (78). Considering the significant role that oxidative stress plays in type 2 diabetes, the use of antioxidant agents is a promising therapeutic approach (77). In addition to T2DM, studies have demonstrated that oxidative stress contributes significantly to various health conditions, including atherosclerosis (79), neurodegenerative disorders (80), arthritis (81), and cancer (82–85).

Cellular signaling pathways regulating proliferation (86,87), growth arrest (88,89), senescence (90–92), DNA repair (93,94), and apoptosis (95–97) have been shown to be affected by oxidative stress. Oxidative stress is a critical factor in regulating apoptosis or programmed cell death. Excessive ROS production can result in cellular damage and trigger uncontrolled apoptotic pathways, resulting in the development of diseases such as cancer and neurodegenerative diseases (96). The impact of oxidative stress (e.g., DNA repair or apoptosis) varies depending on the cell type, duration, and amount of exposure to ROS (74,75).

1.1.3. PKD1's Role In ROS-Mediated Signaling

Previous research has demonstrated the function of PKD1 in apoptosis and ROS-mediated signaling pathways. For example, HeLa cells were treated with the oxidative stress inducer H_2O_2 to investigate whether other stimuli that activate PKD also lead to the activation of nuclear factor kappa-light-chain-enhancer of activated B cells (NF-kB) in these cells. The study revealed a novel signaling cascade where oxidative stress activates the Src/Abelson (Src/Abl) tyrosine kinases, which then phosphorylate and activate PKD. Activated PKD, in turn, activates the NF-κB transcription factor via the inhibitor of the kappa B kinase (IKK)

complex, leading to a pro-survival response that protects cells from oxidative stress-induced death (54). The researchers also treated HeLa cells with mitochondrial oxidative stress inducers other than H_2O_2, like rotenone (complex I inhibitor) and diphenyleneiodonium (DPI), to generate mitochondrial ROS (mROS). They described another signaling pathway where mitochondrial oxidative stress activates PKD at the mitochondria, which then induces manganese superoxide dismutase (MnSOD) expression via NF-κB to protect cells from oxidative damage (98). Moreover, PKD1 has been shown to have a protective role in rat intestinal epithelial cells (RIE-1) from H_2O_2-induced oxidative stress by upregulating NF-κB and downregulating the p38 MAPK pathway without affecting ERK1/2 or JNK (99).

Our research group examined mouse embryonic fibroblasts (MEFs) lacking PKD1, which had been generated through gene targeting to assess their response to ROS. PKD1 has been identified as a detector for oxidative stress and the mitochondrial outer membrane permeabilization regulator. PKD1 deficiency increased ROS sensitivity in MEFs, which subsequently caused mitochondrial membrane depolarization and led to apoptosis when exposed to oxidative stress and serum starvation (100).

In mouse models, doublecortin-like kinase 1 positive (DCLK1+) cells in pancreatic intraepithelial neoplasia lesions experience higher oxidative stress and epithelial growth factor receptor (EGFR) pathway activation (101). Inhibition of EGFR signaling increases suppression of PKD1 activation, expanding the DCLK1+ stem cell population, which may potentially contribute to tumor progression and therapeutic resistance. Additionally, it has been shown that different factors that cause acinar to ductal metaplasia (ADM) in pancreatic cancer, including inflammatory cytokines and growth factors, can elevate PKD1 levels, which are activated by hydrogen peroxide (102). PKD1 activation results in gene expression

modifications that promote a ductal phenotype over an acinar one. The expression of PKD1 in acinar cells affects their survival and contributes to ADM, partly through its interaction with NF-κB. Immunohistochemistry (IHC) was employed to investigate PKD1 expression and activation in transgenic mouse models' tissue sections during the development of ADM and pancreatic intraepithelial neoplasia (PanIN) lesions, which may develop into pancreatic ductal adenocarcinoma (PDAC) (103). The findings indicated that PKD1 plays a critical role in mediating acinar-to-ductal reprogramming and initiating early pancreatic neoplasia initiation through Kirsten rat sarcoma viral oncogene (Kras) signaling and the Notch pathway. Inhibition of PKD1 effectively blocked these processes, suggesting it as a potential therapeutic target for treating pancreatic cancer.

In one study, it has been shown that oxidative stress in dopaminergic neuronal cells, induced by H_2O_2 or 6-hydroxydopamine (6-OHDA), causes early activation of PKD1 through phosphorylation at Ser744/748 (activation loop) and Ser916, which occurs before cell death(104). This early activation of PKD1 facilitates the neutralization of oxidative damage as PKD1 translocates to the nucleus, and its overexpression provides protection against oxidative stress-induced cytotoxicity, while the PKD1 S916A phospho-defective mutant exacerbated cell death, suggesting an anti-apoptotic role for PKD1. Enhancing PKD1's protective mechanism against oxidative damage may suggest a therapeutic strategy for Parkinson's disease treatment. The involvement PKD in autophagy was demonstrated in Human embryonic kidney 293 T cells (HEK 293T) treated with H_2O_2, where PKD1 acts as a positive regulator functioning downstream of death-associated protein kinase (DAPK) (57). PKD interacts with and phosphorylates the lipid kinase Vps34, activating it and initiating the production of phosphatidylinositol 3-phosphate (PI3P), a key step in autophagy induction,

highlighting the necessity of both PKD and DAPK for autophagy induction under oxidative stress conditions.

A study investigated the effect of oxidative stress on bone marrow mesenchymal stem cells (BM-MSCs) induced by hydrogen peroxide, focusing on the role of PKD1 overexpression and knockdown in osteogenesis (105). The findings indicated that oxidative stress inhibits the osteogenic differentiation of BM-MSCs by activating cellular stress pathways that decrease PKD1 expression while increasing Cellular Myelocytomatosis (c-MYC) and Sirtuin 1 (Sirt1) levels, ultimately leading to reduced cell viability. PKD1 has been found to mitigate these negative effects on osteogenesis, with its protective role potentially facilitated by the transcriptional co-activator with PDZ-binding motif (TAZ).

1.1.4. ROS-Mediated Signal Transduction

In response to oxidative stress, PKD1 is activated through a mechanism that requires non-receptor tyrosine kinases and PKCδ (56). The Src family tyrosine kinases (SFKs) include Src, a critical component in various cell processes, including proliferation, survival, and apoptosis (106). The activation of Src can occur due to oxidative stress through a variety of mechanisms involving redox regulation and signaling pathways. Multiple cysteine residues in Src kinase are conserved and can be oxidized by ROS, thereby making the kinase sensitive to changes in redox status. The oxidation of residues Cys^{245} and Cys^{487} (located in the SH2 and kinase domains) leads to a conformational change in Src and its activation. The conformational change may involve the movement of its various components, which can result in the exposure or formation of the active site, and it can facilitate the interaction between Src's catalytic domain and its substrates (107). In addition, it has been shown that oxidative stress increases the autophosphorylation of Tyr^{418} in Src, which serves as a marker

for Src's activity. Another study revealed that epidermal growth factor receptor (EGFR) and Src are essential upstream kinases crucial in oxidative-induced phosphorylation, resulting in decreased cell adhesion, morphological changes, and apoptosis in epithelial cells (108). Hydrogen peroxide (H_2O_2) inhibits protein-tyrosine phosphatases (PTPs), resulting in the hyperphosphorylation of EGFR, which consequently activates Src kinase.

The PKD activation pathway is initiated by Src non-receptor protein kinase (Src), which activates the Abelson tyrosine kinase (Abl). Src and Abl also activate PKCδ by phosphorylating the tyrosine residues in its regulatory domain (Tyr^{311}, Tyr^{332}). Abl kinase phosphorylates PKD1 at the pleckstrin homology (PH) domain (Tyr^{463}) (54). This phosphorylation leads to the removal of PKD1 autoinhibition by triggering conformational changes and releasing its catalytic domain (54,109). Src kinase phosphorylates Tyr^{95} in the PKD1 regulatory domain, and subsequently, it creates a motif that matches the consensus sequence for the binding site of the PKCδ-C2 domain (54). Following this, PKCδ phosphorylates Ser^{738} and Ser^{742} in the activation loop of PKD1, leading to PKD1 activation (104).

Consequently, PKD1 undergoes full activation. The final step in PKD1 activation is the autophosphorylation of Ser^{910} at the C-terminus. However, it remains unclear whether this step is essential for activation (56,110). The localization of PKD1 to the mitochondrial outer membrane in response to ROS is achieved by binding mitochondrial DAG to PKD1 (111). PKCδ and PKD1 have been recognized as a signaling pair in ROS-mediated signaling pathways (55). PKD1 binds to PKCδ and acts as a moderator of NF-κB-mediated response,

ultimately leading to the transcription of SOD for cellular detoxification and survival (55,112). A summary of the signaling mediated by ROS is illustrated in Figure 3.

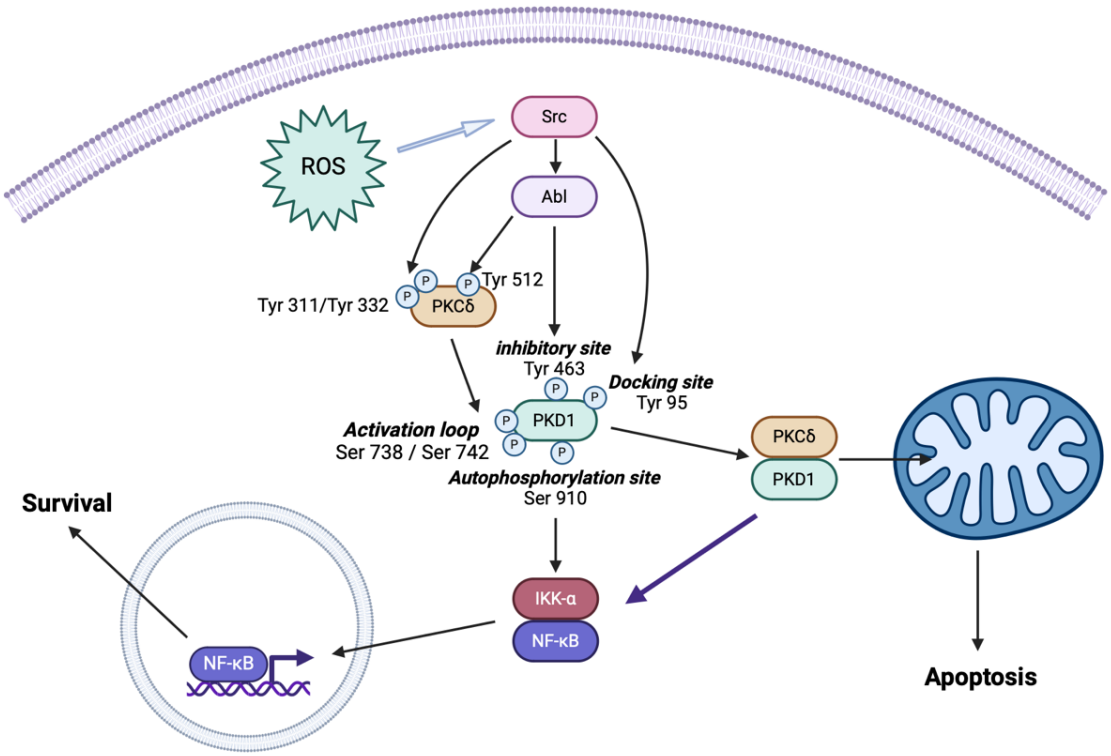
ROS
Src
Abl
Tyr 311/Tyr 332
PKCδ
Tyr 512
inhibitory site
Tyr 463
Docking site
Tyr 95
Activation loop
Ser 738 / Ser 742
PKD1
Autophosphorylation site
Ser 910
PKCδ
PKD1
Survival
IKK-α
NF-κB
NF-κB
Apoptosis

Figure 3 ROS-mediated signaling. Following oxidative stress, Src and Abl activate PKCδ. The phosphorylation of PKD1 by Src, Abl, and active PKCδ leads to the activation of PKD1. Subsequently, PKCδ and PKD1 translocate to the mitochondria, where, depending on the extent of damage, PKD1 regulates the apoptotic response through mitochondria or promotes survival by activating the NF-κB transcription factor. This process is illustrated in the image created in Biorender.com.

1.1.5. MITOCHONDRIAL-MEDIATED APOPTOSIS

Mitochondria are the main origin of ROS in cells. Superoxide produced by mitochondria is transformed into hydrogen peroxide, which is then detoxified in the cytosol (113). In response to oxidative stress, PKCδ and PKD1 translocate to the mitochondria (75). PKD1 lacks a known targeting sequence for the mitochondrial matrix, so it is likely to reside on the outer mitochondrial membrane. This localization allows for detecting mitochondrial ROS and activating protective signaling pathways to prevent damage to mitochondrial macromolecules.

When exposed to oxidative stress, mitochondrial apoptosis-induced channels form in the outer membrane of the mitochondria, releasing cytochrome C and initiating an apoptotic signaling pathway that results in cell death (114). Bcl-2-associated protein (Bax) and Bcl-2-antagonist/killer (Bak) are two pro-apoptotic B-cell lymphoma-2 (Bcl-2) family members that help this process and are involved in apoptosis caused by ROS (115). In the presence of ROS, Bax translocates to the outer mitochondrial membrane, where it regulates permeabilization by forming homomeric or heteromeric pores in combination with Bak (116). It then undergoes conformational changes, forming oligomeric pores that release cytochrome C, leading to apoptosis (116). B-cell lymphoma extra-large (Bcl-XL), another Bcl-2 family member, has a direct inhibitory interaction with Bax that prevents pore formation (117,118). Studies conducted on *PKCδ-/-* and *PKD1-/-* MEFs indicate a significant reduction in the levels of Bcl-XL protein, which may disrupt the balanced levels between Bax and Bcl-XL, ultimately leading to apoptosis (100). During oxidative stress, mitochondrial permeability transition (PT) occurs, significantly enhancing the permeability of the inner mitochondrial membrane to molecules larger than 1500 Da, including protons

and calcium ions (119). The mitochondrial permeability transition pore is the second type of mitochondrial pore, which comprises various proteins, including the voltage-dependent anion channel (VDAC), which facilitates cytochrome C release into the cytosol along with Bax (120,121).

The functions of PKCδ and PKD1 in the above process have been previously elucidated (55,112). Intrinsic apoptosis, which is initiated by the mitochondria, results in the activation of caspases. Caspases are cysteine proteases that are expressed as inactive form and known as proenzymes. Upon apoptosis, the proenzyme is cleaved to produce active caspase (121). Cytochrome C, once released from the mitochondria, binds to the C-terminus of apoptotic protease activating factor-1 (Apaf-1), inducing its open conformation and activation (122,123). The new conformation of Apaf-1 co-assembles with six other subunits to form the active apoptosome in the presence of cytochrome C and ATP (124). Cytochrome c is a critical element of the apoptosome complex and activates caspase-9 (125). Caspase-9 subsequently activates caspase-3 via its protease activity, resulting in caspase-3 activation (126). Caspase-3 has been found to have a significant role in activating apoptotic DNA fragmentation, leading to programmed cell death (127). Figure 4 illustrates the summary of mitochondrial apoptosis signal transduction.

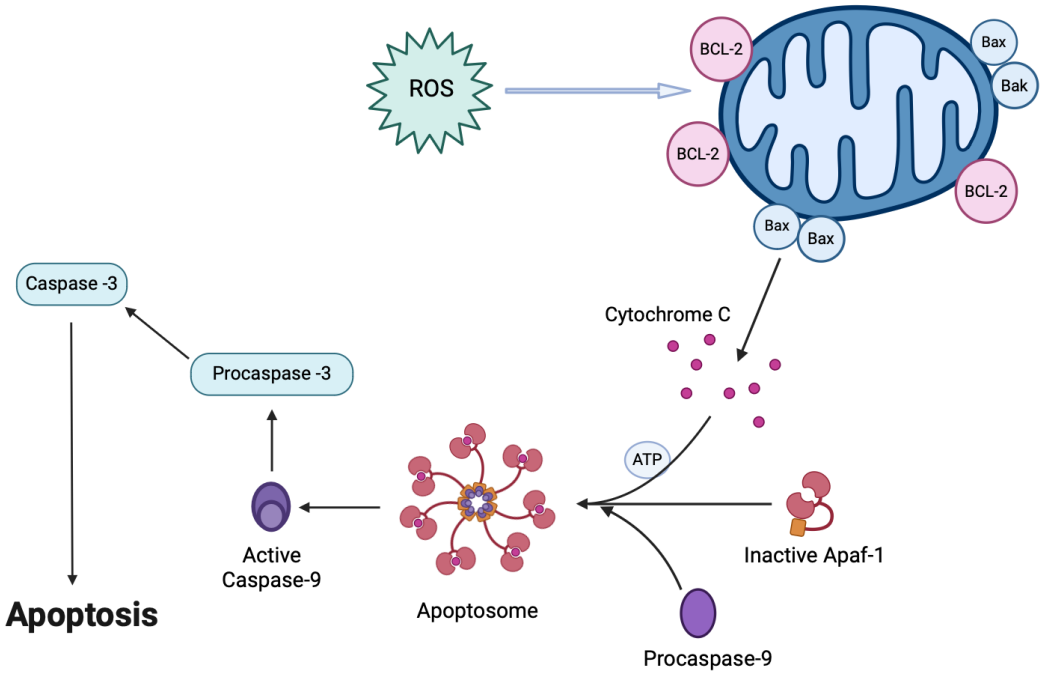
ROS
BCL-2
Bax
Bak
BCL-2
BCL-2
Bax
Bax
Cytochrome C
ATP
Caspase -3
Procaspase -3
Active
Caspase-9
Apoptosome
Inactive Apaf-1
Procaspase-9
Apoptosis

Figure 4 Mitochondria-induced apoptosis. Upon exposure to oxidative stress, the mitochondrial membrane undergoes pore formation or activation, releasing Cytochrome C and initiating a subsequent apoptotic signaling pathway that ultimately leads to cell death. This process is illustrated in the image created in Biorender.com.

1.2. PURPOSE OF STUDY

Previous studies by our group and others have shown that PKD1 has significant roles in oxidative stress and ROS-mediated signaling. Oxidative stress can activate various signaling cascades involving Src/Abl, extracellular signal-regulated kinase (ERK), and NF-κB pathways. For instance, HeLa cells treated with H_2O_2 showed that oxidative stress activates Src/Abl kinases, which subsequently phosphorylate and activate PKD. Activated PKD then induces NF-κB activation via the IKK complex, promoting cell survival under oxidative stress conditions (54). PKD1 also protects cells from oxidative damage induced by mitochondrial ROS through the NF-κB pathway (98).

This study was designed to build upon previous research that investigated mitochondrial membranes depolarization in MEFs of different genotypes (wild-type and PKD1-deficient). Previous findings indicated distinct depolarization patterns in the wild-type (WT), PKD1-deficient (*PKD1-/-)*, and PKC**δ**-deficient (*PKC**δ**-/-*) genotypes, highlighting the involvement of PKD1 and PKC**δ** in regulating mitochondrial depolarization following H_2O_2 treatment (100). The study also showed the translocation of PKD1 to the mitochondria at low ROS levels (low H_2O_2 concentration) in WT and *PKC**δ**-/-* genotypes. However, PKC**δ** was found to be required for activating PKD1 after ROS-induced translocation. Although this translocation alone cannot trigger mitochondrial depolarization at lower levels of ROS, it is a crucial factor for achieving depolarization (100).

Cumulative evidence from these experiments revealed that PKD1 plays a crucial role in regulating the mitochondrial depolarization threshold in response to increased ROS levels, ultimately resulting in cytochrome C release and subsequent apoptosis. The primary objective of this research was to identify the specific substrates and binding proteins of PKD1

in MEFs and to analyze these potential PKD1 substrates under conditions of oxidative stress, focusing on their roles in apoptotic signaling pathways. To further elucidate the molecular mechanisms underlying PKD1's protective function against oxidative stress, we performed RNA sequencing (RNA-Seq) analysis to detect differentially expressed (DE) genes and pathways between WT and *PKD1-/-* cells.

2. Materials and Methods

2.1. Cells and Cell Culture

2.1.1. Cells

WT and *PKD1-/-* MEFs were generated previously in our group using gene targeting. These cells were derived from transgenic mouse embryos between 12.5-13.5 days post coitum and were immortalized using the National Institutes of Health 3T3 cells (NIH 3T3) protocol (100). *PKD1-/-* MEFs lack approximately 8 kb of the *PKD1* gene (exons 3 and 4), resulting in a frameshift and the production of nonsense messenger RNA (mRNA) (100). The specific cell counts varied depending on the experiment, with at least three independent experiments conducted for each.

2.1.2. Cell Culture

MEFs were cultured in Dulbecco's Modified Eagle's Medium (DMEM)-high glucose (MilliporeSigma, Oakville, ON, Canada, Cat# D5796-500ML) medium supplemented with 10% fetal calf serum (FCS) (FisherScientific, Nepean, ON, Canada, Cytiva, Cat# SH3412IH345), 1X MEM Non-essential amino acids (FisherScientific, Nepean, ON, Canada, Cytiva, Cat# SH30238.01), 1% Pen Strep (FisherScientific, Nepean, ON, Canada, Gibco, 15070-063), β-mercaptoethanol (FisherScientific, Nepean, ON, Canada, Gibco, Cat# 21985023) at 37°C with 5% CO_2. Depending on the specific experiment, the cells were plated in 10 cm plastic dishes or 6/24-well dishes. MEFs were passaged once they reached 80% confluence to minimize potential stress. Non-supplemented DMEM medium was applied for stimulation and starvation experiments.

2.1.3. Cell Passage

Cell passage was carried out in cell culture dishes at 80% confluence to maintain cell viability and facilitate experimental procedures. The process involved carefully aspirating the old medium, washing the cells with cold phosphate-buffered saline (PBS) (MilliporeSigma, Oakville, ON, Canada, Dulbecco's, Cat# D8537), and adding 1X trypsin-EDTA (FisherScientific, Nepean, ON, Canada, Gibco, 0.5% Trypsin-EDTA (10X), Cat# 15400054) to the plate, which was then incubated for 5-10 minutes. After examination under the light microscope, the complete medium was added to the trypsin. The mixture was gently pipetted to obtain single cells. The cells were counted using the hemocytometer, and the desired number of cells was added to a new plate based on the experimental requirements.

2.2. Stimulation

Oxidative stress was induced by H_2O_2 (MilliporeSigma, Oakville, ON, Canada, hydrogen peroxide solution in H_2O containing a stabilizer, Cat# H1009) at varying concentrations, according to the experimental specifications. MEFs at 80% confluence (5×10^6 cells) were used for stimulation. The cells were washed once with room temperature PBS buffer, followed by the addition of the pre-warmed, non-supplemented DMEM medium and the desired concentration of H_2O_2. The cells were then incubated at 37°C for a designated period upon the experimental protocol. Once incubation was complete, the cells were promptly washed with cold PBS. The cells were detached from the well as described below or fixed depending on the experiment. Table 1 in the appendices lists the concentrations of H_2O_2 used in this study.

2.3. Western Blot

2.3.1. Protein Extraction and Subcellular Fractionation

Several protocols have been developed for protein extraction and subcellular fractionation. Ultimately, a protocol has been optimized that proved to be more efficient for our samples, which is a combination of the Mitochondrial Extraction Kit for mammalian cells (Thermo Fisher Scientific, Waltham, MA, USA, Cat# 89874) and our custom protocol for an 80% confluent 10cm dish (approximately 5×10^6 cells), outlined as follows (all steps should be done on ice). 10 ml of cold PBS was added to the washed, stimulated cells (as described in section 2.2), and the well was scraped entirely using a disposable scraper. The cells were collected in a 15 ml tube and centrifuged for 5 min at 1000rpm to pellet the cells. PBS Buffer was discarded, and the cells were resuspended in 400µl of the kit's reagent A, including a 1X protease inhibitor (Roche- EDTA free Protease inhibitor Cocktail tablets, Basel, Switzerland, Cat# 04693159001). They were transferred to a 1.5 ml microtube afterward. After 6-8 minutes of incubation on ice, sonication (Branson Digital Sonifier 450 Ultra Sonic Cell Disruptor Desintegrator, Danbury, CT, USA, Cat# Catalog Number: 101-063-596R) was done once for 10 seconds at 30% amplitude. 400µl of reagent C, including a 1X protease inhibitor, was added before centrifugation for 10 minutes at 700g at 4°C. The supernatant contained the mitochondrial and cytosolic fractions. In contrast, the pellet contained cell debris, nuclei, and intact cells. The supernatant was transferred to a new tube, and the pellet was discarded. The supernatant was centrifuged for 15 min at 12,000g at 4°C. The supernatant includes the cytosolic fraction, whereas the pellet contains the mitochondrial fraction. A volume of 50-100µl of radioimmunoprecipitation assay (RIPA) buffer (50mM Tris-Hcl, pH 7.5, 150mM NaCl, 1% Triton x-100, 1% sodium deoxycholate (NaDOC), 0.1%

sodium dodecyl sulfate (SDS), and 2mM EDTA)) was added to the mitochondrial pellet and incubated for 10 minutes on ice. The samples were quantified using the Bradford assay (MilliporeSigma, Bradford Reagent, St. Louis, MO, USA, Cat# B6916-500). After measuring the optical density (OD) of the samples using an Eppendorf spectrophotometer (Eppendorf AG, Hamburg, Germany, Cat# 2231), protein concentrations were determined using a bovine serum albumin (BSA) standard curve (Figure5). Lastly, 4X Laemmli sample buffer (1M Tris-Hcl pH 6.8, 8% SDS, 20% glycerol, 15.5 mg/ml dithiothreitol (DTT), and 0.1 mg/ml bromophenol blue) was added in a 1:4 ratio to the mitochondrial and cytosolic fractions, followed by 5 minutes of boiling at 95°C.

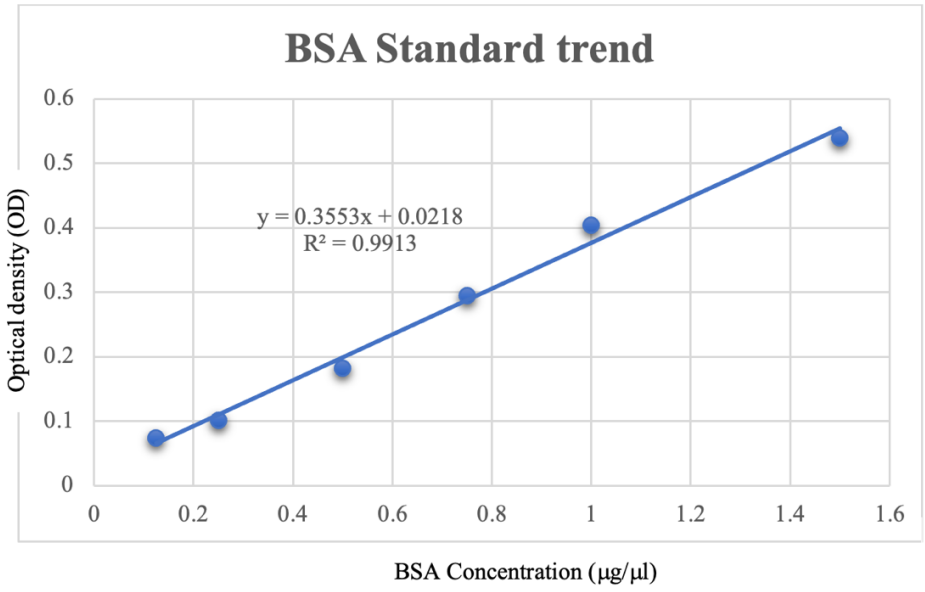

FIGURE 5. BOVINE SERUM ALBUMIN (BSA) STANDARD TREND.

2.3.2. SDS-PAGE

Sodium dodecyl sulfate-polyacrylamide gel electrophoresis (SDS-PAGE) is a widely used method for resolving proteins in a protein mixture with high resolution (128). Separating the proteins through SDS-PAGE is necessary to ensure successful protein detection in western blotting. Protein samples obtained from subcellular fractionation were then loaded into the 12% polyacrylamide gel, and electrophoresis was conducted for 90 min at 110 V to facilitate separation.

2.3.3. WESTERN BLOT

Western blotting is a common laboratory technique to detect and quantify specific proteins in samples. This method involves the separation of proteins based on their molecular weights through SDS-PAGE. Once the SDS-PAGE was done, the separated proteins were transferred from the gel to the nitrocellulose membranes. This was achieved through a process known as tank transfer, which involved blotting the gel onto the membrane for 45 min at 4°C using a tank transfer unit (Hoefer Mighty Small transfer unit) at 400 mA. After transfer, the membrane was washed quickly with 1X PBS buffer. Ponceau S staining was used to observe the protein bands. The membrane was rewashed with 1X PBS buffer for 5-10 minutes at room temperature. Next, it was blocked with 5% skim milk for one hour. The specific antibody was then added to the membrane and incubated overnight at 4°C at a specified dilution ratio. This investigation utilized various antibodies to detect subcellular fractionation and cytochrome C localization. To ensure the accuracy of the extraction, western blotting was performed on Mitochondrial and Cytosolic fractions using anti- voltage-dependent anion channels (VDAC) (Rabbit monoclonal, Cell Signaling Technology, Danvers, MA, USA, Cat# 4661), anti- Prohibitin 1 (PHB1) (Rabbit monoclonal, Cell Signaling Technology,

Danvers, MA, USA, Cat# 2426) specific primary antibodies (1:1000 dilution), and anti-rabbit- Human Prohibitin (HPRO) (Rabbit polyclonal, Invitrogen, Carlsbad, CA, USA, Cat#701629RP488) secondary antibodies (1:5000 dilution) according to the manufacturer's instructions. Anti-cytochrome C (Cyto C) antibody (Rabbit monoclonal, Cell Signaling Technology, Danvers, MA, USA, Cat# 4272) (1:500 dilution) was used and detected using Horseradish peroxidase (HRP)-conjugated rabbit secondary antibody. Anti-Glyceraldehyde-3-phosphate dehydrogenase (GAPDH) (14c10) (Rabbit monoclonal, HRP conjugate, Cell Signaling Technology, Danvers, MA, USA, Cat# 3683) (1:1000 dilution) served as the loading control.

Following the overnight incubation with the specific primary antibody, the membrane was washed three times with 1X PBS buffer for 10-15 minutes each. The secondary antibody was then added and incubated for two hours at room temperature. Finally, the membrane was rewashed three times with 1X PBS buffer for 10-15 minutes.

2.3.4 Imaging

SuperSignal™ West Pico Plus Chemiluminescent Substrates Kit (Thermo Fisher Scientific, Waltham, MA, USA, Cat# 34580) was added to the washed membrane at a 1:1 ratio, followed by a one-minute incubation at room temperature. This was followed by visualizing the membrane using the Analytic Jena UVP Chem Studio Plus imaging machine following the manufacturer's instructions. The resulting signal confirmed the presence of a target protein.

2.4. TUNEL Assay

Cells undergoing apoptosis exhibit alterations in their nuclear structure, including DNA fragmentation. The TUNEL assay was performed throughout the later stages of apoptosis

using the TUNEL in Situ Apoptosis Kit (HRP-DAB method) (Elabscience, Houston, TX, USA, Cat# E-CK-A351) according to the manufacturer's instructions. During this procedure, the exposed 3'-OH of damaged DNA was identified by attaching biotin-labeled Deoxy uridine triphosphate (dUTP) using the Terminal Deoxynucleotidyl Transferase (TdT) enzyme. Antibodies targeting biotin-labeled dUTP were employed as an indirect detection approach. Combining HRP-labeled streptavidin (streptavidin-HRP) and biotin can visualize apoptotic cells. The reaction with peroxide substrate, 3,3'-diaminobenzidine (DAB), produced a dark brown signal under the light microscope. The WT and *PKD1-/-* cells were treated with different hydrogen peroxide concentrations to induce oxidative stress-induced apoptosis. At least three distinct experiments were conducted for both WT and *PKD1-/-* genotypes. Following cell enumeration, statistical analysis was performed using standard deviation.

2.4.1. Stimulation, Fixation, And Permeabilization

Each well of a 24-well plate was plated with 0.2% gelatine-coated coverslips and seeded with 1×10^5 cells the day before the experiment. The cells were stimulated via incubation with hydrogen peroxide (H_2O_2) at 250µM and 500µM concentrations for 25 min at 37°C, as specified in section 2.2. The positive controls were prepared in accordance with the TUNEL Kit protocol, and unstimulated cells were utilized as negative controls.

After stimulation, the cells were washed gently three times with PBS and fixed on coverslips using 4% Paraformaldehyde (MilliporeSigma, Oakville, ON, Canada, Cat# 30525894) for 10-15 minutes at room temperature. The cells were washed for 5 min in PBS buffer. Next, the cells were blocked with 3% H_2O_2 for 10 min at room temperature and rewashed three times with PBS buffer for 5 min each. To permeabilize the cells, they were incubated with

0.2% Triton X-100 (Thermo Fisher Scientific, Waltham, MA, USA, Cat# BP151-100) for 10 minutes at 37°C. Finally, the cells were washed three times with PBS buffer for 5 min each and were ready for labeling.

2.4.3. Labeling & Developing

Labeling for stimulated, negative, and positive samples was performed according to the TUNEL assay kit protocol. Haematoxylin staining was done as a counterstain in the final step. The coverslips were then fixed on glass slides with a Leica Micromount mounting medium after dehydration using 100% ethanol and xylene. Light microscopy was used to visualize the fixed labeled cells for detecting apoptotic cells and imaging.

2.5. Starvation Experiment

Each well of a 24-well plate was prepared using 0.2% gelatine-coated coverslips and seeded with 1×10^5 cells the day before the experiment. To induce starvation, the cells were incubated in a non-supplemented DMEM medium for up to four days at 37°C. After the designated time points (0, 24, 48, 72, and 96 h), fixation with 4% paraformaldehyde was performed according to the procedure outlined in Section 2.4.1. The cells were then permeabilized with 0.1% Triton X-100 for 10 minutes and stained with trypan blue for 1-2 minutes, then washed with PBS before imaging. The fixed cells were counted at each time point to determine the cell death rate of MEFs and compare the WT and PKD1-/- genotypes. At each time point, a minimum of ten images were captured for each well. Table 2 in the appendices represents the original cell counts (#) and normalized cell counts (Norm.) for WT and *PKD1-/-* MEFs during 96-hour starvation experiments. The cell counts have been normalized [$Normalized\ cell\ count = \frac{\text{cell count}\times100}{\text{Initial cell count}}$] to ensure accurate representation in the graph.

2.6. Proliferation Assay

Each well of a 24-well plate was equipped with 0.2% gelatin-coated coverslips and seeded with 5×10^3 cells one day in advance. These cells were incubated for four days in DMEM with 10% FBS at 37°C to assess their proliferation rate. Following the procedures outlined in sections 2.4.1 and 2.5, fixation, permeabilization, and Trypan blue staining were performed. A minimum of 10 images were captured for each well at every time point, and the cells were counted to evaluate the growth rate and compare the WT and *PKD1-/-* genotypes. The proliferation assay was also performed using the hemocytometer for cell enumeration.

2.7. RNA-Seq Analysis

RNA-seq analysis was conducted on primary and immortalized WT and *PKD1-/-* mouse embryonic fibroblasts. This investigation aimed to identify differentially expressed genes (DEGs) between two genotypes, which were validated through subsequent data analysis. All experiments were conducted with at least two different clones for each genotype, and data are presented as standard deviation unless otherwise stated.

2.7.1. Cells & Cell Culture

Primary WT and *PKD1-/-* MEFs were isolated previously from transgenic mouse embryos in our group following the procedures outlined in section 2.1.1. A modified NIH 3T3 protocol was used for our primary MEFs immortalization. Primary MEFs were plated on 10 cm dishes for the first two passages. They were transferred to 6-well dishes and cultured for 5-6 passages using 10% FBS DMEM until they reached senescence. Once the cells were no longer proliferating, the medium was switched to 20% FBS DMEM, and the culture medium was changed every three days. The development of spontaneously immortalized cells,

observable as individual colonies, resulted from prolonged cell culture. These cells then went on to form immortalized MEF cell lines. Passages were subsequently performed at a 1:1 or 1:2 ratio until immortalized clones were identified.

2.7.2. RNA Extraction

When the cells reached 80-90% confluence in a 10 cm plate (1×10^6 cells), they were harvested for total RNA extraction and subsequent RNA analysis using the AllPrep DNA/RNA Mini Kit (Qiagen, Hilden, Germany, Cat# 80204), following the manufacturer's instructions. The concentration and purity of the extracted RNA were determined using a NanoDrop 1000 spectrophotometer (Thermo Fisher Scientific). Samples with A260/A280 ratios between 1.5 and 2.5 were considered for further analysis. RNA integrity was assessed by gel electrophoresis on a 1% agarose gel.

2.7.3. Sequencing & Data Analysis

High-quality RNA derived from both primary and immortalized cells of WT and *PKD1-/-* genotypes were utilized for RNA sequencing using the Illumina NovaSeq 6000 PE100 at the Centre d'expertise et de services Génome Québec in Montreal, QC, Canada. The resulting paired-end reads (an average length of 100bp for each read) were examined for base quality using the FASTQC (fast quality control) tool (version 0.12.0) (https://www.bioinformatics.babraham.ac.uk/projects/fastqc/). Subsequently, the reads were mapped to the mouse reference genome (mm10) utilizing the STAR (spliced transcripts alignment to a reference) tool (version 2.7.10a) (129) under default settings. SAM (sequence alignment/map) files were transformed into BAM (Binary alignment/map) format by applying Samtools (version 1.18) (130). Using FeatureCounts (version 2.0.6), reads

specifically aligned to annotated genes in the Ensemble *Mus musculus* GRCm 38.102.gtf for subsequent downstream differential expression analysis (131). The analysis of gene expression differences between WT and *PKD1-/-* genotypes was performed using the Bioconductor DESeq2 package (version 1.41.13) in R software (version 4.3.2 https://www.r-project.org/) (132). The R codes for the RNA-Seq analysis are presented in the appendices. Genes exhibiting a statistically significant 2-fold change (log2(FC)>1) with an adjusted p-value < 0.05 were deemed differentially expressed. The DESeq2 package (version 1.41.13) (132) was used to compute the adjusted p-value. To explore the biological processes and pathways linked to these DEGs, Gene Ontology (GO) and pathway analyses were conducted (133). These analyses were performed using the Kyoto Encyclopedia of Genes and Genomes (KEGG) database (134) via the Gene Set Analysis Toolkit WebGestalt 2019 online tool and clusterProfiler (version 4.10) (135).

RNA-Seq analysis was conducted using both R software and the Galaxy platform. The Galaxy analysis involved uploading the RNA-Seq data to the platform and utilizing tools such as FastQC (Galaxy version 0.74) for quality control (https://www.bioinformatics.babraham.ac.uk/projects/fastqc/), HISAT2 (Hierarchical indexing for spliced transcript alignment 2) (Galaxy version 2.2.1) for alignment (136), FeatureCounts (Galaxy Version 2.0.3) for gene quantification (131), and DESeq2 (differential expression analysis based on the negative binomial distribution, version2) (Galaxy Version 2.11.40.8) for differential expression analysis (132). The results were visualized and exported for further interpretation and comparison with the R-based analysis.

2.8. Statistical Analysis

All statistical analyses for the proliferation, starvation, and TUNEL assays were performed using Microsoft Excel 365 (Microsoft Corporation, Redmond, WA, USA). Two-way analysis of variance (ANOVA) with replication was employed to assess the effects of genotype (WT and *PKD1-/-*) and the second factor, such as starvation time (0, 24, 48, 72, and 96 hours), on cell viability/numbers, as well as any potential interaction between these factors. Following the detection of statistically significant interactions or main effects in the ANOVA, Tukey's post-hoc test was conducted to perform multiple pairwise comparisons between groups to identify significant differences. The threshold for statistical significance was set at $p < 0.05$ for all comparisons. Data are expressed as the mean ± standard error of the mean (SEM) from three independent experiments. Data were graphically represented using Microsoft Excel 365 and Minitab 21.1 software to visualize the analysis outcomes.

3. Results

3.1. Analysis of PKD1 Translocation Upon H_2O_2 Treatment

3.1.1. Identification of a Suitable Subcellular Fractionation Protocol

To identify proteins acting downstream of PKD1 in ROS-mediated signaling, it was imperative to demonstrate cytochrome C translocation from the mitochondria to the cytosol before undertaking proteomics analysis. Ensuring our samples' high quality of mitochondrial and cytosolic fractions through subcellular fractionation was crucial. These fractions were used to indicate the translocation of cytochrome C from mitochondria to cytosol as a marker for the intermediate stage of mitochondrial-induced apoptosis. Seven distinct protocols were evaluated to achieve this objective by assessing their effectiveness. Subsequently, three protocols were selected for further optimization and testing, prioritizing those better aligned with our laboratory facilities and the limited amount of cellular material available for experimentation.

Subcellular fractionation was conducted on WT and *PKD1-/-* cell pellets to obtain mitochondrial and cytosolic fractions. The extraction procedure was established using the Mitochondrial Extraction Kit for mammalian cells (Thermo Fisher Scientific, 89874) and our custom protocol for MEFs (approximately 5×10^6 cells), as outlined in section 2.3.1. To evaluate the efficacy of our fractionation protocol, we performed Western blotting to validate the mitochondrial and cytosolic fractions. We prioritized qualitative validation over quantitative analysis to effectively distinguish the mitochondrial fraction from the cytosolic fraction (Figure 6). As shown in Figure 6A, in the top row, the anti-VDAC antibody identifies

the VDAC protein, which represents a specific marker for the mitochondrial outer membrane and thus determines the mitochondrial fraction (137). In addition, the PHB1 protein was used as a second marker for the mitochondrial fraction in the third row (138). The VDAC positive fractions were also positive for PHB1, underlining that the purified fraction contains mitochondria. Figure 6B compares the scraping and trypsinization techniques utilized for cell detachment using anti-VDAC antibodies. No significant difference was observed regarding fractionation; consequently, the scraping method was selected due to its reduced cellular stress compared to trypsinization.

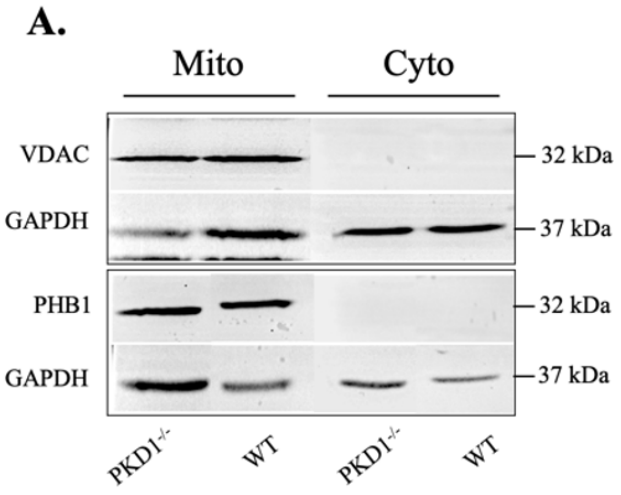
A.
Mito
Cyto
VDAC
GAPDH
PHB1
GAPDH
32 kDa
37 kDa
32 kDa
37 kDa
PKD1-/-
WT
PKD1-/-
WT

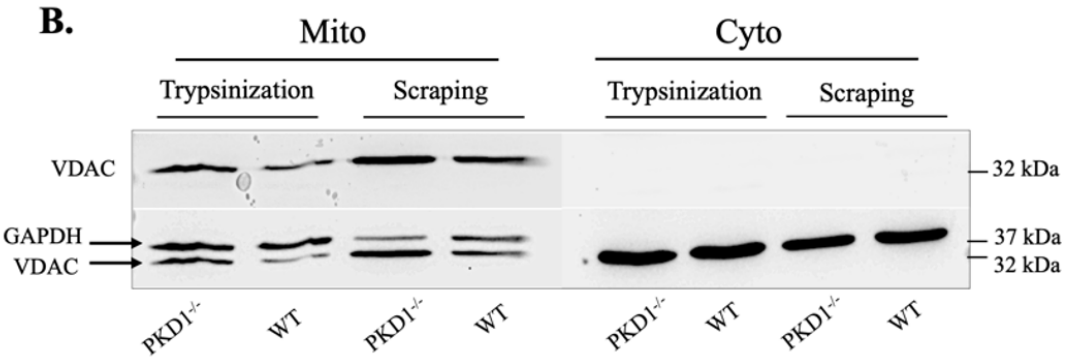
B.
Mito
Cyto
Trypsinization
Scraping
Trypsinization
Scraping
VDAC
GAPDH
VDAC
32 kDa
37 kDa
32 kDa
PKD1-/-
WT
PKD1-/-
WT
PKD1-/-
WT
PKD1-/-
WT

Figure 6 Western blot analysis of mitochondrial (Mito) and cytosolic (Cyto) fractions from WT and PKD1-/- protein extracts. **A.** Subcellular fractionation validation: The specificity of mitochondrial fractions was confirmed using antibodies against VDAC and PHB1 (1:1000 dilution). 20-25 µg protein per lane was loaded. Anti-GAPDH (anti-Glyceraldehyde-3-phosphate dehydrogenase) served as the loading control. **B.** Comparison of scraping and trypsinization methods: Fractionation was assessed in MEFs detached by trypsinization or scraping. Anti-VDAC antibody (1:1000 dilution) applied as indicated. Anti-GAPDH served as the loading control. 25-30 µg protein per lane was loaded. Shown are representative blots of at least three independent experiments.

3.1.2. Analysis of Cytochrome C Translocation in WT and *PKD1-/-* MEFs Upon ROS-Mediated Apoptosis

The original intention of this study was to identify PKD1's specific substrates and/or binding proteins in the mitochondrial outer membrane upon ROS-mediated apoptosis. To achieve this, H_2O_2-induced PKD1 mitochondrial translocation and subsequent induced apoptosis were intended to serve as a stimulus. Our lab previously showed (100) that PKD1 translocated at low H_2O_2 concentrations (25μM) to the outer mitochondrial membrane without any signs of mitochondrial depolarization, while its deficiency led to mitochondrial depolarization at these concentrations. Moreover, they demonstrated that in the WT genotype, cytochrome C is transferred from the mitochondrial fraction to the cytosolic after being stimulated with 50μM H_2O_2. In *PKD1-/-* cells, the threshold for this transfer is lower, and this occurs following stimulation with 25μM H_2O_2.

As one early indicator of induced apoptosis, the release of cytochrome C from the mitochondria to the cytosol is established as a marker (139). We conducted several experiments to identify the correct window and stimulation conditions since a precisely defined protein fraction for the subsequent planned proteomics analysis was a prerequisite for success. Unlike the previous data from our lab (100), the present investigation reveals that the patterns of cytochrome C translocation after H_2O_2 stimulation vary across different experiments with the *PKD1-/-* genotype and show inconsistency, as illustrated in Figures 7 and 8. Due to the inconsistency of our Western blotting analysis, we were unable to conduct at least three independent experiments with consistent outcomes. As a result, reliable quantification was not possible. The images provided are representative and highlight the qualitative aspect of these experiments.

Figure 7 demonstrates the stimulation of WT MEFs under different concentrations of hydrogen peroxide. In Figure 7A, WT MEFs were subjected to stimulation with 500μM, 5 mM, and 50 mM H_2O_2 for five- and ten-minute incubation periods. Cytochrome C was detected in both mitochondrial and cytosolic fractions in unstimulated and 500μM H_2O_2-treated samples. The Cytochrome C signal weakened at 5 mM H_2O_2, and no signal was observed at 50 mM H_2O_2, likely due to the excessively high concentration. Lower concentrations with extended incubation times were investigated in Figure 7B. WT cells were stimulated using 50, 250, and 500 μM hydrogen peroxide for 15min. In unstimulated cells, cytochrome C was found in the mitochondrial fraction and began translocating to the cytosol at 50μM H_2O_2, with increased cytochrome C signal observed after 250μM H_2O_2 stimulation. In contrast, as demonstrated in Figure 7C, stimulation of WT cells with 500μM H_2O_2 resulted in the translocation of cytochrome C to the cytosol after 15 min of incubation. In Figure 7D, WT MEFs were stimulated with 50μM H_2O_2 for 15 and 30 minutes, showed a complete translocation of cytochrome C from mitochondria to the cytosol and a decrease in cytosolic fraction after 30 min incubation. Cytochrome C was present in the cytosolic fraction of both unstimulated and stimulated cells with 25μM H_2O_2.

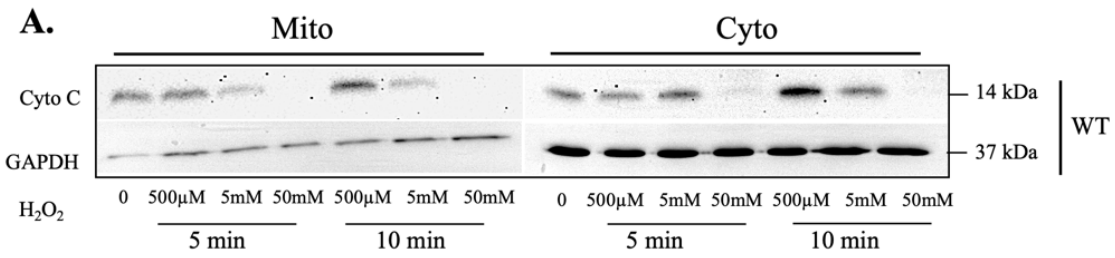
A.
Mito
Cyto
Cyto C
GAPDH
14 kDa
37 kDa
WT
H2O2
0 500μM 5mM 50mM 500μM 5mM 50mM
0 500μM 5mM 50mM 500μM 5mM 50mM
5 min
10 min
5 min
10 min

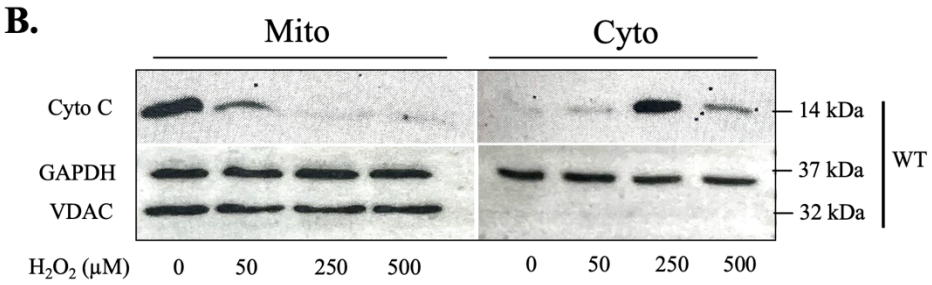
B.
Mito
Cyto
Cyto C
GAPDH
VDAC
14 kDa
37 kDa
32 kDa
WT
H2O2 (μM)
0 50 250 500
0 50 250 500

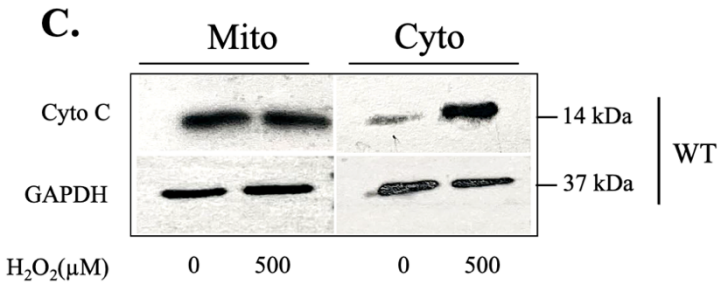
C.
Mito
Cyto
Cyto C
GAPDH
14 kDa
37 kDa
WT
H2O2(μM)
0 500
0 500

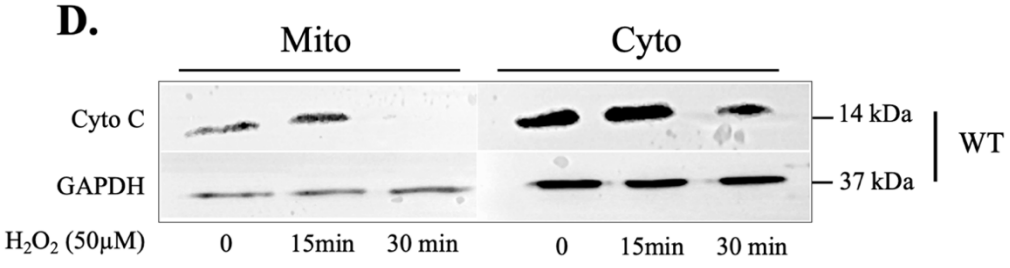
D.
Mito
Cyto
Cyto C
GAPDH
14 kDa
37 kDa
WT
H2O2 (50μM)
0 15min 30 min
0 15min 30 min

Figure 7 H_2O_2 stimulation of WT MEFs. **A.** Western blot analysis of WT MEFs following 5- and 10-min stimulation with 500 μM, 5 mM, and 50 mM. Cytochrome C localization was detected using anti-Cyto C in the top panel, with anti-GAPDH in the bottom panel as a loading control. **B.** Western blot analysis of WT MEFs after 15-min stimulation with different H_2O_2 concentrations. Probed with anti-Cyto C, anti-VDAC, and anti-GAPDH antibodies. **C.** Western blot analysis of WT MEFs after 15-min incubation with 500 μM H_2O_2. Anti-Cyto C and anti-GAPDH antibodies were utilized. **D.** Western blot analysis of WT MEFs following 15- and 30-min incubation with 50 μM H_2O_2. Blots were probed with anti-Cyto C and anti-GAPDH antibodies. A minimum of three replicates were performed for each experiment.

The experiments described in Figure 8 compare the cytochrome C translocation patterns between WT and *PKD1-/-* MEFs under various H_2O_2 concentrations. Figure 8A represents WT and *PKD1-/-* genotypes stimulation with 0, 25, and 50μM H_2O_2 concentrations for 15min. No cytochrome C translocation was observed in the WT MEFs following 50μM H_2O_2 stimulation. In contrast, cytochrome C translocated to the cytosol in *PKD1-/-* cells after incubation with 25μM H_2O_2 in accordance with the earlier study from our group (100). In contrast, the translocation of cytochrome C was observed to occur in the WT genotype following stimulation with 25 and 50μM of H_2O_2, as shown in Figure 8B, while there is no change in cytochrome C localization in *PKD1-/-* MEFs. Cytochrome C relocation from the mitochondrial fraction was observed in *PKD1-/-* cells (Figure 8C) after 15 minutes of stimulation with 25 μM H_2O_2. However, it is present in both fractions of unstimulated cells. In WT cells, cytochrome C translocated to the cytosol after 50 μM H_2O_2 stimulation as expected.

Western blotting experiments using different clone and sub-clone variants with different stimulation conditions revealed a high degree of inconsistency in the oxidative stress response of both WT *PKD1-/-* MEFs. Consequently, these samples were not qualified for subsequent proteomics analysis and identification of PKD1 substrates and/or binding proteins in ROS-induced apoptosis.

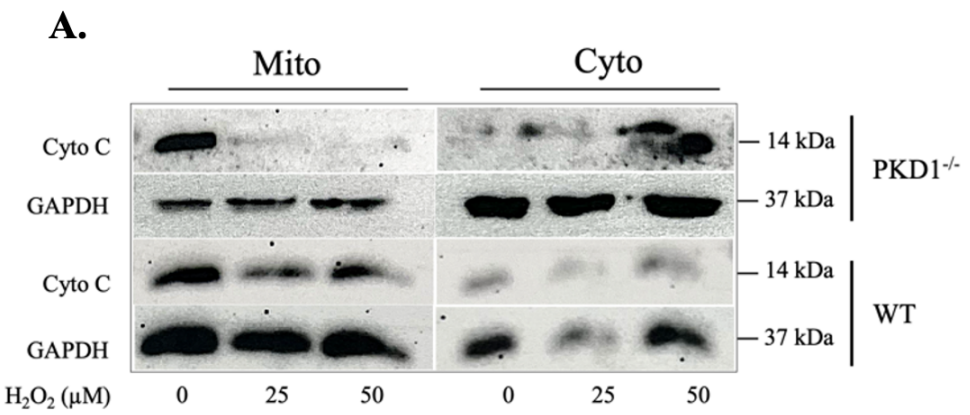
A.
Mito
Cyto
Cyto C
GAPDH
14 kDa
37 kDa
PKD1-/-
Cyto C
GAPDH
14 kDa
37 kDa
WT
H2O2 (μM)
0
25
50
0
25
50

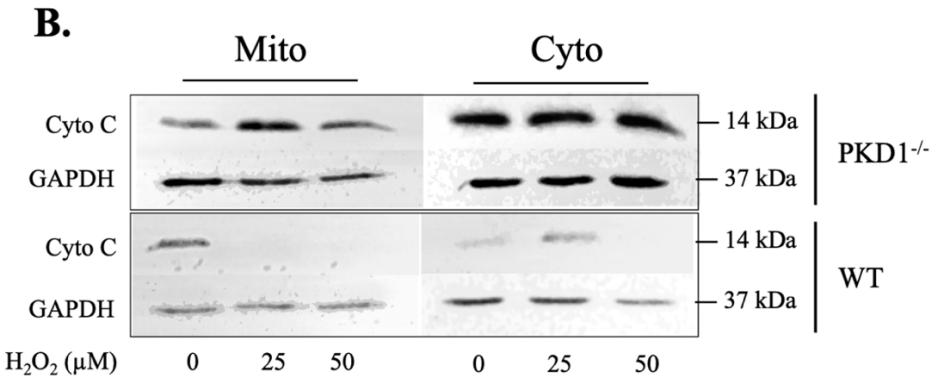
B.
Mito
Cyto
Cyto C
GAPDH
14 kDa
37 kDa
PKD1-/-
Cyto C
GAPDH
14 kDa
37 kDa
WT
H2O2 (μM)
0
25
50
0
25
50

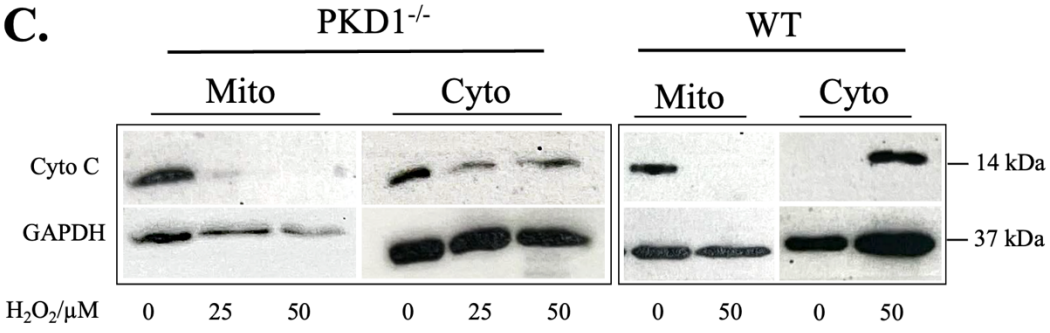
C.
PKD1-/-
WT
Mito
Cyto
Mito
Cyto
Cyto C
GAPDH
14 kDa
37 kDa
H2O2/μM
0
25
50
0
25
50
0
50
0
50

Figure 8 H_2O_2 stimulation of WT and PKD1-/-MEFs. **A, B.** Western blot analysis of WT and *PKD1-/-* MEFs stimulated with 25 μM and 50 μM $H_2O_2$for 15 minutes, probed with anti-Cyto C and anti-GAPDH antibodies. **C.** Western blot analysis of WT and *PKD1-/-* MEFs. *PKD1-/-* cells were treated with 25 μM and 50 μM H_2O_2, while WT cells were stimulated with 50 μM H_2O_2 for 15 minutes. Cytochrome C localization was assessed with anti-Cyto C, and anti-GAPDH was the loading control. Equal protein loading (30 μg per lane) was confirmed for all experiments. At least three independent experiments were done for each experiment.

3.1.3. Analysis of Cytochrome C translocation in Various Mammalian Cell Lines

Considering the inconsistency of cytochrome C release from the mitochondria following H_2O_2 stimulation in WT and *PKD1-/-* MEFs, further experiments were employed applying different mammalian cell lines (HeLa, Chinese hamster ovary (CHO), and human embryonic kidney (HEK-293)) to verify whether the issue was specific to the MEFs in a hydrogen peroxide stimulation. Figure 9 illustrates the western blotting analysis, detecting cytochrome C translocation in these cell lines. HeLa cells exhibited a mild decrease in Cyto C localization in the cytosolic fraction after stimulation with 25 µM H_2O_2 but not with 50 µM H_2O_2 stimulation, while Cyto C was detected in all other samples, including the cytosol of unstimulated cells. HeLa cells did not respond as anticipated following oxidative stress induction. This observation was consistent across the different cell lines examined.

Overall, similar to the MEFs, HeLa, CHO, and HEK-293 cell lines demonstrated inconsistency in cytochrome C translocation in response to stimulation with different H_2O_2 concentrations. Complete translocation of cytochrome C was not observed in any cell lines, while it was present in all unstimulated cytosolic fractions, which may be due to the stress conditions prior to stimulation. Consequently, we lacked a minimum of three independent experiments showing consistent results to perform quantitative analysis. The examples shown in Figure 9 serve to demonstrate the qualitative aspects of these experimental studies.

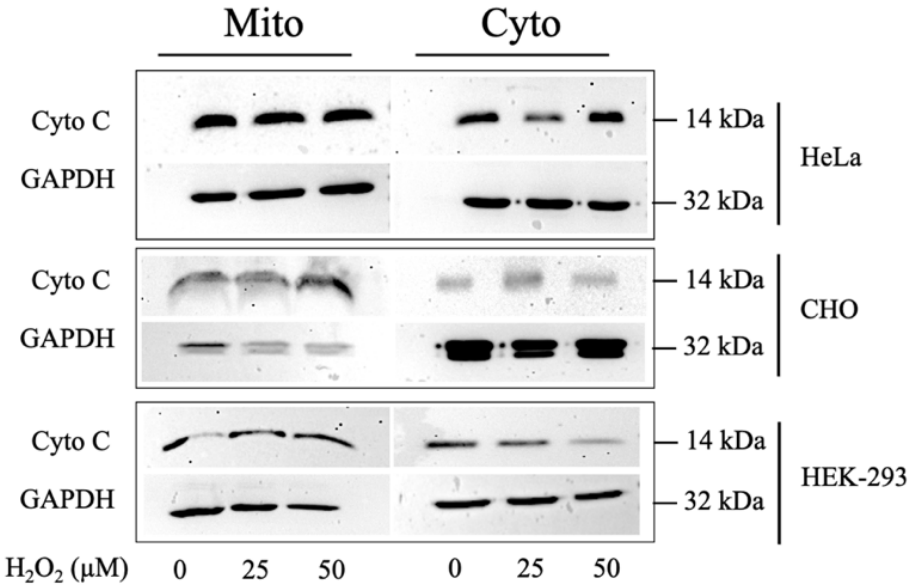
Mito
Cyto
Cyto C
GAPDH
14 kDa
32 kDa
HeLa
Cyto C
GAPDH
14 kDa
32 kDa
CHO
Cyto C
GAPDH
14 kDa
32 kDa
HEK-293
H2O2 (μM) 0 25 50 0 25 50

Figure 9 Detection of Cytochrome C Translocation upon H_2O_2 Stimulation in HeLa, HEK-293, and CHO Cell Lines. Western blotting analysis of HeLa, CHO, and HEK-293 cell lines after stimulation with 25μM-H_2O_2 and 50μM-H_2O_2 for 15 minutes. 30 μg protein was loaded per lane. Blots were probed against Cyto C and GAPDH as loading control. A minimum of three independent experiments were performed for each experiment.

3.2. Proliferation Analysis of WT and *PKD1-/-* MEFs

We conducted the proliferation assay over four days to identify the growth difference between the two genotypes (as illustrated in Figure 10). Figure 10B shows the growth rate differences between WT and *PKD1-/-* MEFs, with Day 0 representing the seeding day. After Day 2, WT cells exhibited a slightly higher increase in cell count than *PKD1-/-* cells. This trend became more pronounced by Day 3, with WT MEFs displaying significantly greater growth, which continued to rise through Day 4. Both cell types showed increased proliferation over time, but WT MEFs demonstrated a more dramatic increase, especially on day 4. In contrast, *PKD1-/-* cells showed a more gradual increase, with a less pronounced difference between later days. Two-way ANOVA with replication with the follow-up TUKEY's analysis revealed significant effects of the time (p-value<0.001), genotype (WT vs. *PKD1-/-*) (p-value<0.001), and interaction between time and genotype (p-value<0.001) in the proliferation assay.

A.

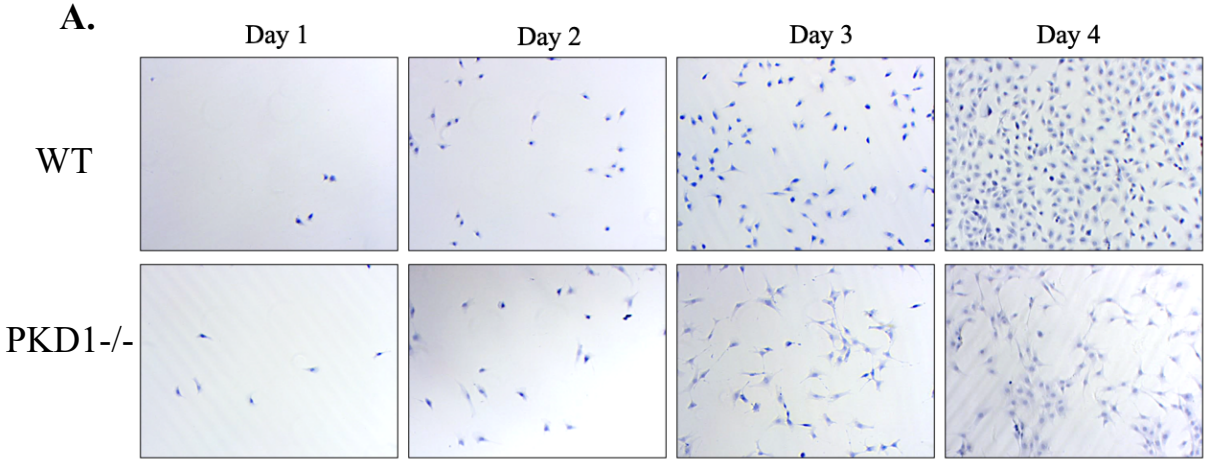
Day 1
Day 2
Day 3
Day 4
WT
PKD1-/-

B.

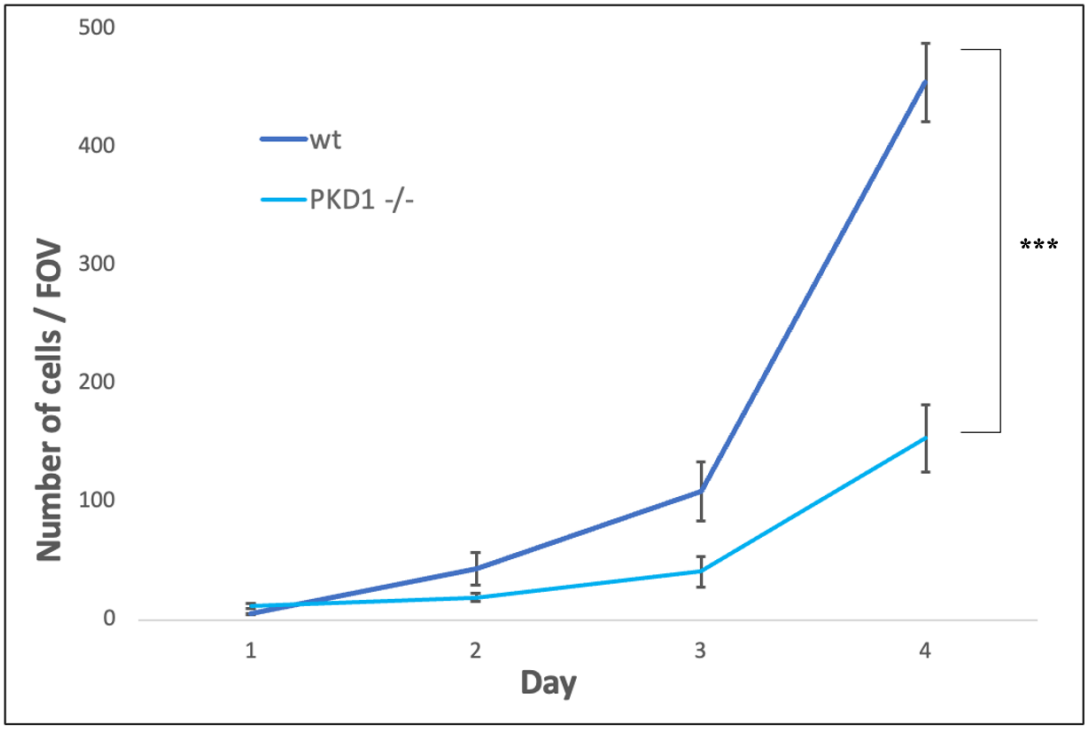
500
400
300
200
100
0
Number of cells / FOV
wt
PKD1 -/-
***
1
2
3
4
Day

Figure 10 Comparison of Cell Proliferation in WT and PKD1-/-MEFs. **A.** The Figure represents the WT and *PKD1-/-* genotypes cell proliferation over four days. **B.** The line graph demonstrates the proliferation comparison of WT and *PKD1-/-* MEFs during four days as the number of cells per FOV (Field of View). n=3. Bars indicate standard errors of the mean. *** p-value< 0.001.

3.3. STARVATION OF WT AND *PKD1-/-* MEFS

Given the fact that the performed H_2O_2 stimulations were not able to provide conclusive results in terms of PKD1's function during the threshold regulation of mitochondrial depolarization, we aimed to examine whether the MEFs used in our lab may have undergone characteristic changes during culturing. Thus, as an alternative approach to investigate the *PKD1-/-* phenotype in that context, we chose starvation as a natural source of ROS. Starvation results in an apoptotic response due to increased oxidative stress. Nutrient deprivation, particularly serum starvation, triggers increasing ROS concentrations within cells, thereby creating an oxidative stress environment (140,141).

As illustrated in Figure 11, the starvation of WT and *PKD1-/-* MEFs revealed that following 24 hours, the *PKD1-/-* genotype showed a significantly reduced cell count compared to the WT. This decrease in cell numbers continued throughout the duration of the experiment, which lasted 96 hours, while WT MEFs continued to proliferate within the first 24 hours after serum withdrawal, as evidenced by the increase in cell counts. This increase in cell numbers could be due to the differential cell growth between WT and *PKD1-/-* MEFs, as demonstrated by the proliferation analysis. However, WT cells subsequently experienced a slight decrease in cell count until 72 hours, after which the cell numbers reached a plateau. This phenomenon contrasts with *PKD1-/-* MEFs, which continuously lose cells in the counts. The cell numbers for each day are documented in Table 2 in the appendices. From seeding to the starvation start point (time 0), both genotypes adhered to the well and initiated proliferation; however, WT cells started cell growth earlier and at a higher rate, continuing to proliferate for the first 24 hours after starvation.

Two-way ANOVA analysis with replication, followed by TUKEY's analysis, showed that the starvation time significantly affects the measured variable (p-value<0.05), particularly after 72 hours of starvation. In addition, the genotype effect is highly significant (p-value<0.0001), with the *PKD1-/-* genotype consistently showing lower values than WT across all the time points. While the interaction between time and genotype is not statistically significant (p-value>0.05), there is a trend suggesting that *PKD1-/-* may be more sensitive to starvation. This is evidenced by a larger decrease over time in *PKD1-/-* MEFs compared to WT.

A

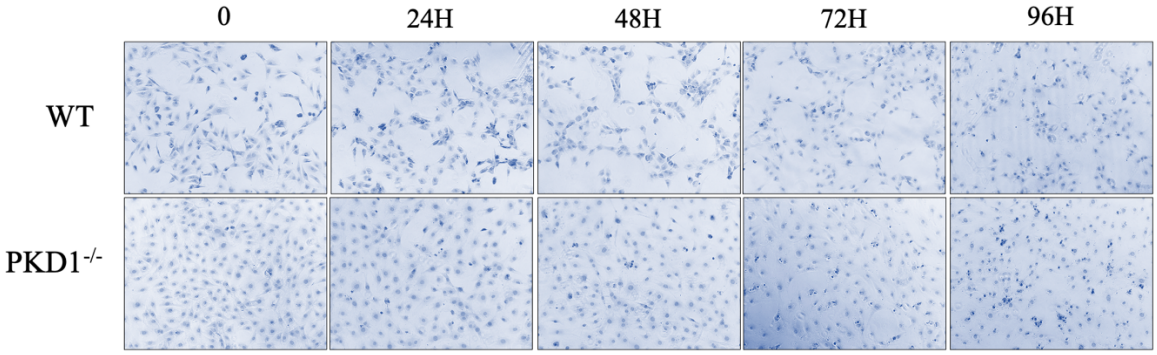
0
24H
48H
72H
96H
WT
PKD1-/-

B

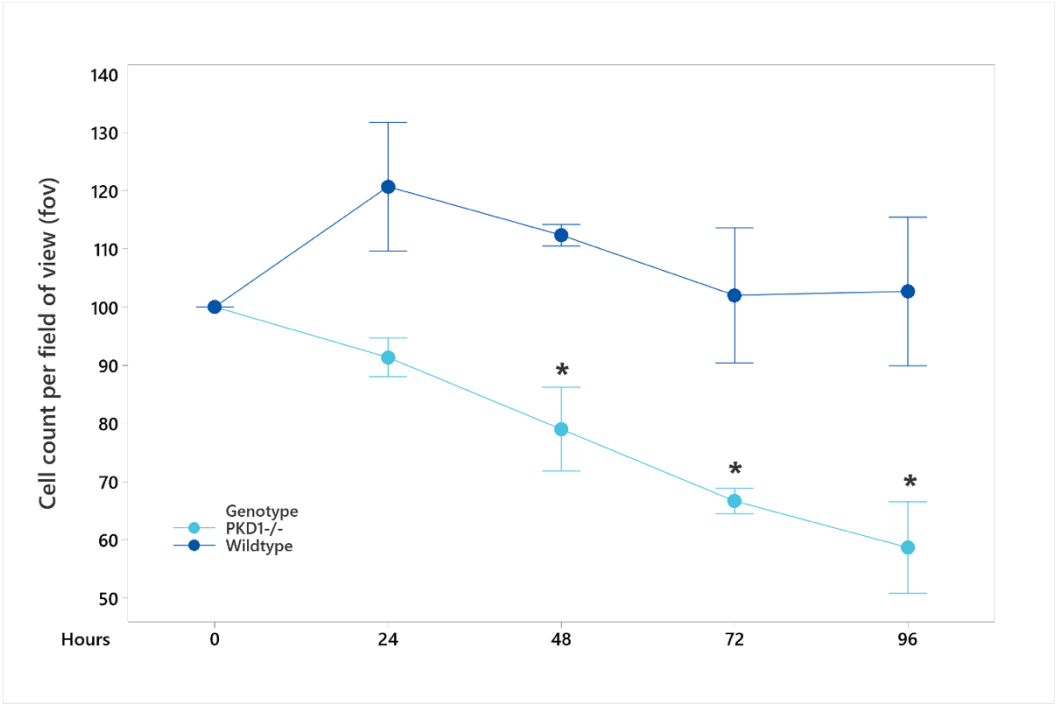
Cell count per field of view (fov)
140
130
120
110
100
90
80
70
60
50
Hours
0
24
48
72
96
Genotype
PKD1-/-
Wildtype
*
*
*

Figure 11 Survival of WT and PKD1-/- MEFs after starvation. **A.** Starvation experiment demonstrates differences in apoptosis between both genotypes. Images present magnification of 100X. **B.** Statistical analysis of WT and *PKD1-/-* cell numbers during four days of starvation as the number of cells per FOV (Field of View). n=3. Bars represent standard errors of the mean. ***p-value<0.0001.

3.4. TUNEL Assay Analysis Comparing Oxidative Stress-Induced Apoptosis in WT and *PKD1-/-* MEFs

Starvation results indicated that *PKD1-/-* MEFs appear to be more susceptible to starvation-induced oxidative stress than the corresponding WT. Based on these findings, we went back to H_2O_2 stimulations to investigate whether an increased apoptotic response could be observed in *PKD1-/-* MEFs. We employed various concentrations and incubation times to determine the conditions under which DNA fragmentation could be detected through TUNEL assay. The optimal conditions for proceeding were confirmed to be 250 and 500μM H_2O_2 for 25 minutes.

As shown in Figure 12, unstimulated MEFs, irrespective of the genotype, do not show any sign of apoptosis above the background. At 0μM H_2O_2, there is no significant difference between WT and *PKD1-/-* MEFs regarding cell death. The results from the two-way ANOVA analysis and multiple comparisons using TUKEY's analysis indicated a statistically significant difference between WT and *PKD1-/-* MEFs at both concentrations of 250 and 500μM H_2O_2 (p-value<0.001), with *PKD1-/-* cells showing a significantly higher percentage of apoptotic cells in comparison to the WT cells at these concentrations. The effect of H_2O_2 concentration was also significant (p-value<0.05). While there is no significant difference in cell death between WT cells at different H_2O_2 concentrations, the susceptibility to apoptosis in *PKD1-/-* cells increases significantly compared to the WT genotype as the concentration of hydrogen peroxide increases.

Cell counts for WT and *PKD1-/-* MEFs are illustrated in Table 3 in the appendices. Comparison between 250 μM H_2O_2 and 500 μM H_2O_2 stimulation revealed a reduction in

cell death for both WT and *PKD1-/-* cells after 500 μM H_2O_2 stimulation. This phenomenon is likely due to the higher concentration of H_2O_2, which induces a decrease in cell adhesion to the wells and results in the loss of dead cells during the stages of the TUNEL assay protocol.

A.

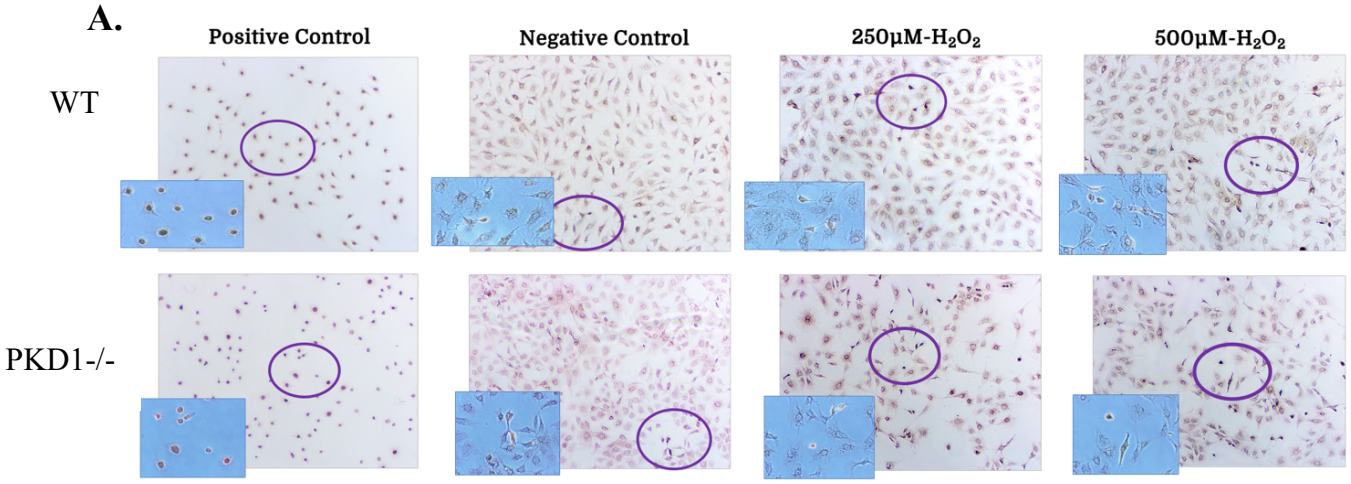
Positive Control
Negative Control
250μM-H_2O_2
500μM-H_2O_2
WT
PKD1-/-

B.

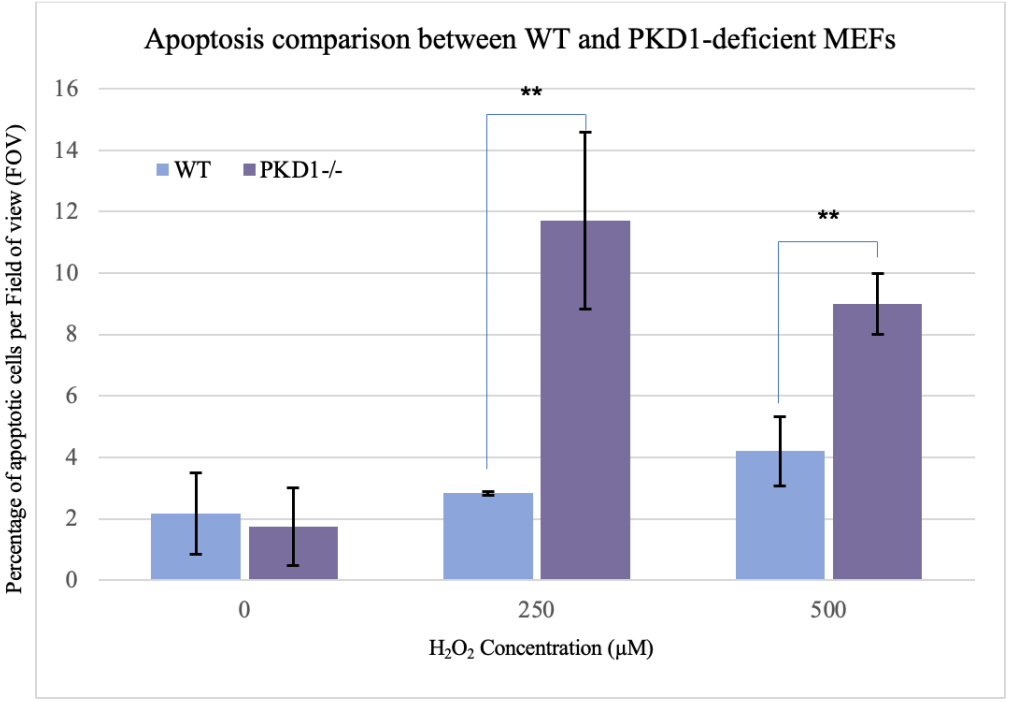
Apoptosis comparison between WT and PKD1-deficient MEFs
Percentage of apoptotic cells per Field of view (FOV)
16
14
12
10
8
6
4
2
0
WT
PKD1-/-
**
**
0
250
500
H_2O_2 Concentration (μM)

Figure 12 TUNEL assay of H2O2 induced WT and PKD1-/- MEFs. **A.** TUNEL assay demonstrates differences in apoptosis between both genotypes. Images present magnifications of 100X and 400X. **B.** Bar graph compares the percentage of apoptotic cells per field of view (FOV) between the WT and *PKD1-/-* MEFs after H_2O_2-stimulation. n=3. Error bars represent the standard errors of the mean (SEM). **p-value<0.01)

3.5. RNA-Seq Analysis of WT and *PKD1-/-* MEFs

3.5.1. Overview Of RNA-Seq Data

RNA-Seq analysis was conducted on WT and *PKD1-/-* MEFs to elucidate the genes and pathways that are differentially expressed and potentially contribute to ROS-induced apoptosis between these genotypes. This approach aimed to provide a more comprehensive understanding of the molecular mechanisms underlying PKD1's protective function.

The RNA-Seq analysis was performed as previously described (Section 2.7). The RNA-Seq experiment generated high-quality sequencing data from WT and *PKD1-/-* MEFs using the Illumina NovaSeq 6000 PE100. The data set included three WT and two *PKD1-/-* clones, with both primary and immortalized MEFs represented. Quality control was conducted using FASTQC (Galaxy version 0.74) (https://www.bioinformatics.babraham.ac.uk/projects/fastqc/), revealing an average mean sequence quality (Phred score) of 36, indicating high sequencing accuracy. The reads were aligned to the mm10 (Mus-Musculus.GRCm38) using the HISAT2 tool (Galaxy version 2.2.1) (136), with an average alignment of 80%. Gene-level quantification was performed using FeatureCounts (Galaxy Version 2.0.3) (131), resulting in BAM file outputs. The high alignment rate and quality scores across all samples confirm the reliability of the sequencing data for subsequent differential gene expression and pathway analyses.

3.5.2. Principal Component Analysis

As a first step in the analysis of the obtained RNA-Seq data set, a principal component analysis (PCA) was carried out using DESeq2 (Galaxy version 2.11.40) (132) to visualize global expression profiles and evaluate variability between WT and *PKD1-/-* MEFs. The

PCA plot shown in Figure 13 displays the distribution of samples defined by PC1, the most significant source of variation in gene expression levels among samples, and PC2, the second largest source of variation. In this study, differences in PC1 are primarily associated with the genotypic variation (WT / *PKD1-/-*) as the primary factor influencing gene expression, while PC2 is associated mainly with variation due to cell clones, which serves as an additional factor in gene expression. Each point represents a sample, and distances between points reflect similarities or differences in overall data patterns. Figure 13A plot reveals a significant difference of 92% between primary WT and *PKD1-/-* MEFs, indicating a considerable variance in transcriptomic profiles between the two genotypes. Additionally, a 6% variance among *PKD1-/-* clones suggests an acceptable degree of heterogeneity. This level of variation within this genotype indicates that the samples show a relative consistency and highlights the existence of some biological or technical variability. The PCA plot for immortalized cells shown in Figure 13B illustrates a 44% variance between WT and *PKD1-/-* genotypes, indicating a relatively significant difference between these two groups. Furthermore, a 22% variance among *PKD1-/-* clones suggests a moderate degree of variability within the *PKD1-/-* clones. This higher variability observed in the immortalized *PKD1-/-* clones shows more difference in their transcriptomic profile, possibly due to increased biological variance or technical factors associated with the immortalization process.

A. Primary PKD1-/- Vs. WT

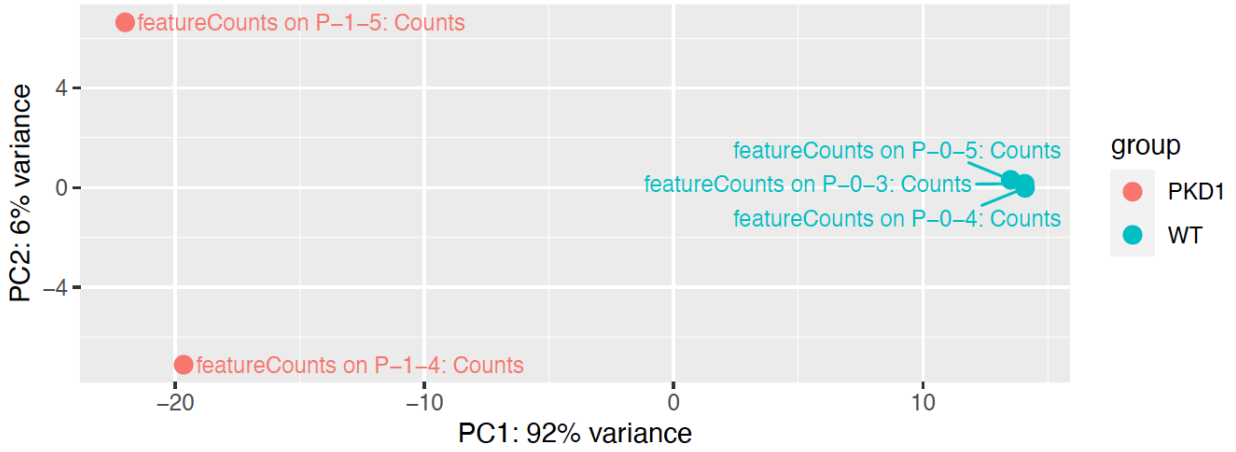

B. Immortalized PKD1-/- Vs. WT

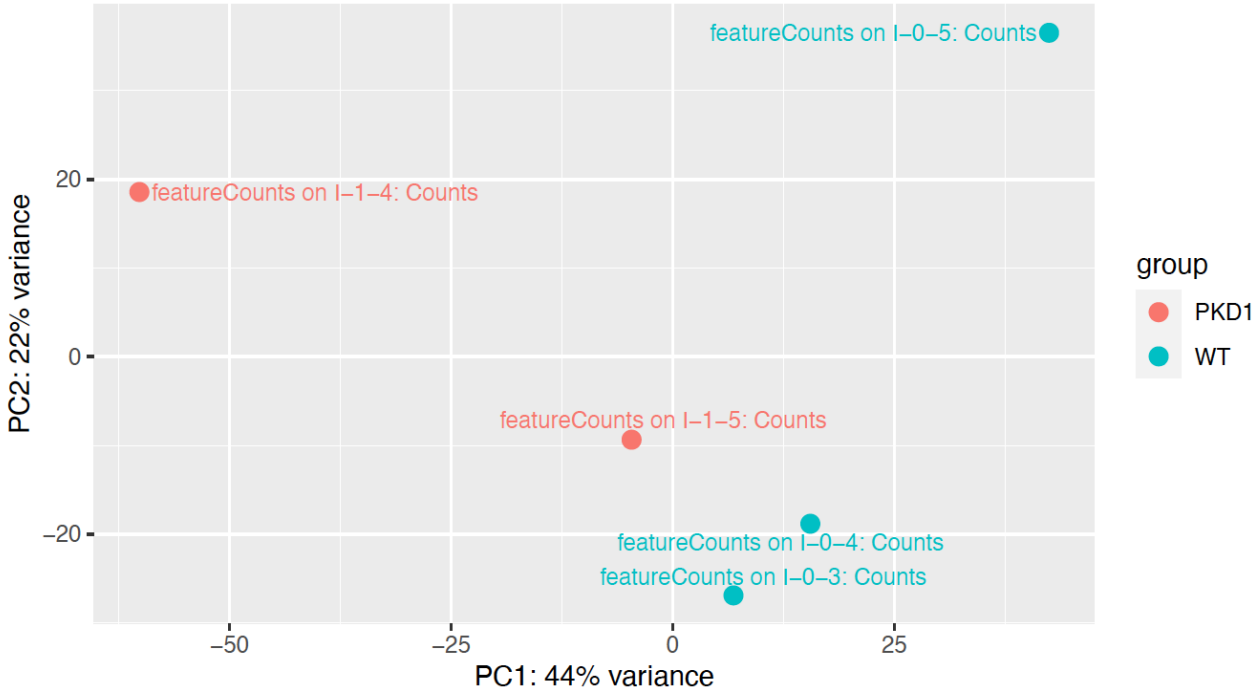

Figure 13 Principal Component Analysis (PCA) of WT and PKD1-/- MEFs. PCA plots illustrate the variability of transcriptomic profiles between WT and *PKD1-/-* MEFs. **A.** PCA plot for primary cells: PC1 reveals a 92% variance between WT and *PKD1-/-* genotypes, while PC2 highlights a 6% heterogeneity between *PKD1-/-* clones. **B.** PCA plot for immortalized cells: PC1 differentiates WT and *PKD1-/-* MEFs (44% variation), and PC2 reflects a 22% variance was identified between *PKD1-/-* clones.

3.5.3. Differential Expression Analysis of WT and *PKD1-/-* Mouse Embryonic Fibroblasts

To investigate the impact of PKD1 deficiency on gene expression, we performed differential expression analysis between WT and *PKD1-/-* MEFs. This analysis aimed to detect genes that show significant changes in expression levels due to PKD1 deficiency, which could provide insights into the molecular mechanisms responsible for its protective function.

Differential expression analysis was conducted on read counts from WT and *PKD1-/-* MEFs using DESeq2 (Bioconductor DESeq2 package (version 1.41.13) in R software) (132). Genes with an adjusted p-value < 0.05 and log2 fold change greater than 1 (log2 (FC) >1) were deemed significantly differentially expressed, revealing a substantial impact of PKD1 deficiency on gene expression.

The analysis resulted in a high number of DEGs in primary and immortalized between WT and *PKD1-/-* genotypes (383 DEGs in primary and 1705 DEGs in immortalized MEFs). The volcano plots in Figure 14 illustrate the distribution of DEGs in WT and *PKD1-/-* primary and immortalized MEFs. The x-axis represents the log2 fold change (log2FC) in gene expression between WT and *PKD1-/-* genotypes, while the y-axis illustrates the negative logarithm (base 10) of the p-value (-log10 p-value), indicating the statistical significance of the difference in gene expression. Each dot on the plot shows a DE gene, with down-regulated genes in blue and up-regulated genes in red. Genes located in the upper-right or upper-left quadrants of the plot are considered significantly differentially expressed.

The volcano plot for primary MEFs (Figure 14A) shows fewer DE genes compared to immortalized cells (Figure 14B), but there is still a significant difference between WT and

PKD1-/- genotypes. The increased number of DEGs in the immortalized cells may be associated with the immortalization process. As illustrated in Figure 14A, the volcano plot demonstrates a dramatically higher number of differentially down-regulated genes compared to up-regulated genes in primary MEFs. We identified 350 down-regulated genes (shown in blue), with genes such as *Tlr13*, *Cx3cr1*, and *Cd68* exhibiting the most significant changes, in contrast to 32 up-regulated genes (shown in red), including *Rpl34*, *Pbp2*, and *Hspa8*. The volcano plot of immortalized MEFs (Figure 14B) reveals a higher number of down-regulated genes compared to up-regulated genes. Specifically, 997 down-regulated genes, including *Ece2*, *Usp13*, and *Uggt2*, were identified, along with 707 up-regulated genes, such as *Rpl34* and *Hoxa13*. Complete lists of all primary and immortalized down and up-regulated genes are presented in Tables 4 and 5 in appendices.

A.

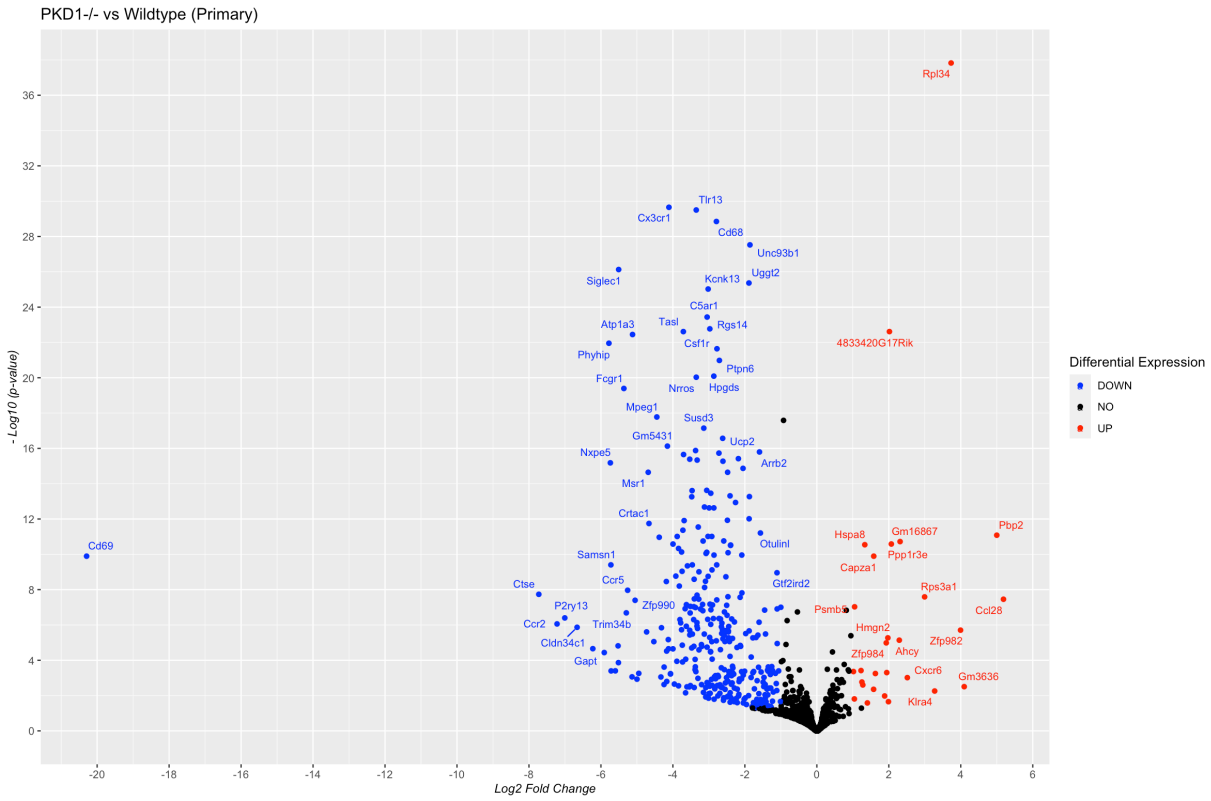
PKD1-/- vs Wildtype (Primary)
- Log10 (p-value)
Log2 Fold Change
Differential Expression
DOWN
NO
UP
Rpl34
Tlr13
Cx3cr1
Cd68
Unc93b1
Siglec1
Kcnk13
Uggt2
C5ar1
Atp1a3
Tasl
Rgs14
4833420G17Rik
Csf1r
Phyhip
Ptpn6
Fcgr1
Nrros
Hpgds
Mpeg1
Susd3
Gm5431
Ucp2
Nxpe5
Arrb2
Msr1
Crtac1
Cd69
Otulinl
Hspa8
Gm16867
Pbp2
Ppp1r3e
Capza1
Samsn1
Ccr5
Gtf2ird2
Rps3a1
Ctse
P2ry13
Zfp990
Psmb8
Ccl28
Ccr2
Trim34b
Hmgn2
Cldn34c1
Zfp982
Ahcy
Gapt
Zfp984
Cxcr6
Gm3636
Klra4

B.

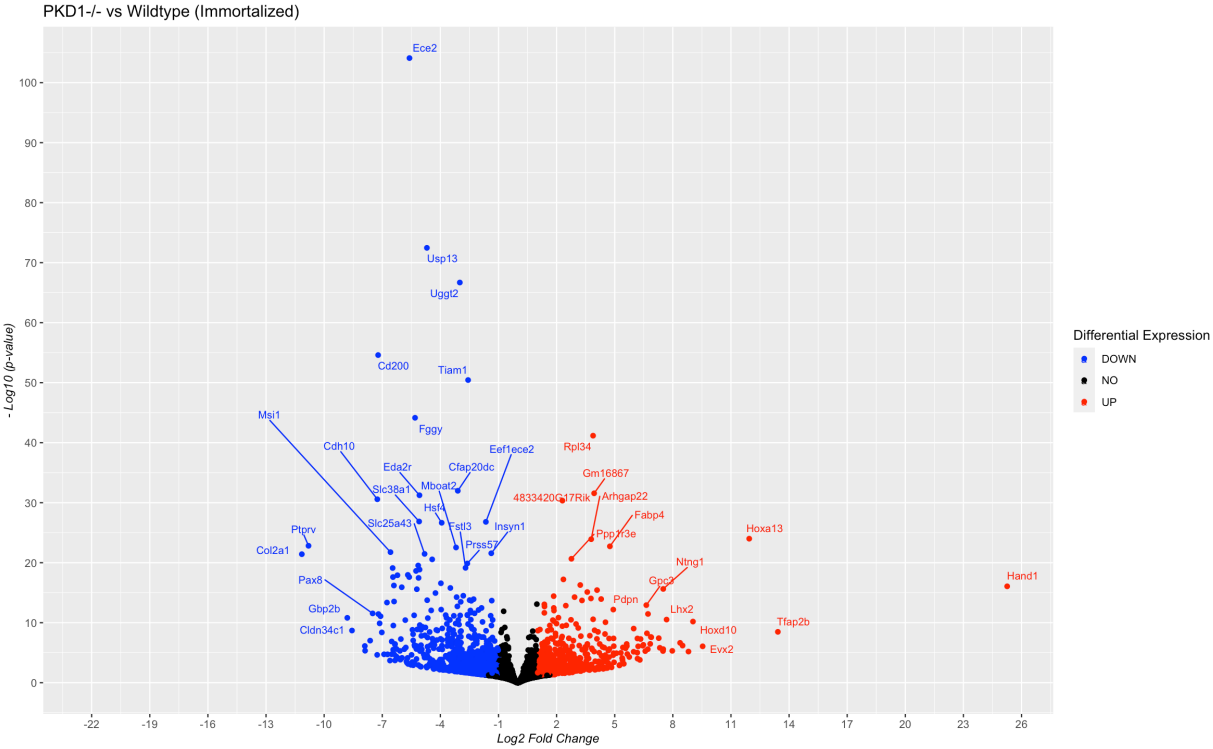
PKD1-/- vs Wildtype (Immortalized)
- Log10 (p-value)
Log2 Fold Change
Differential Expression
DOWN
NO
UP
Ece2
Usp13
Uggt2
Cd200
Tiam1
Msi1
Fggy
Cdh10
Eef1ece2
Rpl34
Eda2r
Cfap20dc
Gm16867
Slc38a1
Mboat2
4833420G17Rik
Arhgap22
Hsf4
Fabp4
Slc25a43
Fstl3
Insyn1
Ppp1r3e
Hoxa13
Ptprv
Prss57
Col2a1
Ntng1
Hand1
Pax8
Gpc3
Pdpn
Gbp2b
Lhx2
Tfap2b
Cldn34c1
Hoxd10
Evx2

Figure 14 Volcano plots of differentially expressed (DE) genes in primary and immortalized WT and PKD1-/- mouse embryonic fibroblasts. **A.** Volcano plot displaying DE genes in primary MEFs, highlighting significant up-regulation and down-regulation between WT and *PKD1-/-* genotypes. **B.** Volcano plot illustrating DE genes in immortalized MEFs, showing the differences in gene expression profiles between WT and *PKD1-/-* MEFs.

3.5.3. Pathway and Gene Ontology Analysis of WT and *PKD1-/-* Mouse Embryonic Fibroblasts

Pathway enrichment analysis was performed using R software and the ShinyGo (version 0.77) (142–144) platform to gain insights into the biological processes and pathways associated with the identified DEGs. R analysis was performed using the Kyoto Encyclopedia of Genes and Genomes (KEGG) (134) database and found 1658 down-regulated and 927 up-regulated pathways in immortalized MEFs (adjusted p-value < 0.05). In contrast, it demonstrated 945 down-regulated pathways in primary cells (adjusted p-value < 0.05), including pathways associated with apoptosis and cell survival. The most significantly enriched KEGG pathways are illustrated in Figure 15. Each bar represents a distinct pathway, and the size of each bar corresponds to the number of genes in that pathway, where the color intensity represents the enrichment significance. Figure 15 shows several enriched pathways, such as those associated with cancer, differentiation, angiogenesis, and cell cycle, were identified. Interestingly, several enriched proliferation pathways are differentially expressed in both primary and immortalized MEFs, validating our observation regarding the growth rate difference between our WT and *PKD1-/-* MEFs.

However, our primary purpose was to investigate pathways linked to apoptosis. Pathways related to apoptosis and their corresponding genes, resulting from the enriched pathway analysis conducted using R software, are presented in Tables 6A and 6B in appendices. Table 6A specifically focuses on pathways involved in apoptosis and cell survival in primary MEFs, while Table 6B shows DE genes in immortalized MEFs. All enriched pathways have adjusted p-values of less than 0.05, indicating statistical significance.

A. Immortalized, Down-regulation

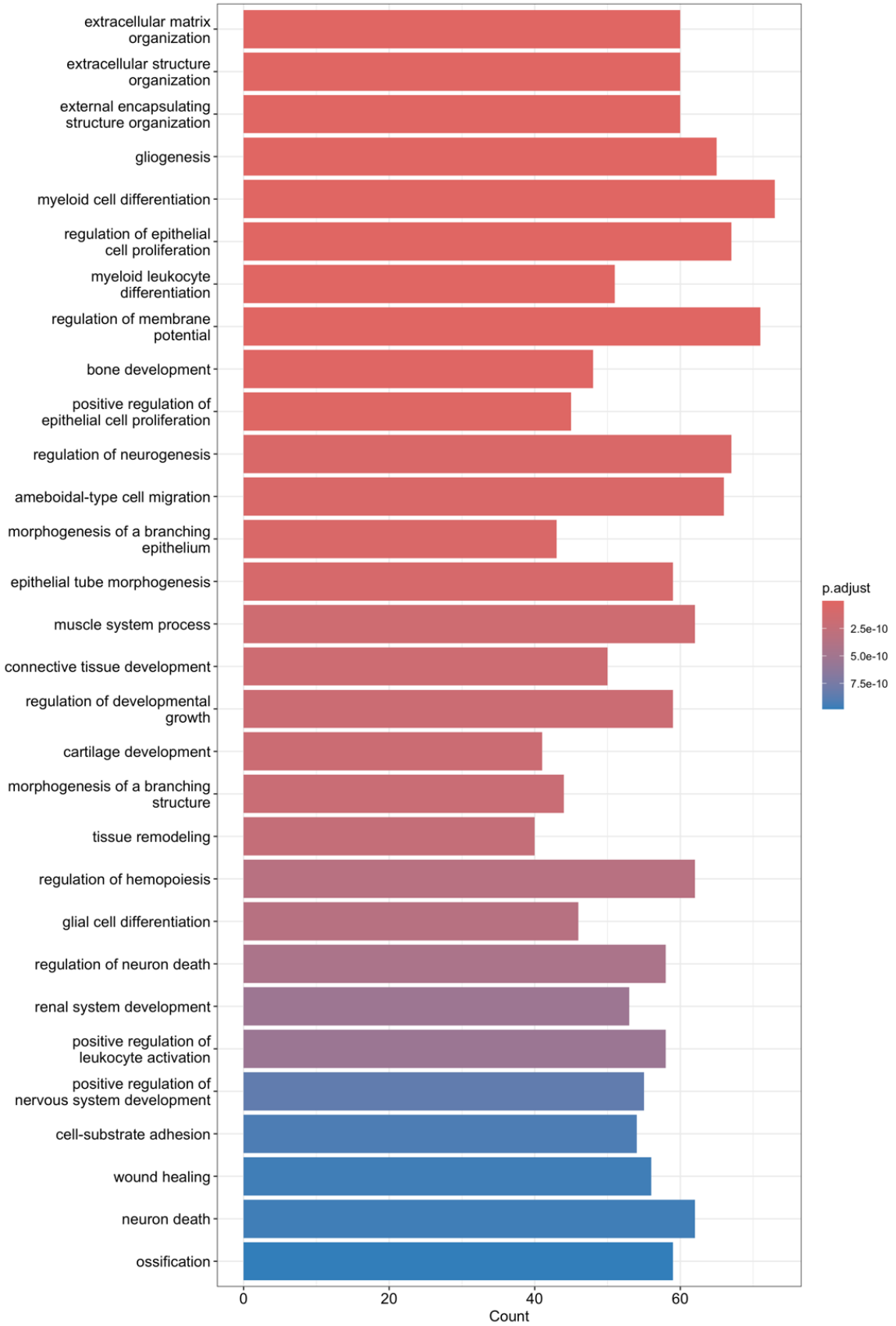

B. Immortalized, Up-regulation

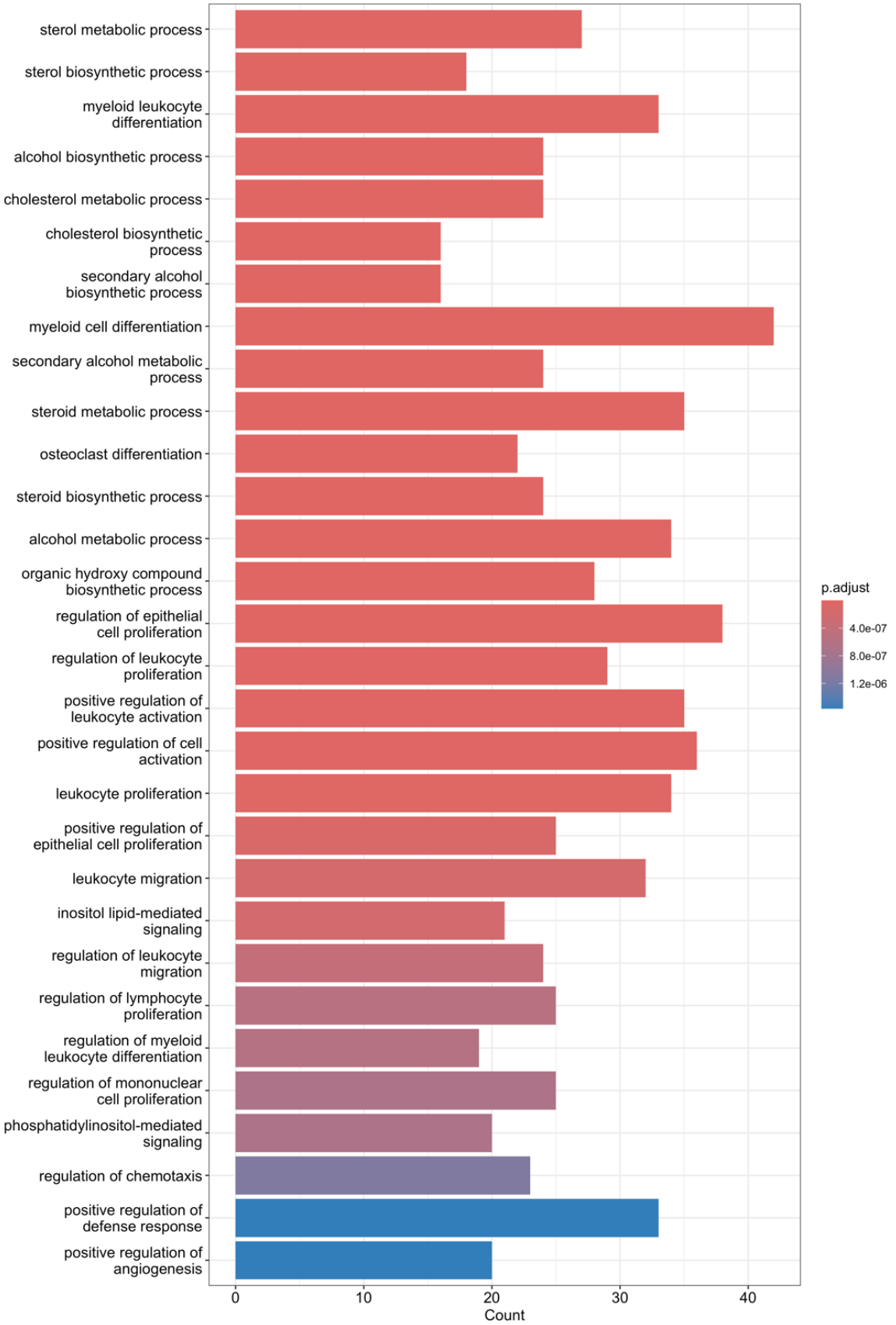

C. Primary, Down-regulation

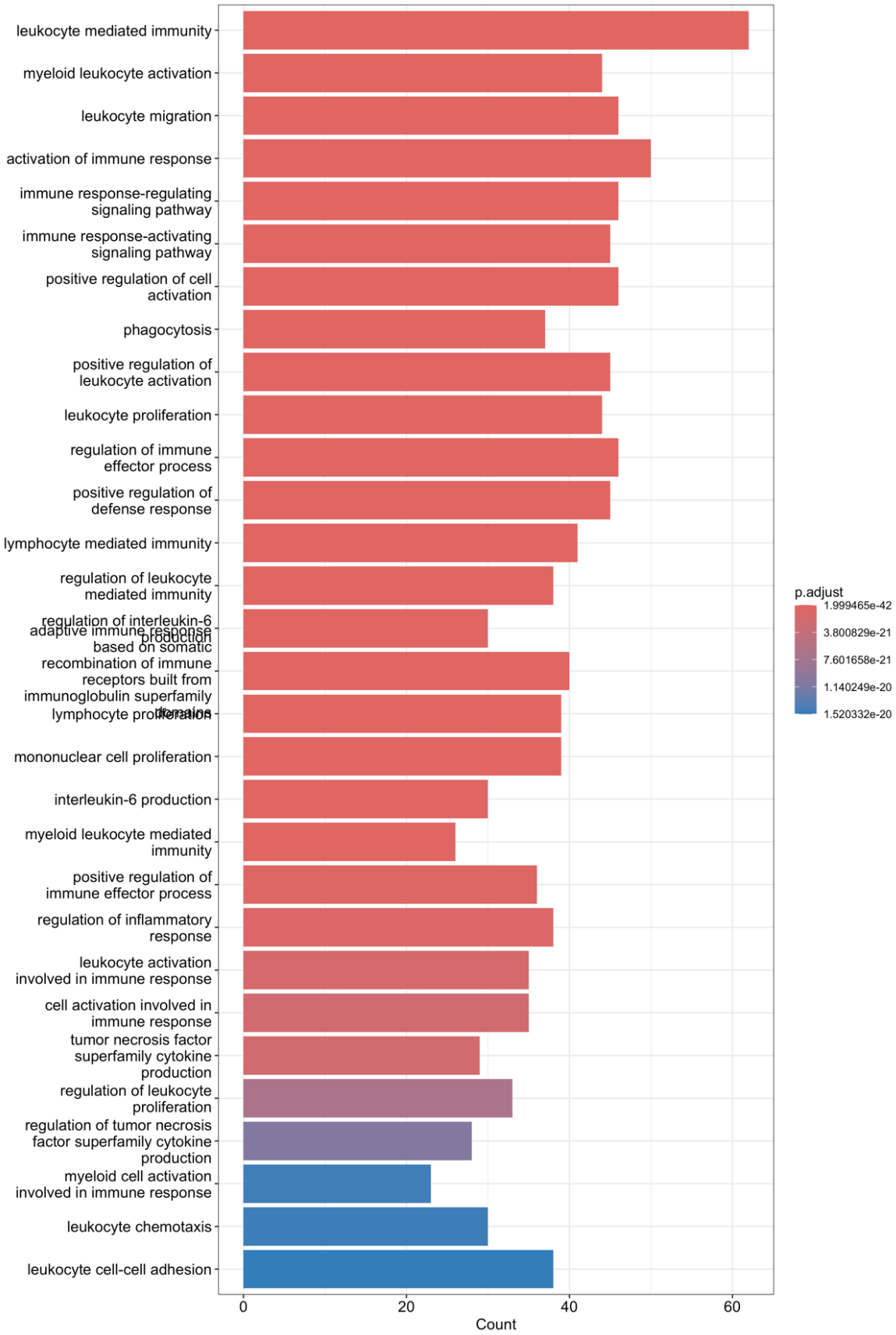

Figure 15 Pathway Analysis of differentially expressed (DE) genes in WT and PKD1-/- MEFs using R analysis. Pathway Analysis illustrates the enriched biological pathways associated with DEGs in WT and *PKD1-/-* genotypes. Figure A demonstrates pathways of down-regulated DE genes, while Figure B highlights pathways of Up-regulated genes in Immortalized cells. Figure C presents pathways associated with down-regulated DE genes in Primary cells. Pathways enriched in either WT or *PKD1-/-* genotypes are represented by bars, where each bar corresponds to a specific biological pathway. The height of each bar indicates the level of enrichment, measured by -log10 (adjusted p-value).

Pathway analysis of DEGs in both primary and immortalized MEFs highlights critical insights into apoptosis. Comparison between primary and immortalized MEFs reveals that genes such as *Bcl2l11 (BIM)*, *Adam8*, *Itgam*, *Trem2*, *Prkd1*, *Btk*, *Trim34b*, *Tifa*, *Hcls1*, *Tnf*, *Dok2*, and *Psd4* were consistently down-regulated in both cell types, suggesting PKD1's critical role in regulating genes involved in apoptosis pathways common to both cellular contexts.

Analysis of pathways in immortalized MEFs revealed an up-regulation of apoptosis-related pathways. Specifically, genes associated with apoptotic processes, including *Tnfaip8l3*, *Tnfa*, *Bmp2*, and *Il12rb1*, were enriched in these upregulated pathways. In contrast, the analysis failed to demonstrate the enriched up-regulated pathway in primary MEFs. This is likely due to the low gene count in up-regulated pathways, which may not have met the significance threshold for enrichment.

The ShinyGo (version 0.77) (142–144) platform was also employed using the Kyoto Encyclopedia of Genes and Genomes (KEGG) database for both the STRING enrichment process and pathway analyses. The ShinyGo application allows for enrichment analysis using gene ontology (GO) and KEGG pathways. The ShinyGo pathway analysis of DE genes was performed for WT and *PKD1-/-* MEFs, indicating the enriched pathways as shown in Figure 16. In this analysis, the false discovery rate (FDR) is a statistical measure used to minimize the false positive while maximizing the true positive results in our analysis. The negative logarithm of FDR (base 10), -log10 (FDR), shows the significance of enriched pathways following pathway analysis, and higher -log10 (FDR) values demonstrate greater significance.

A. Immortalized, Down-regulation

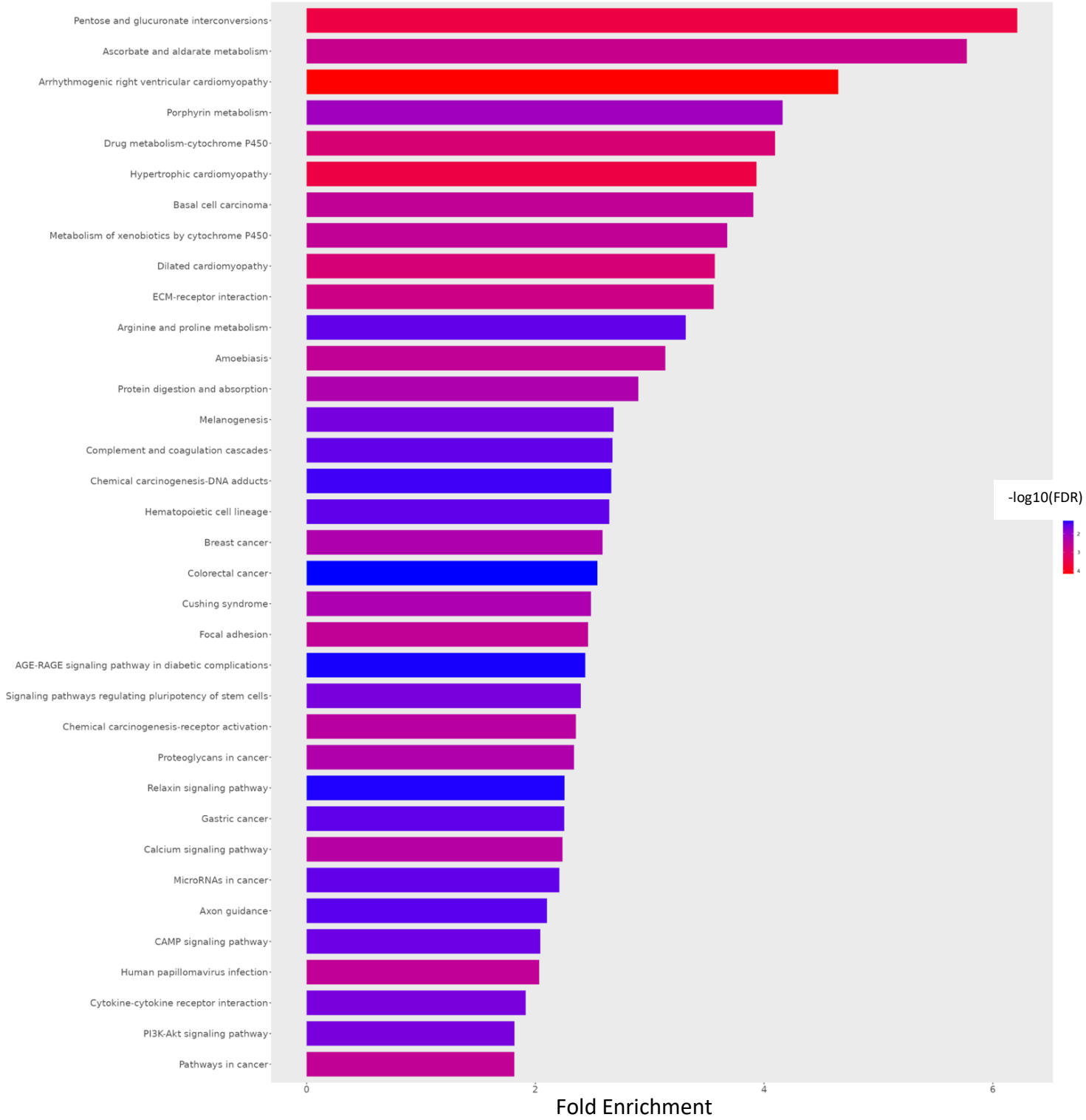

B. Immortalized, Up-regulation

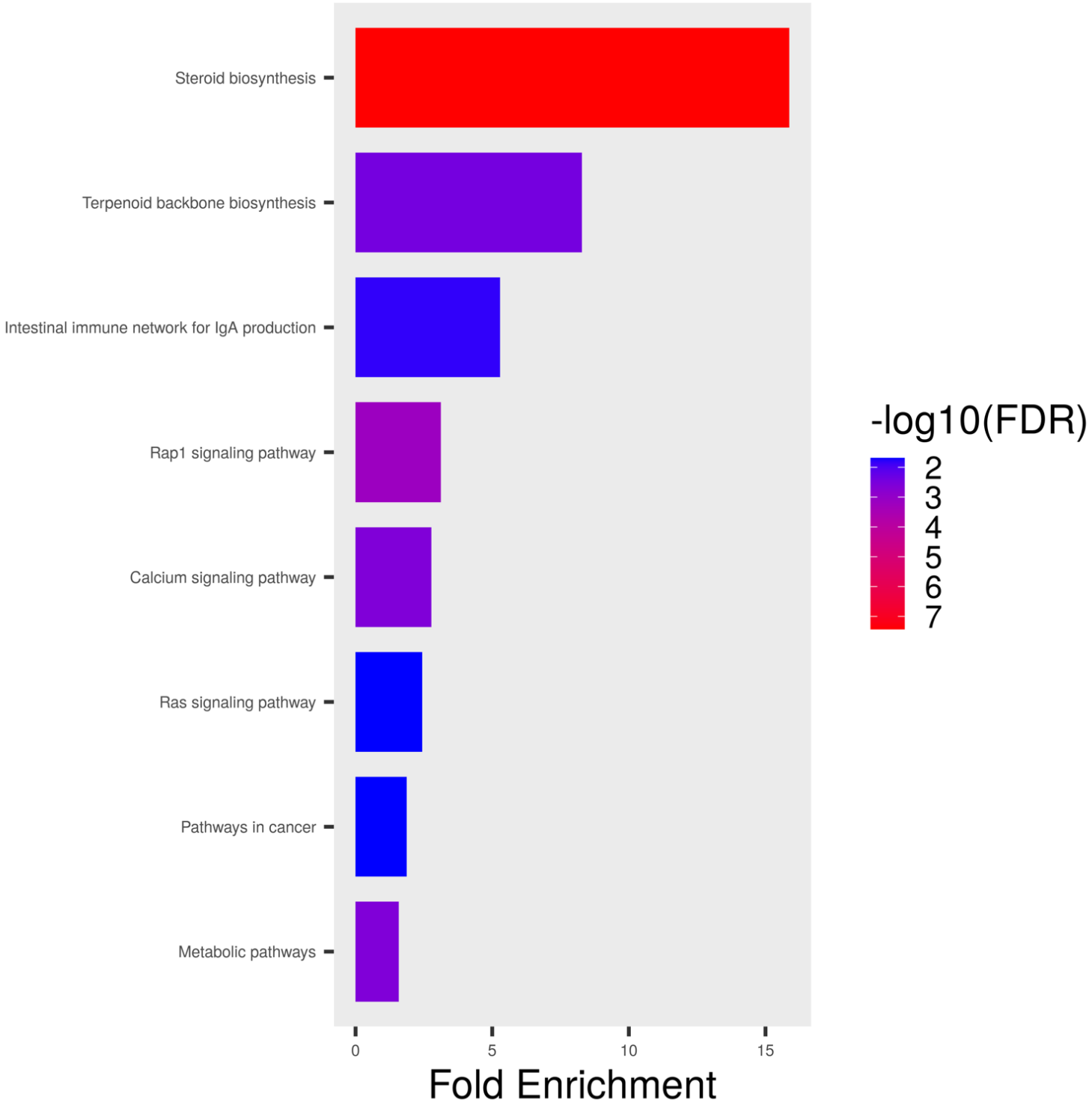

C. Primary, Down-regulation

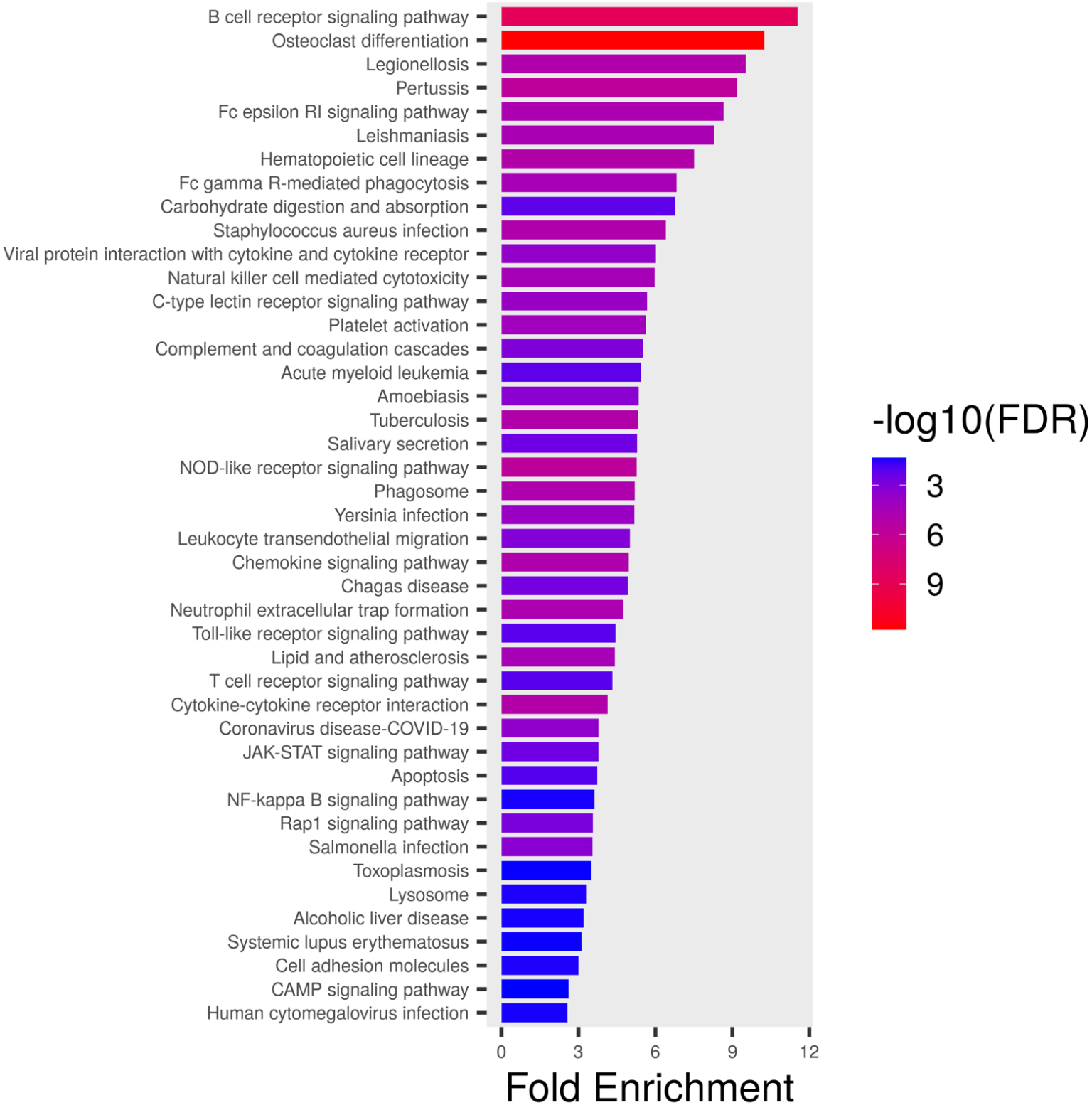

Figure 16 Pathway Analysis of DEGs in WT and PKD1-/- in MEFs using ShinyGo (0.77) pathway analysis. Pathway analysis indicates the enriched biological pathways of DE genes in WT and *PKD1-/-* genotypes. Figure A illustrates enriched pathways of down-regulated DE genes in immortalized MEFs, while Figure B shows pathways of Up-regulated genes. In Figure C, pathways associated with down-regulated DE genes in primary cells are displayed. Pathways enriched in either WT or *PKD1-/-* genotypes are represented by bars, where each bar corresponds to a specific biological pathway. The -log10 (FDR) implies the significance of enriched pathways, with an FDR of less than 0.05. The fold change indicates the amount of change in expression levels of DE genes in the pathway analysis.

Like the R analysis, pathways in various cellular processes were identified, such as pathways in apoptosis, cell survival, cancer, cellular signaling, and metabolism. We continued to focus on apoptosis-related pathways. Table 7 in appendices provides an overview of enriched pathways associated with apoptosis and oxidative stress. All enriched pathways illustrated in Table 7 have adjusted p-values of less than 0.05, indicating statistical significance. In the comparison of primary and immortalized down-regulated pathways, *Bcl2l11 (BIM)*, *Lama3*, and *Csf3r* are identified as common genes between these two cell types that are associated with apoptosis. Up-regulated pathways in immortalized MEFs demonstrate genes involved in regulating apoptosis or cell survival, including *Erbb4*, *Csf2rb*, *Csf2rb2*, *Il7r*, *Pim1*, *Vegfb*, *Vegfc*, *Fgf2*, and *Stmn1*. Consistent with the R analysis, there were no enriched up-regulated pathways in primary MEFs due to the low number of up-regulated genes.

The STRING database uses a comprehensive collection of known and predicted protein-protein interactions (PPIs) to identify enriched pathways and functional networks within a gene set. This facilitates the identification of important biological processes and pathways. STRING analysis identified enriched pathways, including pathways involved in apoptosis and regulation of apoptosis, and pathways related to cell survival, like I-kappaB kinase/NF-kappaB signaling. The STRING enrichment processes related to apoptosis are summarized in Tables 8A and 8B in the appendices. The p-value and the false discovery rate (FDR) of pathways shown in Tables 8A and 8B are less than 0.05, indicating the statistical significance. The comparison of the results between primary and immortalized MEFs reveals several common genes in down-regulated pathways, including *Bcl2l11 (BIM)*, *Ucp2*, *Ctsc*, and *Tgm2*. Analysis of up-regulated enriched pathways in immortalized MEFs revealed several genes, including *Adam8*, *Bmp2*, *Cdkn2d*, *Cx3cr1*, *Gata3*, *Itgam*, *Mef2c*, *Pdpn*, *Trem2*, and

Vegfb. These genes appear to play a critical function in the regulation of apoptotic mechanisms and cellular responses to stress within these cells.

In summary, pathway analyses for WT and *PKD1-/-* MEFs (using R software and ShinyGo platform) identified enriched differentially expressed pathways associated with apoptosis, including common genes in both primary and immortalized cells crucial in programmed cell death and cell survival. These findings highlight similarities between primary and immortalized cells in terms of down-regulated genes in *PKD1-/-* versus WT MEFs. However, the lack of enriched up-regulated pathways in primary MEFs may indicate a reduced apoptotic response, possibly due to fewer DEGs exceeding the significance threshold. Consequently, these results show that PKD1 have a key function in regulating genes involved in cellular survival and apoptosis pathways common to both primary and immortalized mouse embryonic fibroblasts.

4. DISCUSSION

The principal focus of our study was to explore the function of PKD1 in ROS-mediated apoptosis. In exploring PKD1's role in oxidative stress-induced apoptosis, our study confirmed the previously uncovered function of PKD1 in determining the threshold of oxidative stress in WT and *PKD1-/-* mouse embryonic fibroblasts. Our results demonstrate that *PKD1-/-* MEFs have a dramatically higher sensitivity under oxidative stress in comparison to the WT genotype. However, WT and *PKD1-/-* MEFs did not consistently show increased cytochrome C translocation from mitochondria to the cytosol when exposed to hydrogen peroxide. This inconsistency, coupled with the need to demonstrate this specific phase of apoptosis where PKD1 is involved, prevented us from investigating PKD1's substrate and/or binding partner in ROS-induced apoptosis. Moreover, RNA-Seq analysis identified DEGs involved in intrinsic apoptotic pathways in *PKD1-/-* cells, suggesting the crucial role of PKD1 in regulating apoptosis and cell survival under oxidative stress.

4.1. Role of PKD1 in Oxidative Stress Response

4.1.1. Western Blotting Analysis Of Oxidative Stress-Induced Apoptosis in WT Vs. *PKD1-/-* Mouse Embryonic Fibroblasts

Our findings are consistent with the previous research demonstrating the protective role of PKD1 in cellular responses to oxidative stress. Previous studies have identified an essential function of PKD1 in ROS-mediated signaling pathways. Research conducted by Storz and Toker showed that oxidative inducers such as H_2O_2 can activate PKD1, leading to NF-kB activation and subsequent transcription of specific genes involved in survival response that protects cells from oxidative stress-induced apoptosis (54,98). In this context, our group previously analyzed MEFs deficient for PKD1, generated by gene targeting, for their response to ROS. It was demonstrated that PKD1 deficiency increases ROS sensitivity in MEFs, which subsequently causes mitochondrial membrane depolarization, resulting in induced apoptosis when exposed to low concentrations of ROS (100). Our western blotting experiments examining cytochrome C translocation from mitochondria to the cytosol in WT and *PKD1-/-* MEFs revealed potential differences between the two genotypes under oxidative stress. However, inconsistent results across repeated experiments in various clones and subclones made our samples not sufficiently reliable to be analyzed through proteomics to find potential PKD1 binding partners.

Several factors could explain why western blotting experiments in our investigation produced inconsistent results, such as the diversity among clones and subclones derived from the same original cell population (145), the sensitivity of our cell lines to minor variations in experimental conditions (146–149), different responses to stressors like oxidative stress in

distinct subpopulations (150,151), western blotting's limitations in detecting minor changes in protein concentration, especially in incomplete translocation of cytochrome C due to its semi-quantitative nature (152).

There are alternative techniques for future investigations detecting cytochrome C using western blotting in the context of ROS-mediated apoptosis as an indicator of the intermediate stage of the process, where PKD1 plays a significant role. Confocal microscopy with fluorescently labeled cytochrome C (153), flow cytometry to measure the mitochondrial membrane potential (154), and utilizing specific fluorescently labeled antibodies to observe the cytochrome C localization within fixed cells (155).

4.1.2. *PKD1-/-* MEFs Exhibit Enhanced Apoptosis In Response To Oxidative Stress

We conducted the 96-hour starvation experiment as a natural generator of ROS to verify the difference between WT and *PKD1-/-* MEFs in apoptosis induced by oxidative stress. Similar to our group's previous research (100), The starvation experiment revealed significantly higher cell apoptosis in *PKD1-/-* compared to WT MEFs, suggesting PKD1's protective role in ROS-mediated signaling.

The TUNEL assay was also employed on WT and *PKD1-/-* MEFs to examine the role of PKD1 in oxidative stress-induced apoptosis. WT and *PKD1-/-* genotypes were stimulated using hydrogen peroxide to induce oxidative stress apoptosis. Consistent with the starvation experiment, the TUNEL assay showed significantly higher apoptosis in *PKD1-/-* compared to WT MEFs, highlighting the importance of PKD1 in regulating cellular sensitivity to oxidative stress.

PKD1 has been shown to play a vital role in cell survival through the NF-kB signaling pathway. A study using HeLa cells exposed to H_2O_2-induced oxidative stress revealed a novel signaling mechanism. In this pathway, oxidative stress activates PKD1 via Src/Abl non-receptor tyrosine kinases (54). Src/Abl, along with protein kinase Cδ (PKCδ), activates PKD1 through the phosphorylation of specific residues in its regulatory domain (104). The activated PKD1, which binds to PKCδ, then phosphorylates the tyrosine residue in the inhibitory IkBα protein in the IKK complex. This phosphorylation leads to the activation of the NF-kB transcription factor, which is involved in pro-survival responses (54). NF-kB's translocation to the nucleus and transcription of the superoxide dismutase (SOD) can protect cells from oxidative stress-induced apoptosis (55,112). In addition, an alternative pathway against oxidative damage was identified in HeLa cells treated with mitochondrial oxidative stress inducers, such as rotenone (a complex I inhibitor) and DPI (an NADPH oxidase inhibitor). These compounds generate mROS, which activate PKD1 at the mitochondria. This activation leads to the expression of MnSOD (manganese superoxide dismutase) through NF-κB, ultimately protecting cells from oxidative damage (98). In *PKD1-/-* MEFs, due to the lack of PKD1-mediated activation of these protective mechanisms, they exhibit increased sensitivity to oxidative stress compared to WT MEFs and demonstrate a higher susceptibility to apoptosis. Consequently, we observed significantly higher cell death under oxidative stress conditions in *PKD1-/-* MEFs compared to the WT genotype.

4.1.3. *PKD1-/-* MEFs Proliferate Slower Than The WT

Previous research uncovered the role of PKD1 in various biological pathways, including proliferation (47,48). A study conducted by Zhukova et al. (48) demonstrated that PKD1 induces cell proliferation in Swiss 3T3 cells upon exposure to G-protein-coupled receptor

(GPCR) agonists like bombesin and vasopressin. This process occurs through the phosphorylation of Ser^{744}, Ser^{748}, and Ser^{916} in PKD1 by PKC. Activated PKD1 subsequently promotes DNA synthesis, resulting in cell growth (48). PKD1 has been shown to have a critical role in cell proliferation, initiated by vascular endothelial growth factor (VEGF), which is essential for cell growth in angiogenesis (47). PKD1 activation is mediated by Ser^{744}, Ser^{748}, and Ser^{916} phosphorylation by PKCα. Upon activation, PKD1 modulates the extracellular signal-regulated kinase (ERK) signaling pathway. This modulation is fundamental for DNA synthesis and cell proliferation in endothelial cells (47). Moreover, PKD1 inhibitors, such as kb-NB142-70 and kb-NB-165-09, were identified to inhibit cell proliferation in prostate cancer promoted by PKD1 via the inhibition of phorbol 12-myristate 13-acetate (PMA)-induced autophosphorylation (46).

We observed a significantly higher cell growth rate in WT cells compared to *PKD1-/-* MEFs during the first 24 hours of serum starvation. Subsequently, a proliferation assay was conducted to examine the growth rate of MEFs over a four-day period. The proliferation assay revealed a dramatically higher proliferation rate in WT MEFs compared to the *PKD1-/-* cells. Subsequent RNA-Seq analyses also identified down-regulated proliferation pathways involved in various cell types, including leukocytes, mononuclear cells in primary PKD1-/- MEFs, as well as epithelial cells in immortalized cells.

Overall, the proliferation experiment validated the significant role of PKD1 in regulating cell growth in MEFs, as evidenced by the difference in cell proliferation between WT and *PKD1-/-* genotypes. WT MEFs exhibited a markedly higher cell growth rate compared to *PKD1-/-* MEFs over a four-day proliferation experiment.

4.2. RNA-Seq Analysis of WT And *PKD1-/-* Mouse Embryonic Fibroblasts

The original purpose of our RNA-Seq analysis was to identify the transcriptomic differences between WT and *PKD1-/-* mouse embryonic fibroblasts. This analysis aimed to investigate DEGs and enriched pathways that could explain the molecular mechanisms by which PKD1 protects cells against apoptosis induced by ROS. The comparison of gene expression profiles between *PKD1-/-* and WT MEFs, in both primary and immortalized states, provided a comprehensive understanding of how PKD1 deficiency affects cellular responses to oxidative stress and apoptotic signaling pathways.

Principal component analysis (PCA) revealed meaningful transcriptomic differences between WT and *PKD1-/-* MEFs in both primary and immortalized cell types. A 22% variation among immortalized *PKD1-/-* clones suggests that the immortalization process may cause additional transcriptional changes, possibly altering the cellular response to oxidative stress. Several potential factors may contribute to disparities among immortalized MEFs, such as genomic instability due to the immortalization process (156), contributing to differences in gene expression and cellular behavior (157). The immortalization process can lead to a progressive accumulation of significant alterations in gene expression, and it may form new DNA methylation patterns at gene promoter regions (158). This genomic instability and gene expression variations resulted in greater transcriptomic profile differences (22% variation) in immortalized *PKD1-/-* MEFs, which were less pronounced (4% variation) in primary *PKD1-/-* cells.

4.2.1. *PKD1-/-* MEFs Revealed Significant Gene Expression Changes In Primary and Immortalized Cell Types

Differential expression analysis revealed a strikingly high number of DEGs between WT and *PKD1-/-* MEFs, highlighting the profound impact of PKD1 deficiency on the cellular transcriptome. In primary MEFs, 383 DEGs were identified, with the majority being down-regulated (350), while only a small fraction (32) was up-regulated. This pattern suggests that PKD1 predominantly functions as a transcriptional activator in primary cells, and its loss leads to widespread gene repression. In contrast, immortalized MEFs exhibited a much more complex transcriptional profile, with a dramatic increase in the number of DEGs,1705 in total, comprising 997 down-regulated and 707 up-regulated genes. The difference between primary and immortalized MEFs points to the influence of immortalization, which appears to alter the cellular context and result in distinct transcriptional profiles in these two cell types.

4.3. Pathway Analysis Found Enriched Differentially Expressed Pathways Involved In Cell Survival And Apoptosis In Mouse Embryonic Fibroblasts

We conducted pathway analysis to gain insights into the biological processes and pathways associated with the identified DEGs. Pathway enrichment analysis using both R software and the ShinyGo platform revealed several apoptosis-related pathways affected by PKD1-deficiency. Genes like *Bcl2l11 (BIM)*, *Adam8*, *Itgam*, *Trem2*, *Prkd1*, *Btk*, *Trim34b*, *Tifa*, *Tnf*, *Dok2*, and *Psd4* were consistently down-regulated in both primary and immortalized *PKD1-/-* MEFs. Moreover, up-regulation of apoptosis-related genes such as *Tnfaip8l3*, *Bmp2*, and

Il12rb1 was observed in immortalized mouse embryonic fibroblasts. On the other hand, the study found no enriched pathways in primary MEFs. This is likely because the number of up-regulated genes was too small to meet the significance threshold necessary for pathway enrichment. The higher number of up-regulated genes in immortalized cells may suggest that they have enhanced apoptotic response compared to primary MEFs.

The STRING (Search Tool for the Retrieval of Interacting Genes/Proteins) analysis was employed as an important component of the pathway analysis on the RNA-Seq data from WT and *PKD1-/-* MEFs, using the ShinyGo platform. The analysis identified enriched pathways, particularly those involved in apoptosis and regulation of apoptosis, as well as pathways related to cell survival. Common down-regulated genes in both primary and immortalized MEFs include *Bcl2l11 (BIM)*, *Ucp2*, *Ctsc*, and *Tgm2*. Up-regulated genes were also observed in immortalized MEFs, such as *Bmp2*, *Cdkn2d*, *Cx3cr1*, *Gata3*, *Mef2c*, *Pdpn*, and *Vegfb*. STRING analysis revealed no enriched up-regulated pathways in primary cells. The identified genes play crucial roles in regulating apoptotic mechanisms and cellular responses to stress. The analysis also identified pathways related to I-kappaB kinase/NF-kappaB signaling, which are involved in cell survival. The STRING analysis supports the other pathway analyses performed (R software and ShinyGo platform), which provides a comprehensive view of the biological processes affected by PKD1 deficiency in MEFs, particularly those related to apoptosis and stress response.

The RNA-Seq analysis results reveal several similarities between the STRING analysis and the pathway analysis (utilizing R software and the ShinoGo platform) for WT and *PKD1-/-* MEFs. *Bcl2l11 (BIM)* was consistently identified in both STRING and pathway analyses as a down-regulated gene in *PKD1-/-* MEFs. This pro-apoptotic gene plays a significant role in

apoptosis regulation (159). Genes including *Ucp2*, *Ctsc*, and *Tgm2* were identified in both pathway and STRING analyses as down-regulated genes in *PKD1-/-* MEFs, potentially involved in apoptosis regulation. *Bmp2*, *Cx3cr1*, and *Vegfb* were also highlighted as up-regulated in immortalized *PKD1-/-* MEFs, involved in regulating apoptosis or cell survival.

Consequently, the comparison between STRING and pathway analyses identifies several common genes involved in apoptosis regulation, particularly highlighting the downregulation of *Bcl2l11 (BIM)* in *PKD1-/-* MEFs. BCL2L11 protein is a member of the BH3-only subfamily within the BCL-2 family (160). It contains a B-cell 2 homology 3 (BH3) domain, which is vital for its role in promoting apoptosis and facilitates its interaction with other BCL-2 family members (159,161). This pro-apoptotic protein in the BCL-2 family enables the release of cytochrome c from mitochondria to the cytosol (162) by interacting with the anti-apoptotic BCL-2 family proteins, like BCL-2 and BCL-XL and subsequently promoting apoptosis(163,164). The binding of BCL2L11 to these anti-apoptotic proteins blocks them from suppressing cytochrome c release(162). Bcl2l11 directly interacts with the pro-apoptotic BCL-2 family members BAX and BAK, resulting in their activation and mitochondrial outer membrane permeabilization (MOMP) (161,165). Active BAX and BAK form pores in the mitochondrial outer membrane and facilitate cytochrome c release into the cytosol (162).

BCL2L11 is primarily located on the outer mitochondrial membrane in its active form, where it is essential for the regulation of apoptosis. When inactive, BCL2L11 is typically present in the cytoplasm and associated with microtubules via its dynein light chain-binding domain (DBD) (166). The localization of BCL2L11 within the cell is dynamic and can be altered in response to apoptotic signals. After apoptotic stimulation, some of the BCL2L11 isoforms

can be released from microtubules in the cytoplasm. Following this release, BCL2L11 moves to the mitochondria and subsequently interacts with other BCL-2 family members to initiate apoptosis (167).

Although there is no specific information regarding BCL2L11 (BIM) interacting with PKD1 or PKCδ, our group's study on *PKCδ-/-* and *PKD1-/-* MEFs highlighted the significant role of these signaling proteins in the regulation of Bcl-XL protein. This was evidenced by a decrease in Bcl-XL levels and an increase in BAX protein under oxidative stress conditions, ultimately leading to apoptosis (100). Since BIM also resides in the mitochondrial outer membrane and interacts with BAX and BAK to promote apoptosis, it can be a good candidate for further study and detection of its potential interaction with PKD1.

Overall, several apoptosis-related pathways were identified as being affected by PKD1 deficiency, particularly in immortalized MEFs. This supports the hypothesis that PKD1 is involved in protecting cells against ROS-induced apoptosis. The consistent down-regulation of *Bcl2l11 (BIM)*, a pro-apoptotic gene, in both primary and immortalized *PKD1-/-* MEFs is particularly captivating. This may suggest a compensatory mechanism in *PKD1-/-* cells to counteract their increased susceptibility to apoptosis. The analyses also consistently showed differences between primary and immortalized MEFs, with more up-regulated apoptosis-associated genes found in immortalized cells. The differences observed between primary and immortalized MEFs highlight the importance of considering cellular context when studying PKD1's role in ROS-induced apoptosis.

4.4. Future Direction

Given our intriguing observation that *PKD1-/-* cells exhibit downregulation of BCL2L11 in both primary and immortalized cells, an essential further investigation for our research is to explore the potential interaction and regulatory relationship between these two proteins. We suggest a comprehensive examination to uncover the molecular mechanisms underlying PKD1's influence on BCL2L11 expression and function. This approach will involve several key experimental strategies: co-immunoprecipitation analysis to evaluate direct protein interactions, phosphorylation studies to identify potential PKD1-mediated modifications of BCL2L11, and subcellular localization experiments to observe how PKD1 affects BCL2L11 distribution within the cell. These approaches could provide extensive insights into PKD1's regulation of BCL2L11, potentially identifying novel mechanisms in cell survival and apoptosis pathways.

4.5. Limitations

Several potential limitations to this study should be considered. The primary challenge arises from the inconsistency observed in cytochrome C translocation experiments upon H_2O_2 stimulation. This variability was evident in both WT and *PKD1-/-* mouse embryonic fibroblasts, as well as other mammalian cell lines (CHO, HeLa, HEK-293). The variation in responses between different cell lines and even between clones, subclones, and passages of the same cell type makes it challenging to identify PKD1's role in ROS-mediated apoptosis. This limitation prohibited further proteomics investigation of PKD1 substrate and/or binding protein in ROS-mediated signaling. Further complicating this issue is the presence of cytochrome C in unstimulated cytosolic fractions across various experiments. This observation suggests that cells may have experienced stress prior to H_2O_2 stimulation,

potentially confounding the results and making it difficult to isolate the specific effects of PKD1 deficiency on ROS-induced apoptosis. Moreover, the relatively narrow range of H_2O_2 concentrations and incubation times tested in this study might not have captured the full spectrum of cellular responses to oxidative stress, limiting the scope of interpretation. Additionally, the study focused on specific apoptotic markers, such as cytochrome C translocation and TUNEL assay, which, while informative, may have limited our understanding of the other aspects of the apoptotic process. While the starvation experiments showed differences between WT and *PKD1-/-* MEFs, other factors beyond PKD1 deficiency could contribute to these differences. Concerns that the MEFs used may have undergone characteristic changes during extended culturing also present a limitation, which may have influenced the results. This limitation highlights the importance of considering cellular context and potential changes in cell behavior that cultured cells may exhibit over time.

Furthermore, while the RNA-Seq analysis provided valuable insights, it did not extensively explore the specific molecular mechanisms underlying the observed differences between WT and *PKD1-/-* cells. This leaves room for further investigation into the precise pathways and interactions involved in PKD1's protective role against ROS-induced apoptosis. Finally, the study was primarily conducted in cell culture systems, which may not fully reflect the complexity of PKD1's role in a living organism. The applicability of the findings to real-life physiological conditions is limited due to the absence of *in vivo* experimental validation. Addressing these limitations in future studies could help strengthen the findings and provide a more comprehensive understanding of PKD1's role in ROS-induced apoptosis. This might include using a wider range of oxidative stress inducers, exploring additional apoptotic markers, conducting longer-term experiments, and validating key findings in *in vivo* models.

4.6. CONCLUSION

This study aimed to investigate the role of PKD1 in oxidative stress-induced apoptosis and the effect of PKD1 deficiency on gene expression. *PKD1-/-* MEFs exhibited increased susceptibility to ROS-mediated apoptosis due to the absence of PKD1's function in cellular protection and survival. The RNA-Seq analysis provided valuable insights into PKD1's impact on gene expression. This study detected numerous DEGs between WT and *PKD1-/-* MEFs, including the downregulation of the pro-apoptotic protein BCL2L11 (BIM) in *PKD1-/-* MEFs. Specific mechanisms of PKD1's protective role against oxidative stress were not examined, and a more robust investigation is needed. Future research should focus on developing more consistent cellular models to study oxidative stress responding, explore alternative methods to investigate cytochrome C's translocation and the ROS-induced apoptosis, and further investigate the genes that are differentially expressed and pathways identified in the RNA-Seq analysis to better understand PKD1's role in cellular stress responses and cell survival mechanisms. This investigation elucidates PKD1's protective role against oxidative stress and its impact on gene expression, potentially paving the way for new therapies targeting diseases associated with oxidative stress.

5. REFERENCES

1. Patterson H, Nibbs R, Mcinnes I, Siebert S. Protein kinase inhibitors in the treatment of inflammatory and autoimmune diseases. Vol. 176, Clinical and Experimental Immunology. 2014. doi: 10.1111/cei.12248.

2. Kiel C, Serrano L. Challenges ahead in signal transduction: MAPK as an example. Vol. 23, Current Opinion in Biotechnology. 2012. p. 305–314. doi: 10.1016/j.copbio.2011.10.004.

3. Arencibia JM, Pastor-Flores D, Bauer AF, Schulze JO, Biondi RM. AGC protein kinases: From structural mechanism of regulation to allosteric drug development for the treatment of human diseases. Vol. 1834, Biochimica et Biophysica Acta - Proteins and Proteomics. 2013. p. 1302–1321. doi: 10.1016/j.bbapap.2013.03.010.

4. Spitaler M, Cantrell DA. Protein kinase C and beyond. Vol. 5, Nature Immunology. 2004. p. 785–790. doi: 10.1038/ni1097.

5. Buchner K. The role of protein kinase C in the regulation of cell growth and in signalling to the cell nucleus. Vol. 126. J Cancer Res Clin Oncol. 2000. doi: 10.1007/pl00008458.

6. Vasavada RC, Wang L, Fujinaka Y, Takane KK, Rosa TC, Mellado-Gil JMD, et al. Protein kinase C-ζ activation markedly enhances β-cell proliferation: An essential role in growth factor-mediated β-cell mitogenesis. Vol. 56. Diabetes. 2007. p. 2732–2743. doi: 10.2337/db07-0461.

7. Lee SW, Kwak HB, Chung WJ, Cheong H, Kim HH, Lee ZH. Participation of protein kinase c β in osteoclast differentiation and function. Vol. 32. Bone. 2003. p. 217–227. doi: 10.1101/gad.213827.113.

8. Savini I, Catani MV, Rossi A, Duranti G, Melino G, Avigliano L. Characterization of Keratinocyte Differentiation Induced by Ascorbic Acid: Protein Kinase C Involvement and Vitamin C Homeostasis. Vol 118. J Invest Dermatol. 2002. p. 372-379. doi: 10.1046/j.0022-202x.2001.01624.x.

9. Feng X, Zhang J, Smuga-Otto K, Tian S, Yu J, Stewart R, et al. Protein kinase C mediated extraembryonic endoderm differentiation of human embryonic stem cells. Vol. 30. Stem Cells. 2012. p. 461–470. doi: 10.1002/stem.1018.

10. Oehrlein SA, Maelicke A, Herget T. Expression of protein kinase C gene family members is temporally and spatially regulated during neural development in vitro. Vol. 77. European Journal of Cell Biology. 1998. p. 323-337. doi: 10.1016/S0171-9335(98)80091-5.

11. Majumder PK, Mishra NC, Sun X, Bharti A, Kharbanda S, Saxena S, et al. Targeting of Protein Kinase C to Mitochondria in the Oxidative Stress Response. Vol. 12. Cell Growth & Differentiation. 2001. p. 456-470.

12. Waldron RT, Rozengurt E. Oxidative stress induces protein kinase D activation in intact cells: Involvement of Src and dependence on protein kinase C. Vo. 275. Journal of Biological Chemistry. 2000. p.17114–17121. doi: 10.1074/jbc.M908959199.

13. Maher P. How Protein Kinase C Activation Protects Nerve Cells from Oxidative Stress-Induced Cell Death. Vol. 21. J Neurosci. 2001. p. 2929-2938. doi: 10.1523/JNEUROSCI.21-09-02929.

14. Ha H, Yu MR, Yoon Jin Choi, Hi Bahl Lee. Activation of protein kinase C-δ and C-ε by oxidative stress in early diabetic rat kidney. Vo. 38. American Journal of Kidney Diseases. 2001. p. S204-S207. doi: 10.1053/ajkd.2001.27446.

15. Matassa AA, Carpenter L, Biden TJ, Humphries MJ, Reyland ME. PKCδ Is Required for Mitochondrial-dependent Apoptosis in Salivary Epithelial Cells. Vol. 276. Journal of Biological Chemistry. 2001. p. 29719–29728. doi: 10.1074/jbc.M100273200.

16. Murriel CL, Churchill E, Inagaki K, Szweda LI, Mochly-Rosen D. Protein kinase Cδ activation induces apoptosis in response to cardiac ischemia and reperfusion damage: A mechanism involving bad and the mitochondria. Vol. 279. Journal of Biological Chemistry. 2004. p. 47985–47991. doi: 10.1074/jbc.M405071200.

17. Brennan AR, Yuan P, Dickstein DL, Rocher AB, Hof PR, Manji H, et al. Protein kinase C activity is associated with prefrontal cortical decline in aging. Vol. 30. Neurobiol Aging. 2009. p. 782–792. doi: 10.1016/j.neurobiolaging.2007.08.020.

18. Ravichandran VS, Patel HJ, Pagani FD, Westfall M V. Cardiac contractile dysfunction and protein kinase C–mediated myofilament phosphorylation in disease and aging. Journal of General Physiology. 2018 Sep 3;151(9):1070–80. doi: 10.1085/jgp.201912353.

19. Murray NR, Weems J, Braun U, Leitges M, Fields AP. Protein kinase C βII and PKCι/λ: Collaborating partners in colon cancer promotion and progression. Vol 69. Cancer Res. 2009. p. 2656–662. doi: 10.1158/0008-5472.CAN-08-3001.

20. Kanashiro CA, Khalil RA. Signal transduction by protein kinase C in mammalian cells. Vol. 25, Clinical and Experimental Pharmacology and Physiology. Blackwell Publishing; 1998. p. 974–985. doi: 10.1111/j.1440-1681.1998.tb02170.x.

21. Pappa H, Murray-Rust J, Dekker L, Parker P, McDonald N. Crystal structure of the C2 domain from protein kinase C. Vol. 6. Biomednet. 1998. p. 885-894. doi: 10.1016/s0969-2126(98)00090-2.

22. Liu JP. Protein kinase C and its substrates. Vol. 116. Molecular and Cellular Endocrinology. 1996. doi: 10.1016/0303-7207(95)03706-3.

23. Cosentino-Gomes D, Rocco-Machado N, Meyer-Fernandes JR. Cell signaling through protein kinase C oxidation and activation. Vol. 13, International Journal of Molecular Sciences. 2012. p. 10697–10721. doi: 10.3390/ijms130910697.

24. Xiao H, Liu M. Atypical protein kinase C in cell motility. Vol. 70, Cellular and Molecular Life Sciences. 2013. p. 3057–3066. doi: 10.1007/s00018-012-1192-1.

25. Yoshida K. PKCδ signaling: Mechanisms of DNA damage response and apoptosis. Vol. 19, Cellular Signalling. 2007. p. 892–901. doi: 10.1016/j.cellsig.2007.01.027.

26. Wetsel W C, Khan W A, Merchenthaler I, Rivera H, Halpern A E, Phung H M, Negro-Vilar A, Hannun Y. Tissue and Cellular Distribution of the Extended Family of Protein Kinase C Isoenzymes. Vol. 117, J Cell Biol. 1992. p. 121–133. doi: 10.1083/jcb.117.1.121.

27. Bhavanasi D, Kim S, Goldfinger LE, Kunapuli SP. Protein Kinase C Delta Mediates the Activation of Protein Kinase D In Platelets. Vol. 116, Blood. 2010. p. 2021–2021. doi: 10.1016/j.bcp.2011.06.032.

28. Azuma K, Ikeda K, Suzuki T, Aogi K, Horie-Inoue K, Inoue S. TRIM47 activates NF-κB signaling via PKC-e/PKD3 stabilization and contributes to endocrine therapy resistance in breast cancer. Vol. 118, PNAS. 2021. doi: 10.1073/pnas.2100784118.

29. Basu A. Involvement of protein kinase C-δ in DNA damage-induced apoptosis. Vol. 7, Journal of Cellular and Molecular Medicine. 2003. p. 341–350. doi: 10.1111/j.1582-4934.2003.tb00237.x.

30. Yamaguchi T, Miki Y, Yoshida K. Protein kinase C δ activates IκB-kinase α to induce the p53 tumor suppressor in response to oxidative stress. Vol. 19, Cell Signal. 2007. p. 2088–2097. doi: 10.1016/j.cellsig.2007.06.002.

31. Kajimoto T, Shirai Y, Sakai N, Yamamoto T, Matsuzaki H, Kikkawa U, et al. Ceramide-induced Apoptosis by Translocation, Phosphorylation, and Activation of Protein Kinase Cδ in the Golgi Complex. Vol. 279, Journal of Biological Chemistry. 2004. p. 12668–12676. doi: 10.1074/jbc.M312350200.

32. Li L, Lorenzo PS, Bogi K, Blumberg PM, Yuspa SH. Protein Kinase C Targets Mitochondria, Alters Mitochondrial Membrane Potential, and Induces Apoptosis in Normal and Neoplastic Keratinocytes When Overexpressed by an Adenoviral Vector. Vol. 19, Molecular And Cellular Biology. 1999. p. 8547-8558. doi: 10.1128/MCB.19.12.8547.

33. Yamada K, Yoshida K. Multiple subcellular localizations and functions of protein kinase Cδ in liver cancer. Vol. 28, World Journal of Gastroenterology. 2022. p. 188–98. doi: 10.3748/wjg.v28.i2.188.

34. Freeley M, Kelleher D, Long A. Regulation of Protein Kinase C function by phosphorylation on conserved and non-conserved sites. Vol. 23, Cellular Signalling. 2011. p. 753–62. doi: 10.1016/j.cellsig.2010.10.013.

35. Pear CJ, Kour G, House C, Kemp BE, Parker PJ. Mutagenesis of the pseudosubstrate site of protein kinase C leads to activation. Vol. 194, Eur J Biochem. 1990. p. 89–94. doi: 10.1111/j.1432-1033.1990.tb19431.x.

36. Johannes FJ, Prestle J, Eis S, Oberhagemann P, Pfizenmaieri K. PKCu Is a Novel, Atypical Member of the Protein Kinase C Family". Vol. 269, The Journal of Biological Chemistry. 1994. p. 6140-6148. DOI URL: https://doi.org/10.1016/S0021-9258(17)37580-4.

37. Valverde AM, Sinnett-Smith J, Van Lint J, Rozengurt E. Molecular cloning and characterization of protein kinase D: A target for diacylglycerol and phorbol esters with a distinctive catalytic domain. Vol. 91, Proc Nath. Acad. Sci. USA. 1994. p. 8572–8576. doi: 10.1073/pnas.91.18.8572

38. Rozengurt E. Protein kinase D signaling: Multiple biological functions in health and disease. Vol. 26, Physiology. 2011. p. 23–33. doi: 10.1152/physiol.00037.2010.

39. Guo Y, Jiang Y, Rose JB, Nagaraju GP, Jaskula-Sztul R, Hjelmeland AB, et al. Protein Kinase D1 Signaling in Cancer Stem Cells with Epithelial-Mesenchymal Plasticity. Vol. 11, Cells. 2022. doi: 10.3390/cells11233885.

40. Du C, Zhang C, Hassan S, Biswas MHU, Balaji KC. Protein kinase D1 suppresses epithelial-to-mesenchymal transition through phosphorylation of snail. Vol. 70, Cancer Res. 2010. p. 7810–7819. doi: 10.1158/0008-5472.CAN-09-4481.

41. Hausser A, Storz P, Märtens S, Link G, Toker A, Pfizenmaier K. Protein kinase D regulates vesicular transport by phosphorylating and activating phosphatidylinositol-4 kinase IIIβ at the Golgi complex. Vol. 7. Nat Cell Biol. 2005. p. 880–886. doi: 10.1038/ncb1289 .

42. Lu G, Chen J, Espinoza LA, Garfield S, Toshiyuki S, Akiko H, et al. Protein kinase D 3 is localized in vesicular structures and interacts with vesicle-associated membrane protein 2. Vol. 19, Cell Signal. 2007. p. 867–879. doi: 10.1074/jbc.M805358200.

43. di Blasio L, Droetto S, Norman J, Bussolino F, Primo L. Protein kinase D1 regulates VEGF-A-induced αvβ3 integrin trafficking and endothelial cell migration. Vol. 11, Traffic. 2010. p. 1107–18. doi: 10.1111/j.1600-0854.2010.01077.x.

44. Kim M, Jang HR, Kim JH, Noh SM, Song KS, Cho JS, et al. Epigenetic inactivation of protein kinase D1 in gastric cancer and its role in gastric cancer cell migration and invasion. Vol. 29, Carcinogenesis. 2008. p. 629–37. doi: 10.1093/carcin/bgm291.

45. Hao Q, Wang L, Joe Zhao Z, Tang H. Identification of protein kinase D2 as a pivotal regulator of endothelial cell proliferation, migration, and angiogenesis. Vol. 284, Journal of Biological Chemistry. 2009. p.799–806. doi: 10.1074/jbc.M807546200.

46. Lavalle CR, Bravo-Altamirano K, Giridhar K V, Chen J, Sharlow E, Lazo JS, et al. Novel protein kinase D inhibitors cause potent arrest in prostate cancer cell growth and motility. Vol. 10, BMC Chemical Biology. 2010. doi: 10.1186/1472-6769-10-5.

47. Wong C, Jin ZG. Protein kinase C-dependent protein kinase D activation modulates ERK signal pathway and endothelial cell proliferation by vascular endothelial growth factor. Vol. 280, Journal of Biological Chemistry. 2005. p. 33262–33269. doi: 10.1074/jbc.M503198200.

48. Zhukova E, Sinnett-Smith J, Rozengurt E. Protein Kinase D Potentiates DNA Synthesis and Cell Proliferation Induced by Bombesin, Vasopressin, or Phorbol Esters in Swiss 3T3 Cells. Vol. 276, Journal of Biological Chemistry. 2001. p. 40298–40305. doi: 10.1074/jbc.M106512200.

49. Qin L, Zeng H, Zhao D. Requirement of protein kinase D tyrosine phosphorylation for VEGF-A 165-induced angiogenesis through its interaction and regulation of phospholipase Cγ phosphorylation. Vol. 281, Journal of Biological Chemistry. 2006. p. 32550–32558. doi: 10.1074/jbc.M604853200.

50. Liu X, Zheng N, Shi YN, Yuan J, Li L. Thyroid hormone induced angiogenesis through the integrin αvβ3/protein kinase D/histone deacetylase 5 signaling pathway. Vol. 52, J Mol Endocrinol. 2014. p. 245–54. doi: 10.1530/JME-13-0252.

51. Gali A, Bijnsdorp I V., Piersma SR, Pham T V., Gutiérrez-Galindo E, Kühnel F, et al. Protein kinase D drives the secretion of invasion mediators in triple-negative breast cancer cell lines. Vol. 27, iScience. 2024. doi: 10.1016/j.isci.2024.108958.

52. Wille C, Köhler C, Armacki M, Jamali A, Gössele U, Pfizenmaier K, et al. Protein kinase D2 induces invasion of pancreatic cancer cells by regulating matrix metalloproteinases. Vol. 25, Mol Biol Cell. p. 324–336. doi: 10.1091/mbc.E13-06-0334.

53. Lemonnier J, Ghayor C, Guicheux J, Caverzasio J. Protein Kinase C-independent Activation of Protein Kinase D Is Involved in BMP-2-induced Activation of Stress Mitogen-activated Protein Kinases JNK and p38 and Osteoblastic Cell Differentiation. Vol. 279, Journal of Biological Chemistry. 2004. p. 259–264. doi: 10.1074/jbc.M308665200.

54. Storz P, Toker A. Protein kinase D mediates a stress-induced NF-κB activation and survival pathway. Vol. 22, EMBO Journal. 2003. p. 109–20. doi: 10.1093/emboj/cdg009.

55. Storz P, Döppler H, Toker A. Protein Kinase Cδ Selectively Regulates Protein Kinase D-Dependent Activation of NF-κB in Oxidative Stress Signaling. Vol. 24, Mol Cell Biol. 2004. p. 2614–2626. doi: 10.1128/MCB.24.7.2614-2626.2004.

56. Döppler H, Storz P. A novel tyrosine phosphorylation site in protein kinase D contributes to oxidative stress-mediated activation. Vol. 282, Journal of Biological Chemistry. 2007. p. 31873–31881. doi: 10.1074/jbc.M703584200.

57. Eisenberg-Lerner A, Kimchi A. PKD is a kinase of Vps34 that mediates ROS-induced autophagy downstream of DAPk. Vol. 19, Cell Death Differ. 2012. p. 788–797. doi: 10.1038/cdd.2011.149.

58. Song J, Li J, Lulla A, Mark Evers B, Chung DH. Protein kinase D protects against oxidative stress-induced intestinal epithelial cell injury via Rho/ROK/PKC-δ pathway activation. Vol. 290, Am J Physiol Cell Physiol. 2006. p. 1469–1476. doi: 10.1152/ajpcell.00486.2005.

59. Song J, Li J, Mourot JM, Mark Evers B, Chung DH. Diacylglycerol kinase regulation of protein kinase D during oxidative stress-induced intestinal cell injury. Vol. 375, Biochem Biophys Res Commun. 2008. p. 200–204. doi: 10.1016/j.bbrc.2008.07.155.

60. Waldron RT, Rey O, Zhukova E, Rozengurt E. Oxidative stress induces protein kinase C-mediated activation loop phosphorylation and nuclear redistribution of protein kinase D. Vol. 279, Journal of Biological Chemistry. 2004. p. 27482–27493. doi: 10.1074/jbc.M402875200.

61. Eisenberg-Lerner A, Kimchi A. DAP kinase regulates JNK signaling by binding and activating protein kinase D under oxidative stress. Vol. 14, Cell Death Differ. 2007. p. 1908–1915. doi: 10.1038/sj.cdd.4402212.

62. Zhang W, Zheng S, Storz P, Min W. Protein kinase D specifically mediates apoptosis signal-regulating kinase 1-JNK signaling induced by H2O2 but not tumor necrosis factor. Vol. 280, Journal of Biological Chemistry. 2005. p. 19036–19044. doi: 10.1074/jbc.M414674200.

63. Dequiedt F, Van Lint J, Lecomte E, Van Duppen V, Seufferlein T, Vandenheede JR, et al. Phosphorylation of histone deacetylase 7 by protein kinase D mediates T cell receptor-induced Nur77 expression and apoptosis. Vol. 201, Journal of Experimental Medicine. 2005. p. 793–804. doi: 10.1084/jem.20042034.

64. Yuan J, Liu Y, Tan T, Guha S, Gukovsky I, Gukovskaya A, et al. Protein kinase D regulates cell death pathways in experimental pancreatitis. Vol. 3, Front Physiol. 2012. doi: 10.3389/fphys.2012.00060.

65. Iglesias T, Rozengurt E. Protein Kinase D Activation by Mutations within Its Pleckstrin Homology Domain. Vol. 273, Journal of Biological Chemistry. 1998. p. 410-416. doi: 10.1074/jbc.273.1.410.

66. Durand N, Borges S, Storz P. Protein Kinase D enzymes as regulators of EMT and cancer cell invasion. Vol. 5, Journal of Clinical Medicine. MDPI. 2016. doi: 10.3390/jcm5020020.

67. Steinberg SF. Regulation of protein kinase D1 activity. Vol. 81, Molecular Pharmacology. 2012. p. 284–291. doi: 10.1124/mol.111.075986.

68. Rykx A, De Kimpe L, Mikhalap S, Vantus T, Seufferlein T, Vandenheede JR, et al. Protein kinase D: A family affair. Vol. 546, FEBS Letters. Elsevier; 2003. p. 81–66. doi: 10.1016/s0014-5793(03)00487-3.

69. Jamora C, Yamanouye N, Vandenheede JR, Faulkner DJ, Malhotra V. Gbg-Mediated Regulation of Golgi Organization Is through the Direct Activation of Protein Kinase D. Vol. 98, Cell Press. 1999. p. 59–68. doi: 10.1016/S0092-8674(00)80606-6.

70. Durand N, Borges S, Storz P. Functional and therapeutic significance of protein kinase D enzymes in invasive breast cancer. Vol. 72, Cellular and Molecular Life Sciences. Birkhauser Verlag AG; 2015. p. 4369–4382. doi: 10.1007/s00018-015-2011-2.

71. Storz P. Mitochondrial ROS - radical detoxification, mediated by protein kinase D. Vol. 17, Trends Cell Biol. 2007. p. 13–18. doi: 10.1016/j.tcb.2006.11.003.

72. Genestra M. Oxyl radicals, redox-sensitive signalling cascades and antioxidants. Vol. 19, Cellular Signalling. 2007. p. 1807–1819. doi: 10.1016/j.cellsig.2007.04.009.

73. Kohen R, Nyska A. Oxidation of Biological Systems: Oxidative Stress Phenomena, Antioxidants, Redox Reactions, and Methods for Their Quantii cation. Vol. 30, Toxicol Pathol. 2002. p. 620–650. doi: 10.1080/01926230290166724.

74. Martindale JL, Holbrook NJ. Cellular response to oxidative stress: Signaling for suicide and survival. Vol. 192, Journal of Cellular Physiology. 2002. doi: 10.1002/jcp.10119.

75. Storz P. Mitochondrial ROS - radical detoxification, mediated by protein kinase D. Vol. 17, Trends Cell Biol. 2007. p. 13–18. doi: 10.1016/j.tcb.2006.11.003.

76. Cadenas E. Mitochondrial free radical production and cell signaling. Vol. 25, Molecular Aspects of Medicine. 2004. p. 17–26. doi: 10.1016/j.mam.2004.02.005.

77. Burgos-Morón E, Abad-Jiménez Z, de Marañón AM, Iannantuoni F, Escribano-López I, López-Domènech S, et al. Relationship between oxidative stress, ER stress, and inflammation in type 2 diabetes: The battle continues. Vol. 8, Journal of Clinical Medicine. MDPI; 2019. doi: 10.3390/jcm8091385.

78. Yaribeygi H, Sathyapalan T, Atkin SL, Sahebkar A. Molecular Mechanisms Linking Oxidative Stress and Diabetes Mellitus. Vol. 2020, Oxid Med Cell Longev. 2020. doi: 10.1155/2020/8609213.

79. Batty M, Bennett MR, Yu E. The Role of Oxidative Stress in Atherosclerosis. Vol. 11, Cells. MDPI; 2022. doi: 10.3390/cells11233843.

80. Teleanu DM, Niculescu AG, Lungu II, Radu CI, Vladâcenco O, Roza E, et al. An Overview of Oxidative Stress, Neuroinflammation and Neurodegenerative Diseases. Vol. 23, International Journal of Molecular Sciences. MDPI; 2022. doi: 10.3390/ijms23115938.

81. López-Armada MJ, Fernández-Rodríguez JA, Blanco FJ. Mitochondrial Dysfunction and Oxidative Stress in Rheumatoid Arthritis. Vol. 11, Antioxidants. MDPI; 2022. doi: 10.3390/antiox11061151.

82. Chen K, Lu P, Beeraka NM, Sukocheva OA, Madhunapantula SR V., Liu J, et al. Mitochondrial mutations and mitoepigenetics: Focus on regulation of oxidative stress-induced responses in breast cancers. Vol. 83, Seminars in Cancer Biology. Academic Press; 2022. p. 556–69. doi: 10.1016/j.semcancer.2020.09.012.

83. Ramos-Tovar E, Muriel P. Molecular mechanisms that link oxidative stress, inflammation, and fibrosis in the liver. Vol. 9, Antioxidants. MDPI; 2020. doi: 10.3390/antiox9121279.

84. Caliri AW, Tommasi S, Besaratinia A. Relationships among smoking, oxidative stress, inflammation, macromolecular damage, and cancer. Vol. 787, Mutation Research - Reviews in Mutation Research. Elsevier B.V.; 2021. doi: 10.1016/j.mrrev.2021.108365.

85. Basak D, Uddin MN, Hancock J. The role of oxidative stress and its counteractive utility in colorectal cancer (CRC). Vol. 12, Cancers. MDPI AG; 2020. doi: 10.3390/cancers12113336.

86. Abrahan CE, Insua MF, Politi LE, German OL, Rotstein NP. Oxidative stress promotes proliferation and dedifferentiation of retina glial cells in vitro. Vol. 87, J Neurosci Res. 2009. p. 964–977. doi: 10.1002/jnr.21903.

87. Galli A, Svegliati-Baroni G, Ceni E, Milani S, Ridolfi F, Salzano R, et al. Oxidative stress stimulates proliferation and invasiveness of hepatic stellate cells via a MMP2-mediated mechanism. Vol. 41, Hepatology. 2005. p. 1074–1084. doi: 10.1002/hep.20683.

88. Clopton DA, Saltman P. Low-level oxidative stress causes cell-cycle specific arrest in cultured cells. Vol. 210, Biochem Biophys Res Commun. 1995. p. 189–196. DOI URL: https://doi.org/10.1006/bbrc.1995.1645

89. Macip S, Kosoy A, Lee SW, O'Connell MJ, Aaronson SA. Oxidative stress induces a prolonged but reversible arrest in p53-null cancer cells, involving a Chk1-dependent G2 checkpoint. Vol. 25, Oncogene. 2006. p. 6037–6047. doi: 10.1038/sj.onc.1209629.

90. Brandl A, Meyer M, Bechmann V, Nerlich M, Angele P. Oxidative stress induces senescence in human mesenchymal stem cells. Vol. 317, Exp Cell Res. p. 1541–1547. doi: 10.1016/j.yexcr.2011.02.015.

91. Bhayadia R, Schmidt BMW, Melk A, Hömme M. Senescence-Induced Oxidative Stress Causes Endothelial Dysfunction. Vol. 71, Journals of Gerontology - Series A Biological Sciences and Medical Sciences. 2016. p. 161–169. doi: 10.1093/gerona/glv008.

92. Gambino V, De Michele G, Venezia O, Migliaccio P, Dall'Olio V, Bernard L, et al. Oxidative stress activates a specific p53 transcriptional response that regulates cellular senescence and aging. Vol. 12, Aging Cell. 2013. p. 435–445. doi: 10.1111/acel.12060.

93. de Oliveira Alves N, Martins Pereira G, Di Domenico M, Costanzo G, Benevenuto S, de Oliveira Fonoff AM, et al. Inflammation response, oxidative stress and DNA damage caused by urban air pollution exposure increase in the lack of DNA repair XPC protein. Vol. 145, Environ Int. 2020. doi: 10.1016/j.envint.2020.106150.

94. Cadet J, Davies KJA. Oxidative DNA damage & repair: An introduction. Vol. 107, Free Radical Biology and Medicine. Elsevier Inc.; 2017. p. 2–12. doi: 10.1016/j.freeradbiomed.2017.03.030.

95. Warren MC, Bump EA, Medeiros D, Braunhut SJ. OXIDATIVE STRESS-INDUCED APOPTOSIS OF ENDOTHELIAL CELLS. Vol. 29, Free Radical Biology and Medicine. 2000. p. 537-547. doi: 10.1016/s0891-5849(00)00353-1.

96. Curtin JF, Donovan M, Cotter TG. Regulation and measurement of oxidative stress in apoptosis. Vol. 265, Journal of Immunological Methods. 2002. p. 49-72. doi: 10.1016/s0022-1759(02)00070-4.

97. Sinha K, Das J, Pal PB, Sil PC. Oxidative stress: The mitochondria-dependent and mitochondria-independent pathways of apoptosis. Vol. 87, Archives of Toxicology. 2013. p. 1157–80. doi: 10.1007/s00204-013-1034-4.

98. Storz P, Döppler H, Toker A. Protein Kinase D Mediates Mitochondrion-to-Nucleus Signaling and Detoxification from Mitochondrial Reactive Oxygen Species. Vol. 25, Mol Cell Biol. 2005. p. 8520–8530. doi: 10.1128/MCB.25.19.8520-8530.2005.

99. Song J, Li J, Qiao J, Jain S, Mark Evers B, Chung DH. PKD prevents H2O2-induced apoptosis via NF-κB and p38 MAPK in RIE-1 cells. Vol. 378, Biochem Biophys Res Commun. 2009. p. 610–614. doi: 10.1016/j.bbrc.2008.11.106.

100. Zhang T, Sell P, Braun U, Leitges M. PKD1 protein is involved in reactive oxygen species-mediated mitochondrial depolarization in cooperation with protein kinase Cδ (PKCδ). Vol. 290, Journal of Biological Chemistry. 2015. p. 10472–10485. doi: 10.1074/jbc.M114.619148.

101. Fleming Martinez AK, Döppler HR, Bastea LI, Edenfield B, Patel T, Leitges M, et al. Dysfunctional EGFR and oxidative stress-induced PKD1 signaling drive formation of DCLK1+ pancreatic stem cells. Vol. 24, iScience. 2021. doi: 10.1016/j.isci.2020.102019.

102. Döppler HR, Liou GY, Storz P. Generation of Hydrogen Peroxide and Downstream Protein Kinase D1 Signaling Is a Common Feature of Inducers of Pancreatic Acinar-to-Ductal Metaplasia. Vol. 11, Antioxidants. 2022. doi: 10.3390/antiox11010137.

103. Liou GY, Döppler H, Braun UB, Panayiotou R, Scotti Buzhardt M, Radisky DC, et al. Protein kinase D1 drives pancreatic acinar cell reprogramming and progression to intraepithelial neoplasia. Vol. 6, Nat Commun. 2015. doi: 10.1038/ncomms7200.

104. Asaithambi A, Kanthasamy A, Saminathan H, Anantharam V, Kanthasamy AG. Protein kinase D1 (PKD1) activation mediates a compensatory protective response during early stages of oxidative stress-induced neuronal degeneration. Vol. 6, Mol Neurodegener. 2011. doi: 10.1186/1750-1326-6-43.

105. Chen T, Wang H, Jiang C, Lu Y. PKD1 alleviates oxidative stress-inhibited osteogenesis of rat bone marrow-derived mesenchymal stem cells through TAZ activation. Vol. 122, J Cell Biochem. 2021. p. 1715–1725. doi: 10.1002/jcb.30124.

106. Giannoni E, Chiarugi P. Redox circuitries driving Src regulation. Vol. 20, Antioxidants and Redox Signaling. Mary Ann Liebert Inc.; 2014. p. 2011–25. doi: 10.1089/ars.2013.5525.

107. Basuroy S, Sheth P, Kuppuswamy D, Balasubramanian S, Ray RM, Rao RK. Expression of kinase-inactive c-Src delays oxidative stress-induced disassembly and accelerates calcium-mediated reassembly of tight junctions in the Caco-2 cell monolayer. Vol. 278, Journal of Biological Chemistry. 2003. p. 11916–11924. doi: 10.1074/jbc.M211710200.

108. Chan HL, Chou HC, Duran MC, Gruenewald J, Waterfield MD, Ridley A, et al. Major role of epidermal growth factor receptor and Src kinases in promoting oxidative stress-dependent loss of adhesion and apoptosis in epithelial cells. Journal of Biological Chemistry. 2010. p. 4307–4318. doi: 10.1074/jbc.M109.047027.

109. Döppler H, Storz P. Mitochondrial and oxidative stress-mediated activation of protein kinase d1 and its importance in pancreatic cancer. Vol. 7, Frontiers in Oncology. Frontiers Research Foundation; 2017. doi: 10.3389/fonc.2017.00041.

110. Waldron RT, Rozengurt E. Protein kinase C phosphorylates protein kinase D activation loop Ser744 and Ser748 and releases autoinhibition by the pleckstrin homology domain. Vol. 278, Journal of Biological Chemistry. 2003. p. 154–63. doi: 10.1074/jbc.M208075200.

111. Cowell CF, Döppler H, Yan IK, Hausser A, Umazawa Y, Storz P. Mitochondrial diacylglycerol initiates protein-kinase-D1-mediated ROS signaling. Vol. 122, J Cell Sci. 2009. p. 919–928. doi: 10.1242/jcs.041061.

112. Storz P, Döppler H, Toker A. Protein Kinase D Mediates Mitochondrion-to-Nucleus Signaling and Detoxification from Mitochondrial Reactive Oxygen Species. Vol. 25, Mol Cell Biol. 2005. p. 8520–8530. doi: 10.1128/MCB.25.19.8520-8530.2005

113. Han D, Williams E, Cadenas E. Mitochondrial respiratory chain-dependent generation of superoxide anion and its release into the intermembrane space. Vol. 353, Biochem. J. 2001. P. 411-416. doi: 10.1042/0264-6021:3530411.

114. Zorov DB, Juhaszova M, Yaniv Y, Nuss HB, Wang S, Sollott SJ. Regulation and pharmacology of the mitochondrial permeability transition pore. Vol. 83, Cardiovascular Research. 2009. p. 213–25. doi: 10.1093/cvr/cvp151.

115. Korsmeyer SJ, Wei MC, Saito M, Weiler S, Oh KJ, Schlesinger PH. Pro-apoptotic cascade activates BID, which oligomerizes BAK or BAX into pores that result in the release of cytochrome c. Vol. 7, Cell Death and Differentiation. 2000. p. 1166-1173. doi: 10.1038/sj.cdd.4400783.

116. Luna-Vargas MPA, Chipuk JE. The deadly landscape of pro-apoptotic BCL-2 proteins in the outer mitochondrial membrane. Vol. 283, FEBS Journal. Blackwell Publishing Ltd; 2016. p. 2676–89. doi: 10.1111/febs.13624.

117. Rudner J, Elsaesser SJ, Müller AC, Belka C, Jendrossek V. Differential effects of anti-apoptotic Bcl-2 family members Mcl-1, Bcl-2, and Bcl-xL on Celecoxib-induced apoptosis. Vol. 79, Biochem Pharmacol. 2010. p. 10–20. doi: 10.1016/j.bcp.2009.07.021.

118. Certo M, Moore VDG, Nishino M, Wei G, Korsmeyer S, Armstrong SA, et al. Mitochondria primed by death signals determine cellular addiction to antiapoptotic BCL-2 family members. Vol. 9, Cancer Cell. 2006. p. 351–365. doi: 10.1016/j.ccr.2006.03.027.

119. Kannan K, Jain SK. Oxidative stress and apoptosis. Vol. 7, Pathophysiology. 2000. p. 153-166. doi: 10.1016/s0928-4680(00)00053-5.

120. Dejean LM, Martinez-Caballero S, Manon S, Kinnally KW. Regulation of the mitochondrial apoptosis-induced channel, MAC, by BCL-2 family proteins. Vol. 1762, Biochimica et Biophysica Acta - Molecular Basis of Disease. 2006. p. 191–201. doi: 10.1016/j.bbadis.2005.07.002.

121. Wang C, Youle RJ. The role of mitochondria in apoptosis. Vol. 43, Annual Review of Genetics. 2009. p. 95–118. doi: 10.1146/annurev-genet-102108-134850.

122. Hu Y, Ding L, Spencer DM, Nú G. WD-40 Repeat Region Regulates Apaf-1 Self-association and Procaspase-9 Activation. Vol. 273, Journal of Biological Chemistry. 1998. P. 33489-33494. doi: 10.1074/jbc.273.50.33489.

123. Reubold TF, Wohlgemuth S, Eschenburg S. Crystal structure of full-length Apaf-1: How the death signal is relayed in the mitochondrial pathway of apoptosis. Vol. 19, Structure. 2011. p. 1074–1083. doi: 10.1016/j.str.2011.05.013.

124. Dorstyn L, Akey CW, Kumar S. New insights into apoptosome structure and function. Vol. 25, Cell Death and Differentiation. Nature Publishing Group; 2018. p. 1194–208. doi: 10.1038/s41418-017-0025-z.

125. Kim HE, Du F, Fang M, Wang X. Formation of apoptosome is initiated by cytochrome c-induced dATP hydrolysis and subsequent nucleotide exchange on Apaf-1. Vol. 102, PNAS. 2005. p. 17545-17550. doi: 10.1073/pnas.0507900102.

126. Li P, Nijhawan D, Budihardjo I, Srinivasula SM, Ahmad M, Alnemri ES, et al. Cytochrome c and dATP-Dependent Formation of Apaf-1/Caspase-9 Complex Initiates an Apoptotic Protease Cascade. Vol. 91, Cell. 1997. p. 479-489. doi: 10.1016/s0092-8674(00)80434-1.

127. Wolf BB, Schuler M, Echeverri F, Green DR. Caspase-3 is the primary activator of apoptotic DNA fragmentation via DNA fragmentation factor-45/inhibitor of caspase-activated DNase inactivation. Vol. 274, Journal of Biological Chemistry. 1999. p. 30651–30656. doi: 10.1074/jbc.274.43.30651.

128. Nowakowski AB, Wobig WJ, Petering DH. Native SDS-PAGE: High resolution electrophoretic separation of proteins with retention of native properties including bound metal ions. Vol. 6, Metallomics. 2014. p. 1068–1078. doi: 10.1039/c4mt00033a.

129. Dobin A, Davis CA, Schlesinger F, Drenkow J, Zaleski C, Jha S, et al. STAR: Ultrafast universal RNA-seq aligner. Vol. 29, Bioinformatics. 2013. P. 15–21. https://doi.org/10.1093/bioinformatics/bts635.

130. Danecek P, Bonfield JK, Liddle J, Marshall J, Ohan V, Pollard MO, et al. Twelve years of SAMtools and BCFtools. Vol. 10, Gigascience. 2021. P. 1-4. https://doi.org/10.1093/gigascience/giab008.

131. Liao Y, Smyth GK, Shi W. FeatureCounts: An efficient general purpose program for assigning sequence reads to genomic features. Vol. 30, Bioinformatics. 2014. P. 923–30. https://doi.org/10.1093/bioinformatics/btt656.

132. Love MI, Huber W, Anders S. Moderated estimation of fold change and dispersion for RNA-seq data with DESeq2. Vol. 15, Genome Biol. 2014. doi: 10.1186/s13059-014-0550-8.

133. Young MD, Wakefield MJ, Smyth GK, Oshlack A. METHOD Gene ontology analysis for RNA-seq: accounting for selection bias GOseq GOseq is a method for GO analysis

of RNA-seq data that takes into account the length bias inherent in RNA-seq. Vol. 11, Genome Biology. 2010. doi: 10.1186/gb-2010-11-2-r14.

134. Kanehisa M, Goto S. KEGG: Kyoto Encyclopedia of Genes and Genomes. Vol. 28, Nucleic Acids Research. 2000. P. 27-30. doi: 10.1093/nar/28.1.27.

135. Liao Y, Wang J, Jaehnig EJ, Shi Z, Zhang B. WebGestalt 2019: gene set analysis toolkit with revamped UIs and APIs. Vol. 47, Nucleic Acids Res. 2019. P. 199–205. doi: 10.1093/nar/gkz401.

136. Kim D, Langmead B, Salzberg SL. HISAT: A fast spliced aligner with low memory requirements. Vol. 12, Nat Methods. 2015. P. 357–60. doi: 10.1038/nmeth.3317.

137. Dubey AK, Godbole A, Mathew MK. Regulation of VDAC trafficking modulates cell death. Vol. 2, Cell Death Discov. 2016. doi: 10.1038/cddiscovery.2016.85.

138. Alula KM, Delgado-Deida Y, Callahan R, Till A, Underwood L, Thompson WE, et al. Inner mitochondrial membrane protein Prohibitin 1 mediates Nix-induced, Parkin-independent mitophagy. Vol. 13, Sci Rep. 2023. doi: 10.1038/s41598-022-26775-x

139. Chen Q, Gong B, Almasan A. Distinct stages of cytochrome c release from mitochondria: evidence for a feedback amplification loop linking caspase activation to mitochondrial dysfunction in genotoxic stress induced apoptosis. Vol. 7, Cell Death and Differentiation. 2000. p. 227-233. doi: 10.1038/sj.cdd.4400629.

140. Brunk UT, Svensson I. Oxidative stress, growth factor starvation and Fas activation may all cause apoptosis through lysosomal leak. Vol. 4, Redox Report. 1999. p. 3–11. doi: 10.1179/135100099101534675.

141. Li R, Kato H, Fumimoto C, Nakamura Y, Yoshimura K, Minagawa E, et al. Essential Amino Acid Starvation-Induced Oxidative Stress Causes DNA Damage and Apoptosis in Murine Osteoblast-like Cells. Vol. 24, Int J Mol Sci. 2023. doi: 10.3390/ijms242015314.

142. Xijin Ge S, Jung D, Yao R. ShinyGO: a graphical gene-set enrichment tool for animals and plants. Vol. 36, Bioinformatics. p. 26-28-2629. doi: 10.1093/bioinformatics/btz931

143. Luo W, Brouwer C. Pathview: An R/Bioconductor package for pathway-based data integration and visualization. Vol. 29, Bioinformatics. 2013. p. 1830–1831. doi: 10.1093/bioinformatics/btt285.

144. Kanehisa M, Furumichi M, Sato Y, Ishiguro-Watanabe M, Tanabe M. KEGG: Integrating viruses and cellular organisms. Vol. 49, Nucleic Acids Res. 2021. p. 545–51. doi: 10.1093/nar/gkaa970.

145. Frattini A, Fabbri M, Valli R, De Paoli E, Montalbano G, Gribaldo L, et al. High variability of genomic instability and gene expression profiling in different HeLa clones. Vol. 5, Sci Rep. 2015. doi: 10.1038/srep15377.

146. Niepel M, Hafner M, Chung M, Sorger PK. Measuring Cancer Drug Sensitivity and Resistance in Cultured Cells. Vol. 9, Curr Protoc Chem Biol. 2017. p. 55–74. doi: 10.1002/cpch.21.

147. Poon MTC, Bruce M, Simpson JE, Hannan CJ, Brennan PM. Temozolomide sensitivity of malignant glioma cell lines – a systematic review assessing consistencies between in vitro studies. Vol. 21, BMC Cancer. 2021. doi: 10.1186/s12885-021-08972-5.

148. Larsson P, Engqvist H, Biermann J, Werner Rönnerman E, Forssell-Aronsson E, Kovács A, et al. Optimization of cell viability assays to improve replicability and reproducibility of cancer drug sensitivity screens. Vol. 10, Sci Rep. 2020. DOI URL: https://doi.org/10.1038/s41598-020-62848-5

149. Wright Muelas M, Ortega F, Breitling R, Bendtsen C, Westerhoff H V. Rational cell culture optimization enhances experimental reproducibility in cancer cells. Vol. 8, Sci Rep. 2018. doi: 10.1038/s41598-018-21050-4.

150. Choudhary D, Lagage V, Foster KR, Uphoff S. Phenotypic heterogeneity in the bacterial oxidative stress response is driven by cell-cell interactions. Vol. 42, Cell Rep. 2023. doi: 10.1016/j.celrep.2023.112168.

151. Hasenauer J, Waldherr S, Doszczak M, Scheurich P, Radde N, Allgöwer F. Analysis of heterogeneous cell populations: A density-based modeling and identification framework. Vol. 21, Journal of Process Control. 2011. p. 1417–1425. DOI URL: https://doi.org/10.1016/j.jprocont.2011.06.020

152. Mahmood T, Yang PC. Western blot: Technique, theory, and trouble shooting. Vol. 4, N Am J Med Sci. 2012. p. 429–34. doi: 10.4103/1947-2714.100998.

153. Goldstein JC, Muñoz-Pinedo C, Ricci JE, Adams SR, Kelekar A, Schuler M, et al. Cytochrome c is released in a single step during apoptosis. Vol. 12, Cell Death Differ. 2005. p. 453–462. doi: 10.1038/sj.cdd.4401596.

154. Cossarizza A, Baccarani-Contri M, Kalashnikova G, Franceschi C. A new method for the cytofluorimetric analysis of mitochondrial membrane potential using the J-aggregate forming lipophilic cation 5,5',6,6'-tetrachloro-1,1',3,3'-tetraethylbenzimidazolcarbocyanine iodide (JC-1). Vol. 197, Biochemical and Biophisics Research Communications. p. 40–45. doi: 10.1006/bbrc.1993.2438.

155. Scorrano L, Ashiya M, Buttle K, Weiler S, Oaks SA, Mannella CA, et al. A Distinct Pathway Remodels Mitochondrial Cristae and Mobilizes Cytochrome c during

Apoptosis. Vol. 2, Developmental Cell. 2002. p. 55-67. doi: 10.1016/s1534-5807(01)00116-2.

156. Yoshioka K ichi. Development of cancer-initiating cells and immortalized cells with genomic instability. Vol. 7, World J Stem Cells. 2015. p. 483-489. doi: 10.4252/wjsc.v7.i2.483

157. Ensminger M, Iloff L, Ebel C, Nikolova T, Kaina B, Löbrich M. DNA breaks and chromosomal aberrations arise when replication meets base excision repair. Vol. 206, Journal of Cell Biology. 2014. p. 29–43. doi: 10.1083/jcb.201312078.

158. Gordon K, Clouaire T, Bao XX, Kemp SE, Xenophontos M, De Las Heras JI, et al. Immortality, but not oncogenic transformation, of primary human cells leads to epigenetic reprogramming of DNA methylation and gene expression. Vol. 42, Nucleic Acids Res. 2014. p. 3529–3541. doi: 10.1093/nar/gkt1351.

159. O'connor L, Strasser A, O'reilly LA, Hausmann G, Adams JM, Cory S, et al. Bim: a novel member of the Bcl-2 family that promotes apoptosis. Vol. 17, The EMBO Journal. 1998. p. 334-395. doi: 10.1093/emboj/17.2.384.

160. Qian S, Wei Z, Yang W, Huang J, Yang Y, Wang J. The role of BCL-2 family proteins in regulating apoptosis and cancer therapy. Vol. 12, Frontiers in Oncology. Frontiers Media S.A.; 2022. doi: 10.3389/fonc.2022.985363.

161. Warren CFA, Wong-Brown MW, Bowden NA. BCL-2 family isoforms in apoptosis and cancer. Vol. 10, Cell Death and Disease. Nature Publishing Group; 2019. doi: 10.1038/s41419-019-1407-6.

162. Shimizu S, Narita M, Tsujimoto Y. Bcl-2 family proteins regulate the release of apoptogenic cytochrome c by the mitochondrial channel VDAC. Vol. 399, Nature. 1999. p. 483–487. doi: 10.1038/20959.

163. Zhang L, Xing D, Chen M. BimL displacing Bcl-xL promotes Bax translocation during TNFα-induced apoptosis. Vol. 13, Apoptosis. 2008. p. 950–958. doi: 10.1007/s10495-008-0226-5.

164. Wang X, Xing D, Liu L, Chen WR. BimL directly neutralizes Bcl-xL to promote Bax activation during UV-induced apoptosis. Vol. 583, FEBS Lett. 2009. p. 1873–1879. doi: 10.1016/j.febslet.2009.04.045.

165. Nechushtan A, Smith CL, Lamensdorf I, Yoon SH, Youle RJ. Bax and Bak Coalesce into Novel Mitochondria-associated Clusters during Apoptosis. Vol. 153, The Journal of Cell Biology. 2001. p. 1265-1276. doi: 10.1083/jcb.153.6.1265

166. Puthalakath H, Huang DCS, O'reilly LA, King SM, Strasser A. The Proapoptotic Activity of the Bcl-2 Family Member Bim Is Regulated by Interaction with the Dynein Motor Complex The antiapoptotic members of the Bcl-2 family-mammalian Bcl-2, Bcl-x L , Bcl-w, A1/Bfl-1, Mcl-1, and Boo as well as C. elegans CED9-contain 3-4

domains. Vol. 3, Molecular Cell. 1999. p. 287-296. doi: 10.1016/s1097-2765(00)80456-6.

167. Sionov RV, Vlahopoulos SA, Granot Z. Regulation of Bim in Health and Disease. Vol. 6, Oncotarget. 2015. 23058-23134. doi: 10.18632/oncotarget.5492.

6. APPENDICES

6.1. Appendix A: Summary of H_2O_2 Concentrations Used in Cell Stimulation Experiments

TABLE 1- H_2O_2 CONCENTRATIONS

	H_2O_2 Concentration (μgr/μl)	**H_2O_2 Dilution**	**H_2O_2 amount in 5ml Medium (μl)**
1	25	1/1000	12.75
2	50	1/1000	25.5
3	100	1/1000	51
4	150	1/1000	76.5
5	250	1/100	12.75
6	500	1/100	25.5

H_2O_2 dilutions:

1/100 → 100 μl of 30% H_2O_2 in 1 ml PBS

1/1000 → 1ml of 1/100 H_2O_2 dilution in 10 ml PBS

6.2. Appendix B: Cell Count Data Across Time Points in Nutrient Starvation Assay

TABLE 2- CELL COUNT DURING STARVATION EXPERIMENT AT VARIOUS TIME POINTS.

	Exp. 1				Exp. 2				Exp. 3				Mean			
G	WT		PKD1-/-		WT		PKD1-/-		WT		PKD1-/-		#		Norm.	
	#	Norm.	#	Norm.	#	Norm.	#	Norm.	#	Norm.	#	Norm.	WT	PKD1-/-	WT	PKD1-/-
Start	144	100	240	100	172	100	260	100	192	100	257	100	169	252	100	100
24 h	203	141	236	98	203	118	230	88	198	103	227	88	201	231	121	91
48 h	160	111	186	75	190	110	180	69	223	116	238	93	191	201	112	79
72 h	180	125	171	71	152	88	170	65	179	93	166	64	170	169	102	79
96 h	184	128	106	44	150	87	186	71	179	93	157	61	171	149	103	59

6.3. Appendix C: Quantification of Apoptotic Cells in H_2O_2-Stimulated MEFs Using TUNEL Assay

TABLE 3- NUMBER OF APOPTOTIC CELLS IN MEFS FOLLOWING H_2O_2-INDUCED TUNEL ASSAY.

G	Exp.	H_2O_2-Stimulation									
		Positive Cont.		Negative Cont.			250µM			500µM		
		Cell Number		Cell Number		Signal	Cell Number		Signal	Cell Number		Signal
		Total	Signal	Total	Signal	%	Total	Signal	%	Total	Signal	%
WT	1	237	237	320	12	3.7	1417	40	2.8	1349	49	3.6
	2	96	96	289	4	1.4	1163	33	2.8	1132	40	3.5
	3	96	96	289	4	1.4	1022	30	2.9	454	25	5.5
	Mean Signal %	100		2.2			2.8			4.2		
PKD1-/-	1	244	244	281	9	3.2	677	93	13.7	1730	170	9.8
	2	128	128	414	4	1	937	122	13	964	76	7.9
	3	128	128	414	4	1	1236	104	8.4	2293	214	9.3
	Mean Signal %	100		1.7			11.7			9		

6.4. Appendix D: Identification of DEGs in Primary and Immortalized MEFs Following R-Based Analysis

TABLE 4- DEGS IDENTIFIED IN PRIMARY WT AND *PKD1-/-* MOUSE EMBRYONIC FIBROBLASTS

symbol	**Gene name**	**p-adj**	**DE**
Ptpn18	protein tyrosine phosphatase, non-receptor type 18	1.15972059223016E-13	DOWN
Mgat4a	mannoside acetylglucosaminyltransferase 4, isoenzyme A	0.000640602	DOWN
Creg2	cellular repressor of E1A-stimulated genes 2	3.470169321286E-14	DOWN
Pou3f3	POU domain, class 3, transcription factor 3	0.017920393	DOWN
Slc11a1	solute carrier family 11 (proton-coupled divalent metal ion transporters), member 1	1.56482798046308E-07	DOWN
B3gnt7	UDP-GlcNAc:betaGal beta-1,3-N-acetylglucosaminyltransferase 7	0.042064017	DOWN
Inpp5d	inositol polyphosphate-5-phosphatase D	7.65963485412802E-11	DOWN
St8sia4	ST8 alpha-N-acetyl-neuraminide alpha-2,8-sialyltransferase 4	7.63976367846301E-10	DOWN
Cxcr4	chemokine (C-X-C motif) receptor 4	0.00173627	DOWN
Ctse	cathepsin E	1.83799283995788E-08	DOWN
Etnk2	ethanolamine kinase 2	0.007460465	DOWN
Ppfia4	protein tyrosine phosphatase, receptor type, f polypeptide (PTPRF), interacting protein (liprin), alpha 4	0.003733438	DOWN
Ptprv	protein tyrosine phosphatase, receptor type, V	0.000340792	DOWN
Ptpn7	protein tyrosine phosphatase, non-receptor type 7	2.09739154563596E-06	DOWN
Ptprc	protein tyrosine phosphatase, receptor type, C	2.50773493700031E-05	DOWN
Rgs1	regulator of G-protein signaling 1	0.000439401	DOWN
Rgs18	regulator of G-protein signaling 18	8.93654731513158E-05	DOWN

Ncf2	neutrophil cytosolic factor 2	2.38674445254442E-14	DOWN
Fcgr2b	Fc receptor, IgG, low affinity IIb	0.000599172	DOWN
Fcgr3	Fc receptor, IgG, low affinity III	1.39864536417255E-05	DOWN
Fcer1g	Fc receptor, IgE, high affinity I, gamma polypeptide	1.64164607313971E-05	DOWN
Arhgap30	Rho GTPase activating protein 30	7.87683480507367E-07	DOWN
Cd48	CD48 antigen	0.00265791	DOWN
Cd84	CD84 antigen	9.24529905758465E-08	DOWN
Kcnj10	potassium inwardly-rectifying channel, subfamily J, member 10	7.35325573824288E-08	DOWN
Slamf9	SLAM family member 9	0.011742925	DOWN
Aim2	absent in melanoma 2	5.05366750329306E-06	DOWN
Atf3	activating transcription factor 3	0.035389216	DOWN
Traf3ip3	TRAF3 interacting protein 3	0.002346691	DOWN
Mrc1	mannose receptor, C type 1	8.80614820277513E-06	DOWN
Psd4	pleckstrin and Sec7 domain containing 4	2.16780159763915E-06	DOWN
Fcna	ficolin A	4.88467870937284E-14	DOWN
Card9	caspase recruitment domain family, member 9	1.10642291102666E-10	DOWN
Fam78a	family with sequence similarity 78, member A	0.000119643	DOWN
Stom	stomatin	0.000104243	DOWN
Arhgap15	Rho GTPase activating protein 15	0.003493173	DOWN
Spi1	spleen focus forming virus (SFFV) proviral integration oncogene	0.023640501	DOWN
Lmo2	LIM domain only 2	1.23042684586426E-12	DOWN
Plcb2	phospholipase C, beta 2	0.001126384	DOWN

Bcl2l11	BCL2-like 11 (apoptosis facilitator)	1.12818175845238E-05	DOWN
Sirpa	signal-regulatory protein alpha	0.003747796	DOWN
Siglec1	sialic acid binding Ig-like lectin 1, sialoadhesin	7.43952365385366E-27	DOWN
Cd93	CD93 antigen	3.66632304642787E-06	DOWN
Acss1	acyl-CoA synthetase short-chain family member 1	1.29229615161076E-05	DOWN
Tspyl3	TSPY-like 3	0.011034936	DOWN
Tgm2	transglutaminase 2, C polypeptide	0.000552123	DOWN
Nfatc2	nuclear factor of activated T cells, cytoplasmic, calcineurin dependent 2	3.12412299510419E-11	DOWN
Was	Wiskott-Aldrich syndrome	5.34837314860179E-16	DOWN
Cybb	cytochrome b-245, beta polypeptide	4.66175036627362E-11	DOWN
Gpr34	G protein-coupled receptor 34	0.002717344	DOWN
Cfp	complement factor properdin	0.000609517	DOWN
Lonrf3	LON peptidase N-terminal domain and ring finger 3	0.028994393	DOWN
Sash3	SAM and SH3 domain containing 3	9.74498416425048E-12	DOWN
Xlr	X-linked lymphocyte-regulated	0.020800554	DOWN
Avpr2	arginine vasopressin receptor 2	0.010392218	DOWN
Tasl	TLR adaptor interacting with endolysosomal SLC15A4	2.43591869548628E-23	DOWN
Tlr13	toll-like receptor 13	3.16588531798027E-30	DOWN
Cysltr1	cysteinyl leukotriene receptor 1	0.01440763	DOWN
Cldn34c1	claudin 34C1	1.35853847502859E-06	DOWN
Btk	Bruton agammaglobulinemia tyrosine kinase	9.23850627197053E-07	DOWN
Tmsb15l	thymosin beta 15b like	3.81884114991561E-06	DOWN

Tmsb15b2	thymosin beta 15b2	4.61226397435795E-07	DOWN
Tmsb15b1	thymosin beta 15b1	0.041043481	DOWN
Zcchc18	zinc finger, CCHC domain containing 18	0.000505833	DOWN
Tlr8	toll-like receptor 8	1.18812025231589E-06	DOWN
Tlr7	toll-like receptor 7	1.32633663352721E-16	DOWN
Sirpb1a	signal-regulatory protein beta 1A	0.003190198	DOWN
Sirpb1c	signal-regulatory protein beta 1C	0.006595656	DOWN
Nceh1	neutral cholesterol ester hydrolase 1	0.037488186	DOWN
P2ry13	purinergic receptor P2Y, G-protein coupled 13	4.00069001420562E-07	DOWN
P2ry12	purinergic receptor P2Y, G-protein coupled 12	0.002229219	DOWN
Cd1d2	CD1d2 antigen	0.001176015	DOWN
Tnfaip8l2	tumor necrosis factor, alpha-induced protein 8-like 2	3.96249985121092E-10	DOWN
Ctss	cathepsin S	1.7527809124736E-11	DOWN
H2bc18	H2B clustered histone 18	0.003209324	DOWN
Fcgr1	Fc receptor, IgG, high affinity I	4.04392274285753E-20	DOWN
I830077J02Rik	RIKEN cDNA I830077J02 gene	0.007724993	DOWN
Cd53	CD53 antigen	0.003205981	DOWN
Vav3	vav 3 oncogene	0.003077977	DOWN
Tifa	TRAF-interacting protein with forkhead-associated domain	0.000693053	DOWN
Bank1	B cell scaffold protein with ankyrin repeats 1	3.36701160123285E-05	DOWN
Gbp2b	guanylate binding protein 2b	0.000573781	DOWN
Mcoln2	mucolipin 2	0.008496992	DOWN

Ifi44	interferon-induced protein 44	0.023720077	DOWN
Ifi44l	interferon-induced protein 44 like	0.000396808	DOWN
Chd7	chromodomain helicase DNA binding protein 7	0.038177305	DOWN
Trim14	tripartite motif-containing 14	0.000719121	DOWN
Coro2a	coronin, actin binding protein 2A	0.001604008	DOWN
Tal2	T cell acute lymphocytic leukemia 2	0.002256522	DOWN
Ambp	alpha 1 microglobulin/bikunin precursor	0.000552123	DOWN
Tal1	T cell acute lymphocytic leukemia 1	5.50559739923195E-14	DOWN
Csf3r	colony stimulating factor 3 receptor (granulocyte)	0.000869219	DOWN
Laptm5	lysosomal-associated protein transmembrane 5	3.21769655459683E-05	DOWN
Ptafr	platelet-activating factor receptor	6.57468026083852E-05	DOWN
Themis2	thymocyte selection associated family member 2	4.98158760659602E-07	DOWN
Fgr	FGR proto-oncogene, Src family tyrosine kinase	0.002803499	DOWN
Cd52	CD52 antigen	0.001056391	DOWN
Cnr2	cannabinoid receptor 2 (macrophage)	8.80693195560322E-06	DOWN
C1qb	complement component 1, q subcomponent, beta polypeptide	4.31334958581328E-12	DOWN
C1qc	complement component 1, q subcomponent, C chain	2.09526334553365E-07	DOWN
C1qa	complement component 1, q subcomponent, alpha polypeptide	9.17751187055756E-10	DOWN
Padi2	peptidyl arginine deiminase, type II	0.002676934	DOWN
Atp13a2	ATPase type 13A2	9.96064437974552E-08	DOWN
Zfp990	zinc finger protein 990	4.00918059686317E-08	DOWN
Zfp985	zinc finger protein 985	1.43733578237721E-06	DOWN

Pik3cd	phosphatidylinositol-4,5-bisphosphate 3-kinase catalytic subunit delta	1.44076656019672E-07	DOWN
Kcnab2	potassium voltage-gated channel, shaker-related subfamily, beta member 2	1.52307886106057E-08	DOWN
Abcb4	ATP-binding cassette, sub-family B (MDR/TAP), member 4	9.70861378894994E-13	DOWN
Sh3bp2	SH3-domain binding protein 2	0.002080935	DOWN
Bst1	bone marrow stromal cell antigen 1	2.25676006832711E-05	DOWN
Tlr1	toll-like receptor 1	0.046371631	DOWN
Tmem156	transmembrane protein 156	0.00239113	DOWN
Stap1	signal transducing adaptor family member 1	2.5760819754355E-05	DOWN
Pf4	platelet factor 4	0.034180445	DOWN
Selplg	selectin, platelet (p-selectin) ligand	1.62462176006704E-05	DOWN
Hcar2	hydroxycarboxylic acid receptor 2	0.000885483	DOWN
Gtf2ird2	GTF2I repeat domain containing 2	1.10431177044728E-09	DOWN
Ncf1	neutrophil cytosolic factor 1	2.58528128596743E-09	DOWN
Lat2	linker for activation of T cells family, member 2	2.34880476719194E-13	DOWN
Nxpe5	neurexophilin and PC-esterase domain family, member 5	6.59696905459524E-16	DOWN
Adap1	ArfGAP with dual PH domains 1	0.001148729	DOWN
Card11	caspase recruitment domain family, member 11	0.013372844	DOWN
Alox5ap	arachidonate 5-lipoxygenase activating protein	9.77640934079911E-10	DOWN
Gmfg-ps	glia maturation factor, gamma, pseudogene	0.022012132	DOWN
Tbxas1	thromboxane A synthase 1, platelet	3.8264512564881E-08	DOWN
Clec5a	C-type lectin domain family 5, member a	2.22884866213386E-16	DOWN

Npy	neuropeptide Y	0.000441426	DOWN
Hpgds	hematopoietic prostaglandin D synthase	8.12588928140598E-21	DOWN
Il12rb2	interleukin 12 receptor, beta 2	0.025201637	DOWN
Arhgap25	Rho GTPase activating protein 25	9.73755468903291E-12	DOWN
Frmd4b	FERM domain containing 4B	0.009010301	DOWN
Plxnd1	plexin D1	0.000228263	DOWN
Alox5	arachidonate 5-lipoxygenase	0.001913322	DOWN
Slc6a12	solute carrier family 6 (neurotransmitter transporter, betaine/GABA), member 12	0.000266322	DOWN
Apobec1	apolipoprotein B mRNA editing enzyme, catalytic polypeptide 1	7.50526361319499E-09	DOWN
Gdf3	growth differentiation factor 3	0.000435617	DOWN
C3ar1	complement component 3a receptor 1	1.81478284783314E-05	DOWN
Clec4n	C-type lectin domain family 4, member n	0.000400872	DOWN
Clec4d	C-type lectin domain family 4, member d	3.36183899014231E-09	DOWN
Ptpn6	protein tyrosine phosphatase, non-receptor type 6	1.04346498129317E-21	DOWN
Lpar5	lysophosphatidic acid receptor 5	1.83031498725099E-06	DOWN
Vwf	Von Willebrand factor	2.00950422026873E-05	DOWN
Cd69	CD69 antigen	1.2748445914739E-10	DOWN
Clec12a	C-type lectin domain family 12, member a	0.047974619	DOWN
Plbd1	phospholipase B domain containing 1	0.046371631	DOWN
Ptpro	protein tyrosine phosphatase, receptor type, O	8.64814565425094E-05	DOWN
Irag2	inositol 1,4,5-triphosphate receptor associated 2	8.92867962763696E-11	DOWN
Itpr2	inositol 1,4,5-triphosphate receptor 2	0.000400872	DOWN

Pirb	paired Ig-like receptor B	2.23836268795608E-06	DOWN
Pira1	paired-Ig-like receptor A1	0.012996969	DOWN
Pira6	paired-Ig-like receptor A6	3.2871085652131E-06	DOWN
Pira2	paired-Ig-like receptor A2	0.001430507	DOWN
Lilra6	leukocyte immunoglobulin-like receptor, subfamily A (with TM domain), member 6	0.016270451	DOWN
Lair1	leukocyte-associated Ig-like receptor 1	2.09171241124908E-13	DOWN
C5ar2	complement component 5a receptor 2	1.88536942493635E-05	DOWN
C5ar1	complement component 5a receptor 1	3.65870630201129E-24	DOWN
Atp1a3	ATPase, Na+/K+ transporting, alpha 3 polypeptide	3.55723864586939E-23	DOWN
Pou2f2	POU domain, class 2, transcription factor 2	0.001203776	DOWN
Gmfg	glia maturation factor, gamma	8.69364807770397E-06	DOWN
Rinl	Ras and Rab interactor-like	6.7518222112327E-07	DOWN
Tyrobp	TYRO protein tyrosine kinase binding protein	6.03931849381428E-05	DOWN
Cd33	CD33 molecule	0.007435089	DOWN
Cd37	CD37 antigen	0.00094559	DOWN
Ppfia3	protein tyrosine phosphatase, receptor type, f polypeptide (PTPRF), interacting protein (liprin), alpha 3	0.006305128	DOWN
Dhdh	dihydrodiol dehydrogenase (dimeric)	0.001826487	DOWN
Tph1	tryptophan hydroxylase 1	0.004140199	DOWN
Anpep	alanyl (membrane) aminopeptidase	0.004335016	DOWN
Zfp710	zinc finger protein 710	1.23495059698456E-07	DOWN
Fes	feline sarcoma oncogene	0.000941059	DOWN

Tm6sf1	transmembrane 6 superfamily member 1	3.25239592964347E-06	DOWN
Sh3gl3	SH3-domain GRB2-like 3	0.017347993	DOWN
Ctsc	cathepsin C	0.001928661	DOWN
Ucp2	uncoupling protein 2 (mitochondrial, proton carrier)	2.69744670935327E-17	DOWN
P2ry6	pyrimidinergic receptor P2Y, G-protein coupled, 6	0.004302541	DOWN
Folr2	folate receptor 2 (fetal)	0.000271798	DOWN
Trim34b	tripartite motif-containing 34B	2.06530141289591E-07	DOWN
Igsf6	immunoglobulin superfamily, member 6	2.98965860409162E-11	DOWN
Il21r	interleukin 21 receptor	0.010409522	DOWN
Coro1a	coronin, actin binding protein 1A	1.76729547450576E-11	DOWN
AI467606	expressed sequence AI467606	0.047482068	DOWN
Spn	sialophorin	3.07844810987898E-06	DOWN
Pycard	PYD and CARD domain containing	0.002346691	DOWN
Itgam	integrin alpha M	2.46943115093835E-14	DOWN
Adam8	a disintegrin and metallopeptidase domain 8	1.35451799031926E-15	DOWN
Zc3h12d	zinc finger CCCH type containing 12D	0.00074366	DOWN
Lilrb4a	leukocyte immunoglobulin-like receptor, subfamily B, member 4A	3.33859235891143E-08	DOWN
Lilrb4b	leukocyte immunoglobulin-like receptor, subfamily B, member 4B	2.61999020405016E-11	DOWN
Lilrb4a	leukocyte immunoglobulin-like receptor, subfamily B, member 4A	3.46266778335515E-08	DOWN
Pkib	protein kinase inhibitor beta, cAMP dependent, testis specific	0.00293671	DOWN
Srgn	serglycin	8.8957439004252E-08	DOWN
Itgb2	integrin beta 2	0.000963865	DOWN

Trpm2	transient receptor potential cation channel, subfamily M, member 2	0.000114467	DOWN
Arhgap45	Rho GTPase activating protein 45	1.10116536948774E-10	DOWN
Gna15	guanine nucleotide binding protein, alpha 15	2.06034948377882E-08	DOWN
Lyz2	lysozyme 2	7.38177700434141E-11	DOWN
Lyz1	lysozyme 1	1.71678483436566E-09	DOWN
Tbc1d30	TBC1 domain family, member 30	0.009084803	DOWN
Arhgap9	Rho GTPase activating protein 9	1.18027556830846E-12	DOWN
Tnfsf13b	tumor necrosis factor (ligand) superfamily, member 13b	0.013429087	DOWN
Msr1	macrophage scavenger receptor 1	2.26132575089067E-15	DOWN
Pdgfrl	platelet-derived growth factor receptor-like	0.000249282	DOWN
Marchf1	membrane associated ring-CH-type finger 1	0.002446505	DOWN
Lrrc25	leucine rich repeat containing 25	0.035394231	DOWN
Mast1	microtubule associated serine/threonine kinase 1	0.000363996	DOWN
Snx20	sorting nexin 20	2.52190980374631E-08	DOWN
Dpep2	dipeptidase 2	7.70676049352072E-08	DOWN
Dpep2	dipeptidase 2	2.83306243499824E-07	DOWN
Irf8	interferon regulatory factor 8	1.08185278961169E-11	DOWN
Gm3373	predicted gene 3373	0.006974389	DOWN
Gm3667	predicted gene 3667	0.000136262	DOWN
Gm10406	predicted gene 10406	3.66440740943986E-05	DOWN
Gm3739	predicted gene 3739	0.000243237	DOWN
Gm2237	predicted gene 2237	0.027080118	DOWN

Gm5458	predicted gene 5458	0.002355397	DOWN
Stab1	stabilin 1	3.29122091094151E-06	DOWN
Tmem273	transmembrane protein 273	7.34895973234665E-07	DOWN
Wdfy4	WD repeat and FYVE domain containing 4	6.65257342525182E-08	DOWN
Prxl2a	peroxiredoxin like 2A	0.041043481	DOWN
Klhl33	kelch-like 33	1.25215273767515E-07	DOWN
Slc7a7	solute carrier family 7 (cationic amino acid transporter, y+ system), member 7	7.00693461535518E-07	DOWN
Slc7a8	solute carrier family 7 (cationic amino acid transporter, y+ system), member 8	1.62890614145556E-05	DOWN
Phf11b	PHD finger protein 11B	0.011967485	DOWN
Arl11	ADP-ribosylation factor-like 11	0.000515027	DOWN
Phyhip	phytanoyl-CoA hydroxylase interacting protein	1.11143938538883E-22	DOWN
Dok2	docking protein 2	1.87364762636786E-09	DOWN
Lcp1	lymphocyte cytosolic protein 1	1.27022980450778E-06	DOWN
Epsti1	epithelial stromal interaction 1 (breast)	0.016150792	DOWN
Uggt2	UDP-glucose glycoprotein glucosyltransferase 2	4.31130404957523E-26	DOWN
Gpr183	G protein-coupled receptor 183	0.000680683	DOWN
Fat3	FAT atypical cadherin 3	8.10284848974687E-11	DOWN
AB124611	cDNA sequence AB124611	2.34880476719194E-13	DOWN
Slc37a2	solute carrier family 37 (glycerol-3-phosphate transporter), member 2	0.006305128	DOWN
Il10ra	interleukin 10 receptor, alpha	4.33891297246272E-07	DOWN
Fxyd2	FXYD domain-containing ion transport regulator 2	1.87562125988596E-06	DOWN

Cadm1	cell adhesion molecule 1	0.022178383	DOWN
Gm32742	predicted gene, 32742	0.038548598	DOWN
Parp16	poly (ADP-ribose) polymerase family, member 16	0.037997051	DOWN
Adamts7	a disintegrin-like and metallopeptidase (reprolysin type) with thrombospondin type 1 motif, 7	0.012608214	DOWN
Zic4	zinc finger protein of the cerebellum 4	0.025099221	DOWN
Trf	transferrin	0.00041725	DOWN
Tlr9	toll-like receptor 9	0.026047392	DOWN
Nbeal2	neurobeachin-like 2	0.000412517	DOWN
Cx3cr1	chemokine (C-X3-C motif) receptor 1	2.22111501440825E-30	DOWN
Ccr2	chemokine (C-C motif) receptor 2	8.74294385945283E-07	DOWN
Ccr5	chemokine (C-C motif) receptor 5	1.084341069643E-08	DOWN
Osm	oncostatin M	0.001586119	DOWN
Myo1g	myosin IG	0.002284432	DOWN
Ikzf1	IKAROS family zinc finger 1	7.08482474344119E-08	DOWN
Plek	pleckstrin	1.02754740383429E-07	DOWN
Dock2	dedicator of cyto-kinesis 2	7.91326493363769E-06	DOWN
Gm5431	predicted gene 5431	7.46924894147488E-17	DOWN
Nlrp3	NLR family, pyrin domain containing 3	7.61509829677177E-07	DOWN
Cd68	CD68 antigen	1.41302338625818E-29	DOWN
Arrb2	arrestin, beta 2	1.59676154573211E-16	DOWN
Nlrp1a	NLR family, pyrin domain containing 1A	0.016682396	DOWN
Nlrp1b	NLR family, pyrin domain containing 1B	4.6012293829542E-16	DOWN

Atp2a3	ATPase, Ca++ transporting, ubiquitous	1.57957029816169E-06	DOWN
Evi2b	ecotropic viral integration site 2b	2.84854388704852E-12	DOWN
Adap2	ArfGAP with dual PH domains 2	0.021759324	DOWN
Ccl12	chemokine (C-C motif) ligand 12	0.014064949	DOWN
Tmem132e	transmembrane protein 132E	0.000432975	DOWN
Slfn5	schlafen 5	0.000235096	DOWN
Fmnl1	formin-like 1	1.77141023068328E-09	DOWN
Milr1	mast cell immunoglobulin like receptor 1	4.50704952290489E-10	DOWN
Cd300a	CD300A molecule	0.017777748	DOWN
Cd300lb	CD300 molecule like family member B	5.79631924654301E-06	DOWN
Cd300ld	CD300 molecule like family member d	0.003534007	DOWN
Cd300c2	CD300C molecule 2	2.72613781045181E-08	DOWN
Cd300lf	CD300 molecule like family member F	8.73828846209404E-05	DOWN
Unc13d	unc-13 homolog D	0.000573781	DOWN
Slc16a3	solute carrier family 16 (monocarboxylic acid transporters), member 3	0.022012132	DOWN
Gpr137b	G protein-coupled receptor 137B	5.38932340506765E-14	DOWN
Ly86	lymphocyte antigen 86	2.48004872159539E-06	DOWN
Cd83	CD83 antigen	0.00046094	DOWN
Susd3	sushi domain containing 3	7.1559219329698E-18	DOWN
Sema4d	sema domain, immunoglobulin domain (Ig), transmembrane domain (TM) and short cytoplasmic domain, (semaphorin) 4D	5.12039917574011E-06	DOWN
Hk3	hexokinase 3	4.98158760659602E-07	DOWN

Rgs14	regulator of G-protein signaling 14	1.69595088445811E-23	DOWN
Dok3	docking protein 3	1.44549819478321E-05	DOWN
Tifab	TRAF-interacting protein with forkhead-associated domain, family member B	4.31199886907693E-07	DOWN
Pcsk1	proprotein convertase subtilisin/kexin type 1	0.000867706	DOWN
Mctp1	multiple C2 domains, transmembrane 1	0.031825015	DOWN
Hexb	hexosaminidase B	0.000239588	DOWN
Naip2	NLR family, apoptosis inhibitory protein 2	0.006917873	DOWN
Naip5	NLR family, apoptosis inhibitory protein 5	0.010481599	DOWN
Naip6	NLR family, apoptosis inhibitory protein 6	0.017458247	DOWN
Cd180	CD180 antigen	5.38723101980433E-06	DOWN
Gapt	Grb2-binding adaptor, transmembrane	2.20983417828305E-05	DOWN
Pik3cg	phosphatidylinositol-4,5-bisphosphate 3-kinase catalytic subunit gamma	1.2019631998117E-07	DOWN
Cdhr3	cadherin-related family member 3	0.032022104	DOWN
Prkd1	protein kinase D1	9.68630579008843E-12	DOWN
Gpr65	G-protein coupled receptor 65	4.81667828124813E-07	DOWN
Kcnk13	potassium channel, subfamily K, member 13	9.46683660687445E-26	DOWN
Pld4	phospholipase D family, member 4	4.10260174370123E-16	DOWN
Rapgef5	Rap guanine nucleotide exchange factor (GEF) 5	0.000850482	DOWN
Dab2	disabled 2, mitogen-responsive phosphoprotein	0.005185687	DOWN
Il7r	interleukin 7 receptor	1.15427225781818E-06	DOWN
Otulinl	OTU deubiquitinase with linear linkage specificity like	6.20376949591941E-12	DOWN

Tmem71	transmembrane protein 71	0.020725391	DOWN
Csf2rb2	colony stimulating factor 2 receptor, beta 2, low-affinity (granulocyte-macrophage)	0.022729534	DOWN
Csf2rb	colony stimulating factor 2 receptor, beta, low-affinity (granulocyte-macrophage)	0.003743915	DOWN
Cyth4	cytohesin 4	1.2255007052281E-06	DOWN
Syngr1	synaptogyrin 1	0.010048624	DOWN
Nfam1	Nfat activating molecule with ITAM motif 1	3.82262703056125E-16	DOWN
Cerk	ceramide kinase	0.018362064	DOWN
Methig1	methyltransferase hypoxia inducible domain containing 1	0.016012487	DOWN
Bin2	bridging integrator 2	6.87943700739897E-08	DOWN
Galnt6	polypeptide N-acetylgalactosaminyltransferase 6	3.03274710937572E-06	DOWN
Gpr84	G protein-coupled receptor 84	6.2972753731727E-09	DOWN
Nckap1l	NCK associated protein 1 like	6.10192330684127E-06	DOWN
Nrros	negative regulator of reactive oxygen species	9.34283965209969E-21	DOWN
Hcls1	hematopoietic cell specific Lyn substrate 1	1.38565002452451E-07	DOWN
Cd200r1	CD200 receptor 1	0.003519444	DOWN
Cd200r4	CD200 receptor 4	1.52653076458845E-05	DOWN
Cd200	CD200 molecule	0.024589115	DOWN
Samsn1	SAM domain, SH3 domain and nuclear localization signals, 1	3.96249985121092E-10	DOWN
Rasal3	RAS protein activator like 3	3.47104007001484E-09	DOWN
Myo1f	myosin IF	3.96249985121092E-10	DOWN
Pram1	PML-RAR alpha-regulated adaptor molecule 1	0.001545288	DOWN

Gpsm3	G-protein signalling modulator 3 (AGS3-like, C. elegans)	0.000218339	DOWN
Tnf	tumor necrosis factor	2.23510547855877E-05	DOWN
H2-T24	histocompatibility 2, T region locus 24	0.015987683	DOWN
Trem1	triggering receptor expressed on myeloid cells 1	3.01582875477124E-05	DOWN
B430306N03Rik	RIKEN cDNA B430306N03 gene	0.018481484	DOWN
Trem2	triggering receptor expressed on myeloid cells 2	8.69364807770397E-06	DOWN
Ebi3	Epstein-Barr virus induced gene 3	0.003274483	DOWN
Dennd1c	DENN domain containing 1C	4.58055548678699E-07	DOWN
Vav1	vav 1 oncogene	0.001112779	DOWN
Nlrc4	NLR family, CARD domain containing 4	0.007756792	DOWN
Lama3	laminin, alpha 3	0.023105241	DOWN
Cd14	CD14 antigen	2.01321533259882E-06	DOWN
Arap3	ArfGAP with RhoGAP domain, ankyrin repeat and PH domain 3	0.000339686	DOWN
Ticam2	TIR domain containing adaptor molecule 2	0.004416901	DOWN
Eno1b	enolase 1B, retrotransposed	0.000384032	DOWN
Csf1r	colony stimulating factor 1 receptor	2.28132759020246E-22	DOWN
Unc93b1	unc-93 homolog B1, TLR signaling regulator	2.98496218689103E-28	DOWN
Ccdc88b	coiled-coil domain containing 88B	1.83614314078925E-07	DOWN
Fermt3	fermitin family member 3	5.33586939959949E-06	DOWN
Ms4a14	membrane-spanning 4-domains, subfamily A, member 14	0.000124674	DOWN
Ms4a7	membrane-spanning 4-domains, subfamily A, member 7	0.004130178	DOWN
Ms4a4c	membrane-spanning 4-domains, subfamily A, member 4C	0.025099221	DOWN

Ms4a6d	membrane-spanning 4-domains, subfamily A, member 6D	6.7477418400136E-06	DOWN
Mpeg1	macrophage expressed gene 1	1.66993763559664E-18	DOWN
Lpxn	leupaxin	2.26132575089067E-15	DOWN
Dock8	dedicator of cytokinesis 8	0.000741531	DOWN
Hhex	hematopoietically expressed homeobox	1.8585571068714E-16	DOWN
Rbp4	retinol binding protein 4, plasma	2.48004872159539E-06	DOWN
Pik3ap1	phosphoinositide-3-kinase adaptor protein 1	0.013626878	DOWN
Crtac1	cartilage acidic protein 1	1.79627802153702E-12	DOWN
Nrap	nebulin-related anchoring protein	3.78133148750576E-06	DOWN
Bend6	BEN domain containing 6	0.000498214	UP
A730008H23Rik	RIKEN cDNA A730008H23 gene	0.000435542	UP
Ahcy	S-adenosylhomocysteine hydrolase	7.29092343746041E-06	UP
Fhdc1	FH2 domain containing 1	0.026063081	UP
Rps3a1	ribosomal protein S3A1	2.56973679138954E-08	UP
Capza1	capping actin protein of muscle Z-line subunit alpha 1	1.2748445914739E-10	UP
Rpl34	ribosomal protein L34	1.49439451946293E-38	UP
Hmgn2	high mobility group nucleosomal binding domain 2	5.38723101980433E-06	UP
Pdpn	podoplanin	0.01052819	UP
Zfp982	zinc finger protein 982	1.97308998917591E-06	UP
Zfp984	zinc finger protein 984	1.03414717623926E-05	UP
Eno1	enolase 1, alpha non-neuron	0.000382581	UP
C1qtnf12	C1q and tumor necrosis factor related 12	0.000562932	UP

Klra4	killer cell lectin-like receptor, subfamily A, member 4	0.005515349	UP
Pbp2	phosphatidylethanolamine binding protein 2	8.27165014225596E-12	UP
Gm3055	predicted gene 3055	0.015473416	UP
Dctd	dCMP deaminase	0.002497591	UP
Hmgb2	high mobility group box 2	0.042712058	UP
Gm3636	predicted gene 3636	0.003125125	UP
Haus4	HAUS augmin-like complex, subunit 4	0.010166821	UP
Psmb5	proteasome (prosome, macropain) subunit, beta type 5	9.39884937920379E-08	UP
Ppp1r3e	protein phosphatase 1, regulatory subunit 3E	2.60593761304349E-11	UP
Gm16867	predicted gene, 16867	1.89965753578791E-11	UP
Hspa8	heat shock protein 8	2.85968810261653E-11	UP
Mpzl2	myelin protein zero-like 2	0.022178383	UP
Mns1	meiosis-specific nuclear structural protein 1	0.001709866	UP
Cxcr6	chemokine (C-X-C motif) receptor 6	0.000963988	UP
4833420G17Rik	RIKEN cDNA 4833420G17 gene	2.43591869548628E-23	UP
Tmem267	transmembrane protein 267	0.046204606	UP
Ccl28	chemokine (C-C motif) ligand 28	3.49878352844632E-08	UP
Pop1	processing of precursor 1, ribonuclease P/MRP family, (S. cerevisiae)	0.04135598	UP
Tslp	thymic stromal lymphopoietin	0.004414234	UP

TABLE 5- DEGS IDENTIFIED IN IMMORTALIZED WT AND *PKD1-/-* MOUSE EMBRYONIC FIBROBLASTS

symbol	**Gene name**	**p-adj**	**DE**
Alkal1	ALK and LTK ligand 1	1.69153765385834E-11	DOWN
Cpa6	carboxypeptidase A6	0.001117761	DOWN
Efhc1	EF-hand domain (C-terminal) containing 1	1.67513545768279E-06	DOWN
Kcnq5	potassium voltage-gated channel, subfamily Q, member 5	0.042921241	DOWN
Rims1	regulating synaptic membrane exocytosis 1	0.029211826	DOWN
Zap70	zeta-chain (TCR) associated protein kinase	0.002723832	DOWN
Mgat4a	mannoside acetylglucosaminyltransferase 4, isoenzyme A	1.83422292961001E-06	DOWN
Ercc5	excision repair cross-complementing rodent repair deficiency, complementation group 5	0.000188834	DOWN
Col3a1	collagen, type III, alpha 1	0.000674076	DOWN
Tmeff2	transmembrane protein with EGF-like and two follistatin-like domains 2	0.001108487	DOWN
Inpp1	inositol polyphosphate-1-phosphatase	0.007572053	DOWN
Ankrd44	ankyrin repeat domain 44	0.023706582	DOWN
Catip	ciliogenesis associated TTC17 interacting protein	0.038857082	DOWN
Cyp27a1	cytochrome P450, family 27, subfamily a, polypeptide 1	9.39377579484185E-07	DOWN
Prkag3	protein kinase, AMP-activated, gamma 3 non-catalytic subunit	4.28079072184948E-06	DOWN
Wnt6	wingless-type MMTV integration site family, member 6	2.94219929367226E-10	DOWN
Wnt10a	wingless-type MMTV integration site family, member 10A	1.360105481481E-06	DOWN
Des	desmin	0.000560376	DOWN
Chpf	chondroitin polymerizing factor	0.009225789	DOWN

Sphkap	SPHK1 interactor, AKAP domain containing	0.016792883	DOWN
Nppc	natriuretic peptide type C	0.023833386	DOWN
Efhd1	EF hand domain containing 1	0.002775445	DOWN
Ugt1a10	UDP glycosyltransferase 1 family, polypeptide A10	0.035586063	DOWN
Ugt1a9	UDP glucuronosyltransferase 1 family, polypeptide A9	0.035200213	DOWN
Ugt1a8	UDP glucuronosyltransferase 1 family, polypeptide A8	0.035461809	DOWN
Ugt1a6b	UDP glucuronosyltransferase 1 family, polypeptide A6B	0.030680706	DOWN
Ugt1a5	UDP glucuronosyltransferase 1 family, polypeptide A5	0.035586063	DOWN
Ugt1a2	UDP glucuronosyltransferase 1 family, polypeptide A2	0.036106985	DOWN
Dnajb3	DnaJ heat shock protein family (Hsp40) member B3	9.67818271208166E-08	DOWN
Ugt1a1	UDP glucuronosyltransferase 1 family, polypeptide A1	0.035650181	DOWN
Ackr3	atypical chemokine receptor 3	1.13276943870768E-15	DOWN
Rab17	RAB17, member RAS oncogene family	0.025584079	DOWN
Crocc2	ciliary rootlet coiled-coil, rootletin family member 2	0.000322819	DOWN
Sned1	sushi, nidogen and EGF-like domains 1	0.010940037	DOWN
Serpinb10	serine (or cysteine) peptidase inhibitor, clade B (ovalbumin), member 10	4.19943669481773E-05	DOWN
Inhbb	inhibin beta-B	0.000452601	DOWN
Tmem37	transmembrane protein 37	1.40121714448728E-19	DOWN
3110009E18Rik	RIKEN cDNA 3110009E18 gene	0.005984265	DOWN
C4bp	complement component 4 binding protein	0.009411764	DOWN
Ctse	cathepsin E	0.046214747	DOWN
Cdk18	cyclin-dependent kinase 18	0.014419179	DOWN

Etnk2	ethanolamine kinase 2	0.001737538	DOWN
Sox13	SRY (sex determining region Y)-box 13	1.36736572748818E-10	DOWN
Atp2b4	ATPase, Ca++ transporting, plasma membrane 4	8.7908373027563E-10	DOWN
Optc	opticin	2.04548987615311E-07	DOWN
Kdm5b	lysine (K)-specific demethylase 5B	0.000152114	DOWN
Ptprv	protein tyrosine phosphatase, receptor type, V	1.51374997312777E-23	DOWN
Phlda3	pleckstrin homology like domain, family A, member 3	0.000139048	DOWN
Pkp1	plakophilin 1	3.50768718036544E-07	DOWN
Kif21b	kinesin family member 21B	0.02332901	DOWN
Brinp3	bone morphogenetic protein/retinoic acid inducible neural specific 3	0.01873842	DOWN
Nmnat2	nicotinamide nucleotide adenylyltransferase 2	0.002905146	DOWN
Teddm2	transmembrane epididymal family member 2	0.033446222	DOWN
Glul	glutamate-ammonia ligase (glutamine synthetase)	0.00960167	DOWN
Mr1	major histocompatibility complex, class I-related	0.010507943	DOWN
Cryzl2	crystallin zeta like 2	0.005164749	DOWN
Sec16b	SEC16 homolog B (S. cerevisiae)	1.45474735759197E-05	DOWN
Fmo4	flavin containing monooxygenase 4	0.04435804	DOWN
Fmo1	flavin containing monooxygenase 1	0.016833568	DOWN
F5	coagulation factor V	0.003847	DOWN
Slc19a2	solute carrier family 19 (thiamine transporter), member 2	0.002013933	DOWN
Fam78b	family with sequence similarity 78, member B	0.046637717	DOWN
Vangl2	VANGL planar cell polarity 2	0.014430912	DOWN

Ifi206	interferon activated gene 206	0.041257034	DOWN
Rgs7	regulator of G protein signaling 7	0.002853831	DOWN
Coq8a	coenzyme Q8A	0.039832335	DOWN
Ephx1	epoxide hydrolase 1, microsomal	0.000586488	DOWN
Susd4	sushi domain containing 4	0.003352498	DOWN
Tlr5	toll-like receptor 5	0.005520528	DOWN
C130074G19Rik	RIKEN cDNA C130074G19 gene	0.00048716	DOWN
Mark1	MAP/microtubule affinity regulating kinase 1	0.006878658	DOWN
Tgfb2	transforming growth factor, beta 2	0.029406507	DOWN
Hhat	hedgehog acyltransferase	4.22383492679788E-05	DOWN
Syt14	synaptotagmin XIV	1.03534631039176E-05	DOWN
Lamb3	laminin, beta 3	0.025888498	DOWN
Plxna2	plexin A2	4.55917948585632E-07	DOWN
Cdnf	cerebral dopamine neurotrophic factor	0.01085072	DOWN
Proser2	proline and serine rich 2	2.65975790371947E-05	DOWN
Msrb2	methionine sulfoxide reductase B2	1.84876355887994E-08	DOWN
Il1rn	interleukin 1 receptor antagonist	7.71597962353957E-07	DOWN
Psd4	pleckstrin and Sec7 domain containing 4	1.67532963811921E-06	DOWN
Pax8	paired box 8	2.80688746139708E-12	DOWN
Cacna1b	calcium channel, voltage-dependent, N type, alpha 1B subunit	3.88442286478973E-05	DOWN
Entpd2	ectonucleoside triphosphate diphosphohydrolase 2	0.018537019	DOWN
Tmem141	transmembrane protein 141	0.000876489	DOWN

Bmyc	brain expressed myelocytomatosis oncogene	0.000206623	DOWN
Col5a1	collagen, type V, alpha 1	0.000287998	DOWN
Ppp1r26	protein phosphatase 1, regulatory subunit 26	8.97112959338576E-05	DOWN
Pierce1	piercer of microtubule wall 1	0.000150948	DOWN
Gbgt1	globoside alpha-1,3-N-acetylgalactosaminyltransferase 1	0.031437468	DOWN
Spaca9	sperm acrosome associated 9	0.045970898	DOWN
Kyat1	kynurenine aminotransferase 1	0.007371749	DOWN
Fibcd1	fibrinogen C domain containing 1	0.043907763	DOWN
Plpp7	phospholipid phosphatase 7 (inactive)	0.002480972	DOWN
Eeig1	estrogen-induced osteoclastogenesis regulator 1	0.009159366	DOWN
Ak1	adenylate kinase 1	0.000191082	DOWN
Olfml2a	olfactomedin-like 2A	0.019526439	DOWN
Arl5a	ADP-ribosylation factor-like 5A	0.011322275	DOWN
Galnt5	polypeptide N-acetylgalactosaminyltransferase 5	0.000395651	DOWN
Cd302	CD302 antigen	2.32052896362922E-07	DOWN
Ly75	lymphocyte antigen 75	0.003231711	DOWN
Pla2r1	phospholipase A2 receptor 1	8.34728407751049E-12	DOWN
Scn2a	sodium channel, voltage-gated, type II, alpha	2.27515574587849E-06	DOWN
Scn7a	sodium channel, voltage-gated, type VII, alpha	0.046930887	DOWN
Dlx1	distal-less homeobox 1	0.022970333	DOWN
Pde1a	phosphodiesterase 1A, calmodulin-dependent	1.10071799019783E-05	DOWN
Tfpi	tissue factor pathway inhibitor	0.000642006	DOWN

Ypel4	yippee like 4	0.027178364	DOWN
Serping1	serine (or cysteine) peptidase inhibitor, clade G, member 1	0.036202188	DOWN
Agbl2	ATP/GTP binding protein-like 2	0.003842808	DOWN
C1qtnf4	C1q and tumor necrosis factor related protein 4	6.87340324899816E-05	DOWN
Creb3l1	cAMP responsive element binding protein 3-like 1	3.43963195132105E-11	DOWN
Syt13	synaptotagmin XIII	0.008321259	DOWN
Tspan18	tetraspanin 18	0.001137404	DOWN
Alx4	aristaless-like homeobox 4	0.012456714	DOWN
Pamr1	peptidase domain containing associated with muscle regeneration 1	0.049571339	DOWN
Slc5a12	solute carrier family 5 (sodium/glucose cotransporter), member 12	0.042322991	DOWN
Ano3	anoctamin 3	2.6221449890181E-16	DOWN
Muc15	mucin 15	8.96330905233019E-08	DOWN
Or4f15	olfactory receptor family 4 subfamily F member 15	0.04334264	DOWN
Disp2	dispatched RND tramsporter family member 2	0.008119238	DOWN
Ganc	glucosidase, alpha; neutral C	0.002903768	DOWN
Dusp2	dual specificity phosphatase 2	0.000111277	DOWN
Fahd2a	fumarylacetoacetate hydrolase domain containing 2A	0.00036723	DOWN
Kcnip3	Kv channel interacting protein 3, calsenilin	8.86968226448004E-13	DOWN
Bcl2l11	BCL2-like 11 (apoptosis facilitator)	2.91532646858566E-08	DOWN
Ebf4	early B cell factor 4	0.004769836	DOWN
Cpxm1	carboxypeptidase X 1 (M14 family)	0.000647313	DOWN
Gfra4	glial cell line derived neurotrophic factor family receptor alpha 4	9.38813756757432E-05	DOWN

Adam33	a disintegrin and metallopeptidase domain 33	0.006421149	DOWN
Dzank1	double zinc ribbon and ankyrin repeat domains 1	0.006539945	DOWN
Dtd1	D-tyrosyl-tRNA deacylase 1	0.012134043	DOWN
Thbd	thrombomodulin	0.004870948	DOWN
Tmem74b	transmembrane protein 74B	0.005157586	DOWN
Slc52a3	solute carrier protein family 52, member 3	0.040195718	DOWN
Rem1	rad and gem related GTP binding protein 1	6.28684470210442E-17	DOWN
Dusp15	dual specificity phosphatase-like 15	0.033735673	DOWN
Nol4l	nucleolar protein 4-like	0.001731477	DOWN
Efcab8	EF-hand calcium binding domain 8	8.55912309852419E-05	DOWN
Procr	protein C receptor, endothelial	6.13723065409634E-06	DOWN
Tgm2	transglutaminase 2, C polypeptide	1.20276349775808E-14	DOWN
Lbp	lipopolysaccharide binding protein	0.000201199	DOWN
Jph2	junctophilin 2	0.014825748	DOWN
Rims4	regulating synaptic membrane exocytosis 4	0.015735299	DOWN
Kcns1	K+ voltage-gated channel, subfamily S, 1	0.039025846	DOWN
Sulf2	sulfatase 2	1.8317463431257E-05	DOWN
Kcnb1	potassium voltage gated channel, Shab-related subfamily, member 1	0.030867859	DOWN
Ptgis	prostaglandin I2 (prostacyclin) synthase	2.47202503510332E-08	DOWN
Ripor3	RIPOR family member 3	0.005554689	DOWN
Atp9a	ATPase, class II, type 9A	6.00183765861459E-09	DOWN
Dok5	docking protein 5	0.014787899	DOWN

Ctsz	cathepsin Z	0.029727877	DOWN
Gm14399	predicted gene 14399	0.004582856	DOWN
Nkain4	Na+/K+ transporting ATPase interacting 4	4.64077650503299E-08	DOWN
AA414768	expressed sequence AA414768	2.50291889219867E-08	DOWN
Maob	monoamine oxidase B	0.010576794	DOWN
Timp1	tissue inhibitor of metalloproteinase 1	0.030773823	DOWN
Zcchc12	zinc finger, CCHC domain containing 12	0.006747328	DOWN
Slc25a43	solute carrier family 25, member 43	3.4183682438589E-22	DOWN
Gria3	glutamate receptor, ionotropic, AMPA3 (alpha 3)	0.038243389	DOWN
Smim10l2a	small integral membrane protein 10 like 2A	0.000106451	DOWN
Dusp9	dual specificity phosphatase 9	0.001160597	DOWN
F8	coagulation factor VIII	0.028588942	DOWN
Cfap47	cilia and flagella associated protein 47	0.039013956	DOWN
Dmd	dystrophin, muscular dystrophy	0.030587769	DOWN
Il1rapl1	interleukin 1 receptor accessory protein-like 1	0.019248389	DOWN
Arhgef9	CDC42 guanine nucleotide exchange factor (GEF) 9	3.09668910442496E-11	DOWN
Eda2r	ectodysplasin A2 receptor	5.7335803678189E-32	DOWN
Ar	androgen receptor	1.98873926198905E-09	DOWN
Stard8	START domain containing 8	0.00651963	DOWN
Slc7a3	solute carrier family 7 (cationic amino acid transporter, y+ system), member 3	0.002079294	DOWN
Rtl5	retrotransposon Gag like 5	1.53959714636767E-09	DOWN
P2ry10	purinergic receptor P2Y, G-protein coupled 10	0.007484935	DOWN

Itm2a	integral membrane protein 2A	0.012707382	DOWN
Pou3f4	POU domain, class 3, transcription factor 4	0.027460546	DOWN
Cldn34c1	claudin 34C1	2.00367055454577E-09	DOWN
Pcdh19	protocadherin 19	0.000642006	DOWN
Tmem35a	transmembrane protein 35A	4.11186200863116E-09	DOWN
Arxes1	adipocyte-related X-chromosome expressed sequence 1	0.001490688	DOWN
Plp1	proteolipid protein (myelin) 1	0.002324134	DOWN
Tmsb15l	thymosin beta 15b like	0.000361456	DOWN
Tmsb15b2	thymosin beta 15b2	0.000139954	DOWN
Tmsb15b1	thymosin beta 15b1	0.001520342	DOWN
Zcchc18	zinc finger, CCHC domain containing 18	2.65801271898058E-17	DOWN
Col4a5	collagen, type IV, alpha 5	3.51206572656196E-09	DOWN
Pak3	p21 (RAC1) activated kinase 3	0.005454847	DOWN
Lhfpl1	lipoma HMGIC fusion partner-like 1	1.86728308555922E-05	DOWN
Il13ra2	interleukin 13 receptor, alpha 2	0.022061442	DOWN
Tro	trophinin	0.035330869	DOWN
Maged2	MAGE family member D2	0.001408086	DOWN
Wnk3	WNK lysine deficient protein kinase 3	0.000187268	DOWN
Mageh1	MAGE family member H1	0.002601715	DOWN
Ptchd1	patched domain containing 1	0.04334264	DOWN
Phex	phosphate regulating endopeptidase homolog, X-linked	0.018102376	DOWN
Egfl6	EGF-like-domain, multiple 6	0.003130562	DOWN

Stmn2	stathmin-like 2	1.27593576071107E-10	DOWN
Cyp7b1	cytochrome P450, family 7, subfamily b, polypeptide 1	0.004128233	DOWN
Tnik	TRAF2 and NCK interacting kinase	6.7575417107376E-07	DOWN
Cldn11	claudin 11	0.023479576	DOWN
Zmat3	zinc finger matrin type 3	0.014719729	DOWN
Usp13	ubiquitin specific peptidase 13 (isopeptidase T-3)	3.37625806226306E-73	DOWN
Slc7a11	solute carrier family 7 (cationic amino acid transporter, y+ system), member 11	0.038163272	DOWN
Mgst2	microsomal glutathione S-transferase 2	0.000969556	DOWN
Maml3	mastermind like transcriptional coactivator 3	0.008493628	DOWN
Trpc4	transient receptor potential cation channel, subfamily C, member 4	0.000357324	DOWN
Med12l	mediator complex subunit 12-like	0.046388638	DOWN
Igsf10	immunoglobulin superfamily, member 10	0.043709242	DOWN
Npy2r	neuropeptide Y receptor Y2	0.003894941	DOWN
Mnd1	meiotic nuclear divisions 1	0.014312167	DOWN
Cd1d2	CD1d2 antigen	0.001221813	DOWN
Cd1d1	CD1d1 antigen	0.04704654	DOWN
Nes	nestin	0.00144997	DOWN
Bcan	brevican	0.020362162	DOWN
Kcnn3	potassium intermediate/small conductance calcium-activated channel, subfamily N, member 3	0.001211427	DOWN
S100a16	S100 calcium binding protein A16	0.011772597	DOWN
Crct1	cysteine-rich C-terminal 1	0.023972794	DOWN

Selenbp1	selenium binding protein 1	0.000211571	DOWN
Mab21l3	mab-21-like 3	0.004492473	DOWN
Tspan2	tetraspanin 2	0.014694653	DOWN
Wnt2b	wingless-type MMTV integration site family, member 2B	0.033344978	DOWN
Inka2	inka box actin regulator 2	0.0375249	DOWN
Celsr2	cadherin, EGF LAG seven-pass G-type receptor 2	0.000261521	DOWN
Fndc7	fibronectin type III domain containing 7	0.038231067	DOWN
Olfm3	olfactomedin 3	0.00522551	DOWN
Gpr88	G-protein coupled receptor 88	0.036273238	DOWN
Palmd	palmdelphin	2.38512781167084E-06	DOWN
Rwdd3	RWD domain containing 3	0.002343074	DOWN
Tram1l1	translocation associated membrane protein 1-like 1	4.44334066389334E-06	DOWN
Arsj	arylsulfatase J	3.18603549206361E-09	DOWN
Alpk1	alpha-kinase 1	0.005120961	DOWN
Pitx2	paired-like homeodomain transcription factor 2	3.10125046487257E-06	DOWN
Enpep	glutamyl aminopeptidase	0.035058611	DOWN
Tacr3	tachykinin receptor 3	0.035650181	DOWN
Ddit4l	DNA-damage-inducible transcript 4-like	0.007849269	DOWN
Gbp2b	guanylate binding protein 2b	1.53693618932453E-11	DOWN
Ptgfr	prostaglandin F receptor	6.83891015473884E-05	DOWN
Ripk2	receptor (TNFRSF)-interacting serine-threonine kinase 2	0.04663289	DOWN
Mmp16	matrix metallopeptidase 16	3.17130799515232E-06	DOWN

Fhl5	four and a half LIM domains 5	0.008075046	DOWN
Cntfr	ciliary neurotrophic factor receptor	8.28052179769764E-08	DOWN
Ccl27a	chemokine (C-C motif) ligand 27A	0.001358557	DOWN
Aldh1b1	aldehyde dehydrogenase 1 family, member B1	4.86400525136222E-08	DOWN
Col15a1	collagen, type XV, alpha 1	0.003273376	DOWN
Pakap	paralemmin A kinase anchor protein	0.01458467	DOWN
Zfp618	zinc finger protein 618	0.00676606	DOWN
Tnc	tenascin C	0.001335765	DOWN
Pappa	pregnancy-associated plasma protein A	0.018294842	DOWN
Astn2	astrotactin 2	0.000310829	DOWN
Brinp1	bone morphogenic protein/retinoic acid inducible neural specific 1	0.000427982	DOWN
Lurap1l	leucine rich adaptor protein 1-like	3.44682345073136E-13	DOWN
Adamtsl1	ADAMTS-like 1	9.64921528431284E-09	DOWN
Fggy	FGGY carbohydrate kinase domain containing	7.05905964096344E-45	DOWN
Cyp2j6	cytochrome P450, family 2, subfamily j, polypeptide 6	7.09650305720938E-06	DOWN
Nfia	nuclear factor I/A	0.023372544	DOWN
Ror1	receptor tyrosine kinase-like orphan receptor 1	0.009732373	DOWN
Fam151a	family with sequence simliarity 151, member A	0.045670205	DOWN
Ssbp3	single-stranded DNA binding protein 3	0.023833386	DOWN
Podn	podocan	0.011772597	DOWN
Tut4	terminal uridylyl transferase 4	0.048654591	DOWN
Dmrta2	doublesex and mab-3 related transcription factor like family A2	0.000844122	DOWN

Pik3r3	phosphoinositide-3-kinase regulatory subunit 3	0.004649925	DOWN
Pik3r3	phosphoinositide-3-kinase regulatory subunit 3	0.005212175	DOWN
Tmem53	transmembrane protein 53	0.024295063	DOWN
Cldn19	claudin 19	0.014419179	DOWN
Ccdc30	coiled-coil domain containing 30	0.006359586	DOWN
Rhbdl2	rhomboid like 2	0.030306353	DOWN
Rspo1	R-spondin 1	0.00642182	DOWN
Csf3r	colony stimulating factor 3 receptor (granulocyte)	0.035251382	DOWN
Gjb5	gap junction protein, beta 5	0.004364121	DOWN
Fndc5	fibronectin type III domain containing 5	1.84129520840379E-05	DOWN
Adgrb2	adhesion G protein-coupled receptor B2	0.006742868	DOWN
Serinc2	serine incorporator 2	2.48019063900536E-18	DOWN
Rab42	RAB42, member RAS oncogene family	0.018344167	DOWN
Sesn2	sestrin 2	0.006430015	DOWN
Sytl1	synaptotagmin-like 1	0.025363544	DOWN
Crybg2	crystallin beta-gamma domain containing 2	0.039485843	DOWN
Cnksr1	connector enhancer of kinase suppressor of Ras 1	0.004930502	DOWN
Extl1	exostosin-like glycosyltransferase 1	0.041113053	DOWN
Asap3	ArfGAP with SH3 domain, ankyrin repeat and PH domain 3	0.026301018	DOWN
Zfp990	zinc finger protein 990	0.000427982	DOWN
Zfp985	zinc finger protein 985	1.04888753760844E-05	DOWN
Per3	period circadian clock 3	0.006933713	DOWN

Rnf207	ring finger protein 207	6.53251764201918E-07	DOWN
Chd5	chromodomain helicase DNA binding protein 5	2.83904697526181E-06	DOWN
Prdm16	PR domain containing 16	0.008680469	DOWN
Mmp23	matrix metallopeptidase 23	7.66858307863885E-20	DOWN
Fndc10	fibronectin type III domain containing 10	0.001432151	DOWN
Tnfrsf18	tumor necrosis factor receptor superfamily, member 18	0.007764998	DOWN
Elapor2	endosome-lysosome associated apoptosis and autophagy regulator family member 2	0.00039612	DOWN
Gnai1	guanine nucleotide binding protein (G protein), alpha inhibiting 1	0.037087482	DOWN
Fbxl13	F-box and leucine-rich repeat protein 13	1.53517316024591E-11	DOWN
Lrrc17	leucine rich repeat containing 17	1.87107358638213E-05	DOWN
Gm7361	predicted gene 7361	0.003682363	DOWN
Lmbr1	limb region 1	0.017869085	DOWN
Il6	interleukin 6	0.007643496	DOWN
Cgref1	cell growth regulator with EF hand domain 1	0.000375879	DOWN
Spon2	spondin 2, extracellular matrix protein	0.030111777	DOWN
Uvssa	UV stimulated scaffold protein A	0.042925234	DOWN
Mxd4	Max dimerization protein 4	0.002978895	DOWN
Wfs1	wolframin ER transmembrane glycoprotein	0.000645448	DOWN
Nsg1	neuron specific gene family member 1	0.010621088	DOWN
Bst1	bone marrow stromal cell antigen 1	0.047470512	DOWN
Cd38	CD38 antigen	0.000272876	DOWN
Ccdc149	coiled-coil domain containing 149	0.00338076	DOWN

Lgi2	leucine-rich repeat LGI family, member 2	0.014446846	DOWN
Arap2	ArfGAP with RhoGAP domain, ankyrin repeat and PH domain 2	0.033940316	DOWN
Tlr6	toll-like receptor 6	6.55308593864467E-05	DOWN
Fam114a1	family with sequence similarity 114, member A1	0.002975307	DOWN
N4bp2	NEDD4 binding protein 2	0.000235872	DOWN
Ociad2	OCIA domain containing 2	0.010091624	DOWN
Ppbp	pro-platelet basic protein	0.002951945	DOWN
Odaph	odontogenesis associated phosphoprotein	0.021115683	DOWN
U90926	cDNA sequence U90926	0.019784502	DOWN
Stbd1	starch binding domain 1	0.000217895	DOWN
Ccdc158	coiled-coil domain containing 158	0.000295851	DOWN
Nkx6-1	NK6 homeobox 1	0.01005653	DOWN
Cds1	CDP-diacylglycerol synthase 1	0.011358613	DOWN
Ptpn13	protein tyrosine phosphatase, non-receptor type 13	0.000674076	DOWN
Slc49a3	solute carrier family 49 member 3	4.87329636542288E-07	DOWN
Trpv4	transient receptor potential cation channel, subfamily V, member 4	0.033157111	DOWN
Msi1	musashi RNA-binding protein 1	1.74682796573381E-22	DOWN
Sdsl	serine dehydratase-like	0.005542327	DOWN
Dtx1	deltex 1, E3 ubiquitin ligase	0.027203666	DOWN
Hcar1	hydrocarboxylic acid receptor 1	0.001064316	DOWN
Abcb9	ATP-binding cassette, sub-family B (MDR/TAP), member 9	0.005975352	DOWN
Pitpnm2	phosphatidylinositol transfer protein, membrane-associated 2	1.84467187720355E-06	DOWN

Rflna	refilin A	0.014667734	DOWN
Adgrd1	adhesion G protein-coupled receptor D1	0.006121187	DOWN
Srrm3	serine/arginine repetitive matrix 3	0.003362169	DOWN
Hspb1	heat shock protein 1	3.29544362582775E-14	DOWN
Tfr2	transferrin receptor 2	0.000192828	DOWN
Pdgfa	platelet derived growth factor, alpha	0.001358557	DOWN
Prkar1b	protein kinase, cAMP dependent regulatory, type I beta	7.83267634700203E-08	DOWN
Zfp853	zinc finger protein 853	2.50682656703099E-05	DOWN
Wasf3	WASP family, member 3	0.017216141	DOWN
Col1a2	collagen, type I, alpha 2	1.45474735759197E-05	DOWN
Asb4	ankyrin repeat and SOCS box-containing 4	1.22439944105326E-16	DOWN
Col28a1	collagen, type XXVIII, alpha 1	0.013596724	DOWN
Ppp1r3a	protein phosphatase 1, regulatory subunit 3A	0.009024579	DOWN
Wnt2	wingless-type MMTV integration site family, member 2	0.007736302	DOWN
Kcnd2	potassium voltage-gated channel, Shal-related family, member 2	0.046163199	DOWN
Aass	aminoadipate-semialdehyde synthase	0.023966976	DOWN
Lrrc4	leucine rich repeat containing 4	0.024698776	DOWN
Flnc	filamin C, gamma	0.00504755	DOWN
Kcp	kielin/chordin-like protein	0.000813235	DOWN
Exoc4	exocyst complex component 4	0.000905749	DOWN
Dennd11	DENN domain containing 11	0.01799016	DOWN
Prss37	protease, serine 37	0.005644683	DOWN

Gstk1	glutathione S-transferase kappa 1	0.000666776	DOWN
Epha1	Eph receptor A1	7.27982919588379E-05	DOWN
Tcaf2	TRPM8 channel-associated factor 2	1.82175000812963E-05	DOWN
Zfp786	zinc finger protein 786	1.91208212345607E-05	DOWN
AI854703	expressed sequence AI854703	0.006933713	DOWN
Hoxa3	homeobox A3	0.008329333	DOWN
Hoxa5	homeobox A5	6.56919893610912E-05	DOWN
Hoxa6	homeobox A6	0.000970005	DOWN
Hoxa7	homeobox A7	0.000126667	DOWN
Pde1c	phosphodiesterase 1C	0.005277042	DOWN
Thnsl2	threonine synthase-like 2 (bacterial)	0.044227889	DOWN
Sema4f	sema domain, immunoglobulin domain (Ig), TM domain, and short cytoplasmic domain	9.86387089711773E-10	DOWN
1700003E16Rik	RIKEN cDNA 1700003E16 gene	0.019604784	DOWN
Tet3	tet methylcytosine dioxygenase 3	0.02029725	DOWN
Actg2	actin, gamma 2, smooth muscle, enteric	0.032119775	DOWN
Gata2	GATA binding protein 2	4.47972144912137E-05	DOWN
Podxl2	podocalyxin-like 2	0.009085757	DOWN
Chst13	carbohydrate sulfotransferase 13	0.003621405	DOWN
Slc41a3	solute carrier family 41, member 3	0.04780765	DOWN
Foxp1	forkhead box P1	0.007397017	DOWN
Lhfpl4	lipoma HMGIC fusion partner-like protein 4	0.004447679	DOWN
Creld1	cysteine-rich with EGF-like domains 1	0.000284765	DOWN

Wnt5b	wingless-type MMTV integration site family, member 5B	2.14782870366565E-05	DOWN
B4galnt3	beta-1,4-N-acetyl-galactosaminyl transferase 3	0.019108773	DOWN
Gm10224	predicted pseudogene 10224	0.000319657	DOWN
P3h3	prolyl 3-hydroxylase 3	9.17378767602449E-09	DOWN
Gpr162	G protein-coupled receptor 162	0.019381961	DOWN
Plekhg6	pleckstrin homology domain containing, family G (with RhoGef domain) member 6	0.047969533	DOWN
Ntf3	neurotrophin 3	0.014134684	DOWN
Cracr2a	calcium release activated channel regulator 2A	6.25343949282652E-10	DOWN
Nrip2	nuclear receptor interacting protein 2	0.02029725	DOWN
Mansc1	MANSC domain containing 1	0.015735299	DOWN
Smco3	single-pass membrane protein with coiled-coil domains 3	0.031620969	DOWN
Pde3a	phosphodiesterase 3A, cGMP inhibited	0.027048545	DOWN
Ldhb	lactate dehydrogenase B	0.001898913	DOWN
Sox5	SRY (sex determining region Y)-box 5	0.003362169	DOWN
Bcat1	branched chain aminotransferase 1, cytosolic	0.002903768	DOWN
Itpr2	inositol 1,4,5-triphosphate receptor 2	2.21783357493389E-09	DOWN
Cacng7	calcium channel, voltage-dependent, gamma subunit 7	3.56205085649556E-05	DOWN
Tmc4	transmembrane channel-like gene family 4	0.018537019	DOWN
Tnnt1	troponin T1, skeletal, slow	0.044995597	DOWN
Cox6b2	cytochrome c oxidase subunit 6B2	2.51720492667458E-06	DOWN
Isoc2b	isochorismatase domain containing 2b	6.7597951678026E-07	DOWN
Isoc2a	isochorismatase domain containing 2a	1.39602185621051E-05	DOWN

Gm36210	predicted gene, 36210	0.003850344	DOWN
Ssc5d	scavenger receptor cysteine rich family, 5 domains	0.004051177	DOWN
Ccdc8	coiled-coil domain containing 8	3.19339079880484E-15	DOWN
Hif3a	hypoxia inducible factor 3, alpha subunit	0.019048297	DOWN
Nova2	NOVA alternative splicing regulator 2	0.002775445	DOWN
Exoc3l2	exocyst complex component 3-like 2	0.000424922	DOWN
Bcam	basal cell adhesion molecule	5.67080457508608E-07	DOWN
Bcl3	B cell leukemia/lymphoma 3	0.028854899	DOWN
Zfp112	zinc finger protein 112	0.025264213	DOWN
Tescl	tescalcin-like	0.020211717	DOWN
Zfp575	zinc finger protein 575	1.53766943802123E-09	DOWN
Sptbn4	spectrin beta, non-erythrocytic 4	0.000166384	DOWN
Blvrb	biliverdin reductase B (flavin reductase (NADPH))	1.56483327491913E-06	DOWN
Fcgbpl1	Fc fragment of IgG binding protein like 1	0.038703818	DOWN
Lrfn1	leucine rich repeat and fibronectin type III domain containing 1	7.07350629745153E-06	DOWN
Fbxo27	F-box protein 27	1.32097944109048E-05	DOWN
Aplp1	amyloid beta (A4) precursor-like protein 1	3.59141931272201E-11	DOWN
Sbsn	suprabasin	0.007520669	DOWN
Lgi4	leucine-rich repeat LGI family, member 4	0.007820521	DOWN
Hpn	hepsin	0.043490602	DOWN
Zfp977	zinc finger protein 977	0.005071968	DOWN
Nkg7	natural killer cell group 7 sequence	0.001846597	DOWN

Clec11a	C-type lectin domain family 11, member a	0.000286272	DOWN
Shank1	SH3 and multiple ankyrin repeat domains 1	2.34519635231173E-06	DOWN
1700008O03Rik	RIKEN cDNA 1700008O03 gene	0.007148562	DOWN
Syt3	synaptotagmin III	0.046366925	DOWN
Kcnc3	potassium voltage gated channel, Shaw-related subfamily, member 3	0.017240972	DOWN
Cpt1c	carnitine palmitoyltransferase 1c	0.00144997	DOWN
Dhdh	dihydrodiol dehydrogenase (dimeric)	1.79763879879248E-06	DOWN
Plekha4	pleckstrin homology domain containing, family A (phosphoinositide binding specific) member 4	0.001655616	DOWN
Fgf21	fibroblast growth factor 21	0.00761006	DOWN
Grin2d	glutamate receptor, ionotropic, NMDA2D (epsilon 4)	3.24771755140953E-06	DOWN
Nell1	NEL-like 1	0.000628048	DOWN
Ano5	anoctamin 5	2.59993690997443E-06	DOWN
Gabrb3	gamma-aminobutyric acid (GABA) A receptor, subunit beta 3	5.3849910295246E-06	DOWN
Ndn	necdin, MAGE family member	0.004003947	DOWN
Entrep2	endosomal transmembrane epsin interactor 2	0.016612413	DOWN
St8sia2	ST8 alpha-N-acetyl-neuraminide alpha-2,8-sialyltransferase 2	3.52429323697544E-05	DOWN
Ntrk3	neurotrophic tyrosine kinase, receptor, type 3	4.34695748657223E-14	DOWN
Aen	apoptosis enhancing nuclease	0.000360189	DOWN
Kif7	kinesin family member 7	8.54232077298321E-05	DOWN
Anpep	alanyl (membrane) aminopeptidase	6.34376781243069E-06	DOWN
Ttll13	tubulin tyrosine ligase-like family, member 13	0.007838189	DOWN

Hddc3	HD domain containing 3	0.019638551	DOWN
Tm6sf1	transmembrane 6 superfamily member 1	0.000562343	DOWN
Hdgfl3	HDGF like 3	7.42974044003815E-07	DOWN
Sh3gl3	SH3-domain GRB2-like 3	3.40756796594636E-08	DOWN
Tmc3	transmembrane channel-like gene family 3	0.001129289	DOWN
Cemip	cell migration inducing protein, hyaluronan binding	0.025627456	DOWN
Ctxnd1	cortexin domain containing 1	0.000139224	DOWN
Fah	fumarylacetoacetate hydrolase	0.009131616	DOWN
Ctsc	cathepsin C	0.031391825	DOWN
Rab38	RAB38, member RAS oncogene family	2.11386836277236E-07	DOWN
Fam181b	family with sequence similarity 181, member B	9.90839258038538E-07	DOWN
Dgat2	diacylglycerol O-acyltransferase 2	0.004098871	DOWN
Gdpd5	glycerophosphodiester phosphodiesterase domain containing 5	2.3864182292093E-06	DOWN
Xrra1	X-ray radiation resistance associated 1	0.011407036	DOWN
P4ha3	procollagen-proline, 2-oxoglutarate 4-dioxygenase (proline 4-hydroxylase), alpha polypeptide III	0.016816473	DOWN
Ucp2	uncoupling protein 2 (mitochondrial, proton carrier)	0.001727871	DOWN
Trim34b	tripartite motif-containing 34B	2.7777893164352E-06	DOWN
Stk33	serine/threonine kinase 33	0.026512512	DOWN
Trim66	tripartite motif-containing 66	0.025997852	DOWN
Dkk3	dickkopf WNT signaling pathway inhibitor 3	0.044093984	DOWN
Apobr	apolipoprotein B receptor	0.044867661	DOWN
Htra1	HtrA serine peptidase 1	9.53920498355514E-05	DOWN

Lhpp	phospholysine phosphohistidine inorganic pyrophosphate phosphatase	0.001951078	DOWN
Adam12	a disintegrin and metallopeptidase domain 12 (meltrin alpha)	0.026481601	DOWN
Insyn2a	inhibitory synaptic factor 2A	0.010771691	DOWN
Mgmt	O-6-methylguanine-DNA methyltransferase	2.92515451843817E-20	DOWN
Sprn	shadow of prion protein	0.030396452	DOWN
Zfp941	zinc finger protein 941	0.045834641	DOWN
B4galnt4	beta-1,4-N-acetyl-galactosaminyl transferase 4	3.06418355331354E-06	DOWN
Akap12	A kinase (PRKA) anchor protein (gravin) 12	0.000541664	DOWN
Vip	vasoactive intestinal polypeptide	0.035926471	DOWN
Rgs17	regulator of G-protein signaling 17	0.00559664	DOWN
Ulbp1	UL16 binding protein 1	1.26339669032059E-08	DOWN
Lrp11	low density lipoprotein receptor-related protein 11	0.0092673	DOWN
Txlnb	taxilin beta	0.047764272	DOWN
Il20ra	interleukin 20 receptor, alpha	7.97642943558389E-07	DOWN
Eya4	EYA transcriptional coactivator and phosphatase 4	0.008261237	DOWN
Enpp1	ectonucleotide pyrophosphatase/phosphodiesterase 1	0.019250085	DOWN
L3mbtl3	L3MBTL3 histone methyl-lysine binding protein	0.020495409	DOWN
Lama2	laminin, alpha 2	2.64217562858251E-08	DOWN
Hey2	hairy/enhancer-of-split related with YRPW motif 2	0.001612739	DOWN
Mettl24	methyltransferase like 24	3.78669285577374E-05	DOWN
Sim1	single-minded family bHLH transcription factor 1	0.032838926	DOWN
Ddit4	DNA-damage-inducible transcript 4	0.045826156	DOWN

Adamts14	a disintegrin-like and metallopeptidase (reprolysin type) with thrombospondin type 1 motif, 14	0.007209717	DOWN
Zfp365	zinc finger protein 365	0.042910222	DOWN
Tmem26	transmembrane protein 26	0.03098023	DOWN
Pcdh15	protocadherin 15	0.00080967	DOWN
Gnaz	guanine nucleotide binding protein, alpha z subunit	0.019875697	DOWN
Col18a1	collagen, type XVIII, alpha 1	0.004867275	DOWN
Slc1a6	solute carrier family 1 (high affinity aspartate/glutamate transporter), member 6	1.59260103366495E-05	DOWN
Fstl3	follistatin-like 3	7.154875307254E-20	DOWN
Prss57	protease, serine 57	1.34050376665105E-20	DOWN
Efna2	ephrin A2	0.01132966	DOWN
Jsrp1	junctional sarcoplasmic reticulum protein 1	0.019096605	DOWN
Celf5	CUGBP, Elav-like family member 5	7.35292173016372E-05	DOWN
Fhl4	four and a half LIM domains 4	0.007722493	DOWN
Abtb3	ankyrin repeat and BTB domain containing 3	0.005752036	DOWN
Dram1	DNA-damage regulated autophagy modulator 1	6.97333092301379E-05	DOWN
Ano4	anoctamin 4	0.026416513	DOWN
Anks1b	ankyrin repeat and sterile alpha motif domain containing 1B	0.000358877	DOWN
Acss3	acyl-CoA synthetase short-chain family member 3	0.00104003	DOWN
Csrp2	cysteine and glycine-rich protein 2	0.000743014	DOWN
Caps2	calcyphosphine 2	0.016686758	DOWN
Irak3	interleukin-1 receptor-associated kinase 3	0.005868946	DOWN

Agap2	ArfGAP with GTPase domain, ankyrin repeat and PH domain 2	0.018317693	DOWN
B4galnt1	beta-1,4-N-acetyl-galactosaminyl transferase 1	9.70547266761728E-05	DOWN
Slc26a10	solute carrier family 26, member 10	0.000336588	DOWN
Mmp19	matrix metallopeptidase 19	0.046333629	DOWN
Evi5l	ecotropic viral integration site 5 like	0.002231303	DOWN
Prr36	proline rich 36	0.000390099	DOWN
Lrrc8e	leucine rich repeat containing 8 family, member E	0.003282515	DOWN
Mcf2l	mcf.2 transforming sequence-like	5.44847342921529E-15	DOWN
F7	coagulation factor VII	0.00184753	DOWN
Ank1	ankyrin 1, erythroid	0.046419771	DOWN
Plekha2	pleckstrin homology domain-containing, family A (phosphoinositide binding specific) member 2	0.000589696	DOWN
Adrb3	adrenergic receptor, beta 3	1.58728577532567E-09	DOWN
Rnf122	ring finger protein 122	0.022942437	DOWN
Nrg1	neuregulin 1	0.000499706	DOWN
Tex15	testis expressed gene 15	4.05530202065034E-06	DOWN
AI429214	expressed sequence AI429214	0.006638669	DOWN
Pdgfrl	platelet-derived growth factor receptor-like	4.33009661622447E-10	DOWN
Fam149a	family with sequence similarity 149, member A	0.000139371	DOWN
Sorbs2	sorbin and SH3 domain containing 2	2.93575606181979E-14	DOWN
Ccdc110	coiled-coil domain containing 110	0.030076199	DOWN
1700029J07Rik	RIKEN cDNA 1700029J07 gene	0.01437542	DOWN
Stox2	storkhead box 2	4.21948151818674E-06	DOWN

Spock3	sparc/osteonectin, cwcv and kazal-like domains proteoglycan 3	0.003003458	DOWN
Npy1r	neuropeptide Y receptor Y1	3.40490995701434E-18	DOWN
Psd3	pleckstrin and Sec7 domain containing 3	7.5561961440636E-13	DOWN
Sh2d4a	SH2 domain containing 4A	0.001678517	DOWN
Zfp964	zinc finger protein 964	0.005834657	DOWN
Tssk6	testis-specific serine kinase 6	0.026970341	DOWN
Slc25a42	solute carrier family 25, member 42	0.027085665	DOWN
Tmem59l	transmembrane protein 59-like	0.04492938	DOWN
Gdf15	growth differentiation factor 15	1.51679621871333E-09	DOWN
Nr3c2	nuclear receptor subfamily 3, group C, member 2	0.00800724	DOWN
Rnf150	ring finger protein 150	0.002998703	DOWN
Adgrl1	adhesion G protein-coupled receptor L1	0.013505218	DOWN
Palm3	paralemmin 3	0.012642592	DOWN
Il27ra	interleukin 27 receptor, alpha	0.002379143	DOWN
Fbxw9	F-box and WD-40 domain protein 9	0.034009161	DOWN
Gpt2	glutamic pyruvate transaminase (alanine aminotransferase) 2	0.012873111	DOWN
Chd9	chromodomain helicase DNA binding protein 9	0.000236023	DOWN
Irx3	Iroquois related homeobox 3	0.00010627	DOWN
Mmp2	matrix metallopeptidase 2	0.004970599	DOWN
Cx3cl1	chemokine (C-X3-C motif) ligand 1	0.004225173	DOWN
Ccl17	chemokine (C-C motif) ligand 17	0.028641962	DOWN
Adgrg1	adhesion G protein-coupled receptor G1	0.014446846	DOWN

Cngb1	cyclic nucleotide gated channel beta 1	0.039388909	DOWN
Mmp15	matrix metallopeptidase 15	6.95446128682684E-05	DOWN
Bean1	brain expressed, associated with Nedd4, 1	1.77083104963495E-14	DOWN
Rrad	Ras-related associated with diabetes	0.013346584	DOWN
Hsf4	heat shock transcription factor 4	2.21853348492698E-27	DOWN
Plekhg4	pleckstrin homology domain containing, family G (with RhoGef domain) member 4	7.3716759517794E-11	DOWN
Smpd3	sphingomyelin phosphodiesterase 3, neutral	0.00090507	DOWN
Zfp612	zinc finger protein 612	0.044227889	DOWN
Il34	interleukin 34	2.96953397032723E-07	DOWN
Sdr42e1	short chain dehydrogenase/reductase family 42E, member 1	0.003702135	DOWN
Jph3	junctophilin 3	0.009558044	DOWN
Spata2l	spermatogenesis associated 2-like	0.012038969	DOWN
Tubb3	tubulin, beta 3 class III	7.86751440094567E-05	DOWN
Gm3373	predicted gene 3373	0.002262976	DOWN
Gm3667	predicted gene 3667	0.001584679	DOWN
Gm10406	predicted gene 10406	7.24291554003902E-05	DOWN
Gm3739	predicted gene 3739	1.79730052565856E-05	DOWN
Gm3558	predicted gene 3558	0.004511642	DOWN
Cfap20dc	CFAP20 domain containing	1.03491158776028E-32	DOWN
Fhit	fragile histidine triad gene	5.2730708046289E-07	DOWN
Gm2244	predicted gene 2244	0.003459208	DOWN
Gm2237	predicted gene 2237	5.39536621898842E-06	DOWN

Gm5458	predicted gene 5458	0.000394892	DOWN
Kat6b	K(lysine) acetyltransferase 6B	0.017203469	DOWN
Kcnma1	potassium large conductance calcium-activated channel, subfamily M, alpha member 1	0.001788006	DOWN
Opn4	opsin 4 (melanopsin)	1.80132509430834E-05	DOWN
Ccser2	coiled-coil serine rich 2	3.34514094368824E-05	DOWN
Rab2b	RAB2B, member RAS oncogene family	0.017216141	DOWN
Slc22a17	solute carrier family 22 (organic cation transporter), member 17	3.85121763199568E-05	DOWN
Efs	embryonal Fyn-associated substrate	3.99224374621188E-07	DOWN
Myh7	myosin, heavy polypeptide 7, cardiac muscle, beta	0.007854199	DOWN
Ltb4r2	leukotriene B4 receptor 2	0.000422222	DOWN
Cryl1	crystallin, lambda 1	0.000187207	DOWN
Amer2	APC membrane recruitment 2	0.00719193	DOWN
Defb42	defensin beta 42	9.32652331430283E-05	DOWN
Neil2	nei like 2 (E. coli)	0.008488929	DOWN
Fzd3	frizzled class receptor 3	0.000101971	DOWN
Fbxo16	F-box protein 16	0.000521147	DOWN
Ephx2	epoxide hydrolase 2, cytoplasmic	3.23911539903758E-05	DOWN
Egr3	early growth response 3	0.000870114	DOWN
Phyhip	phytanoyl-CoA hydroxylase interacting protein	3.46648314300704E-11	DOWN
Lgi3	leucine-rich repeat LGI family, member 3	1.8317463431257E-05	DOWN
Dmtn	dematin actin binding protein	0.000369992	DOWN
Lacc1	laccase domain containing 1	0.002916173	DOWN

Ccdc122	coiled-coil domain containing 122	0.002916173	DOWN
Cnmd	chondromodulin	0.020388686	DOWN
Uggt2	UDP-glucose glycoprotein glucosyltransferase 2	2.02526617950999E-67	DOWN
Nalcn	sodium leak channel, non-selective	0.0063356	DOWN
Mmp13	matrix metallopeptidase 13	0.001727871	DOWN
Sesn3	sestrin 3	0.019109801	DOWN
Vstm5	V-set and transmembrane domain containing 5	0.000205185	DOWN
Col5a3	collagen, type V, alpha 3	0.007965619	DOWN
Tmem205	transmembrane protein 205	0.029788119	DOWN
Plppr2	phospholipid phosphatase related 2	0.005212175	DOWN
Igsf9b	immunoglobulin superfamily, member 9B	1.71291172471268E-08	DOWN
St14	suppression of tumorigenicity 14 (colon carcinoma)	0.024236953	DOWN
Robo3	roundabout guidance receptor 3	0.000748622	DOWN
Panx3	pannexin 3	0.007483236	DOWN
Abcg4	ATP binding cassette subfamily G member 4	0.038442836	DOWN
Fxyd6	FXYD domain-containing ion transport regulator 6	1.22154917523309E-18	DOWN
Nxpe4	neurexophilin and PC-esterase domain family, member 4	1.1297971205466E-07	DOWN
Ttc12	tetratricopeptide repeat domain 12	2.22309154542415E-14	DOWN
Dixdc1	DIX domain containing 1	6.15971176795217E-06	DOWN
2310030G06Rik	RIKEN cDNA 2310030G06 gene	2.93587214167008E-05	DOWN
Cib2	calcium and integrin binding family member 2	0.03098023	DOWN
Lingo1	leucine rich repeat and Ig domain containing 1	2.6641096300199E-07	DOWN

Sema7a	sema domain, immunoglobulin domain (Ig), and GPI membrane anchor, (semaphorin) 7A	0.008226096	DOWN
Stra6	stimulated by retinoic acid gene 6	5.2969022173546E-06	DOWN
Islr2	immunoglobulin superfamily containing leucine-rich repeat 2	0.042983078	DOWN
Insyn1	inhibitory synaptic factor 1	2.69021167686629E-22	DOWN
Larp6	La ribonucleoprotein 6, translational regulator	0.006290367	DOWN
Itga11	integrin alpha 11	1.99522494471004E-05	DOWN
Calml4	calmodulin-like 4	0.032654564	DOWN
Igdcc4	immunoglobulin superfamily, DCC subclass, member 4	1.80925424309763E-05	DOWN
Rasl12	RAS-like, family 12	4.88180954739086E-12	DOWN
Car12	carbonic anhydrase 12	0.008465513	DOWN
Myzap	myocardial zonula adherens protein	0.043907763	DOWN
Cgnl1	cingulin-like 1	0.015108528	DOWN
Pygo1	pygopus 1	0.000236613	DOWN
Dnaaf4	dynein axonemal assembly factor 4	0.026092451	DOWN
Wdr72	WD repeat domain 72	0.000134398	DOWN
Atosa	atos homolog A	0.008141863	DOWN
Lysmd2	LysM, putative peptidoglycan-binding, domain containing 2	1.9830722788913E-12	DOWN
Col12a1	collagen, type XII, alpha 1	0.029730455	DOWN
Bckdhb	branched chain ketoacid dehydrogenase E1, beta polypeptide	0.000724032	DOWN
Ctsh	cathepsin H	0.023240748	DOWN
Zic1	zinc finger protein of the cerebellum 1	0.001112915	DOWN
Plod2	procollagen lysine, 2-oxoglutarate 5-dioxygenase 2	0.021874242	DOWN

Slc9a9	solute carrier family 9 (sodium/hydrogen exchanger), member 9	0.00061657	DOWN
Slc35g2	solute carrier family 35, member G2	1.580214265233E-05	DOWN
Slco2a1	solute carrier organic anion transporter family, member 2a1	1.86728308555922E-05	DOWN
Acad11	acyl-Coenzyme A dehydrogenase family, member 11	0.026155987	DOWN
Ackr4	atypical chemokine receptor 4	0.010576794	DOWN
Nek11	NIMA (never in mitosis gene a)-related expressed kinase 11	0.002324134	DOWN
Col6a6	collagen, type VI, alpha 6	9.79134819316685E-05	DOWN
Cish	cytokine inducible SH2-containing protein	0.001613068	DOWN
6430571L13Rik	RIKEN cDNA 6430571L13 gene	0.046260235	DOWN
Mst1r	macrophage stimulating 1 receptor (c-met-related tyrosine kinase)	0.003316052	DOWN
P4htm	prolyl 4-hydroxylase, transmembrane (endoplasmic reticulum)	0.023833386	DOWN
Celsr3	cadherin, EGF LAG seven-pass G-type receptor 3	0.004522409	DOWN
Plxnb1	plexin B1	0.000271267	DOWN
Trim71	tripartite motif-containing 71	0.002174789	DOWN
Tgfbr2	transforming growth factor, beta receptor II	1.48566463466454E-05	DOWN
Itga9	integrin alpha 9	0.048961131	DOWN
Osbp2	oxysterol binding protein 2	0.035330869	DOWN
Sec14l2	SEC14-like lipid binding 2	2.40561083057869E-09	DOWN
Castor1	cytosolic arginine sensor for mTORC1 subunit 1	0.000585758	DOWN
Gck	glucokinase	0.001925565	DOWN
Zpbp	zona pellucida binding protein	1.51679621871333E-09	DOWN
Spata48	spermatogenesis associated 48	6.55741805606714E-05	DOWN

Cobl	cordon-bleu WH2 repeat	5.9282526550072E-08	DOWN
Egfr	epidermal growth factor receptor	1.65740529269217E-10	DOWN
Meis1	Meis homeobox 1	0.020315579	DOWN
Slc1a4	solute carrier family 1 (glutamate/neutral amino acid transporter), member 4	0.040090583	DOWN
Ccdc85a	coiled-coil domain containing 85A	0.001952084	DOWN
Efemp1	epidermal growth factor-containing fibulin-like extracellular matrix protein 1	0.010764759	DOWN
Sh3pxd2b	SH3 and PX domains 2B	1.79502084837999E-06	DOWN
Rnf145	ring finger protein 145	0.000212886	DOWN
Sgcd	sarcoglycan, delta (dystrophin-associated glycoprotein)	0.012845054	DOWN
Flt4	FMS-like tyrosine kinase 4	3.06680464595715E-06	DOWN
Gfpt2	glutamine fructose-6-phosphate transaminase 2	8.25943531979175E-07	DOWN
Ltc4s	leukotriene C4 synthase	0.047137369	DOWN
Adamts2	a disintegrin-like and metallopeptidase (reprolysin type) with thrombospondin type 1 motif, 2	0.029079099	DOWN
Zfp879	zinc finger protein 879	0.018141997	DOWN
Zfp454	zinc finger protein 454	0.017171749	DOWN
Cdkl3	cyclin-dependent kinase-like 3	0.036259058	DOWN
Tcf7	transcription factor 7, T cell specific	0.019048297	DOWN
Shroom1	shroom family member 1	3.90985557896536E-05	DOWN
Pdlim4	PDZ and LIM domain 4	3.71051275864506E-11	DOWN
P4ha2	procollagen-proline, 2-oxoglutarate 4-dioxygenase (proline 4-hydroxylase), alpha II polypeptide	0.012251084	DOWN

Lyrm7	LYR motif containing 7	0.000275763	DOWN
Gpx3	glutathione peroxidase 3	2.28412441639162E-05	DOWN
Sparc	secreted acidic cysteine rich glycoprotein	5.79027039457633E-08	DOWN
Zfp39	zinc finger protein 39	0.001077371	DOWN
Zfp867	zinc finger protein 867	0.049361401	DOWN
Slc5a10	solute carrier family 5 (sodium/glucose cotransporter), member 10	0.049068914	DOWN
Adora2b	adenosine A2b receptor	0.028343616	DOWN
Zswim7	zinc finger SWIM-type containing 7	6.6765074492785E-06	DOWN
Myh10	myosin, heavy polypeptide 10, non-muscle	0.043029635	DOWN
Arhgef15	Rho guanine nucleotide exchange factor (GEF) 15	0.001408064	DOWN
Slc25a35	solute carrier family 25, member 35	2.74351612725914E-05	DOWN
Kdm6b	KDM1 lysine (K)-specific demethylase 6B	3.36710710770812E-06	DOWN
Atp1b2	ATPase, Na+/K+ transporting, beta 2 polypeptide	0.003131098	DOWN
Sat2	spermidine/spermine N1-acetyl transferase 2	0.004356585	DOWN
Fgf11	fibroblast growth factor 11	0.000185552	DOWN
Tmem95	transmembrane protein 95	0.009319767	DOWN
Kctd11	potassium channel tetramerisation domain containing 11	0.006453952	DOWN
Slc16a11	solute carrier family 16 (monocarboxylic acid transporters), member 11	4.98720399823402E-06	DOWN
Slc16a13	solute carrier family 16 (monocarboxylic acid transporters), member 13	5.52974941760165E-07	DOWN
Bcl6b	B cell CLL/lymphoma 6, member B	0.00041927	DOWN
Alox12	arachidonate 12-lipoxygenase	0.043430287	DOWN

Gp1ba	glycoprotein 1b, alpha polypeptide	0.017909009	DOWN
Inca1	inhibitor of CDK, cyclin A1 interacting protein 1	0.046881286	DOWN
Aipl1	aryl hydrocarbon receptor-interacting protein-like 1	0.001909348	DOWN
Pitpnm3	PITPNM family member 3	5.58647124793611E-07	DOWN
Spns2	SPNS lysolipid transporter 2, sphingosine-1-phosphate	0.001084036	DOWN
Camkk1	calcium/calmodulin-dependent protein kinase kinase 1, alpha	6.7789847763988E-05	DOWN
Serpinf1	serine (or cysteine) peptidase inhibitor, clade F, member 1	0.01097303	DOWN
Doc2b	double C2, beta	6.26768661732888E-05	DOWN
Lgals9	lectin, galactose binding, soluble 9	0.003868368	DOWN
Rhbdl3	rhomboid like 3	0.002262976	DOWN
Rasl10b	RAS-like, family 10, member B	0.00074392	DOWN
Wfdc18	WAP four-disulfide core domain 18	0.037698128	DOWN
Tspoap1	TSPO associated protein 1	0.003892335	DOWN
Mks1	MKS transition zone complex subunit 1	3.41891586611081E-07	DOWN
Msi2	musashi RNA-binding protein 2	0.042132963	DOWN
Wfikkn2	WAP, follistatin/kazal, immunoglobulin, kunitz and netrin domain containing 2	0.002614297	DOWN
Cacna1g	calcium channel, voltage-dependent, T type, alpha 1G subunit	2.33952804744216E-19	DOWN
Mycbpap	MYCBP associated protein	0.000323866	DOWN
Col1a1	collagen, type I, alpha 1	0.00040869	DOWN
Sgca	sarcoglycan, alpha (dystrophin-associated glycoprotein)	0.00370545	DOWN
Nxph3	neurexophilin 3	0.0326829	DOWN
Copz2	coatomer protein complex, subunit zeta 2	0.005514835	DOWN

Sp6	trans-acting transcription factor 6	0.02360438	DOWN
Scrn2	secernin 2	0.004036931	DOWN
Cacnb1	calcium channel, voltage-dependent, beta 1 subunit	0.00285034	DOWN
Csf3	colony stimulating factor 3 (granulocyte)	0.000943298	DOWN
Rapgefl1	Rap guanine nucleotide exchange factor (GEF)-like 1	0.013678185	DOWN
Igfbp4	insulin-like growth factor binding protein 4	4.04682683832607E-05	DOWN
Krt20	keratin 20	4.17698193028407E-07	DOWN
Klhl10	kelch-like 10	0.016115779	DOWN
Odad4	outer dynein arm complex subunit 4	0.008369177	DOWN
Tubg2	tubulin, gamma 2	0.018456523	DOWN
Wnk4	WNK lysine deficient protein kinase 4	0.000730126	DOWN
Asb16	ankyrin repeat and SOCS box-containing 16	0.000143438	DOWN
Itga2b	integrin alpha 2b	7.81930509247606E-07	DOWN
Adam11	a disintegrin and metallopeptidase domain 11	1.58132494456791E-05	DOWN
Arhgap27	Rho GTPase activating protein 27	0.026638756	DOWN
1810010H24Rik	RIKEN cDNA 1810010H24 gene	0.014590446	DOWN
Cep112	centrosomal protein 112	5.44066128601809E-06	DOWN
Sox9	SRY (sex determining region Y)-box 9	0.034028728	DOWN
Sdk2	sidekick cell adhesion molecule 2	7.63439816450728E-07	DOWN
Dnai2	dynein axonemal intermediate chain 2	0.039630568	DOWN
Kif19a	kinesin family member 19A	0.009751556	DOWN
Gprc5c	G protein-coupled receptor, family C, group 5, member C	2.48205207642461E-18	DOWN

Nat9	N-acetyltransferase 9 (GCN5-related, putative)	0.014663896	DOWN
Cdr2l	cerebellar degeneration-related protein 2-like	1.00414344031248E-05	DOWN
Rhbdf2	rhomboid 5 homolog 2	0.007278182	DOWN
Mgat5b	mannoside acetylglucosaminyltransferase 5, isoenzyme B	0.027707273	DOWN
Tbc1d16	TBC1 domain family, member 16	0.00017903	DOWN
Slc38a10	solute carrier family 38, member 10	0.001149643	DOWN
Bahcc1	BAH domain and coiled-coil containing 1	2.93173006181329E-10	DOWN
Pycr1	pyrroline-5-carboxylate reductase 1	0.010483693	DOWN
Rac3	Rac family small GTPase 3	9.81685997070784E-08	DOWN
Slc16a3	solute carrier family 16 (monocarboxylic acid transporters), member 3	0.03098023	DOWN
Rab40b	Rab40B, member RAS oncogene family	0.000818474	DOWN
Zfp750	zinc finger protein 750	1.03110382993088E-06	DOWN
Ryr2	ryanodine receptor 2, cardiac	0.043713091	DOWN
Inhba	inhibin beta-A	0.013824915	DOWN
Foxc1	forkhead box C1	2.22970375001413E-08	DOWN
Serpinb1a	serine (or cysteine) peptidase inhibitor, clade B, member 1a	0.011604603	DOWN
Serpinb9	serine (or cysteine) peptidase inhibitor, clade B, member 9	0.047006719	DOWN
Cage1	cancer antigen 1	0.03974576	DOWN
Dsp	desmoplakin	8.88803123624851E-10	DOWN
Nhlrc1	NHL repeat containing 1	0.000637244	DOWN
Ptpdc1	protein tyrosine phosphatase domain containing 1	1.580214265233E-05	DOWN
Ogn	osteoglycin	0.040419159	DOWN

S1pr3	sphingosine-1-phosphate receptor 3	0.022863865	DOWN
Gadd45g	growth arrest and DNA-damage-inducible 45 gamma	0.031102958	DOWN
Prr7	proline rich 7 (synaptic)	0.004023655	DOWN
Dbn1	drebrin 1	7.79172317606226E-05	DOWN
Zfp457	zinc finger protein 457	0.032044496	DOWN
Zfp456	zinc finger protein 456	2.00279030095274E-10	DOWN
Edil3	EGF-like repeats and discoidin I-like domains 3	5.03979455092685E-06	DOWN
Vcan	versican	0.014063746	DOWN
Foxd1	forkhead box D1	0.01741691	DOWN
Serf1	small EDRK-rich factor 1	4.63561784382677E-07	DOWN
Ccdc125	coiled-coil domain containing 125	0.038451756	DOWN
Adamts6	a disintegrin-like and metallopeptidase (reprolysin type) with thrombospondin type 1 motif, 6	0.000236023	DOWN
Plk2	polo like kinase 2	5.52188207296504E-05	DOWN
Ankrd55	ankyrin repeat domain 55	1.27744952152746E-05	DOWN
Il6st	interleukin 6 signal transducer	0.000365266	DOWN
Itga2	integrin alpha 2	0.008595101	DOWN
Nim1k	NIM1 serine/threonine protein kinase	0.00021386	DOWN
Adcy3	adenylate cyclase 3	0.000148651	DOWN
Pfn4	profilin family, member 4	1.01139603298136E-07	DOWN
Fkbp1b	FK506 binding protein 1b	0.015438393	DOWN
Mboat2	membrane bound O-acyltransferase domain containing 2	2.8908518510849E-23	DOWN
Sox11	SRY (sex determining region Y)-box 11	8.15236727649545E-09	DOWN

Fam110c	family with sequence similarity 110, member C	0.009232217	DOWN
Ahr	aryl-hydrocarbon receptor	0.001684703	DOWN
Scin	scinderin	0.006742868	DOWN
Prkd1	protein kinase D1	6.12291827084291E-12	DOWN
Akap6	A kinase (PRKA) anchor protein 6	0.000461905	DOWN
Slc25a21	solute carrier family 25 (mitochondrial oxodicarboxylate carrier), member 21	2.48913724697301E-10	DOWN
Gpr135	G protein-coupled receptor 135	1.01139603298136E-07	DOWN
L3hypdh	L-3-hydroxyproline dehydratase (trans-)	0.001011536	DOWN
Six1	sine oculis-related homeobox 1	0.002076734	DOWN
Six4	sine oculis-related homeobox 4	0.017419645	DOWN
Slc38a6	solute carrier family 38, member 6	0.001156445	DOWN
Ppp1r36	protein phosphatase 1, regulatory subunit 36	0.002380726	DOWN
Rab15	RAB15, member RAS oncogene family	1.56788011168936E-10	DOWN
Plek2	pleckstrin 2	0.001906147	DOWN
Tmem229b	transmembrane protein 229B	0.041656492	DOWN
Zfp36l1	zinc finger protein 36, C3H type-like 1	0.008940652	DOWN
Smoc1	SPARC related modular calcium binding 1	5.30151261820957E-08	DOWN
Ttc9	tetratricopeptide repeat domain 9	1.78788129201378E-09	DOWN
Acot1	acyl-CoA thioesterase 1	7.07453342734555E-12	DOWN
Acot6	acyl-CoA thioesterase 6	0.038760657	DOWN
Pgf	placental growth factor	1.7503643871195E-07	DOWN
Mlh3	mutL homolog 3	0.001602922	DOWN

Batf	basic leucine zipper transcription factor, ATF-like	0.031764531	DOWN
Vash1	vasohibin 1	1.74329748896438E-06	DOWN
Ism2	isthmin 2	0.021956969	DOWN
Ston2	stonin 2	3.82539442364664E-05	DOWN
Kcnk10	potassium channel, subfamily K, member 10	7.36928357729144E-05	DOWN
Asb2	ankyrin repeat and SOCS box-containing 2	0.013760327	DOWN
Otub2	OTU domain, ubiquitin aldehyde binding 2	0.002158562	DOWN
Ppp4r4	protein phosphatase 4, regulatory subunit 4	9.18734445351892E-06	DOWN
Clmn	calmin	6.55421537253042E-13	DOWN
Bdkrb2	bradykinin receptor, beta 2	0.002102299	DOWN
Hhipl1	hedgehog interacting protein-like 1	3.78211887146526E-08	DOWN
Eml1	echinoderm microtubule associated protein like 1	0.011469639	DOWN
Tnfaip2	tumor necrosis factor, alpha-induced protein 2	5.79373318455454E-12	DOWN
Gm266	predicted gene 266	0.004364626	DOWN
Inf2	inverted formin, FH2 and WH2 domain containing	0.007907338	DOWN
Itgb8	integrin beta 8	0.031476446	DOWN
Card6	caspase recruitment domain family, member 6	0.00693502	DOWN
C1qtnf3	C1q and tumor necrosis factor related protein 3	0.00099207	DOWN
Adamts12	a disintegrin-like and metallopeptidase (reprolysin type) with thrombospondin type 1 motif, 12	0.002642707	DOWN
Npr3	natriuretic peptide receptor 3	4.77136162177178E-05	DOWN
Cdh10	cadherin 10	2.66469331293343E-31	DOWN
Cdh18	cadherin 18	0.001909348	DOWN

Marchf11	membrane associated ring-CH-type finger 11	0.012977792	DOWN
Nipal2	NIPA-like domain containing 2	0.000674076	DOWN
Cthrc1	collagen triple helix repeat containing 1	3.65742750658174E-12	DOWN
Rspo2	R-spondin 2	0.017240972	DOWN
Tnfrsf11b	tumor necrosis factor receptor superfamily, member 11b (osteoprotegerin)	1.70336825595119E-09	DOWN
Psca	prostate stem cell antigen	0.005164749	DOWN
Lynx1	Ly6/neurotoxin 1	0.001959585	DOWN
Rhpn1	rhophilin, Rho GTPase binding protein 1	0.043329919	DOWN
Smpd5	sphingomyelin phosphodiesterase 5	0.040678589	DOWN
Myh9	myosin, heavy polypeptide 9, non-muscle	0.031981792	DOWN
C1qtnf6	C1q and tumor necrosis factor related protein 6	0.002359358	DOWN
Kcnj4	potassium inwardly-rectifying channel, subfamily J, member 4	1.72584593321021E-14	DOWN
Pheta2	PH domain containing endocytic trafficking adaptor 2	0.000449295	DOWN
Cyp2d22	cytochrome P450, family 2, subfamily d, polypeptide 22	0.003725274	DOWN
Scube1	signal peptide, CUB domain, EGF-like 1	4.39378808841167E-05	DOWN
Parvb	parvin, beta	5.14252494259144E-08	DOWN
Shisal1	shisa like 1	0.033157111	DOWN
Rtl6	retrotransposon Gag like 6	0.017874266	DOWN
Prr5	proline rich 5 (renal)	0.046756245	DOWN
Arhgap8	Rho GTPase activating protein 8	0.017240972	DOWN
Phf21b	PHD finger protein 21B	0.007760437	DOWN
Tafa5	TAFA chemokine like family member 5	5.86713856221758E-12	DOWN

Mapk11	mitogen-activated protein kinase 11	0.003311284	DOWN
Shank3	SH3 and multiple ankyrin repeat domains 3	3.7885874711203E-05	DOWN
Pdzrn4	PDZ domain containing RING finger 4	0.042208812	DOWN
Slc38a1	solute carrier family 38, member 1	1.36085516678915E-27	DOWN
Vdr	vitamin D (1,25-dihydroxyvitamin D3) receptor	0.036720941	DOWN
Col2a1	collagen, type II, alpha 1	3.78164077167945E-22	DOWN
Zfp641	zinc finger protein 641	0.00013763	DOWN
Fkbp11	FK506 binding protein 11	0.000730126	DOWN
Wnt10b	wingless-type MMTV integration site family, member 10B	1.07341042872245E-18	DOWN
Slc4a8	solute carrier family 4 (anion exchanger), member 8	2.22970375001413E-08	DOWN
Fignl2	fidgetin-like 2	0.008605986	DOWN
Krt84	keratin 84	0.032903602	DOWN
Sp7	Sp7 transcription factor 7	0.000179269	DOWN
Nfe2	nuclear factor, erythroid derived 2	0.013478627	DOWN
Pde1b	phosphodiesterase 1B, Ca2+-calmodulin dependent	0.001374112	DOWN
Ppp1r1a	protein phosphatase 1, regulatory inhibitor subunit 1A	8.23974079969465E-09	DOWN
Srl	sarcalumenin	0.000180755	DOWN
Rogdi	rogdi homolog	0.000375879	DOWN
Ppl	periplakin	0.010953028	DOWN
Rbfox1	RNA binding protein, fox-1 homolog (C. elegans) 1	1.32187745215227E-09	DOWN
Ciita	class II transactivator	0.017171749	DOWN
Clec16a	C-type lectin domain family 16, member A	5.79561235388655E-06	DOWN

Socs1	suppressor of cytokine signaling 1	0.007585273	DOWN
Snx29	sorting nexin 29	0.041256088	DOWN
A930007A09Rik	RIKEN cDNA A930007A09 gene	0.019017176	DOWN
Ifitm7	interferon induced transmembrane protein 7	0.003073758	DOWN
Bmerb1	bMERB domain containing 1	4.88151075669895E-10	DOWN
2610318N02Rik	RIKEN cDNA 2610318N02 gene	2.53085676484875E-07	DOWN
Ydjc	YdjC homolog (bacterial)	0.039545647	DOWN
Eef1ece2	Eef1akmt4-endothelin converting enzyme 2 readthrough	1.56056679964803E-27	DOWN
Ece2	endothelin converting enzyme 2	8.05223743904562E-105	DOWN
Fam131a	family with sequence similarity 131, member A	0.004023655	DOWN
2510009E07Rik	RIKEN cDNA 2510009E07 gene	0.001761696	DOWN
Dgkg	diacylglycerol kinase, gamma	2.89919158098043E-08	DOWN
Kng1	kininogen 1	0.005113562	DOWN
Cldn1	claudin 1	7.63439816450728E-07	DOWN
Cpn2	carboxypeptidase N, polypeptide 2	0.041302099	DOWN
Kalrn	kalirin, RhoGEF kinase	5.49398425331749E-12	DOWN
Fstl1	follistatin-like 1	3.75628569495656E-06	DOWN
Gap43	growth associated protein 43	0.021958365	DOWN
Gramd1c	GRAM domain containing 1C	2.7152932550379E-12	DOWN
Cd200	CD200 molecule	2.49401950324408E-55	DOWN
Tagln3	transgelin 3	0.038689985	DOWN

Nfkbiz	nuclear factor of kappa light polypeptide gene enhancer in B cells inhibitor, zeta	0.008595101	DOWN
Abi3bp	ABI family member 3 binding protein	0.000567774	DOWN
Pros1	protein S (alpha)	0.045497491	DOWN
Htr1f	5-hydroxytryptamine (serotonin) receptor 1F	0.014808011	DOWN
Nrip1	nuclear receptor interacting protein 1	9.48944874202002E-05	DOWN
Tiam1	T cell lymphoma invasion and metastasis 1	3.64305390675113E-51	DOWN
Sh3bgr	SH3-binding domain glutamic acid-rich protein	0.036481218	DOWN
Rps6ka2	ribosomal protein S6 kinase, polypeptide 2	0.047332842	DOWN
Fndc1	fibronectin type III domain containing 1	0.006968139	DOWN
Prkn	parkin RBR E3 ubiquitin protein ligase	0.025282014	DOWN
Lix1	limb and CNS expressed 1	0.004098871	DOWN
Mmp25	matrix metallopeptidase 25	0.000605128	DOWN
Sox8	SRY (sex determining region Y)-box 8	0.015401047	DOWN
Fbxl16	F-box and leucine-rich repeat protein 16	9.2602875480089E-13	DOWN
Nme4	NME/NM23 nucleoside diphosphate kinase 4	4.50226333296517E-06	DOWN
Arhgdig	Rho GDP dissociation inhibitor (GDI) gamma	9.83199864020084E-06	DOWN
Syngap1	synaptic Ras GTPase activating protein 1 homolog (rat)	0.020388686	DOWN
Scube3	signal peptide, CUB domain, EGF-like 3	7.83267634700203E-08	DOWN
Slc26a8	solute carrier family 26, member 8	0.019083014	DOWN
Cdkn1a	cyclin-dependent kinase inhibitor 1A (P21)	0.004727758	DOWN
Mdga1	MAM domain containing glycosylphosphatidylinositol anchor 1	0.020970881	DOWN
Rsph1	radial spoke head 1 homolog (Chlamydomonas)	0.000284144	DOWN

Pde9a	phosphodiesterase 9A	2.2814587134662E-05	DOWN
Notch3	notch 3	6.75844723055816E-05	DOWN
Zfp811	zinc finger protein 811	0.014864948	DOWN
Cyp4f13	cytochrome P450, family 4, subfamily f, polypeptide 13	0.000139954	DOWN
Col11a2	collagen, type XI, alpha 2	0.049205198	DOWN
H2-DMb1	histocompatibility 2, class II, locus Mb1	0.003669047	DOWN
Tap1	transporter 1, ATP-binding cassette, sub-family B (MDR/TAP)	0.029788119	DOWN
Notch4	notch 4	0.000645733	DOWN
Prrt1	proline-rich transmembrane protein 1	0.005343688	DOWN
H2-T10	histocompatibility 2, T region locus 10	0.042882688	DOWN
Tubb4a	tubulin, beta 4A class IVA	0.008465513	DOWN
Vit	vitrin	0.001068697	DOWN
Qpct	glutaminyl-peptide cyclotransferase (glutaminyl cyclase)	0.000309069	DOWN
Kdm5d	lysine (K)-specific demethylase 5D	0.002974969	DOWN
Eif2s3y	eukaryotic translation initiation factor 2, subunit 3, structural gene Y-linked	0.022209503	DOWN
Uty	ubiquitously transcribed tetratricopeptide repeat containing, Y-linked	0.002532829	DOWN
Ddx3y	DEAD box helicase 3, Y-linked	0.006861904	DOWN
Svil	supervillin	6.69574003324058E-05	DOWN
Zfp438	zinc finger protein 438	0.030507976	DOWN
Mpp7	membrane protein, palmitoylated 7 (MAGUK p55 subfamily member 7)	0.010109451	DOWN
Riok3	RIO kinase 3	1.08777309815948E-07	DOWN

Lama3	laminin, alpha 3	6.66395482820443E-07	DOWN
Ttc39c	tetratricopeptide repeat domain 39C	0.000101541	DOWN
Psma8	proteasome subunit alpha 8	0.000680345	DOWN
Kctd1	potassium channel tetramerisation domain containing 1	0.004248846	DOWN
Dsc2	desmocollin 2	0.020889895	DOWN
Rnf125	ring finger protein 125	0.018122421	DOWN
Klhl14	kelch-like 14	4.65271722618844E-06	DOWN
Asxl3	ASXL transcriptional regulator 3	1.90619651445466E-13	DOWN
Nrep	neuronal regeneration related protein	0.015543023	DOWN
Reep2	receptor accessory protein 2	6.55308593864467E-05	DOWN
Lrrtm2	leucine rich repeat transmembrane neuronal 2	0.001634456	DOWN
Nrg2	neuregulin 2	0.025832519	DOWN
Pcdhb7	protocadherin beta 7	0.002654062	DOWN
Pcdhb15	protocadherin beta 15	0.038403671	DOWN
Pcdhb16	protocadherin beta 16	0.008840134	DOWN
Pcdhb17	protocadherin beta 17	0.036259058	DOWN
Pcdhb18	protocadherin beta 18	7.12823343718813E-06	DOWN
Pcdh1	protocadherin 1	6.43619549094492E-05	DOWN
Nr3c1	nuclear receptor subfamily 3, group C, member 1	4.58763731450884E-05	DOWN
Jakmip2	janus kinase and microtubule interacting protein 2	0.000485603	DOWN
Lox	lysyl oxidase	6.04137289448062E-05	DOWN
Ppic	peptidylprolyl isomerase C	1.67583300126298E-06	DOWN

Gramd2b	GRAM domain containing 2B	0.000949829	DOWN
Fbn2	fibrillin 2	2.14843885622624E-07	DOWN
Smim3	small integral membrane protein 3	1.61857550849384E-16	DOWN
Synpo	synaptopodin	1.329649073182E-05	DOWN
Arsi	arylsulfatase i	0.007656886	DOWN
Afap1l1	actin filament associated protein 1-like 1	0.003300708	DOWN
Sh3tc2	SH3 domain and tetratricopeptide repeats 2	0.008160744	DOWN
Piezo2	piezo-type mechanosensitive ion channel component 2	0.004036931	DOWN
Zfp532	zinc finger protein 532	6.86135466031837E-12	DOWN
Rax	retina and anterior neural fold homeobox	0.010201855	DOWN
Mc2r	melanocortin 2 receptor	0.0297566	DOWN
Ccdc68	coiled-coil domain containing 68	0.023564953	DOWN
Dcc	deleted in colorectal carcinoma	0.026631687	DOWN
Mro	maestro	0.008724107	DOWN
Mapk4	mitogen-activated protein kinase 4	9.4844113180184E-05	DOWN
Katnal2	katanin p60 subunit A-like 2	2.10636792325081E-05	DOWN
Slc14a1	solute carrier family 14 (urea transporter), member 1	0.000341191	DOWN
Zfp516	zinc finger protein 516	0.000185588	DOWN
Dok6	docking protein 6	1.3371755902808E-07	DOWN
Gm45871	predicted gene 45871	0.006933713	DOWN
Aldh3b1	aldehyde dehydrogenase 3 family, member B1	0.033882745	DOWN
Unc93b1	unc-93 homolog B1, TLR signaling regulator	2.07825465325893E-14	DOWN

Ctsf	cathepsin F	0.000157658	DOWN
Actn3	actinin alpha 3	0.048796324	DOWN
Bbs1	Bardet-Biedl syndrome 1 (human)	0.014467802	DOWN
Npas4	neuronal PAS domain protein 4	0.000205274	DOWN
Cnih2	cornichon family AMPA receptor auxiliary protein 2	4.90513205841175E-05	DOWN
Asrgl1	asparaginase like 1	0.001441626	DOWN
Myrf	myelin regulatory factor	1.73270450578127E-05	DOWN
Dagla	diacylglycerol lipase, alpha	0.00691265	DOWN
Syt7	synaptotagmin VII	2.38944742576343E-06	DOWN
Lrrc10b	leucine rich repeat containing 10B	0.000958882	DOWN
Gcnt1	glucosaminyl (N-acetyl) transferase 1, core 2	6.36883946217042E-06	DOWN
Aldh1a1	aldehyde dehydrogenase family 1, subfamily A1	0.002013933	DOWN
Fas	Fas (TNF receptor superfamily member 6)	0.000268242	DOWN
Hoga1	4-hydroxy-2-oxoglutarate aldolase 1	2.39085152088682E-07	DOWN
Pyroxd2	pyridine nucleotide-disulphide oxidoreductase domain 2	1.54439650177339E-08	DOWN
Sema4g	sema domain, immunoglobulin domain (Ig), transmembrane domain (TM) and short cytoplasmic domain, (semaphorin) 4G	0.000599876	DOWN
Ina	internexin neuronal intermediate filament protein, alpha	0.023831045	DOWN
Neurl1a	neuralized E3 ubiquitin protein ligase 1A	2.7841302381914E-21	DOWN
Prex2	phosphatidylinositol-3,4,5-trisphosphate-dependent Rac exchange factor 2	0.004638602	UP
Slco5a1	solute carrier organic anion transporter family, member 5A1	0.01567607	UP
Kcnb2	potassium voltage gated channel, Shab-related subfamily, member 2	8.65053607619093E-07	UP

Tfap2b	transcription factor AP-2 beta	3.31224728461151E-09	UP
Mcm3	minichromosome maintenance complex component 3	0.04654406	UP
Col9a1	collagen, type IX, alpha 1	0.006643787	UP
Bend6	BEN domain containing 6	6.21624245117928E-06	UP
Ptpn18	protein tyrosine phosphatase, non-receptor type 18	0.039630568	UP
Aff3	AF4/FMR2 family, member 3	4.79579700659607E-06	UP
Creg2	cellular repressor of E1A-stimulated genes 2	0.002380726	UP
Mfsd6	major facilitator superfamily domain containing 6	0.000323866	UP
Stk17b	serine/threonine kinase 17b (apoptosis-inducing)	0.00023777	UP
Hecw2	HECT, C2 and WW domain containing E3 ubiquitin protein ligase 2	0.000156996	UP
Cd28	CD28 antigen	0.001962986	UP
Zdbf2	zinc finger, DBF-type containing 2	0.017802337	UP
Map2	microtubule-associated protein 2	0.017698729	UP
Erbb4	erb-b2 receptor tyrosine kinase 4	0.018041125	UP
Igfbp5	insulin-like growth factor binding protein 5	0.045092291	UP
Dock10	dedicator of cytokinesis 10	0.032644759	UP
Nyap2	neuronal tyrosine-phophorylated phosphoinositide 3-kinase adaptor 2	9.54794764378574E-06	UP
Htr2b	5-hydroxytryptamine (serotonin) receptor 2B	9.51150418202673E-10	UP
A730008H23Rik	RIKEN cDNA A730008H23 gene	3.62648917648837E-06	UP
Klhl30	kelch-like 30	8.05987461417143E-05	UP
Gal3st2	galactose-3-O-sulfotransferase 2	0.011032048	UP
St8sia4	ST8 alpha-N-acetyl-neuraminide alpha-2,8-sialyltransferase 4	3.15715751182778E-06	UP

Rnf152	ring finger protein 152	1.31168208036132E-06	UP
Tnfrsf11a	tumor necrosis factor receptor superfamily, member 11a, NFKB activator	0.000714413	UP
Htr5b	5-hydroxytryptamine (serotonin) receptor 5B	0.027776207	UP
Cxcr4	chemokine (C-X-C motif) receptor 4	0.000645448	UP
Cd55	CD55 molecule, decay accelerating factor for complement	0.044600716	UP
Ube2t	ubiquitin-conjugating enzyme E2T	0.017240972	UP
Lhx9	LIM homeobox protein 9	3.06418355331354E-06	UP
Rgs1	regulator of G-protein signaling 1	0.014904629	UP
Rgs18	regulator of G-protein signaling 18	0.034156798	UP
Hmcn1	hemicentin 1	1.19634581776196E-05	UP
Rgl1	ral guanine nucleotide dissociation stimulator,-like 1	0.008151546	UP
Ncf2	neutrophil cytosolic factor 2	0.03935719	UP
Lamc2	laminin, gamma 2	0.031110597	UP
Astn1	astrotactin 1	0.002295806	UP
Tnn	tenascin N	0.001089962	UP
Rxrg	retinoid X receptor gamma	0.004870715	UP
Hsd17b7	hydroxysteroid (17-beta) dehydrogenase 7	0.021630243	UP
Gm7694	predicted gene 7694	0.00381504	UP
Nos1ap	nitric oxide synthase 1 (neuronal) adaptor protein	0.003130562	UP
Kcnj10	potassium inwardly-rectifying channel, subfamily J, member 10	0.023397357	UP
Igsf9	immunoglobulin superfamily, member 9	7.59440351302567E-05	UP
Aim2	absent in melanoma 2	0.015480843	UP

Dnah14	dynein, axonemal, heavy chain 14	0.000394858	UP
Lbr	lamin B receptor	0.002242237	UP
Esrrg	estrogen-related receptor gamma	0.029452364	UP
Flvcr1	feline leukemia virus subgroup C cellular receptor 1	7.8400897875242E-06	UP
Nmt2	N-myristoyltransferase 2	0.001905572	UP
Bend7	BEN domain containing 7	0.022907181	UP
Gata3	GATA binding protein 3	0.000218238	UP
Cubn	cubilin (intrinsic factor-cobalamin receptor)	0.009751556	UP
Otud1	OTU domain containing 1	0.007760437	UP
Hnmt	histamine N-methyltransferase	8.73171059869494E-05	UP
Dpp7	dipeptidylpeptidase 7	0.01522216	UP
Fcna	ficolin A	0.001213725	UP
Sh2d3c	SH2 domain containing 3C	0.026529115	UP
Ttll11	tubulin tyrosine ligase-like family, member 11	0.012602231	UP
Lhx2	LIM homeobox protein 2	3.02106020715016E-11	UP
Lypd6	LY6/PLAUR domain containing 6	0.026469003	UP
Cytip	cytohesin 1 interacting protein	1.79502084837999E-06	UP
Spc25	SPC25, NDC80 kinetochore complex component, homolog (S. cerevisiae)	0.005652488	UP
Abcb11	ATP-binding cassette, sub-family B (MDR/TAP), member 11	0.003473233	UP
Evx2	even-skipped homeobox 2	8.56086362098313E-07	UP
Hoxd13	homeobox D13	6.46653804179922E-07	UP
Hoxd12	homeobox D12	4.8847649040139E-06	UP

Hoxd11	homeobox D11	2.5554591888473E-06	UP
Hoxd10	homeobox D10	6.41361292697324E-11	UP
Hoxd3	homeobox D3	5.39207178970483E-05	UP
Selenoh	selenoprotein H	0.000274142	UP
Mdk	midkine	7.86751440094567E-05	UP
Hsd17b12	hydroxysteroid (17-beta) dehydrogenase 12	8.00837017234412E-14	UP
Depdc7	DEP domain containing 7	0.029274447	UP
Katnbl1	katanin p80 subunit B like 1	0.001840446	UP
Scg5	secretogranin V	0.039486116	UP
Oip5	Opa interacting protein 5	0.015946946	UP
Wdr76	WD repeat domain 76	0.018102376	UP
Frmd5	FERM domain containing 5	1.21740361542121E-05	UP
Trim69	tripartite motif-containing 69	0.040015006	UP
Duoxa1	dual oxidase maturation factor 1	0.03451623	UP
Rassf2	Ras association (RalGDS/AF-6) domain family member 2	0.013955294	UP
Pcna	proliferating cell nuclear antigen	0.000444951	UP
Bmp2	bone morphogenetic protein 2	0.000156373	UP
Flrt3	fibronectin leucine rich transmembrane protein 3	0.013092987	UP
Cd93	CD93 antigen	2.22428000986083E-06	UP
Cst3	cystatin C	3.94485712377604E-06	UP
Ahcy	S-adenosylhomocysteine hydrolase	1.65740529269217E-10	UP
Acss2	acyl-CoA synthetase short-chain family member 2	0.005277042	UP

Pkig	protein kinase inhibitor, gamma	0.005134672	UP
Tnnc2	troponin C2, fast	0.010339098	UP
Neurl2	neuralized E3 ubiquitin protein ligase 2	0.001064316	UP
Pard6b	par-6 family cell polarity regulator beta	0.044309159	UP
Nfatc2	nuclear factor of activated T cells, cytoplasmic, calcineurin dependent 2	0.021375234	UP
Tshz2	teashirt zinc finger family member 2	2.39957278979425E-06	UP
Aurka	aurora kinase A	0.017788266	UP
Pmepa1	prostate transmembrane protein, androgen induced 1	0.045454594	UP
Was	Wiskott-Aldrich syndrome	2.52818736740515E-07	UP
Ebp	phenylalkylamine Ca2+ antagonist (emopamil) binding protein	0.020623654	UP
Tspan7	tetraspanin 7	8.62756940890157E-07	UP
Atp6ap2	ATPase, H+ transporting, lysosomal accessory protein 2	0.000333458	UP
Lonrf3	LON peptidase N-terminal domain and ring finger 3	0.000392582	UP
Gpc3	glypican 3	1.17329665735651E-13	UP
Slitrk2	SLIT and NTRK-like family, member 2	0.004002991	UP
Nsdhl	NAD(P) dependent steroid dehydrogenase-like	7.97642943558389E-07	UP
Mpp1	membrane protein, palmitoylated	0.009169619	UP
Heph	hephaestin	0.000698913	UP
Fgf16	fibroblast growth factor 16	0.002950795	UP
Tlr13	toll-like receptor 13	6.59253417869345E-05	UP
Sytl4	synaptotagmin-like 4	0.001269344	UP
Cenpi	centromere protein I	0.000982698	UP

Timm8a1	translocase of inner mitochondrial membrane 8A1	0.029536336	UP
Btk	Bruton agammaglobulinemia tyrosine kinase	0.035586063	UP
Rtl9	retrotransposon Gag like 9	0.01234546	UP
Fancb	Fanconi anemia, complementation group B	0.040433111	UP
Tlr7	toll-like receptor 7	0.008155875	UP
Fabp4	fatty acid binding protein 4, adipocyte	1.86817002676322E-23	UP
Ralyl	RALY RNA binding protein-like	0.039032341	UP
Ect2	ect2 oncogene	0.025268019	UP
Nceh1	neutral cholesterol ester hydrolase 1	0.010859286	UP
Gpr160	G protein-coupled receptor 160	0.013257746	UP
Fgf2	fibroblast growth factor 2	0.000145747	UP
Nudt6	nudix hydrolase 6	4.16993418171354E-05	UP
Spata5	spermatogenesis associated 5	2.25159032777568E-09	UP
Hspa4l	heat shock protein 4 like	5.8244776241235E-06	UP
Larp1b	La ribonucleoprotein 1B	0.017396032	UP
Jade1	jade family PHD finger 1	0.015365119	UP
Exosc8	exosome component 8	0.036064811	UP
Mab21l1	mab-21-like 1	0.020970881	UP
Tm4sf4	transmembrane 4 superfamily member 4	0.01458467	UP
P2ry1	purinergic receptor P2Y, G-protein coupled 1	0.007593878	UP
Tiparp	TCDD-inducible poly(ADP-ribose) polymerase	8.69522850036211E-14	UP
Fnip2	folliculin interacting protein 2	0.046666774	UP

Tmem144	transmembrane protein 144	0.000157548	UP
Gucy1b1	guanylate cyclase 1, soluble, beta 1	0.006523044	UP
Dchs2	dachsous cadherin related 2	1.72778623492669E-08	UP
Sfrp2	secreted frizzled-related protein 2	5.83680359338947E-09	UP
Rps3a1	ribosomal protein S3A1	0.01151623	UP
Fcrl1	Fc receptor-like 1	0.01356601	UP
Hdgf	heparin binding growth factor	0.005198143	UP
Glmp	glycosylated lysosomal membrane protein	6.14884066435124E-05	UP
Smg5	SMG5 nonsense mediated mRNA decay factor	0.01028172	UP
Pmf1	polyamine-modulated factor 1	0.008289225	UP
Fdps	farnesyl diphosphate synthetase	0.000236023	UP
Gba	glucosidase, beta, acid	0.001072105	UP
Cks1b	CDC28 protein kinase 1b	0.003851191	UP
Pmvk	phosphomevalonate kinase	0.000565802	UP
Mrpl9	mitochondrial ribosomal protein L9	0.012351466	UP
Cgn	cingulin	0.046866217	UP
Tnfaip8l2	tumor necrosis factor, alpha-induced protein 8-like 2	0.037848311	UP
Ctss	cathepsin S	5.43811459733731E-15	UP
Prpf3	pre-mRNA processing factor 3	0.007888428	UP
Gja5	gap junction protein, alpha 5	2.61176970581155E-05	UP
Acp6	acid phosphatase 6, lysophosphatidic	0.012479621	UP
Atp1a1	ATPase, Na+/K+ transporting, alpha 1 polypeptide	3.30649132946559E-07	UP

Capza1	capping actin protein of muscle Z-line subunit alpha 1	3.74621595393745E-15	UP
Adora3	adenosine A3 receptor	0.023304477	UP
Vav3	vav 3 oncogene	7.71523279652806E-16	UP
Ntng1	netrin G1	2.35502412510495E-16	UP
Ndst3	N-deacetylase/N-sulfotransferase (heparan glucosaminyl) 3	6.95446128682684E-05	UP
Ugt8a	UDP galactosyltransferase 8A	0.011461223	UP
Ank2	ankyrin 2, brain	0.012637993	UP
Mcub	mitochondrial calcium uniporter dominant negative beta subunit	0.001665638	UP
Rpl34	ribosomal protein L34	6.76201950378137E-42	UP
Emcn	endomucin	0.017001021	UP
H2az1	H2A.Z variant histone 1	0.019658969	UP
Lamtor3	late endosomal/lysosomal adaptor, MAPK and MTOR activator 3	0.000159055	UP
Syde2	synapse defective 1, Rho GTPase, homolog 2 (C. elegans)	7.12599242206084E-05	UP
St6galnac3	ST6 (alpha-N-acetyl-neuraminyl-2,3-beta-galactosyl-1,3)-N-acetylgalactosaminide alpha-2,6-sialyltransferase 3	0.007994379	UP
Lhx8	LIM homeobox protein 8	0.049162969	UP
Tnni3k	TNNI3 interacting kinase	0.00234955	UP
Car8	carbonic anhydrase 8	0.000334537	UP
Gdf6	growth differentiation factor 6	1.42861243728256E-06	UP
Fsbp	fibrinogen silencer binding protein	0.032379523	UP
Wwp1	WW domain containing E3 ubiquitin protein ligase 1	0.001232726	UP
Atp6v0d2	ATPase, H+ transporting, lysosomal V0 subunit D2	6.5086634763812E-05	UP
Mob3b	MOB kinase activator 3B	0.044149626	UP

Atp8b5	ATPase, class I, type 8B, member 5	0.013658813	UP
Arhgef39	Rho guanine nucleotide exchange factor (GEF) 39	0.017028877	UP
Hrct1	histidine rich carboxyl terminus 1	0.00168009	UP
Coro2a	coronin, actin binding protein 2A	0.000150948	UP
Gabbr2	gamma-aminobutyric acid (GABA) B receptor, 2	0.041540584	UP
Ctnnal1	catenin (cadherin associated protein), alpha-like 1	3.94977069593426E-05	UP
Epb41l4b	erythrocyte membrane protein band 4.1 like 4b	1.8317463431257E-05	UP
Lpar1	lysophosphatidic acid receptor 1	0.031095996	UP
Tek	TEK receptor tyrosine kinase	0.001209643	UP
Kank4	KN motif and ankyrin repeat domains 4	0.041153265	UP
Dnajc6	DnaJ heat shock protein family (Hsp40) member C6	0.025691772	UP
Lepr	leptin receptor	0.022643162	UP
Pcsk9	proprotein convertase subtilisin/kexin type 9	0.030057662	UP
Rab3b	RAB3B, member RAS oncogene family	0.020623654	UP
Pdzk1ip1	PDZK1 interacting protein 1	0.000183092	UP
Zswim5	zinc finger SWIM-type containing 5	0.019803402	UP
Atp6v0b	ATPase, H+ transporting, lysosomal V0 subunit B	2.1831051178154E-05	UP
Slc2a1	solute carrier family 2 (facilitated glucose transporter), member 1	0.001157605	UP
Mfsd2a	MFSD2 lysolipid transporter A, lysophospholipid	0.008160868	UP
Yrdc	yrdC domain containing (E.coli)	0.033297617	UP
Stk40	serine/threonine kinase 40	0.009590093	UP
Sh3d21	SH3 domain containing 21	0.003550214	UP

Med18	mediator complex subunit 18	2.16338007917033E-06	UP
Ptafr	platelet-activating factor receptor	2.67685840453554E-06	UP
Rpa2	replication protein A2	0.032654564	UP
Trnp1	TMF1-regulated nuclear protein 1	0.010859286	UP
Sfn	stratifin	0.016664337	UP
Hmgn2	high mobility group nucleosomal binding domain 2	3.67930199453222E-07	UP
Stmn1	stathmin 1	0.001034134	UP
Aunip	aurora kinase A and ninein interacting protein	0.001580264	UP
E2f2	E2F transcription factor 2	0.001759038	UP
Pla2g2e	phospholipase A2, group IIE	1.64830666323302E-05	UP
Htr6	5-hydroxytryptamine (serotonin) receptor 6	0.042378981	UP
Slc66a1	solute carrier family 66 member 1	5.17392835727442E-06	UP
Padi2	peptidyl arginine deiminase, type II	0.008119238	UP
Pdpn	podoplanin	6.45834871445969E-13	UP
Pramel13	PRAME like 13	9.59027559189681E-05	UP
Tnfrsf1b	tumor necrosis factor receptor superfamily, member 1b	0.004995324	UP
Zfp991	zinc finger protein 991	6.04876309179744E-05	UP
Zfp982	zinc finger protein 982	3.50768718036544E-07	UP
Zfp984	zinc finger protein 984	2.71004051766728E-10	UP
Nppb	natriuretic peptide type B	0.018397693	UP
Clcn6	chloride channel, voltage-sensitive 6	1.82482917351324E-05	UP
Mad2l2	MAD2 mitotic arrest deficient-like 2	0.000360189	UP

Fbxo44	F-box protein 44	0.004191204	UP
Disp3	dispatched RND transporter family member 3	0.014697844	UP
Angptl7	angiopoietin-like 7	3.35958478497294E-07	UP
Casz1	castor zinc finger 1	0.008369177	UP
Slc25a33	solute carrier family 25, member 33	0.002262732	UP
Eno1	enolase 1, alpha non-neuron	3.76903732188957E-08	UP
Tas1r3	taste receptor, type 1, member 3	0.003282515	UP
Ube2j2	ubiquitin-conjugating enzyme E2J 2	1.00825966790302E-05	UP
C1qtnf12	C1q and tumor necrosis factor related 12	3.27977726613213E-11	UP
B3galt6	UDP-Gal:betaGal beta 1,3-galactosyltransferase, polypeptide 6	6.43059895000183E-08	UP
Noc2l	NOC2 like nucleolar associated transcriptional repressor	1.90903591816633E-05	UP
Samd11	sterile alpha motif domain containing 11	6.74014274528665E-07	UP
Cyp51	cytochrome P450, family 51	0.004376033	UP
Dbf4	DBF4 zinc finger	0.025604739	UP
Abcb4	ATP-binding cassette, sub-family B (MDR/TAP), member 4	0.001425788	UP
Sema3d	sema domain, immunoglobulin domain (Ig), short basic domain, secreted, (semaphorin) 3D	4.25012368614143E-08	UP
Gm21083	predicted gene, 21083	0.048352028	UP
Insig1	insulin induced gene 1	0.034966513	UP
Cib4	calcium and integrin binding family member 4	0.002829413	UP
Kcnk3	potassium channel, subfamily K, member 3	9.01827046337675E-15	UP
Cenpa	centromere protein A	0.019571068	UP
Gm5553	predicted gene 5553	0.00243	UP

Sh3bp2	SH3-domain binding protein 2	0.014411335	UP
Msx1	msh homeobox 1	4.10702785002602E-08	UP
Hs3st1	heparan sulfate (glucosamine) 3-O-sulfotransferase 1	8.08608059916378E-07	UP
Fgfbp1	fibroblast growth factor binding protein 1	0.018122421	UP
Prom1	prominin 1	0.01114175	UP
0610040J01Rik	RIKEN cDNA 0610040J01 gene	0.001011536	UP
Rbm47	RNA binding motif protein 47	0.001328037	UP
Bend4	BEN domain containing 4	0.025135322	UP
Kctd8	potassium channel tetramerisation domain containing 8	7.12599242206084E-05	UP
Gabra4	gamma-aminobutyric acid (GABA) A receptor, subunit alpha 4	0.020970881	UP
Txk	TXK tyrosine kinase	0.005355507	UP
Kdr	kinase insert domain protein receptor	0.000949829	UP
Afp	alpha fetoprotein	0.008369177	UP
Cxcl15	chemokine (C-X-C motif) ligand 15	0.034504343	UP
Prdm8	PR domain containing 8	2.72773692711848E-05	UP
Fgf5	fibroblast growth factor 5	6.42718726820124E-06	UP
Cfap299	cilia and flagella associated protein 299	0.004859724	UP
Bmp3	bone morphogenetic protein 3	1.83422292961001E-06	UP
Prkg2	protein kinase, cGMP-dependent, type II	0.000108086	UP
Mvk	mevalonate kinase	7.69213708598881E-06	UP
Tbx5	T-box 5	0.000322819	UP
Kmt5a	lysine methyltransferase 5A	0.001025907	UP

Tmem132c	transmembrane protein 132C	5.24438691248698E-06	UP
Lat2	linker for activation of T cells family, member 2	0.014891323	UP
Cldn15	claudin 15	0.000424198	UP
Gpr146	G protein-coupled receptor 146	0.000176697	UP
C130050O18Rik	RIKEN cDNA C130050O18 gene	0.04681849	UP
Tmem184a	transmembrane protein 184a	0.048745019	UP
Sdk1	sidekick cell adhesion molecule 1	5.27805838813043E-08	UP
Cpsf4	cleavage and polyadenylation specific factor 4	0.02360438	UP
Alox5ap	arachidonate 5-lipoxygenase activating protein	0.000538238	UP
Hsph1	heat shock 105kDa/110kDa protein 1	2.10159708592101E-09	UP
Fry	FRY microtubule binding protein	0.003586996	UP
Tfpi2	tissue factor pathway inhibitor 2	0.003696071	UP
Ica1	islet cell autoantigen 1	0.003473233	UP
Foxp2	forkhead box P2	0.004769123	UP
Tfec	transcription factor EC	0.001259093	UP
Cttnbp2	cortactin binding protein 2	0.00693502	UP
Strip2	striatin interacting protein 2	0.002354403	UP
Bpgm	2,3-bisphosphoglycerate mutase	0.022942437	UP
Fam180a	family with sequence similarity 180, member A	0.031009473	UP
Fmc1	formation of mitochondrial complex V assembly factor 1	0.029662522	UP
Clec5a	C-type lectin domain family 5, member a	0.006523044	UP
Prss2	protease, serine 2	2.48741600719682E-05	UP

Npy	neuropeptide Y	2.24407346808297E-05	UP
Snx10	sorting nexin 10	1.38527669656724E-10	UP
Hoxa13	homeobox A13	9.93588146402198E-25	UP
Chn2	chimerin 2	0.003460942	UP
Aqp1	aquaporin 1	6.46653804179922E-07	UP
Herc3	hect domain and RLD 3	0.026469003	UP
Ccser1	coiled-coil serine rich 1	0.00104003	UP
Grid2	glutamate receptor, ionotropic, delta 2	0.002559466	UP
Hpgds	hematopoietic prostaglandin D synthase	5.99335839029719E-09	UP
Ndnf	neuron-derived neurotrophic factor	0.04769007	UP
Lrrtm1	leucine rich repeat transmembrane neuronal 1	0.010196382	UP
Eva1a	eva-1 homolog A (C. elegans)	0.00078256	UP
Tacr1	tachykinin receptor 1	5.44066128601809E-06	UP
Cd207	CD207 antigen	1.13987634214174E-14	UP
Tgfa	transforming growth factor alpha	0.004180799	UP
Fam136a	family with sequence similarity 136, member A	0.000278152	UP
Pcyox1	prenylcysteine oxidase 1	0.015020712	UP
Mgll	monoglyceride lipase	1.93651891654023E-14	UP
Slc6a6	solute carrier family 6 (neurotransmitter transporter, taurine), member 6	0.001560251	UP
Adamts9	a disintegrin-like and metallopeptidase (reprolysin type) with thrombospondin type 1 motif, 9	0.007450401	UP
Mitf	melanogenesis associated transcription factor	0.032999802	UP

Gxylt2	glucoside xylosyltransferase 2	0.005146017	UP
Oxtr	oxytocin receptor	0.00691265	UP
Irak2	interleukin-1 receptor-associated kinase 2	2.53259648223342E-05	UP
Tatdn2	TatD DNase domain containing 2	2.57952608413284E-06	UP
Rasgef1a	RasGEF domain family, member 1A	7.12599242206084E-05	UP
Rimklb	ribosomal modification protein rimK-like family member B	0.04387047	UP
Aicda	activation-induced cytidine deaminase	0.02853679	UP
Slc2a3	solute carrier family 2 (facilitated glucose transporter), member 3	0.028921746	UP
Clec4d	C-type lectin domain family 4, member d	0.00651963	UP
Cd9	CD9 antigen	0.000219641	UP
Vwf	Von Willebrand factor	0.010507943	UP
Clec9a	C-type lectin domain family 9, member a	0.018736545	UP
Clec1a	C-type lectin domain family 1, member a	0.001316826	UP
Clec7a	C-type lectin domain family 7, member a	0.018096632	UP
Klra4	killer cell lectin-like receptor, subfamily A, member 4	0.034536242	UP
Apold1	apolipoprotein L domain containing 1	0.007149572	UP
Pbp2	phosphatidylethanolamine binding protein 2	4.89102752504759E-08	UP
Grin2b	glutamate receptor, ionotropic, NMDA2B (epsilon 2)	0.01233949	UP
Arhgdib	Rho, GDP dissociation inhibitor (GDI) beta	3.79064894931694E-08	UP
Pde6h	phosphodiesterase 6H, cGMP-specific, cone, gamma	1.87274638760891E-07	UP
Pirb	paired Ig-like receptor B	0.001999036	UP
Pira6	paired-Ig-like receptor A6	0.000498178	UP

Pira2	paired-Ig-like receptor A2	5.5595930889514E-05	UP
Lair1	leukocyte-associated Ig-like receptor 1	3.67930199453222E-07	UP
Usp29	ubiquitin specific peptidase 29	0.004362191	UP
C5ar2	complement component 5a receptor 2	1.24331778470682E-05	UP
C5ar1	complement component 5a receptor 1	1.43474275454636E-11	UP
Slc1a5	solute carrier family 1 (neutral amino acid transporter), member 5	0.001374859	UP
Pvr	poliovirus receptor	0.009069785	UP
Psmd8	proteasome (prosome, macropain) 26S subunit, non-ATPase, 8	0.047764272	UP
Wdr62	WD repeat domain 62	0.033891177	UP
Tyrobp	TYRO protein tyrosine kinase binding protein	0.006637072	UP
Fam187b	family with sequence similarity 187, member B	0.043064708	UP
Chst8	carbohydrate sulfotransferase 8	0.041060082	UP
Ccnb1-ps	cyclin B1, pseudogene	0.042541456	UP
Cd37	CD37 antigen	0.014467802	UP
Ftl1	ferritin light polypeptide 1	5.27210411644125E-08	UP
Gabrg3	gamma-aminobutyric acid (GABA) A receptor, subunit gamma 3	0.027805005	UP
Fam169b	family with sequence similarity 169, member B	7.97642943558389E-07	UP
Pde2a	phosphodiesterase 2A, cGMP-stimulated	0.016664337	UP
Pde2a	phosphodiesterase 2A, cGMP-stimulated	6.20696510145652E-05	UP
Folr2	folate receptor 2 (fetal)	3.9591555256237E-06	UP
Olfml1	olfactomedin-like 1	0.00027701	UP
Spon1	spondin 1, (f-spondin) extracellular matrix protein	0.01501904	UP

Pde3b	phosphodiesterase 3B, cGMP-inhibited	0.024938596	UP
Kdm8	lysine (K)-specific demethylase 8	0.000150722	UP
Coro1a	coronin, actin binding protein 1A	0.024839533	UP
Septin1	septin 1	0.013505218	UP
Itgam	integrin alpha M	0.043195634	UP
Tcerg1l	transcription elongation regulator 1-like	0.022873127	UP
Lrrc27	leucine rich repeat containing 27	2.89596873172007E-10	UP
Adam8	a disintegrin and metallopeptidase domain 8	1.71010481116944E-07	UP
Pkp3	plakophilin 3	0.01746471	UP
Syt8	synaptotagmin VIII	0.032044496	UP
Dhcr7	7-dehydrocholesterol reductase	0.018992034	UP
Samd5	sterile alpha motif domain containing 5	0.009804358	UP
Arfgef3	ARFGEF family member 3	0.001207496	UP
Raet1e	retinoic acid early transcript 1E	0.001003847	UP
Raet1a	retinoic acid early transcript 1, alpha	0.023767542	UP
Enpp3	ectonucleotide pyrophosphatase/phosphodiesterase 3	7.59535080145771E-10	UP
Arhgap18	Rho GTPase activating protein 18	6.92368343089441E-05	UP
Cenpw	centromere protein W	1.64192506310743E-06	UP
Col10a1	collagen, type X, alpha 1	1.04888753760844E-05	UP
Slc16a10	solute carrier family 16 (monocarboxylic acid transporters), member 10	9.59681145600085E-08	UP
Scml4	Scm polycomb group protein like 4	3.44559178070423E-07	UP
Crybg1	crystallin beta-gamma domain containing 1	0.022643162	UP

Lilrb4a	leukocyte immunoglobulin-like receptor, subfamily B, member 4A	0.046341717	UP
Lilrb4b	leukocyte immunoglobulin-like receptor, subfamily B, member 4B	0.015088904	UP
Lilrb4a	leukocyte immunoglobulin-like receptor, subfamily B, member 4A	0.03524291	UP
Vps26a	VPS26 retromer complex component A	0.000752041	UP
Ctnna3	catenin (cadherin associated protein), alpha 3	0.029179767	UP
Rtkn2	rhotekin 2	0.009931405	UP
Cdk1	cyclin-dependent kinase 1	0.007807249	UP
Gstt2	glutathione S-transferase, theta 2	0.003785578	UP
Mif	macrophage migration inhibitory factor (glycosylation-inhibiting factor)	0.028538426	UP
Lss	lanosterol synthase	0.002387372	UP
Icosl	icos ligand	0.047764272	UP
Agpat3	1-acylglycerol-3-phosphate O-acyltransferase 3	0.001852337	UP
Cstb	cystatin B	0.001580264	UP
Arhgap45	Rho GTPase activating protein 45	0.000361781	UP
Eid3	EP300 interacting inhibitor of differentiation 3	0.028138326	UP
Pmch	pro-melanin-concentrating hormone	0.008091776	UP
Gas2l3	growth arrest-specific 2 like 3	0.044956552	UP
Kitl	kit ligand	0.001005775	UP
Ptprq	protein tyrosine phosphatase, receptor type, Q	0.000245415	UP
Trhde	TRH-degrading enzyme	0.002761165	UP
Myrfl	myelin regulatory factor-like	0.002295806	UP
Rab3ip	RAB3A interacting protein	0.001955266	UP

Hmga2	high mobility group AT-hook 2	0.016866772	UP
Wif1	Wnt inhibitory factor 1	0.039296643	UP
Arhgap9	Rho GTPase activating protein 9	2.85749942605145E-06	UP
Itga7	integrin alpha 7	0.000188025	UP
Tnfsf13b	tumor necrosis factor (ligand) superfamily, member 13b	0.000291242	UP
Myo16	myosin XVI	0.029733557	UP
Irs2	insulin receptor substrate 2	0.017465517	UP
Ankrd10	ankyrin repeat domain 10	4.77136162177178E-05	UP
Angpt2	angiopoietin 2	1.54384841002431E-05	UP
Thsd1	thrombospondin, type I, domain 1	0.002859523	UP
Unc5d	unc-5 netrin receptor D	0.007964942	UP
Asah1	N-acylsphingosine amidohydrolase 1	1.44268465833E-05	UP
Dctd	dCMP deaminase	0.021336811	UP
Neil3	nei like 3 (E. coli)	0.040856478	UP
Vegfc	vascular endothelial growth factor C	0.005943863	UP
Hpgd	hydroxyprostaglandin dehydrogenase 15 (NAD)	4.7379512580895E-05	UP
Sap30	sin3 associated polypeptide	0.006718829	UP
Hmgb2	high mobility group box 2	0.002013933	UP
Mfap3l	microfibrillar-associated protein 3-like	0.04867008	UP
Msmo1	methylsterol monoxygenase 1	0.00040404	UP
Cilp2	cartilage intermediate layer protein 2	0.041579632	UP
Il12rb1	interleukin 12 receptor, beta 1	0.040090583	UP

Slc5a5	solute carrier family 5 (sodium iodide symporter), member 5	0.008563245	UP
Gm10654	predicted gene 10654	0.005859663	UP
Ankle1	ankyrin repeat and LEM domain containing 1	0.002386474	UP
Plvap	plasmalemma vesicle associated protein	0.013135279	UP
Slc27a1	solute carrier family 27 (fatty acid transporter), member 1	0.016363225	UP
B3gnt3	UDP-GlcNAc:betaGal beta-1,3-N-acetylglucosaminyltransferase 3	0.000382964	UP
Il15	interleukin 15	0.001945543	UP
Adcy7	adenylate cyclase 7	0.046596537	UP
Snx20	sorting nexin 20	0.004956516	UP
Sall1	spalt like transcription factor 1	6.42220537222243E-06	UP
Cmtm4	CKLF-like MARVEL transmembrane domain containing 4	0.005739054	UP
Agrp	agouti related neuropeptide	0.007483236	UP
Dpep2	dipeptidase 2	0.038231067	UP
Dpep2	dipeptidase 2	0.037999622	UP
Cdh1	cadherin 1	0.005519548	UP
Maf	MAF bZIP transcription factor	0.013887226	UP
Mvd	mevalonate (diphospho) decarboxylase	0.011300437	UP
Cbfa2t3	CBFA2/RUNX1 translocation partner 3	0.045454594	UP
Acta1	actin alpha 1, skeletal muscle	0.026135363	UP
Pgbd5	piggyBac transposable element derived 5	1.10535999204453E-06	UP
Gm3636	predicted gene 3636	0.019390825	UP
Cadps	Ca2+-dependent secretion activator	0.00989378	UP

Fut11	fucosyltransferase 11	0.026386418	UP
Adk	adenosine kinase	1.36180107170149E-09	UP
Chdh	choline dehydrogenase	0.006345282	UP
Uqcc5	ubiquinol-cytochrome c reductase complex assembly factor 5	0.037698128	UP
Galnt15	polypeptide N-acetylgalactosaminyltransferase 15	0.033296237	UP
Ncoa4	nuclear receptor coactivator 4	3.68844085975819E-05	UP
Tmem273	transmembrane protein 273	0.041844945	UP
Wdfy4	WD repeat and FYVE domain containing 4	0.002535343	UP
Arhgap22	Rho GTPase activating protein 22	1.21224069072189E-24	UP
Gdf10	growth differentiation factor 10	1.5098521102497E-06	UP
Prxl2a	peroxiredoxin like 2A	1.99011981282162E-08	UP
Cdkn3	cyclin-dependent kinase inhibitor 3	0.018343505	UP
Lgals3	lectin, galactose binding, soluble 3	0.001045321	UP
Peli2	pellino 2	0.00306804	UP
Rnase6	ribonuclease, RNase A family, 6	0.020715656	UP
Haus4	HAUS augmin-like complex, subunit 4	0.000884453	UP
Psmb5	proteasome (prosome, macropain) subunit, beta type 5	1.96366560615078E-13	UP
Slc7a8	solute carrier family 7 (cationic amino acid transporter, y+ system), member 8	3.03034482406652E-07	UP
Ppp1r3e	protein phosphatase 1, regulatory subunit 3E	2.21814881068413E-21	UP
Zfhx2	zinc finger homeobox 2	0.014430912	UP
Il17d	interleukin 17D	1.41737372939511E-05	UP
Shisa2	shisa family member 2	7.6350628276815E-09	UP

Atp8a2	ATPase, aminophospholipid transporter-like, class I, type 8A, member 2	0.02088554	UP
Arl11	ADP-ribosylation factor-like 11	0.000391562	UP
Fdft1	farnesyl diphosphate farnesyl transferase 1	0.001527631	UP
Xkr6	X-linked Kx blood group related 6	0.045221384	UP
Dock5	dedicator of cytokinesis 5	0.007376113	UP
Slc25a37	solute carrier family 25, member 37	1.94381366425026E-07	UP
Entpd4	ectonucleoside triphosphate diphosphohydrolase 4	1.04934708235241E-06	UP
Gm16867	predicted gene, 16867	2.70587414925551E-32	UP
Entpd4b	ectonucleoside triphosphate diphosphohydrolase 4B	0.028825125	UP
Rhobtb2	Rho-related BTB domain containing 2	0.000131461	UP
Reep4	receptor accessory protein 4	0.001066972	UP
Hr	lysine demethylase and nuclear receptor corepressor	0.00017928	UP
Dok2	docking protein 2	0.023705842	UP
Rgcc	regulator of cell cycle	0.040453833	UP
Pcdh20	protocadherin 20	2.69545679292696E-11	UP
Hs6st3	heparan sulfate 6-O-sulfotransferase 3	3.50768718036544E-07	UP
Dock9	dedicator of cytokinesis 9	0.000633075	UP
Zic5	zinc finger protein of the cerebellum 5	5.14153316746743E-05	UP
Zic2	zinc finger protein of the cerebellum 2	2.27082308265795E-07	UP
Pdgfd	platelet-derived growth factor, D polypeptide	0.003895283	UP
Mmp12	matrix metallopeptidase 12	0.032455356	UP
Pgr	progesterone receptor	0.005120961	UP

Fat3	FAT atypical cadherin 3	0.000233712	UP
Cdkn2d	cyclin dependent kinase inhibitor 2D	0.026817309	UP
AB124611	cDNA sequence AB124611	0.000435977	UP
Ldlr	low density lipoprotein receptor	0.01899812	UP
Tbx20	T-box 20	0.007643496	UP
Adamts8	a disintegrin-like and metallopeptidase (reprolysin type) with thrombospondin type 1 motif, 8	0.000966814	UP
Kirrel3	kirre like nephrin family adhesion molecule 3	0.002768387	UP
Hspa8	heat shock protein 8	2.25744309505244E-12	UP
Ubash3b	ubiquitin associated and SH3 domain containing, B	0.000414447	UP
Sorl1	sortilin-related receptor, LDLR class A repeats-containing	0.002997944	UP
Sc5d	sterol-C5-desaturase	0.006750191	UP
Cbl	Casitas B-lineage lymphoma	0.000406533	UP
Cadm1	cell adhesion molecule 1	1.80124562453763E-09	UP
Layn	layilin	4.38597569548699E-06	UP
Exph5	exophilin 5	0.025827385	UP
Tnfaip8l3	tumor necrosis factor, alpha-induced protein 8-like 3	0.007045079	UP
Gldn	gliomedin	3.36727358733598E-09	UP
Isl2	insulin related protein 2 (islet 2)	3.23911539903758E-05	UP
Cspg4	chondroitin sulfate proteoglycan 4	0.019048297	UP
Rec114	REC114 meiotic recombination protein	0.023419602	UP
Pkm	pyruvate kinase, muscle	0.00054212	UP
Pclaf	PCNA clamp associated factor	0.013955947	UP

Tln2	talin 2	1.4259414322008E-13	UP
Aldh1a2	aldehyde dehydrogenase family 1, subfamily A2	0.004270901	UP
Mns1	meiosis-specific nuclear structural protein 1	0.007604518	UP
Fam83b	family with sequence similarity 83, member B	0.006532941	UP
Tinag	tubulointerstitial nephritis antigen	0.012603162	UP
Tbx18	T-box18	0.01693188	UP
Pcolce2	procollagen C-endopeptidase enhancer 2	0.00358283	UP
Pls1	plastin 1 (I-isoform)	0.001045321	UP
Atp1b3	ATPase, Na+/K+ transporting, beta 3 polypeptide	0.001102727	UP
Trf	transferrin	0.003515407	UP
Gpx1	glutathione peroxidase 1	0.000264752	UP
Prkar2a	protein kinase, cAMP dependent regulatory, type II alpha	0.037364737	UP
Eomes	eomesodermin	0.004910928	UP
Xylb	xylulokinase homolog (H. influenzae)	0.019416232	UP
Scn5a	sodium channel, voltage-gated, type V, alpha	0.038231067	UP
Cx3cr1	chemokine (C-X3-C motif) receptor 1	0.022752715	UP
Vipr1	vasoactive intestinal peptide receptor 1	1.00058784042954E-05	UP
Camk2b	calcium/calmodulin-dependent protein kinase II, beta	1.47270418521757E-09	UP
Otx1	orthodenticle homeobox 1	0.001156445	UP
Bcl11a	B cell CLL/lymphoma 11A (zinc finger protein)	2.57434962074149E-06	UP
Ranbp17	RAN binding protein 17	0.013983778	UP
Atp10b	ATPase, class V, type 10B	0.012813547	UP

Gm5431	predicted gene 5431	0.014400474	UP
9930111J21Rik2	RIKEN cDNA 9930111J21 gene 2	0.020316297	UP
N4bp3	NEDD4 binding protein 3	0.035321686	UP
Fstl4	follistatin-like 4	0.007186703	UP
Hand1	heart and neural crest derivatives expressed 1	8.60437277080202E-17	UP
Shmt1	serine hydroxymethyltransferase 1 (soluble)	0.000192828	UP
Zfp286	zinc finger protein 286	0.018669582	UP
Myh1	myosin, heavy polypeptide 1, skeletal muscle, adult	0.001433096	UP
Usp43	ubiquitin specific peptidase 43	0.021866161	UP
Cd68	CD68 antigen	3.44682345073136E-13	UP
Nlrp1a	NLR family, pyrin domain containing 1A	0.00140021	UP
Aspa	aspartoacylase	0.014559515	UP
Evi2b	ecotropic viral integration site 2b	0.037153037	UP
Tbx2	T-box 2	0.034009161	UP
Tbx4	T-box 4	3.76903732188957E-08	UP
Hlf	hepatic leukemia factor	0.004970599	UP
Gngt2	guanine nucleotide binding protein (G protein), gamma transducing activity polypeptide 2	0.002951945	UP
Krtap1-5	keratin associated protein 1-5	0.018600052	UP
Grn	granulin	0.003279831	UP
Fmnl1	formin-like 1	0.005963182	UP
Ace	angiotensin I converting enzyme (peptidyl-dipeptidase A) 1	0.029452364	UP
Cd300a	CD300A molecule	0.0001041	UP

Cd300lb	CD300 molecule like family member B	0.038949814	UP
Cd300c2	CD300C molecule 2	0.002191517	UP
Pcyt2	phosphate cytidylyltransferase 2, ethanolamine	0.003502247	UP
Idi1	isopentenyl-diphosphate delta isomerase	1.8317463431257E-05	UP
Ero1b	endoplasmic reticulum oxidoreductase 1 beta	0.022752715	UP
H4c11	H4 clustered histone 11	0.046333629	UP
H4c12	H4 clustered histone 12	0.016210783	UP
H2ac12	H2A clustered histone 12	0.003972503	UP
H3c8	H3 clustered histone 8	0.007397017	UP
H2bc9	H2B clustered histone 9	0.014430912	UP
D130043K22Rik	RIKEN cDNA D130043K22 gene	0.008155875	UP
Prl3a1	prolactin family 3, subfamily a, member 1	0.00041927	UP
Foxq1	forkhead box Q1	3.4686876544083E-12	UP
Foxf2	forkhead box F2	3.91216252977762E-08	UP
Serpinb1c	serine (or cysteine) peptidase inhibitor, clade B, member 1c	0.015006189	UP
Gfod1	glucose-fructose oxidoreductase domain containing 1	3.23911539903758E-05	UP
Rnf182	ring finger protein 182	0.000296303	UP
Ninj1	ninjurin 1	2.93543459355979E-06	UP
Fgd3	FYVE, RhoGEF and PH domain containing 3	0.047378755	UP
Shc3	src homology 2 domain-containing transforming protein C3	0.003550214	UP
Sema4d	sema domain, immunoglobulin domain (Ig), transmembrane domain (TM) and short cytoplasmic domain, (semaphorin) 4D	5.99143385316251E-06	UP
Rgs14	regulator of G-protein signaling 14	5.52974941760165E-07	UP

Tifab	TRAF-interacting protein with forkhead-associated domain, family member B	0.008369177	UP
Ntrk2	neurotrophic tyrosine kinase, receptor, type 2	0.006878658	UP
Zfp367	zinc finger protein 367	0.000558104	UP
Zfp429	zinc finger protein 429	0.044519462	UP
Zfp273	zinc finger protein 273	0.019868963	UP
Srd5a1	steroid 5 alpha-reductase 1	0.003481912	UP
Ftl1-ps2	ferritin light polypeptide, pseudogene 2	3.72464192329842E-11	UP
Pcsk1	proprotein convertase subtilisin/kexin type 1	0.016459448	UP
Polr3g	polymerase (RNA) III (DNA directed) polypeptide G	0.003108599	UP
Mef2c	myocyte enhancer factor 2C	0.002654062	UP
Cenpk	centromere protein K	0.022229164	UP
Ddx4	DEAD box helicase 4	4.22478170580082E-08	UP
Plpp1	phospholipid phosphatase 1	0.000965087	UP
Mtrex	Mtr4 exosome RNA helicase	2.3864182292093E-06	UP
Ccno	cyclin O	0.015383816	UP
Hcn1	hyperpolarization activated cyclic nucleotide gated potassium channel 1	3.68803897599378E-16	UP
4833420G17Rik	RIKEN cDNA 4833420G17 gene	4.52900882427228E-31	UP
Tmem267	transmembrane protein 267	1.8317463431257E-05	UP
Ccl28	chemokine (C-C motif) ligand 28	2.35186484493848E-08	UP
Rrm2	ribonucleotide reductase M2	0.007371749	UP
Meox2	mesenchyme homeobox 2	6.7597951678026E-07	UP

Mdga2	MAM domain containing glycosylphosphatidylinositol anchor 2	2.63101572484958E-08	UP
Rgs6	regulator of G-protein signaling 6	9.07551664827105E-05	UP
Erg28	ergosterol biosynthesis 28	0.003770293	UP
Galc	galactosylceramidase	0.000116817	UP
Kcnk13	potassium channel, subfamily K, member 13	1.60167558199861E-08	UP
Pld4	phospholipase D family, member 4	1.65242947554484E-05	UP
Vipr2	vasoactive intestinal peptide receptor 2	0.00079283	UP
Ranbp3l	RAN binding protein 3-like	4.32041002475117E-06	UP
Nadk2	NAD kinase 2, mitochondrial	0.030147307	UP
Il7r	interleukin 7 receptor	1.75770535548109E-05	UP
Pdzd2	PDZ domain containing 2	0.006995423	UP
Sema5a	sema domain, seven thrombospondin repeats (type 1 and type 1-like), transmembrane domain (TM) and short cytoplasmic domain, (semaphorin) 5A	0.01649602	UP
Pop1	processing of precursor 1, ribonuclease P/MRP family, (S. cerevisiae)	0.049338304	UP
Osr2	odd-skipped related 2	0.000680345	UP
Dcstamp	dendrocyte expressed seven transmembrane protein	0.023867706	UP
Abra	actin-binding Rho activating protein	7.27982919588379E-05	UP
Sybu	syntabulin (syntaxin-interacting)	0.023938865	UP
Atad2	ATPase family, AAA domain containing 2	0.013363329	UP
Fbxo32	F-box protein 32	0.001193962	UP
Klhl38	kelch-like 38	0.000895414	UP
Sqle	squalene epoxidase	0.0027467	UP

Ly6f	lymphocyte antigen 6 complex, locus F	0.046780515	UP
Csf2rb2	colony stimulating factor 2 receptor, beta 2, low-affinity (granulocyte-macrophage)	5.23879132319451E-17	UP
Csf2rb	colony stimulating factor 2 receptor, beta, low-affinity (granulocyte-macrophage)	3.24771755140953E-06	UP
Gcat	glycine C-acetyltransferase (2-amino-3-ketobutyrate-coenzyme A ligase)	0.002997944	UP
Gcat	glycine C-acetyltransferase (2-amino-3-ketobutyrate-coenzyme A ligase)	0.002286196	UP
Maff	v-maf musculoaponeurotic fibrosarcoma oncogene family, protein F (avian)	0.004072031	UP
Nfam1	Nfat activating molecule with ITAM motif 1	6.21164710091275E-08	UP
Slc38a4	solute carrier family 38, member 4	0.00082807	UP
Amigo2	adhesion molecule with Ig like domain 2	0.000408235	UP
Troap	trophinin associated protein	0.016303737	UP
Racgap1	Rac GTPase-activating protein 1	0.035158526	UP
Smagp	small cell adhesion glycoprotein	1.09546157873226E-06	UP
Bin2	bridging integrator 2	0.031104652	UP
Galnt6	polypeptide N-acetylgalactosaminyltransferase 6	0.048796324	UP
Rpl39l	ribosomal protein L39-like	0.000393505	UP
Atf7ip2	activating transcription factor 7 interacting protein 2	0.002077614	UP
Shisa9	shisa family member 9	0.000261521	UP
Cdc45	cell division cycle 45	0.000438453	UP
Tfrc	transferrin receptor	0.000607773	UP

Sema5b	sema domain, seven thrombospondin repeats (type 1 and type 1-like), transmembrane domain (TM) and short cytoplasmic domain, (semaphorin) 5B	0.005318461	UP
Hcls1	hematopoietic cell specific Lyn substrate 1	0.03465508	UP
Lsamp	limbic system-associated membrane protein	0.02126966	UP
Cxadr	coxsackie virus and adenovirus receptor	1.46592562401665E-08	UP
Btg3	BTG anti-proliferation factor 3	0.000810223	UP
Mrps6	mitochondrial ribosomal protein S6	9.53474745581692E-13	UP
Slc5a3	solute carrier family 5 (inositol transporters), member 3	6.01980445506606E-18	UP
Tagap1	T cell activation GTPase activating protein 1	0.001666134	UP
Acat2	acetyl-Coenzyme A acetyltransferase 2	5.65927676215682E-11	UP
Pgp	phosphoglycolate phosphatase	0.002218034	UP
Tpsg1	tryptase gamma 1	0.04435804	UP
Neurl1b	neuralized E3 ubiquitin protein ligase 1B	0.037397947	UP
Ip6k3	inositol hexaphosphate kinase 3	0.000908429	UP
Smim29	small integral membrane protein 29	0.006991	UP
Pim1	proviral integration site 1	0.002681642	UP
Abcg1	ATP binding cassette subfamily G member 1	0.022746018	UP
Myo1f	myosin IF	0.000375116	UP
Tapbp	TAP binding protein	0.043709242	UP
H2-Ab1	histocompatibility 2, class II antigen A, beta 1	0.01033744	UP
Neu1	neuraminidase 1	0.019403454	UP
Tcf19	transcription factor 19	0.030306353	UP

Or5v1b	olfactory receptor family 5 subfamily V member 1B	0.003108413	UP
Cenpq	centromere protein Q	0.025166966	UP
Cyp39a1	cytochrome P450, family 39, subfamily a, polypeptide 1	0.006894306	UP
Polh	polymerase (DNA directed), eta (RAD 30 related)	0.000846541	UP
Trem2	triggering receptor expressed on myeloid cells 2	0.014808011	UP
Plin4	perilipin 4	0.006160755	UP
Dennd1c	DENN domain containing 1C	0.021111989	UP
Dlgap1	DLG associated protein 1	8.34450951897514E-11	UP
Galm	galactose mutarotase	0.000145747	UP
Tmem178	transmembrane protein 178	6.90738059102955E-06	UP
Gata6	GATA binding protein 6	3.7885874711203E-05	UP
Tslp	thymic stromal lymphopoietin	0.007009101	UP
Cystm1	cysteine-rich transmembrane module containing 1	5.71200624145375E-05	UP
Kctd16	potassium channel tetramerisation domain containing 16	0.045221384	UP
Lvrn	laeverin	0.038296777	UP
Arl14epl	ADP-ribosylation factor-like 14 effector protein-like	0.000394892	UP
Prdm6	PR domain containing 6	0.010590735	UP
Lipg	lipase, endothelial	0.022752715	UP
Siglec15	sialic acid binding Ig-like lectin 15	0.008642131	UP
Hsbp1l1	heat shock factor binding protein 1-like 1	0.00642182	UP
Chka	choline kinase alpha	0.019390825	UP
Ctsw	cathepsin W	0.022845462	UP

Slc25a45	solute carrier family 25, member 45	0.011469639	UP
Cdca5	cell division cycle associated 5	0.023850417	UP
Vegfb	vascular endothelial growth factor B	0.033820771	UP
Fen1	flap structure specific endonuclease 1	0.027320855	UP
Vwce	von Willebrand factor C and EGF domains	0.015106683	UP
Ptgdr2	prostaglandin D2 receptor 2	0.000135509	UP
Stx3	syntaxin 3	3.38533679396022E-06	UP
Lpxn	leupaxin	8.34975368730168E-06	UP
Gna14	guanine nucleotide binding protein, alpha 14	0.01220339	UP
Entrep1	endosomal transmembrane epsin interactor 1	0.005370505	UP
Pip5k1b	phosphatidylinositol-4-phosphate 5-kinase, type 1 beta	0.000797591	UP
Dmrt2	doublesex and mab-3 related transcription factor 2	0.001314548	UP
Mlana	melan-A	7.70031291144205E-07	UP
Lipo3	lipase, member O3	0.022752715	UP
Lipo2	lipase, member O2	0.007483236	UP
Pcgf5	polycomb group ring finger 5	8.81235221564925E-05	UP
Hhex	hematopoietically expressed homeobox	3.74982310062059E-10	UP
Exoc6	exocyst complex component 6	3.64957140535869E-05	UP
Slc35g1	solute carrier family 35, member G1	0.000474187	UP
Plce1	phospholipase C, epsilon 1	0.006551709	UP
Entpd1	ectonucleoside triphosphate diphosphohydrolase 1	0.004810409	UP
Arhgap19	Rho GTPase activating protein 19	0.0475105	UP

Cnnm1	cyclin M1	4.87329636542288E-07	UP
Scd1	stearoyl-Coenzyme A desaturase 1	0.002791628	UP
Mfsd13a	major facilitator superfamily domain containing 13a	0.035321686	UP
Gsto1	glutathione S-transferase omega 1	0.021276513	UP
Gsto2	glutathione S-transferase omega 2	5.86281679912733E-06	UP
Add3	adducin 3 (gamma)	3.75715414216302E-05	UP
Nrap	nebulin-related anchoring protein	2.48741600719682E-05	UP

6.5. Appendix E: Differential Expression of Apoptosis and Cell Survival Pathway Genes in WT vs. PKD1-/- MEFs Identified via R Analysis

TABLES 6A AND 6B- DEGS IN APOPTOSIS AND CELL SURVIVAL PATHWAYS OF WT VS. *PKD1-/-* MEFS IDENTIFIED BY R ANALYSIS

6A. Primary MEFs		
DE	**Pathway**	**Gene ID**
Down-reg	Regulation of apoptotic process in various cell types (e.g., neurons, T-cell, myeloid, leucocytes, etc.)	Bcl2l11, Pik3cd, Siglect1, Tnf, Adam8, Fcgr2b, Card9, etc.
	ROS / Superoxide metabolic processes and regulation	Ncf11, Ncf2, Cybb, Itgam, Nross, Alox5, Tnf, etc.
	Cellular response to oxidative stress and regulation	Sirpa, Btk, Alox5, Itgam, Hk3, Prkd1, Tnf, Trem2, etc.
	NF-kappa B signaling and regulation	Card9, Card11, Sirpa, Btk, Tifa, Trim34b, Trem2, Tnf, Ticam2, Pycard, Prkd1, etc.
	Phosphatidylinositol 3-kinase signaling and regulation	Pik3cd, Pik3cg, Pik3ap1, Tnf, Trem2, Sema4d, Osm, Fgr, Hcls1
	Receptor signaling pathway via JAK-STAT	Ptprc, Il12rb2, Il10ra, Osm, Cd300a, Csf2rb, Csf2rb2, Hcls1, Tnf
	AKT / Protein kinase B signaling and regulation	Pik3cd, Pik3cg, Osm, Hcls1, Tnf, Adam8, Bank1, P2ry12, etc.
	Ras protein Signal transduction	Pik3cg, Rasal3, Dok2, Dok3, Dock2, Psd4, Was, Rapgef5, etc.

6B. Immortalized MEFs		
DE	**Pathway**	**Gene ID**
Down-reg	Regulation of apoptotic process in various cell types (e.g., neurons, myeloid, leucocytes, epithelial cells, etc.)	Bcl2l11, Tgfb2, Tgfbr2, Gata3, Gata6, Fas, Itgam, Adam8, Trem2, Prkn, Bcl3, E2f2, Fgf21, Hcls1, Slc7a11, Mif, Noc2, Tifa, Tifab, etc.
	Cellular response to starvation	Prkd1, Fas, Slc2a1, Wnt2b, Rnf152, Gck, etc.
	NF-kappa B signaling and regulation	Btk, Riok2, Riok3, Tgm2, Eda2r, Ripk2, Trem2, Prkn, Trim34b, Adam8, Alpk1, Bcl3, etc.
	Regulation of MAP kinase	Adam8, Mif, Tgfa, Fgf2, Egfr, etc.
	Phosphatidylinositol 3-kinase signaling and regulation	Egfr, Fgf2, Tgfb2, Sox9, Trem2, etc.
	Regulation of Wnt signaling	Fgf2, Prkn, Wnt5b, Tiam1, Egfr, Sox9, etc.
	AKT / Protein kinase B signaling and regulation	Adam8, Gata3, Fgf2, Egfr, Sox9, Pik3r3, Tnfa, Sox9, Hcls1, etc.
	Regulation of Ras protein signal transduction	Dok2, Dok5, Dok6, Rasgef1a, Dock5, Pds4, Was, Rac3, Tiam1, Rapgefl1, etc.
Up-reg	Regulation of apoptotic process in various cell types (e.g., neurons, myeloid, leucocytes, epithelial cells, etc.)	Trem2, Itgam, Adam8, Gata3, Mef2c, Tek, Kdr, Ndnf, Sema5a, Mif, E2f2, Hcls1, etc.
	AKT / Protein kinase B signaling and regulation	Igfbp5, Gata3, Fgf2, Tek, Adam8, Tnfaip8l3, Sema5a, Hcls1, etc.
	Regulation of Ras protein signal transduction	Rgl1, Was, Syde2, Stmn1, Pdpn, Rasgef1a, Dok2, Dock5, Cbl, Racgap1, etc.
	Phosphatidylinositol 3-kinase signaling and regulation	Fgf2, Vav3, Tek, Tnfaip8l3
	Regulation of Wnt signaling	Bmp2, Gpc3, Fgf2, Wf1, Cdh1, Sema5a, etc.
	Receptor signaling pathway via JAK-STAT	Il12rb1, Il15, Csf2rb, Csf2rb2, Hcls1, Erbb4, etc.

6.6. Appendix F: DEGs in Apoptosis and Survival Pathways of WT vs. PKD1-/- MEFs Analyzed with ShinyGo

TABLE 7- DEGS IN WT VS. *PKD1-/-* MEFS USING SHINYGO ANALYSIS.

MEFs	DE	Pathway	Gene ID
Immortalized	Down-reg	Pathways in cancer (e.g., breast, gastric, colorectal, etc.)	Adcy3, Ar, Bdkrb2, Bcl2l11, Cdkn1a, Col4a5, Csf3r, Dcc, Egfr, Fas, Flt4, Fzd3, Gnai1, Hey2, Il6, Il6st, Itga2, Itga2b, Kif7, Kng1, Lama2, Lama3, Lamb3, Rac3, Mmp2, Notch3, Notch4, Pax8, Pdgfa, Pgf, Pik3r3, Mgst2, Tcf7, Tgfb2, Tgfbr2, Wnt10a, Wnt10b, Wnt2, Wnt2b, Wnt5b, Wnt6, Gadd45g, Fgf21, Calml4
		JAK-STAT signaling pathway	Itga9, Bcl2l11, Cdkn1a, Col2a1, Col4a5, Col1a1, Col1a2, Csf3, Csf3r, Efna2, Egfr, Flt4, Il6, Itga2, Lama2, Lama3, Lamb3, Ntf3, Pdgfa, Pgf, Pik3r3, Tnc, Col6a6, Creb3l1, Itga11, Itgb8, Fgf21, Ddit4
		PI3K-Akt signaling pathway	Cdkn1a, Cish, Socs1, Cntfr, Csf3, Egfr, Il13ra2, Il6, Il6st, Pdgfa, Pik3r3, Il20ra, Il27ra
	Up-reg	Pathways in cancer	Adcy7, Bmp2, Camk2b, Cbl, Cdh1, Cxcr4, Csf2rb, Csf2rb2, Fgf2, Fgf5, Gngt2, Lpar1, Gstt2, Gsto1, Il12rb1, Il15, Il7r, Lamc2, Kitl, Mitf, Pim1, Rxrg, Slc2a1, Ctnna3, Tgfa, Vegfb, Vegfc, E2f2, Ncoa4, Cks1b, Gsto2, Fgf16
		PI3K-Akt signaling pathway	Angpt2, Col9a1, Erbb4, Fgf2, Fgf5, Gngt2, Lpar1, Il7r, Itga7, Kdr, Lamc2, Kitl, Ntrk2, Tek, Tgfa, Vegfb, Vegfc, Vwf, Tnn, Pdgfd, Fgf16
		MAPK signaling pathway	Angpt2, Erbb4, Fgf2, Fgf5, Hspa8, Kdr, Stmn1, Kitl, Ntrk2, Tek, Tgfa, Tgfa, Vegfb, Vegfc, Lamtor3, Pdgfd, Fgf16
		Ras signaling pathway	Angpt2, Fgf2, Fgf5, Gngt2, Grin2b, Kdr, Kitl, Ntrk2, Rgl1, Shc3, Tek, Tgfa, Vegfb, Vegfc, Pla2g2e, Pdgfd, Plce1, Fgf16
Primary	Down-reg	Apoptosis	Bcl2l11, Csf2rb, Csf2rb2, Ctsc, Ctss, Itpr2, Pik3cd, Tnf
		NF-kappa B signaling pathway	Card11, Btk, Cd14, Tnf, Ticam2, Tnfsf13b, Pik3cd, Vwf, Pik3cg, Lpar5, Pik3ap1
		PI3K-Akt signaling pathway	Bcl2l11, Csf1r, Csf3r, Lama3, Osm,
		JAK-STAT signaling pathway	Csf2rb, Csf2rb2, Cstf3r, Ptpn6, Il10ra, Il12rb2, Il7r, Osm, Pik3cd, Il21r

6.7. Appendix G: STRING-Enriched Biological Processes in WT vs. PKD1-/-MEFs

TABLES 8A AND 8B- ENRICHED BIOLOGICAL PROCESSES IN WT AND *PKD1-/-*MEFS IDENTIFIED BY STRING ENRICHMENT PROCESS

8A. Immortalized				
DE	**process**	**Gene ID**	**p-value**	**FDR**
Down-reg	Regulation of apoptotic process	Alox12, Sox9, Bdkrb2, Scin, Hspb1, Timp1, Gata2, Ctsz, Ptgis, Vip, Hey2, Il20ra, Egfr, Flt4, Zfp36l1, Gadd45g, Plk2, Vdr, Col2a1, Wnt10b, Cdkn1a, Sox8, Nme4, Fas, Il6, Ercc5, Pax8, Creb3l1, Zmat3, Slc7a11, Ptgfr, Cd38, Ctsc, Fgf21, Mmp2, Cx3cl1, Ctsh, Akap12, Six4, Aipl1, Egr3, Ntrk3, Gabrb3, Pde3a, Ripk2, Hoxa5, Rnf122, Phlda3, Efhc1, Dlx1, Agap2, Tgfb2, Inhbb, Prr7, Inhba, Alx4, Wfs1, Foxc1, Ar, Kcnb1, Six1, Ackr3, Inca1, Pou3f4, Syngap1, Mgmt, Nell1, Tcf7, Aldh1a1, Nes, Eya4, Nr3c1, Tgm2, Tnfrsf18, Kcnip3, Pde1a, Cntfr, Col18a1, Hpn, Rps6ka2, Bcl2l11, Neurl1a, Ntf3, Pak3, Il1rn, Bcl3, Fzd3, Ucp2, Acot1, Lox, Foxp1, Wnk3, Kcnma1, Park2	0.00034	0.0259
Up-reg	Regulation of apoptotic process	Cdh1, Ace, Il7r, Aqp1, Tnfaip8l2, Hspa8, Cdk1, Rgcc, Fbxo32, Tfrc, Hcls1, Trem2, Pim1, Tslp, Vegfb, Tfap2b, Stk17b, Htr2b, Mdk, Rassf2, Bmp2, Aurka, Sfrp2, Rps3a1, Pdpn, Tnfrsf1b, Tgfa, Tyrobp, Coro1a, Angpt2, Hpgd, Aldh1a2, Foxq1, Irs2, Hoxa13, Mif, Gata6, Cbl, Mitf, Grn, Sfn, Ndnf, Lpar1, Pcsk9, Msx1, Amigo2, Pgr, Cx3cr1, Hmgb2, Itgam, Sema5a, Hmga2, Hsph1, Ntrk2, Gpx1, Cdkn2d, Stk40, Grid2, Tnfaip8l3, Tek, Gata3, Kitl, Adam8, Ect2, Nlrp1a, Camk2b, Kdr, Cflar, Rtkn2, Erbb4, Lgals3, Clec5a, C5ar1, Gba, Mef2c, Evi2b, Noc2l, Ncf2	8.3E-06	0.00071
	Regulation of response to stress	Il12rb1, Ace, Mmp12, Kiaa0319, Tnfaip8l2, Ctss, Enpp3, Fam132a, Trem2, Tslp, Vegfb, Cd28, Tnfrsf11a, Fcna, Mdk, Wdr76, Rassf2, Pcna, Bmp2, Fabp4, Sfrp2, Pdpn, Tnfrsf1b, Mad2l2, Cd9, Was, Sytl4, Btk, Il15, Ldlr, Trf, Polr3g, Mvk, Fgf2, Mif, Ubash3b, Grn, Setd8, Cxcr4, Insig1, Gdf6, Cx3cr1, Hmgb2, Pld4, Itgam, Alox5ap, Hmga2, Hsph1, Gpx1, Cadm1, Cdkn2d, Myo1f, Cd37, Fancb, Rpa2, Gata3, Aunip, Adam8, Duoxa1, Clec7a, Mgll, Ankle1, Aim2, Txk, Adcy7, Mef2c, Raet1c	1.94E-05	0.0014

8B. Primary				
DE	**process**	**Gene ID**	**p-value**	**FDR**
Down-reg	Apoptotic process	Spi1, Prkd1, Ncf1, Atp2a3, Tnf, Ctsc, Tyrobp, Pycard, Btk, Spn, Hcar2, Naip5, Nlrc4, Pik3cg, Itgam, Gpr65, Dab2, Cadm1, Nlrp1b, Nlrp1a, Bcl2l11, Naip6, Naip2, Aim2, Srgn, Inpp5d, C5ar1	0.00028	0.0071
	Regulation of apoptosis	Ccl12, Il7r, Tnfaip8l2, Atp2a3, Hcls1, Trem2, Tnf, Csf1r, Dock8, Atf3, Fcgr2b, Siglec1, Pf4, Ctsc, Tyrobp, Coro1a, Pycard, Nckap1l, Hk3, Pou3f3, Cxcr4, Hcar2, Naip5, Nlrc4, Pik3cg, Cx3cr1, Itgam, Osm, Fcer1g, Dab2, Card11, Card9, Nlrp3, Tgm2, Pik3cd, Adam8, Nlrp1b, Nlrp1a, Arrb2, Bcl2l11, Ccr5, Naip6, Naip2, Ucp2, Clec5a, Inpp5d, C5ar1, Evi2b, Ptprc, Ncf2	4.31E-07	2.21E-05
	Regulation of response to stress	Vav1, Tnfaip8l2, Ctss, Ncf1, Trem2, Tnf, Alox5, Fcgr2b, Fcna, Fcgr1, Gbp5, Fgr, Stap1, Ctsc, Pycard, Was, Btk, Trf, Gpsm3, Spn, Hk3, Pik3ap1, Cxcr4, Nlrc4, Pik3cg, Cx3cr1, Pld4, Itgam, Alox5ap, Osm, Fcer1g, Dab2, Tlr9, Cadm1, Myo1f, Cnr2, Cd37, Card9, Nlrp3, Bst1, Tgm2, Sirpa, Plek, Trpm2, Adam8, Arrb2, Ccr5, Tlr8, Mctp1, Aim2, Fcgr3, Ccr2	2.94E-10	2.71E-08
	I-kappaB kinase/NF-kappaB signaling	Btk, Avpr2, Tifa, Tlr7, Tlr9, Card11, Card9, Tlr8, Tifab	3.35E-07	1.78E-05
	Regulation of I-kappaB kinase/NF-kappaB signaling	Prkd1, Clec4n, Tnf, Pycard, Tifa, Cx3cr1, Ticam2, Tlr9, Card11, Card9, Tgm2, Sirpa	7.87E-05	0.0024

6.8. Appendix H: R Code Workflow for RNA-Seq Data Analysis

#**Installation of Packages Relevant to the Analysis**

```
if (!require("BiocManager", quietly = TRUE))
install.packages("BiocManager")
BiocManager::install("DESeq2")
BiocManager::install("pheatmap")
BiocManager::install("apeglm")
BiocManager::install("dplyr")
BiocManager::install("RColorBrewer")
BiocManager::install("ggplot2")
BiocManager::install("ggrepel")
BiocManager::install("ComplexHeatmap")
BiocManager::install("org.Mm.eg.db")
BiocManager::install("ashr")
BiocManager::install("AnnotationDbi"
BiocManager::install("clusterProfiler")

BiocManager::install("DESeq2")
BiocManager::install("ComplexHeatmap")
install.packages("ggrepel")
BiocManager::install("apeglm")
BiocManager::install("ashr")
BiocManager::install("AnnotationDbi")
BiocManager::install("clusterProfiler")
```

#Calling Libraries

```
library(DESeq2)
library(pheatmap)
library(apeglm)
library(dplyr)
library(RColorBrewer)
```

```
library(ggplot2)

library(ggrepel)

library(ComplexHeatmap)

library("org.Mm.eg.db")

library("ashr")

library(AnnotationDbi)

library(clusterProfiler)
```

#Set Directory

```
setwd("/Users/smed-jmloaizamoss/Desktop")
```

#Two types of data: a) the raw counts of each sample, b) Sample Info or Metadata: shows the factors or variables of each sample.

#Loading Count Data

```
rawcounts <- read.csv("Counts.raw.csv", header = TRUE, row.names = 1, sep = ",")

rawcounts

head(rawcounts)
```

#Loading Sample Info

```
Meta <- read.csv("MetaData.csv", header = TRUE, row.names = 1, sep = ",")

Meta

head(Meta)
```

#Setting Factors

```
Meta$Genotype <- factor(Meta$Genotype)

Meta$Status <- factor(Meta$Status)
```

#DESeq object creation

```
dds <- DESeqDataSetFromMatrix(countData = rawcounts, colData = Meta, design = ~ Genotype + Status + Genotype:Status)
```

#Filtering table for genes expressed

```
smallestGroupSize <- 3

keep <- rowSums(counts(dds) >= 10) >= smallestGroupSize

dds2 <- dds[keep,]

#Creating the new factor of Genotype:Status interaction for design

dds2$group <- factor(paste0(dds2$Genotype, dds2$Status))

design(dds2) <- ~ group

#DESeq statistical test

dds3 <- DESeq(dds2)

#Search names of levels for comparison

dds2$group

#Contrasts combinations of PKD1

ResP1.P0 <- results(dds3, contrast=c("group", "PKD1-/-Primary", "WildtypePrimary"))

ResI1.P1 <- results(dds3, contrast=c("group", "PKD1-/-Immortalized", "PKD1-/-Primary"))

ResI1.I0 <- results(dds3, contrast=c("group", "PKD1-/-Immortalized", "WildtypeImmortalized"))

ResI0.P0 <- results(dds3, contrast=c("group", "WildtypeImmortalized", "WildtypePrimary"))

#Change DESeq object to Dataframe

RP1.P0 <- as.data.frame(ResP1.P0)

RI1.P1 <- as.data.frame(ResI1.P1)

RI1.I0 <- as.data.frame(ResI1.I0)

RI0.P0 <- as.data.frame(ResI0.P0)

#Adding Gene Symbols, Gene Name, RNA biotype


RP1.P0$symbol <- mapIds(org.Mm.eg.db, keys = rownames(RP1.P0), keytype = "ENSEMBL", column = "SYMBOL")

RP1.P0$Genename <- mapIds(org.Mm.eg.db, keys = rownames(RP1.P0), keytype = "ENSEMBL", column =
"GENENAME")

RP1.P0$biotype <- mapIds(org.Mm.eg.db, keys = rownames(RP1.P0), keytype = "ENSEMBL", column =
"GENETYPE")
```

#Adding DE Classification

```
RP1.P0$DE <- "NO"

RP1.P0$DE[RP1.P0$log2FoldChange > 1 & RP1.P0$padj < 0.05] <- "UP"

RP1.P0$DE[RP1.P0$log2FoldChange< -1 & RP1.P0$padj < 0.05] <- "DOWN"

RP1.P0s <- na.omit(RP1.P0)

RP1.P0s


RI1.P1$symbol <- mapIds(org.Mm.eg.db, keys = rownames(RI1.P1), keytype = "ENSEMBL", column = "SYMBOL")

RI1.P1$Genename <- mapIds(org.Mm.eg.db, keys = rownames(RI1.P1), keytype = "ENSEMBL", column =
"GENENAME")

RI1.P1$biotype <- mapIds(org.Mm.eg.db, keys = rownames(RI1.P1), keytype = "ENSEMBL", column = "GENETYPE")
```

#Adding DE Classification

```
RI1.P1$DE <- "NO"

RI1.P1$DE[RI1.P1$log2FoldChange > 1 & RI1.P1$padj < 0.05] <- "UP"

RI1.P1$DE[RI1.P1$log2FoldChange< -1 & RI1.P1$padj < 0.05] <- "DOWN"

RI1.P1s <- na.omit(RI1.P1)

RI1.P1s


RI1.I0$symbol <- mapIds(org.Mm.eg.db, keys = rownames(RI1.I0), keytype = "ENSEMBL", column = "SYMBOL")

RI1.I0$Genename <- mapIds(org.Mm.eg.db, keys = rownames(RI1.I0), keytype = "ENSEMBL", column =
"GENENAME")

RI1.I0$biotype <- mapIds(org.Mm.eg.db, keys = rownames(RI1.I0), keytype = "ENSEMBL", column = "GENETYPE")

#Adding DE Classification

RI1.I0$DE <- "NO"

RI1.I0$DE[RI1.I0$log2FoldChange > 1 & RI1.I0$padj < 0.05] <- "UP"

RI1.I0$DE[RI1.I0$log2FoldChange< -1 & RI1.I0$padj < 0.05] <- "DOWN"

RI1.I0s <- na.omit(RI1.I0)

RI1.I0s


RI0.P0$symbol <- mapIds(org.Mm.eg.db, keys = rownames(RI0.P0), keytype = "ENSEMBL", column = "SYMBOL")
```

```
RI0.P0$Genename <- mapIds(org.Mm.eg.db, keys = rownames(RI0.P0), keytype = "ENSEMBL", column = "GENENAME")

RI0.P0$biotype <- mapIds(org.Mm.eg.db, keys = rownames(RI0.P0), keytype = "ENSEMBL", column = "GENETYPE")
```

#Adding DE Classification

```
RI0.P0$DE <- "NO"

RI0.P0$DE[RI0.P0$log2FoldChange > 1 & RI0.P0$padj < 0.05] <- "UP"

RI0.P0$DE[RI0.P0$log2FoldChange< -1 & RI0.P0$padj < 0.05] <- "DOWN"

RI0.P0s <- na.omit(RI0.P0)

RI0.P0s
```

#Extract the DE genes

```
RP1.P0DE <- subset(RP1.P0s, DE != "NO")

RI1.P1DE <- subset(RI1.P1s, DE != "NO")

RI1.I0DE <- subset(RI1.I0s, DE != "NO")

RI0.P0DE <- subset(RI0.P0s, DE != "NO")
```

#Extract the DE protein-coding genes

```
RP1.P0DEc <- subset(RP1.P0DE, biotype == "protein-coding")

RI1.P1DEc <- subset(RI1.P1DE, biotype == "protein-coding")

RI1.I0DEc <- subset(RI1.I0DE, biotype == "protein-coding")

RI0.P0DEc <- subset(RI0.P0DE, biotype == "protein-coding")
```

#Compare the total number of transcripts versus the DE ones

```
dim(RP1.P0s)

dim(RP1.P0DE)

dim(RP1.P0DEc)

dim(RI1.P1s)

dim(RI1.P1DE)

dim(RI1.P1DEc)

dim(RI1.I0s)

dim(RI1.I0DE)
```

```
dim(RI1.P1DEc)

dim(RI0.P0s)

dim(RI0.P0DE)

dim(RI0.P0DEc)
```

GeneOntology

#pPKD1-/- vs pWT

#Upregulated

```
RP1.P0up <-RP1.P0DEc[(RP1.P0DEc$log2FoldChange > 1), ]

RP1.P0ups <- RP1.P0up$symbol

GOupA <- enrichGO(gene = RP1.P0ups, OrgDb = org.Mm.eg.db, keyType = "SYMBOL", ont = "BP", pvalueCutoff = 0.05, qvalueCutoff = 0.05)

P1.P0GOup <- as.data.frame(GOupA)

write.csv(P1.P0GOup, file = "P1.P0GOup.csv")

plotGOupA <- plot(barplot(GOupA, showCategory = 30))
```

#Downregulated

```
RP1.P0down <- RP1.P0DEc[(RP1.P0DEc$log2FoldChange < -1), ]

RP1.P0downs <- RP1.P0down$symbol

GOdownA <- enrichGO(gene = RP1.P0downs, OrgDb = org.Mm.eg.db, keyType = "SYMBOL", ont = "BP", pvalueCutoff = 0.05, qvalueCutoff = 0.05)

P1.P0GOdown <- as.data.frame(GOdownA)

write.csv(P1.P0GOdown, file = "P1.P0GOdown.csv")

plotGOdownA <- plot(barplot(GOdownA, showCategory = 30))
```

#iPKD1-/- vs iWT

#Upregulated

```
RI1.I0up <-RI1.I0DEc[(RI1.I0DEc$log2FoldChange > 1), ]

RI1.I0ups <- RI1.I0up$symbol

GOupB <- enrichGO(gene = RI1.I0ups, OrgDb = org.Mm.eg.db, keyType = "SYMBOL", ont = "BP", pvalueCutoff = 0.05, qvalueCutoff = 0.05)

I1.I0GOup <- as.data.frame(GOupB)
```

```
write.csv(I1.I0GOup, file = "I1.I0GOup.csv")

plotGOupB <- plot(barplot(GOupB, showCategory = 30))


#Downregulated

RI1.I0down <- RI1.I0DEc[(RP1.P0DEc$log2FoldChange < -1), ]

RI1.I0downs <- RI1.I0down$symbol

GOdownB <- enrichGO(gene = RI1.I0downs, OrgDb = org.Mm.eg.db, keyType = "SYMBOL", ont = "BP", pvalueCutoff
= 0.05, qvalueCutoff = 0.05)

I1.I0down <- as.data.frame(GOdownB)

write.csv(I1.I0down, file = "I1.I0down.csv")

plotGOdownB <- plot(barplot(GOdownB, showCategory = 30))
```